N69-35125

NASA CR-72569
R-7775

ASE FILE
COPY

PROTECTIVE COATING SYSTEM FOR A REGENERATIVELY COOLED THRUST CHAMBER

TASKS I AND II
FINAL REPORT

(30 June 1967 through 31 January 1969)

by

H. W. Carpenter

prepared for

NATIONAL AERONAUTICS AND SPACE ADMINISTRATION

Contract NAS3-11187

ROCKETDYNE
A Division of North American Rockwell Corporation
Canoga Park, California

NOTICE

This report was prepared as an account of Government-sponsored work. Neither the United States, nor the National Aeronautics and Space Administration (NASA), nor any person acting on behalf of NASA:

1. Makes any warranty or representation, expressed or implied, with respect to the accuracy, completeness, or usefulness of the information contained in this report, or that the use of any information, apparatus, method, or process disclosed in this report may not infringe privately-owned rights; or
2. Assumes any liabilities with respect to the use of, or for damages resulting from the use of, any information, apparatus, method or process disclosed in this report.

As used above, "person acting on behalf of NASA" includes any employee or contractor of NASA, or employee of such contractor, to the extent that such employee or contractor of NASA or employee of such contractor prepares, disseminates, or provides access to any information pursuant to his employment or contract with NASA, or his employment with such contractor.

Requests for copies of this report should be referred to:

National Aeronautics and Space Administration
Scientific and Technical Information Facility
P.O. Box 33
College Park, Md. 20740

NASA CR-72569
R-7775

PROTECTIVE COATING SYSTEM FOR A REGENERATIVELY COOLED THRUST CHAMBER

Tasks I and II
Final Report

(30 June 1967 through 31 January 1969)

By

H. W. Carpenter

Prepared For
National Aeronautics and Space Administration

February 1969

Contract NAS3-11187

Technical Management
NASA Lewis Research Center
Cleveland, Ohio
Chemical Rocket Division
Mr. Charles Zalabak

Rocketdyne
A Division of North American Rockwell Corporation
Canoga Park, California

FOREWORD

The effort described herein was performed under Contract NAS3-11187 from 30 June 1967 through 31 January 1969. It is comprised of two major tasks. Task I (analytical) occupied the period from 30 June 1967 to 30 November 1968 and Task II (experimental) from 1 December 1967 to 31 January 1969. The Technical Manager was Mr. Charles Zalabak, Chemical Rocket Division, National Aeronautics and Space Administration, Lewis Research Center, Cleveland, Ohio 44135. This report is submitted in fulfillment of the requirements of Exhibit A, par. II.3 and of Exhibit B, par. E of the subject contract.

ACKNOWLEDGEMENTS

Contributions of the following people are gratefully acknowledged: Dr. Stephen C. Carniglia, who was Responsible Engineer for the latter part of the program; Dr. Sherman D. Brown, who was Responsible Engineer for the major portion of the program, for his guidance and support early in the program; Dr. George Y. Onoda, Jr., for his valuable technical assistance at the onset of the program; Dr. Oliver E. Accountius for providing test specimens coated with the cementitiously bonded ThO_2 coatings; Mr. Robert J. Hall for performing the X-ray diffraction and electron-beam microprobe analyses; and Mr. Mark M. Nakata of Atomics International Division, North American Rockwell Corporation, for the thermal diffusivity measurements of the phosphate-bonded ZrO_2 material.

ABSTRACT

A ceramic coating system is desired for thermal protection of the thrust chamber wall in a high-performance, liquid hydrogen-, liquid oxygen-fueled rocket engine. This heat-barrier coating is intended to reduce the heat flux through the chamber wall from 50 to 20 Btu/in.^{2}-sec, reduce the metal wall temperature to less than 1600 F, operate with a 4000 F surface temperature, and survive multiple engine starts.

Cementitiously bonded heat-barrier coatings were considered analytically and through examination of the literature in Task I. Several material systems were selected for initial experimental evaluation of Task II. Based on screening-type arc-plasma jet tests that simulated the thermal conditions of the reference rocket engine, one coating system out of those selected appeared capable of meeting all program objectives. The remainder of Task II was devoted to the development and further detailed evaluation of this one system. The coating consists essentially of zirconia powder bonded with orthophosphoric acid plus a small amount of hydrofluoric acid. The phosphate-bonded ZrO_2 coatings were found to be hard, strong, refractory, resistant to thermal shock, and similar to phosphate-free zirconia in degree of thermal protectiveness. The coatings were applied on Hastelloy-X sheet by several aqueous slurry coating methods, and only a 600 F curing treatment was required before service.

Advantages of this slurry-applied coating are simplicity, low cost, and ability to coat thrust chambers under minimum restrictions with respect to size and shape. This coating system has survived multiple thermal shocks between room temperature and apparent surface temperatures above 4000 F, while protecting the water-cooled substrate, in arc-plasma jet tests. It appears ready to be evaluated in small-scale rocket engine tests.

CONTENTS

Foreword iii

Acknowledgements iii

Abstract v

Introduction 1

Review of Task I 5

  Basis for Selection of Coating Systems 5

  Selected Coating Systems 6

Summary of Task II 9

  Accomplishments 9

  The Phosphate-Bonded ZrO_2 Coating System 9

  Disqualified Coating Systems 12

Task II Procedures 15

  Specimen Preparation 15

  Flexural Strength and Density Measurement 17

  Adherence Tests 18

  Arc-Plasma Jet Tests 21

The Phosphate-Bonded ZrO_2 System: Results and Discussion . . . 33

  Introduction 33

  Formulation Studies 34

  Adherence 65

  Arc-Plasma Jet Tests 77

Disqualified Coating Systems: Results and Discussion 89

  Fluorosilicic Acid-Bonded Systems 89

  Potassium Silicate-Bonded ZrO_2 91

  Barium Zirconate Systems 94

  Hafnia-Rich Mixed Oxide Systems 101

  Thoria-Based Systems 103

Conclusions and Recommendations 111

  Conclusions 111

  Recommendations 112

References 117

Appendix A

Task I Final Report A-1

Appendix B

Evaluation of the Thermal Shock Test for Adherence B-1

Appendix C

Heat Flux Calibration of the Arc-Plasma Jet Test C-1

Appendix D

Particle Size Distribution Study D-1

Appendix E

Special Substrate Preparation Studies E-1

Appendix F

Arc-Plasma Jet Test Data of Specimens Coated With
Phosphate-Bonded ZrO_2 . . . . F-1

Appendix G

Thermal Diffusivity Measurement of Phosphate-Bonded ZrO_2 . . . G-1

ILLUSTRATIONS

1. Adherence Specimen Showing Cohesive Failure 22
2. Exploded View of Arc-Plasma Jet Test Fixture 25
3. Specimens Melted in the Arc-Plasma Jet 50
4. Microstructure of Bars Composed of Formulations of B44, 45, 47, and 49 That Have Annealed for 1/2 Hour 54
5. Photomicrograph of the Area That Was Analyzed With the Electron-Beam Microprobe 60
6. Electron-Beam Microprobe Analysis of a Phosphate-Bonded ZrO_2 Coating That Has Been Tested in an Arc-Plasma Jet 61
7. Melting Temperature of Phosphate-Bonded ZrO_2 as a Function of Binder Content 63
8. Specimens After the Thermal Shock Test 67
9. Photomicrographs of Adherence Test Specimens That Have Special Adherence-Promoting Base Layers 70
10. Specimen 116 After Flexing Back and Forth Over Progressively Smaller Mandrels 76
11. Cross Sections of the Coating on Specimen 72-6 After Testing in the Arc-Plasma Jet 81
12. Cross Sections of Coatings That Were Subjected to Thermal Conditions in the Arc-Plasma Jet Much More Severe Than Service Conditions in a Thrust Chamber . . 83
13. Silicate-Bonded ZrO_2 Specimens After Arc-Plasma Jet Tests 97
14. Cementitiously Bonded $BaZrO_3$ Specimens After Testing in the Arc-Plasma Jet 100
15. Phosphate-Bonded ThO_2-Coated Specimens After Testing in the Arc-Plasma Jet 110

TABLES

1. Cross-Section of Heat Transfer Parameters Across Test Specimens 30
2. Flexural Strength of Phosphate-Bonded Zirconia as a Function of Fluoride Content 43
3. Effect of Fluoride Content on the Shelf Life of Phosphate-Bonded Zirconia Slurry Compositions 44
4. Phosphate-Bonded ZrO_2 Slurry Formulations 51
5. The Effect of Relative Strength and Hardness of Selected Composition of Phosphate-Bonded ZrO_2 as a Function of Annealing Temperature 53
6. The Effect on Strength and Hardness of Selected Compositions of Phosphate-Bonded ZrO_2 as a Function of Annealing Temperature 57
7. Adherence Data: Thermal Shock Test of Coated Hastelloy-X Tabs That Were Prepared Using Selected Techniques 66
8. Summary of Adherence Data: Bend Test Type A 73
9. Summary of Adherence Data: Bend Test Type B 74
10. Composition and Properties of Selected ZrO_2 Systems Containing H_2SiF_6 and $NH_4H_2PO_4$ 90
11. Arc-Plasma Test Results of Specimens Coated With Silicate-Bonded ZrO_2: A Summary 95
12. Arc-Plasma Test Results of Specimens Coated With Cementitiously Bonded $BaZrO_2$: A Summary 99
13. Arc-Plasma Test Results for Specimens Coated With Phosphate-Bonded ThO_2 107

INTRODUCTION

Dependable heat-barrier coatings will be extremely advantageous, if not a necessity, on the chamber walls of advanced liquid-fueled, regeneratively cooled rocket engines. The heat flux through the chamber walls of these advanced high-performance engines will be four or five times present levels because of increased chamber pressures. Metals and alloys that are used in current thrust chamber applications are presently near their service limits. Potential designs for future thrust chambers include use of either refractory metal alloys or novel, highly efficient schemes of cooling. But uncoated refractory metals are not useful in oxidizing atmospheres at the temperatures anticipated, and it is improbable that dependable oxidation protective coatings for service in high-performance rocket engines will be developed in the near future. Although auxiliary cooling schemes exist (e.g., film cooling), they entail inefficient use of fuel. The amplified pumping demanded for increased regenerative cooling is not satisfactory either, because it lessens efficiency and increases engine weight.

Use of effective, passive heat-barrier coatings therefore becomes very attractive as a means for reducing the heat flux through the walls of regeneratively cooled thrust chambers, and for reducing the service temperature of metal components. Reduced service temperatures will result in extended fatigue life and reduced corrosion rates of alloys that are presently used, in lower thermal stresses, and in increased flexibility of design. Weight reductions will also result from the decreased heat flux, through a decrease in the required coolant flowrate.

To date, the only successful heat-barrier coatings for rocket engine applications have been applied by melt-spraying methods, the most successful being applied by arc-plasma spraying. Arc-plasma spraying processes offer several favorable qualities:

1. Flexibility in coating design and application (e.g., graded coatings)

2. Ability to obtain comparatively adherent coatings
3. Utility for a wide range of coating materials (e.g., any material that melts stably and has a reasonably low vapor pressure)
4. Adequate process control

While coatings applied by slurry methods have not yet been used for heat barriers in rocket engine applications, slurry methods offer several potential advantages over melt-spraying methods. Slurry methods require no elaborate, expensive equipment, fixtures, or cooling. Most importantly, slurry methods are not restricted by substrate size and geometry as is arc-plasma spraying. Arc-plasma spraying is a line-of-sight process, and best results are obtained when the coating material is applied at a 90-degree angle to the substrate. Thus, only surfaces that are accessible to the melt-spraying equipment can be coated, and the minimum diameter of a long chamber would have to be about 10 inches to conveniently accommodate a conventional arc-plasma spray gun. Slurry processes, conversely, are not intrinsically limited by size or shape of the part to be coated. Inaccessible surfaces can be coated by dipping the entire part into the slurry or by pouring the slurry into the inaccessible area. Therefore, the most economical and, in some cases, the only feasible coating application technique is one in which the coating is applied as a slurry.

The types of coating systems commonly applied by slurry-coating methods include diffusion coatings (such as an aluminide coating on a refractory metal), fused-glass coatings (such as procelain enamels and glazes), and cementitiously bonded coatings. Because the last-named type of coating is the only type that was potentially useful in this program, the term "slurry coating" as used in this report will refer only to cementitiously bonded coating systems. Fused-glass and diffusion coatings are not stable at 4000 F, and they do not offer sufficient resistance to the flow of heat.

Cohesive bonding in slurry-applied coatings is accomplished by chemical energy rather than by thermal energy alone as in sintering. Cementitiously bonded slurry coatings consist of three main constituents: a filler material, a binder material, and a liquid suspension medium. In this program these constituents are, respectively, refractory oxide fillers, phosphate and silicate binders, and water.

Heat-barrier design criteria for this program included the following:

1. The coating must be capable of reducing the design heat flux of 50 Btu/in.^{2}-sec to 20 Btu/in.^{2}-sec.
2. The temperature of the coated side of the metal wall must not exceed 1600 F.
3. The gas-side surface temperature of the coating must be approximately 4000 F.
4. The specified gas temperature is 6000 F (combustion of hydrogen in oxygen).
5. Coolant temperatures may range from 50 to 500 R (-410 to 40 F).
6. One of the materials presently used for construction of thrust chambers (e.g., type 347 stainless steel or Hastelloy-X) will be used for the structural wall.

This program, directed toward meeting these conditions by means of a slurry coating, was divided into two consecutive tasks. Task I included an analytical evaluation of the performance of heat-barrier, slurry-coating systems, and the selection of four potential slurry-coating systems that appeared to be best. Selection was based on the literature and on the analytical evaluation. Coatings selected in Task I were then evaluated in Task II in arc-plasma jet tests. Based on failure analysis after each test, coating materials and coating designs were improved for following tests. The final goal was a dependable coating that would be capable of satisfactory performance in the environment described by the design criteria. Within the scope of Task II, evaluation of performance was based solely on arc-plasma jet tests that simulated thermal conditions of the design environment, and on other appropriate laboratory tests: testing of coatings in rocket engine thrust chambers under the design conditions was excluded.

Because this was not a materials development program, coating materials and processes were originally limited to those of existing technology, or those that were commercially available. The program, by necessity, overreached this original intent because existing coating technology and materials were inadequate to cope with the hostile environment of the design thrust chamber. Significant advancements were achieved in the formulation and processing of phosphate-bonded zirconia coatings for extreme high-temperature, high heat-flux service. Confirmation of the performance potential of these coatings, through laboratory testing and examination, has led to the recommendation that the coating system be evaluated in a small H_2-O_2-fueled rocket engine as the next step toward qualification.

This publication is the final report of this program. A final report of Task I was previously prepared (Rocketdyne Report R-7273, issued 21 November 1967); that report is reproduced in its entirety as Appendix A hereto, while its content is reviewed briefly in the following pages as an introduction to the specific undertakings of Task II. After a summary, the subsequent sections and their Appendices treat Task II in full, followed finally by the program conclusions and recommendations.

REVIEW OF TASK I*

BASIS FOR SELECTION OF COATING SYSTEMS

A literature search showed that four past heat-barrier coating programs were relevant to this program. This literature information was useful for evaluating potential coating materials systems; but it was of limited value in designing coating systems for this program because of the large differences in design criteria between past and present application concepts. The general literature on the cementitious bonding of ceramics was also critically reviewed.

Heat transfer analyses for the steady-state and transient conditions of the design rocket engine were:

Thermal resistance required for a thermal barrier to reduce the heat flux from 50 to 20 Btu/in.^{2}-sec	140 in.^{2}-sec-F/Btu
Surface temperature of the coating	4000 F
Coating/metal chamber wall interface temperature	1200 F
Temperature drop across the coating	2800 F
Temperature gradient across a 3.5-mil thick coating	10^6 F/inch
Approximate time for the coating to reach steady state	5×10^{-2} second
Average heating rate	10^5 F/second

Heat-barrier coating thickness required to provide the design thermal resistance was estimated to be 3.5 mils for all coating systems. An accurate thickness value for each cementitiously bonded system was not possible based on existing thermal property data, owing to variables of composition and porosity and to uncertainties of reaction, vaporization, and consolidation in the service environment.

---

*The full Task I report appears as Appendix A

Thermal stress analyses revealed that the stresses in the coating critically depend on the overall design of the coating system. The effects of material properties (heat conductivity, expansion coefficient, and elastic modulus) and coating thickness on the magnitude of stresses in the coating and at the coating-substrate interface were considered. Also evaluated were the usefulness of graded coatings and of stress-relief devices such as coatings that soften at high temperatures, and ductile metal interlayers between the coating and substrate. The overall analyses suggested that a simple monolithic coating probably would not be suitable for sustaining the thermal shock conditions and that either a graded coating or some stress-relief device would probably be necessary. Materials for special sublayer coatings and reinforcements could not be selected, however, until more was known concerning their requirements in the coating design. These requirements were to be deduced from failure analyses of the specimens tested in arc-plasma jet tests.

Factors that might affect the performance and reliability of the coating were considered. These factors included important properties affecting chemical and physical stability, in addition to resistance to thermal shock, such as: melting point, vapor pressure, adherence, density, strength, and reaction rates with hydrogen, oxygen, and water.

SELECTED COATING SYSTEMS

Based on the literature search and the described analyses and criteria, ZrO_2, ThO_2, $BaZrO_3$, and a HfO_2-rich mixture of oxides were selected as coating filler materials. Binders H_2PO_3F, H_2SiF_6, K_2SiO_3, and $Th(NO_3)_4$ (for use in ThO_2 system only) were selected for bonding the filler materials and thereby providing strength to the coating system. ZrO_2 appeared by far the most promising filler candidate based on the state of the art. Cementitiously bonded ZrO_2 materials that were used as thick heat shields had showed very encouraging results in oxyacetylene torch tests. Cementitiously bonded ThO_2, although not tested so extensively, appeared promising in similar tests; and it was considered potentially more chemically and thermally stable than ZrO_2 in the rocket engine environment. The two other oxides that were selected, on the other hand, had not been used previously as cementitiously bonded materials. These oxides were selected because of potential complementary properties to those of ZrO_2 and ThO_2. $BaZrO_3$ was selected because of possible advantages from the standpoint of chemical bonding reactions, and because it was reported to have a lower thermal expansion coefficient than ZrO_2. A hafnia-rich mixture of oxides (HfO_2-ZrO_2-TiO_2) was also selected because it has a very low macroscopic thermal expansion. Low expansion would be an important asset in reducing thermal stress in the outer (hotter) coating stratum.

Hastelloy-X was selected as the reference substrate material because it has a 30-percent lower thermal expansion coefficient than type 347 stainless steel and because a uniform, tenacious oxide layer can be easily formed on its surface. This was felt to be a potential advantage for providing good wetting and strong bonding of the heat-barrier coating.

SUMMARY OF TASK II

ACCOMPLISHMENTS

One heat-barrier coating system that is applied by slurry-coating techniques, among the combinations identified in Task I, best survived initial screening tests. This system was designed, developed, and exhaustively evaluated in arc-plasma jet tests which simulated the thermal conditions of the reference rocket engine. Based on the information obtained, this coating has the following attributes:

1. It is capable of reducing the heat flux through the thrust chamber wall from 50 to 20 Btu/in.^{2}-sec.
2. It is capable of reducing the metal surface (i.e., the coating/metal interface) temperature to below 1600 F, nominally to 1200 F.
3. It is resistant to thermal shock and thermal stress. It survived 25 thermal shocks from 70 to 4000 to 70 F, and steady-state testing to indicated temperatures above 4000 F.
4. It can be applied to virtually any size and shape of thrust chamber.
5. It requires only a 600 F cure before service to 4000 F.
6. It is made from inexpensive commercial materials.
7. It can be refurbished, even in the field.

THE PHOSPHATE-BONDED ZrO_2 COATING SYSTEM

The successful coating is a phosphate-bonded ZrO_2 system having the compositional range:

ZrO_2 (-325 mesh)	10 grams
Binder Solution No. 4 (40 parts by volume 85-percent aqueous H_3PO_4 plus 1 part 60-percent aqueous HF)	0.5 to 1.1 grams
Water (As needed to yield a suitable slurry)	1.5 to 2 grams

Working time of the slurry is about 10 minutes. After 10 minutes, it thickens. More water can be added to thin it but this practice was avoided because the consequence was unknown. Coatings can be applied by spraying, dipping, pouring, or troweling; they are cured at room temperature, 150 F, and 600 F for 1 hour each.

A significant change in state-of-the-art formulations in the phosphate-bonded ZrO_2 system was made. H_2PO_3F, which is the binder in the state-of-the-art formulation, was replaced by H_3PO_4 plus a small amount of HF. This change eliminated the highly corrosive nature of the existing slurry, which was completely unacceptable for this program, and simplified the chemical system for systematic studies of reactions and application variables.

The performance evaluation and the optimum slurry formulations were arrived at primarily by arc-plasma jet tests and secondly through other useful laboratory tests. For the arc-plasma jet test, coatings from 2 to 5 mils thick were applied on Hastelloy-X tabs measuring 1-1/2 inches by 4 inches by 0.015 inch thick. These coated tabs were supported in a picture-frame fixture in which cooling water was flowed on the uncoated backside, and the coating was exposed to an arc-plasma jet on the front side. Because a nucleate boiling condition existed in the coolant, the backside surface temperature never rose to more than about 400 F, even when the coating temperature was driven to the melting point of CaO-stabilized ZrO_2, 4625 F. Thus, a severe temperature gradient, near that of the reference conditions, existed during these tests. Severe thermal shocks were obtained by manually moving the specimens in and out of the arc-plasma jet with a rapid lateral motion. Arc-plasma jet test results of coatings 5 mils and less in thickness, plus pertinent coating properties, are listed below:

Arc Plasma Jet Tests

Conditions

Surface Temperature, F	to 4100
Temperature Gradient, F/in.	$\sim 10^6$
Thermal Shocks	25
Total Time, minutes	>5

Results

No Failures - no spalling
no melting
no cracking
no erosion

Properties of Phosphate - Bonded ZrO_2 (600 F Cured)

Hardness	could not be scratched with a blunt steel probe
Surface Roughness, μ in. rms	100
Flexual Strength (of cast bars), psi	to 4000
Density (of cast bars), gm/cm^3	3.4
Theoretical Density of ZrO_2, gm/cm^3	5.6
Thermal Diffusivity at 1800 F, cm^2/sec	0.002
Efficiency of Thermal Protectiveness	Similiar to phosphate-free ZrO_2

Calibration studies and thermal diffusivity measurements indicated that the degree of thermal protection of the phosphate-bonded ZrO_2 coating was similar to that of CaO-stabilized ZrO_2. A coating thickness of 3.5 mils, then, should provide the design thermal resistance.

All of the arc-plasma jet tests were on specimens that were prepared by grit blasting before the coating was applied. Adherence of coatings on grit-blasted Hastelloy-X substrates was satisfactory, but it was predominantly of a mechanical nature. Subsequently, other methods for providing adherence were evaluated in thermal shock, tensile, and flexural types of adherence tests. Ranking of selected methods of preparing the Hastelloy-X substrate for increasing adherence was, listing the best first:

1. A base layer of a commercial, high-temperature glass coating
2. A base layer of melt-sprayed metal
3. Grit blasting or chemical etching

4. Oxidation

5. Cleaned, as-received surface

Bonds that were developed by the methods used in 1 and 2 above were stronger than the cohesive strength of the coating. These techniques for developing strong adherence may not be amenable with fabrication process of a large thrust chamber, however.

The CaO-stabilized ZrO_2 in the phosphate-bonded ZrO_2 coating partially destabilized at an intermediate temperature over 2700 F, but not at 4000 F. This behavior could pose a potential problem because, although it did not affect performance in the arc-plasma jet environment, it could affect coating performance in rocket engine service depending on temperature/time history. The substitution of other stabilizing agents for CaO appears quite feasibile, if this problem proves to be real.

DISQUALIFIED COATING SYSTEMS

All other coating systems were inferior to the phosphate-bonded ZrO_2 system, based on arc-plasma jet and other appropriate laboratory tests. As soon as a coating system was definitely shown to be inferior, it was dropped from contention; hence, it remains possible that detailed development of certain of these could result in competitive behavior, in time.

Binders

Of the four binder systems that were evaluated, H_2SiF_6 and $Th(NO_3)_4$ provided no bonding. The water-soluble potassium silicate glass imparted high strength to coating systems, but these systems afforded poor resistance to thermal shock and poor thermal stability at 4000 F. Phosphate binder provided the best coating systems. Strengths reported in the literature for systems bonded with H_2SiF_6 originated from the phosphate content in a small amount of $NH_4H_2PO_4$ which had been added to these systems for other reasons. $Th(NO_3)_4$ provided green strength to ThO_2-based coating systems at low temperatures, but not after it was decomposed at about 1000 F.

Phosphate-Bonded ThO_2

Most of the phosphate-bonded ThO_2 specimens performed very poorly in arc-plasma jet tests. One particular formulation, in contrast, performed well in three arc-plasma jet tests. Although this system showed promise, it was dropped from consideration in favor of the more successful phosphate-bonded ZrO system because:

1. This cementetiously bonded system required more developmental efforts.
2. ThO_2 powder is 10 times more expensive than ZrO_2, slightly toxic and radioactive, and unavailable in as many varieties as ZrO_2 powders (e.g., particle size distribution, purity, and fused or sintered derived).
3. Coating properties and performance were highly dependent on the nature of the raw material, whereas this was not the case for ZrO_2 systems which tolerated a wide range of ZrO_2 powders.

Remaining Systems

All remaining coating systems were significantly inferior in strength, thermal stability, and/or resistance to thermal shock. These systems included:

Phosphate-Bonded $BaZrO_3$
Phosphate-Bonded HfO_2-Rich Mixed Oxides
Silicate-Bonded ZrO_2
Silicate-Bonded $BaZrO_3$
Silicate-Bonded HfO_2-Rich Mixed Oxides

TASK II PROCEDURES

SPECIMEN PREPARATION

Slurry Preparation

Slurries of candidate coating systems were prepared initially in small quantities. Binder solutions were always premixed with the water addition before they were mixed with the ZrO_2 powder. Undiluted binder solutions were not added directly to dry powders because reaction was too rapid in most cases to allow adequate mixing. Weighing was to an accuracy of ±0.01 gram.

As soon as the binder was added, the slurry was vigorously mixed, manually, for at least 1 minute. Although more mixing might have been desired, time was limited in some systems because of chemical reactions that occurred in the slurry. Because the consequences in resultant coating properties of allowing these reactions to occur was unknown, mixing time was limited so that the slurry could be applied to the substrate before any appreciable reaction took place. Thus, specimens were prepared from fresh slurries that were never more than a few minutes old.

This same procedure and sequence was used later in the program when larger batches of phosphate-bonded ZrO_2 were prepared. Substrates were always prepared ahead so that even when a 100-gram batch of slurry was prepared, it was applied to the specimen substrates in less than 10 minutes.

Slurry consistency, or viscosity, was adjusted by the solid-to-water ratio. Adding more water to dilute thick slurries was satisfactory. The only disadvantage of excess water might be when chemical bonding occurs before the water is evaporated. In such a case, coating porosity might be higher than otherwise desired. For this type of screening test, however, this possibility and its consequences seemed minor. Electrolytes or control of chemical reactions was not used to adjust slurry consistency. Time did not allow such a systematic study using these techniques on the large number of experimental slurries that were evaluated.

Substrate Preparation

All Hastelloy-X substrates were cleaned thoroughly before any coating was applied. Substrates were degreased in acetone or trichlorethylene, then rinsed, first in distilled water and finally in ethanol to facilitate drying and to prevent the deposition of the film left by either water or acetone.

Mechanical bonding of coatings to Hastelloy-X was found to be generally desirable, because chemcial bonds in most cases were poorly developed. Thus, roughening the substrate by grit blasting was a standard practice before coatings were applied to it.

Precise quality control of grit blasted substrates was not possible. Because a coarse -20 mesh alumina powder had to be used to roughen the Hastelloy-X sufficiently, high air pressure was required to propel the alumina grains fast enough to penetrate the hard Hastelloy-X surface. Use of an air pressure of 60 psi created a very rough, uniform substrate condition, but the 0.015-inch-thick Hastelloy-X sheet stock bowed outward significantly (toward the grit blasting nozzle) because of the cold work on the one side of the thin sheet stock. To reduce bowing, the air pressure was regulated as low as possible (the pressure gage indicated 5 psi, but it was not accurate at this level), and degree of grit blasting was kept to a minimum. The result was that surface roughness was inconsistent: It varied between 150 and 220 microinches rms. Moreover, distortion could not be prevented completely, even under the mildest grit blasting conditions. Distortion was kept to a minimum by grit blasting a large sheet, usually 4-1/2 inches by 4-1/2 inches, and then cutting smaller specimens from the flatter portions (usually in the center) of the larger sheet.

A number of techniques were evaluated for eliminating distortion of the Hastelloy-X sheet stock due to grit blasting but none was successful. These unsuccessful techniques included:

1. Holding the Hastelloy-X sheet stock against a thick backup plate during grit blasting using cement, solder, or vacuum

2. Use of soft and elastic backup plates
3. Holding over a concave backup plate
4. Use of no backup plate
5. Bending concave before grit blasting
6. Grit blasting a small portion of the total surface at a time
7. Grit blasting both sides
8. Annealing the bowed specimen while it was clamped flat, after grit blasting

Slurry Application

Slurries were applied to Hastelloy-X substrates initially by dipping or pour-coating, depending on specimen size. Hastelloy-X specimens 2 inches long or less were dipped into the slurry, and larger specimens were coated by pouring the slurry over the specimen. Thickness was adjusted by the drain angle of the slurry and/or by shaking or tapping off excess slurry. This procedure was satisfactory for initial screening, but thickness control was difficult.

Spray coating was adopted as a standard application technique after the initial screening tests. Spraying was accomplished using thinner slurries than those used for pour coating and dipping. A small commercial air-pressure spray gun was used.* Slurry capacity in the spray gun was 150 milliliters, but quantities as small as 30 milliliters were conveniently used by reducing the volume capacity with a small polyethylene container. Bottled nitrogen gas was used to pressurize the gun. Specimens were sprayed in a vertical or slanted position, and then laid flat before the slurry dried so that thickness was relatively uniform.

FLEXURAL STRENGTH AND DENSITY MEASUREMENT

Specimens for measuring flexural strength were bars, 1/4 inch by 1/4 inch by 1 or 2 inches, cast in Teflon molds using slurries with relatively thick consistencies. Drying and curing schedules were much slower than for thin coatings to reduce cracking in the bars. Bars were removed from the Teflon molds for curing above 300 F.

---

*Model 15, Binks Manufacturing Company, Chicago, Illinois

One- and 2-inch bars were broken using 3- and 4-point loading, respectively, at ambient temperature. Density was calculated from the dimensions and weights of the bars before breaking.

ADHERENCE TESTS

A good test for adherence was required for evaluating design features and process variables intended to promote better adherence. Satisfactory tests for glass and enamel coatings on metals, which are described in the literature and in ASTM publications, have been in use for many years. Adherence tests for crystalline ceramic coatings on metals, on the other hand, are reported infrequently in the literature, and the particular test method and reported data are useful only for evaluating the coating specified in each report. That is to say, adherence tests for crystalline ceramic coating/metal systems are not standard, and a single method of testing is not completely satisfactory for all systems or, for that matter, for any one system. The ASTM Committee for evaluating and defining methods for testing high-temperature coating/metal systems has been able to recommend for qualified use only one method of testing, a tensile adherence test. But this adherence test alone was insufficient for evaluating adherence of coatings on this program. Consequently, three different methods of testing adherence were used. These methods were expedient in that only small, simple specimens and easy testing procedures were required. Although these tests were convenient, and comparative rather than absolute, they provided meaningful data as shown from the results reported in the section on phosphate-bonded ZrO_2 coatings and in Appendix B. The methods were (1) bend, (2) thermal shock, and (3) tensile tests.

Bend Test

The bend test consisted of bending a coated Hastelloy-X tab, 1/2 inch by 2 inches by 0.015 inch thick, around progressively smaller mandrels. Specimens were bent such that the coating was on the convex side, in tension, and mandrel diameters were 4-1/2, 3-1/2, 2-1/2, 2, 1-1/2, 1 and 3/4 inches. Bending around smaller mandrels was not practical because the total portion of the coated area that was flexed decreased and the ends of the specimen eventually touched, making a complete bend impossible. Also, bending around mandrels, particularly with a diameter less than 3 inches, required a special technique to avoid crimping. One end of the specimen was held firmly with the thumb while the fingers of the other hand bent the specimen around the mandrel gradually starting nearest the fixed end.

A second procedure was used for coatings that did not fail using the above procedure. Coated specimens were alternately bent back and forth, ten times over progressively smaller mandrels. The coating was thus cycled in tension and compression. This was a very severe test because the coating was crushed on the compressive cycle. Mandrels were covered with masking tape and cleaned after each time that the coating touched the tape to protect the coating surface during testing. Loose coating material was removed by rubbing the specimen surface, and cracks and edges of broken coatings were pried up with a fingernail. Reasoning was that any coating that could be removed this easily was practically nonadherent. This procedure was referred to as bend test type B, whereas the former bend test was referred to as type A.

These tests were simple and yet provided useful information. Most importantly, they showed the condition of the interface after the coating had been broken off. A clean metal substrate indicated a bonding failure, whereas a metal substrate covered with an adhering film or fragments of the coating indicated strong bonding.

Thermal Shock Test

In the thermal shock test, coatings were made to fail by thermal cycling at progressively higher temperatures. Coatings were stressed due to the mismatch in thermal expansion with the Hastelloy-X substrate. Although temperature levels were much less than the service temperature, 4000 F, stresses due to the expansion mismatch in this test can be greater than those under service conditions because the specimens were heated isothermally. Under service conditions, the coating-metal system is heated under a temperature differential such that the higher expansion Hastelloy-X is at lower temperatures while the lower expansion ceramic is at higher temperatures. Test specimens were Hastelloy-X tabs, 1/2 inch x 2 inches by 0.015 inch thick, coated on one side.

The coated tabs were cemented in a vertical position to a depth of 1/4 inch in a refractory brick. An entire series of test specimens being compared were cemented in the same brick (up to 50 specimens), so that test conditions were the same for all specimens. An identical but smaller brick containing a thermocouple, placed beside the brick containing the specimens, was used to monitor test temperature. Specimens were heated 15 minutes in a muffle furnace (long enough to reach thermal equilibrium) and then removed from the furnace and cooled in front of a large fan. The first thermal cycle was from ambient to 700 F to ambient temperature. Each following cycle was 100 F higher than the last. Cycling was continued until 50 percent or more of the coating spalled. Loose sections of coatings were rubbed and picked off.

Specimens were easy to prepare, and the test was relatively reproducible. Another advantage was that handling of specimens was avoided. Variations in specimen thickness were accounted for by plotting thickness vs temperature from which coatings failed. Initial studies, which were made to determine the validity of this test procedure (Appendix B), showed that failure temperature was relatively independent of coating thickness when thickness was 10 mils or greater. Also, failure of these thicker coatings was by an adherence mode, whereas failure of thinner coatings was by a cohesive mode. Cohesive failure of the coating was less useful for interpreting degree of bonding of the coating to the metal substrate. Consequently, test specimens were coated with a thickness greater then 10 mils.

"Cohesive" failure was recorded when the exposed metal substrate under the spalled coating was covered with more than 75 percent of strongly adherent fragments of coating (Fig. 1). "Adhesive" failure was defined when the exposed metal surface was covered with less than 25 percent of adherent fragments.

Tensile Test

The tensile test consisted of applying the coating on one side of a thick 1-inch-diameter, Hastelloy-X disc, epoxy bonding the coated disc between two mandrels that fit a tensile test machine, and then pulling the coating off in a standard tensile test.

This test procedure has several limitations for this application. Results of tensile tests on brittle, porous materials are highly dependent on the way in which specimens are mounted and on the penetration depth of the epoxy that is used to attach the coated side to the mandrel. The coated specimen must be mounted exactly perpendicular to the direction of pull and exactly parallel to the surfaces of the adjoining mandrels, and the epoxy cannot be allowed to penetrate the coating near the metal substrate.

ARC-PLASMA JET TESTS

Arc-Plasma Heating

Rocket engineers recognize that the only truly valid test for heat-barrier coatings designed for service in a rocket engine environment is test firing in an actual rocket engine under the conditions in which the coatings are expected to operate. Testing an entire series of developmental coatings in rocket engines is not practical, however, from the standpoint of

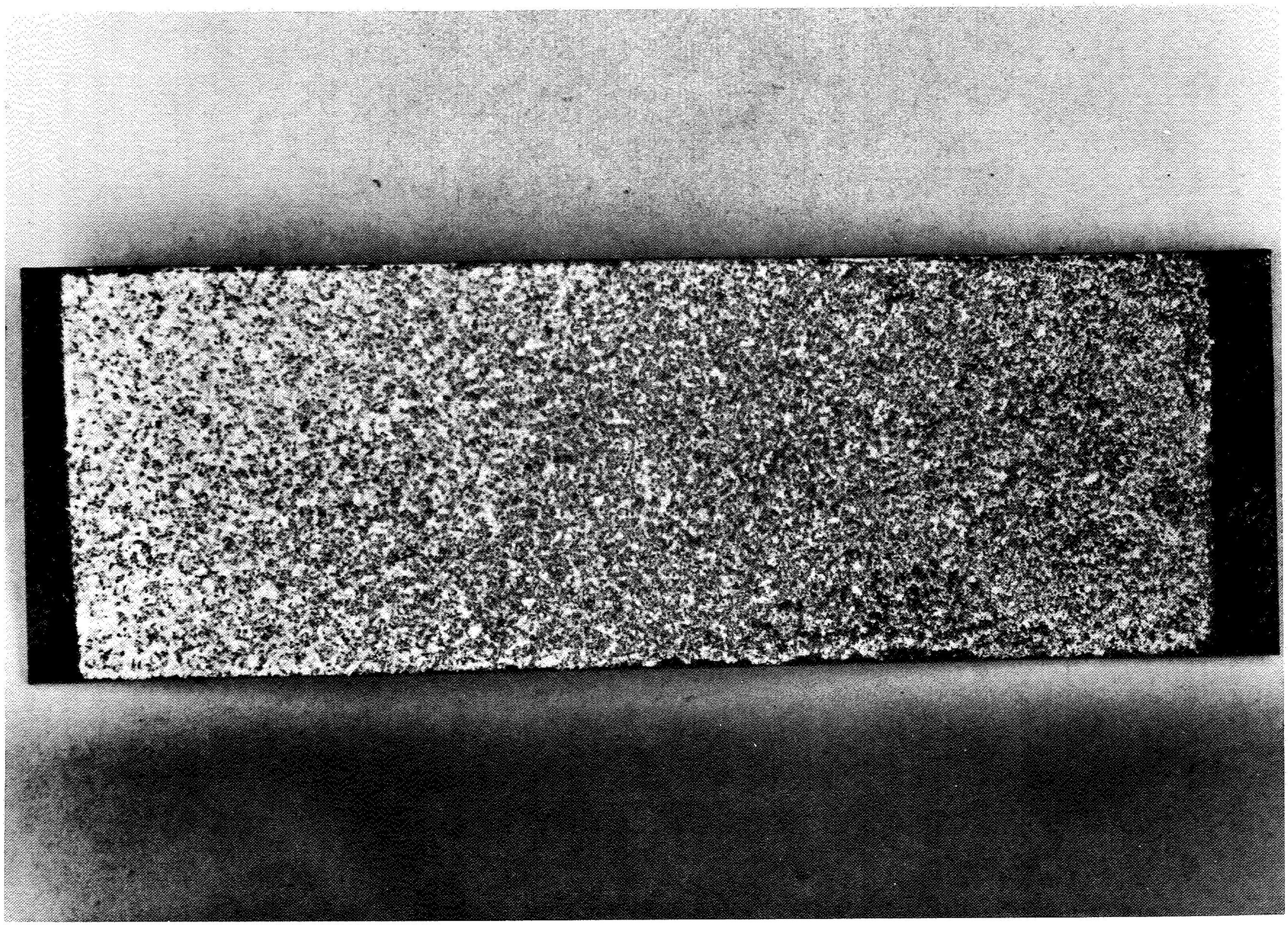

5AG13-12/10/68-C1C

Figure 1. Adherence Specimen Showing Cohesive Failure (Magnification X5)

the time and cost involved, A satisfactory screening test must be used to evaluate coatings so that only a few of the best formulations actually need to be tested in a rocket engine.

Selection of a practical yet meaningful screening test requires a compromise among several factors. The test must simulate as many as possible of the environmental conditions in the thrust chamber. Heat flux, gas composition, shear forces due to gas/wall momentum transport, mechanical constraints and loads, and heating and cooling rates are among the environmental characteristics of the engine which ought to be simulated. It is not possible to simulate all of these conditions adequately in one simple test. Short of actual rocket engine firings, the best kind of screening test available makes use of a high-pressure d-c arc-plasma jet. The arc-plasma provides (1) test temperatures high engough to melt and/or vaporize any material, (2) heat fluxes over a wide range which includes and substantially exceeds 20 Btu/in.^{2}-sec, (3) heating rates of 10^4 F/sec and higher, and (4) reducing, neutral, or oxidizing test atmospheres. Arc-plasma jet testing is also simple and expeditious. In a single working day, dozens of tests can be made by two technicians using inexpensive test hardware.

The only significant drawbacks in testing with an arc-plasma jet are the small size of the heated area on the test specimen and the low shear forces generated by the gas/wall momentum transport as compared with those in an actual thrust chamber. The approximate heated area of the jet produced by conventional arc-plasma guns is a circle about 1/4 inch in diameter. Temperature distributions parallel to the coating surface and restraint conditions imposed on the coating are, therefore, different in this small heated area compared with those in a large heated area such as the wall of a thrust chamber. The resistance of coatings to the shear forces of the high-velocity gases in a rocket engine cannot be adequately tested. In spite of these drawbacks, however, arc-plasma jet heating is nonetheless the most economical, expeditious, and meaningful method of screening coating materials available.

A temperature drop across the coated specimen was achieved by water-cooling the backside (uncoated side) while the coated side was heated with the arc-plasma jet. Because a nucleate boiling condition existed on the back side, the cooled side of the substrate never rose to more than 50 F above the saturation temperature of the coolant water, nominally 300 to 400 F at the particular water pressure used for cooling, 40 to 60 psi, (Ref. 12). Had film boiling occurred, the surface temperature would have immediately risen to above the melting point of Hastelloy-X (Ref. 13 and 14). Metallographic studies of sectioned Hastelloy-X substrates that had been coated and tested in a variety of arc-plasma jet tests showed no evidence of grain growth or other microstructural changes indicative of heating above the design temperatures.

Simultaneously, on the front side, the coating surface temperature could easily be driven above the melting point of all materials tested (i.e., above 5600 F). All reported surface temperatures are uncorrected disappearing-filament optical pyrometer temperatures, unless otherwise stated.

The arc-plasma gun was always positioned 1 inch from the specimen, and heat flux was regulated by arc amperage. Argon at a flowrate of 1 scfm was used as the arc-plasma gas, and power settings varied from 200 to 500 amperes at about 28 to 30 volts. Oxygen was added through the powder feed port of the arc-plasma gun during special tests.

Specimen and Holding Fixture

Coatings to be tested were applied on one side of and to within 1/8 inch of the edges of Hastelloy-X coupons, 1-1/2 inches wide by 4 inches long by 0.015 inch thick. During testing, the coated specimen formed the front face of a box in which water was flowing at a rate sufficient to keep the cold side at the saturation temperature of the water. The specimen was held to the box, or holding fixture, by a copper picture frame (Fig. 2). Another copper frame that was sandwiched between the specimen and a steel backup plate formed the coolant water channel. Coolant water was fed in and out of the channel through 3/8-inch-diameter steel tubes welded into and perpendicular to the steel backup plate. Water pressure and flowrate were measured at the inlet side, whereas water temperature was measured

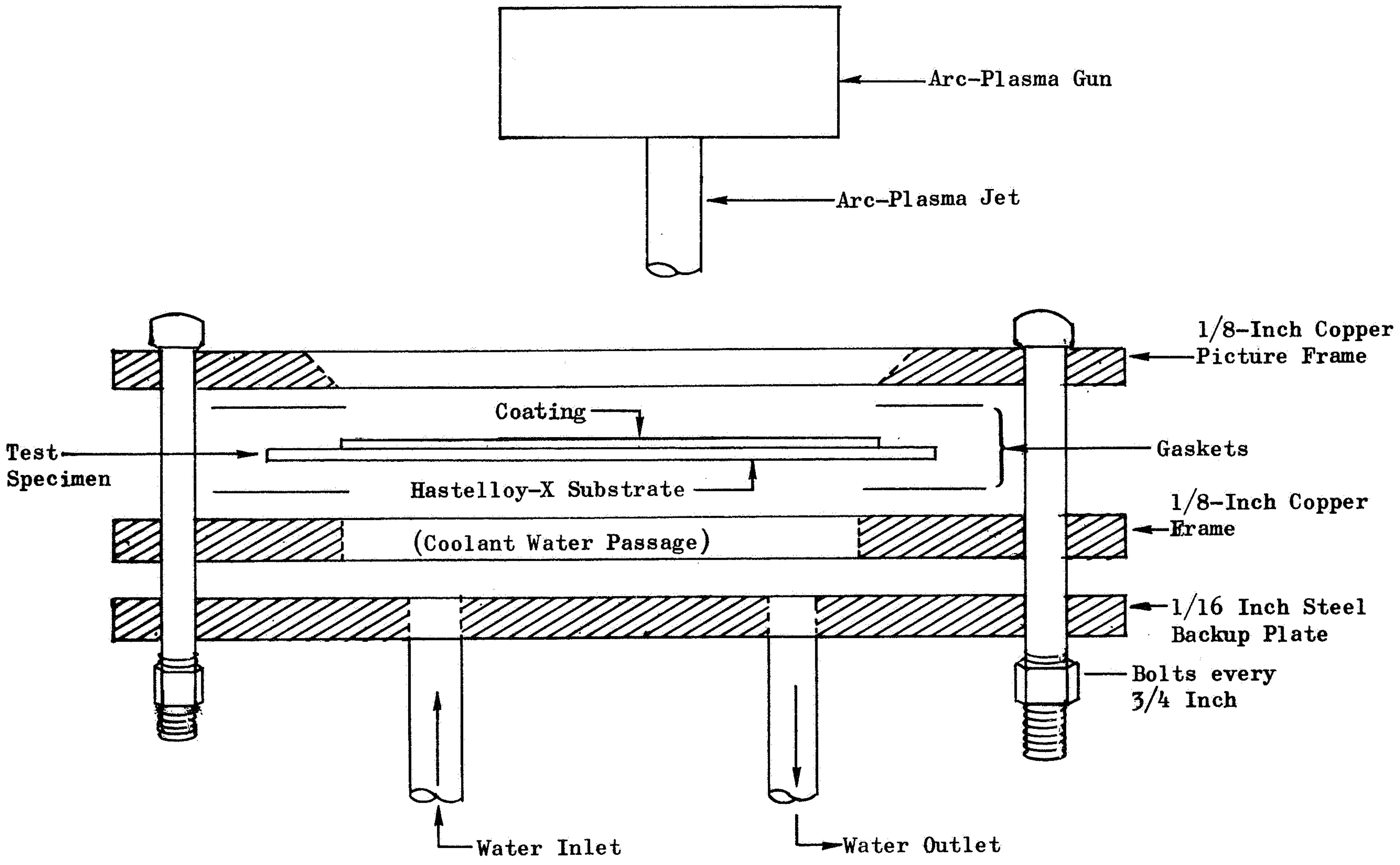
Arc-Plasma Gun
Arc-Plasma Jet
1/8-Inch Copper Picture Frame
Coating
Test Specimen
Gaskets
Hastelloy-X Substrate
1/8-Inch Copper Frame
(Coolant Water Passage)
1/16 Inch Steel Backup Plate
Bolts every 3/4 Inch
Water Inlet
Water Outlet

Figure 2. Exploded View of Arc-Plasma Jet Test Fixture

at the outlet side. The specimen was large enough for at least six tests, obtained by positioning the fixture with respect to the fixed arc-plasma gun.

Testing Sequence

Specimens, held in the test fixture, were swung laterally into the arc-plasma jet. To visual observation, heating appeared instantaneous. The specimen was then tested at steady-state for 3 minutes while the surface temperature was obtained with an optical pyrometer and while the change in the temperature of the cooling water was recorded (Test Phase A). Then the specimen was swung in and out of the arc-plasma jet, for a few seconds in each position, to simulate heating and cooling of the coated system in a rocket engine (Test Phase B). Thermal cycling continued either until failure of the coating or through 25 complete cycles, whichever occurred first. After thermal cycling, the coolant water temperature and the coating surface temperature were again measured in a steady-state exposure to determine whether any change had occurred (Test Phase C). Because coatings which failed almost always did so during or as a result of thermal cycling, duration of the steady-state testing was not critical, particularly at the beginning of the program.

The first test on each specimen was at a low heat flux level. Usually the heat flux was first adjusted to drive the coating surface temperature to 3500 F. If the specimen survived the three test phases at this heat flux, it was repositioned and tested again in a new area at a higher heat flux level. This sequence was repeated until failure was induced. Tests at critical heat flux levels, or atypical tests, were usually repeated.

The heat flux through the coated specimens, which was calibrated by three different methods, is presented in Appendix C. Although the absolute heat flux value could not be stated with precision, it was shown that it exceeded 20 Btu/in.^{2}-sec during testing of successful coatings.

Failure Analysis

Failure of the coating during testing was recorded when the coating visibly melted, spalled, or when the surface temperature changed more than

100 F. An appreciable decrease in surface temperature indicated that the thermal resistance of the coating had decreased. This condition, which was unusual, could be caused by erosion or possibly by sintering of the coating system. A rise in surface temperature, on the other hand, was more common. Such an increase in temperature was probably due to a small increase in the contact resistance at the coating/metal interface. When the coating separated completely at the interface, it melted immediately. Calculations showed that heat transfer by radiation to the Hastelloy-X substrate was at least ten times smaller than the heat input from the arc-plasma jet, so that the thin coating would melt in a fraction of a second if the coating were separated from the substrate.

All visual changes occurring during testing were recorded. After testing, changes such as severe loss in strength or hardness, surface cracking, melting, spalling, loss of adherence, sintering, and shrinkage were also noted. A low-power binocular microscope was used to observe these changes on the coating surface. After nondestructive examination, appropriate specimens were sectioned and mounted for microscopic analysis.

Standard ceramographic mounting procedures were found unsatisfactory for preparing cementitiously coated specimens. Most of the cementitiously bonded grains in the coatings broke away during standard polishing operations. A successful procedure for preparing mounts of cementitiously coated specimens was to vacuum infiltrate at room temperature with a low-viscosity, cold-setting epoxy*. Once the cementitiously bonded grains were reinforced with the epoxy, standard polishing procedures could be used.

Heat Flux Measurement

Calibration of the arc-plasma jet test was needed to verify that coated specimens were actually tested at a maximum heat flux level of 20 Btu/in.^{2}-sec.

For a coated metal system heated at ca. 20 Btu/in.^{2}-sec heat flux by a high-intensity arc-plasma jet, such as in this program, a satisfactory method for measuring heat flux has yet to be demonstrated. Measurements of heat flux in tests similar to those performed in this program have been made using a large cold-wall calorimeter. Results using this relatively simple method can be misleading, however, when compared to tests on coated systems. Heat transfer conditions can be different in the two cases; viz., through the cold copper wall of the calorimeter and through the coated specimen that is heated to 4000 F. Reasons are:

---

*Hysol R8-038 epoxy plus Hysol 3416 hardener, Hysol Corporation of Olean, New York, Los Angeles, California, and Toronto, Canada.

1. Most importantly, the value for area that is used to calculate heat flux in the large cold-wall calorimeter is never known with precision. Because heat flux is obtained by dividing heat input per unit time by the heated area, accuracy of the calculated heat flux value is directly dependent on the accuracy of this estimated area.

2. The heat transfer coefficient across the boundary layer at the coated surface is different because the roughness of a coated surface is greater than that of a smooth copper surface. This parameter could be significant when interpreting heat transfer results of an arc-plasma jet-heated system because a very substantial temperature drop occurs across the boundary layer.

3. The coated system is radiating at 4000 F, whereas the cold wall of the calorimeter is radiating at ca. 300 F.

A seemingly simple and accurate method of measuring heat flux would be to use a heat-flux gage smaller than the diameter of the arc-plasma jet. The front face could be made of Hastelloy-X and covered with the reference heat-barrier coating. But because the diameter would have to be 1/4-inch or less, design and construction of such a device were beyond the scope of this program. Cooling the front face at 20 Btu/in.^{2}-sec, while at the same time obtaining an accurate measurement of the rise in heat content of the coolant water, would have required unique fabrication techniques and a special high-pressure water system. Even greater difficulties were confronted in considering measuring the ΔT across the thickness of the Hastelloy-X itself.

In this program, measurement of heat flux was attempted by three basic methods:

1. Calculation based on heat transfer data using the Fourier equation
2. Calorimetric measurement based on rise in heat content in the cooling water and on the estimated effective area
3. Measurement using a commercial heat-flux gage

As stated earlier, none of these methods was satisfactory and results were questionable. For this reason, interpretation and comparison of arc-plasma jet test results were based mainly on surface temperature and coating thickness rather than on the measured heat flux through the coated specimens. This way of interpreting data was valid for these screening-type tests because results were qualified according to the thermal resistance of the coating. Surface temperature was measured optically and corrected for emittance (the correction factor is discussed on page C-4).

Arc-plasma jet test conditions of the reference heat-barrier coating are shown in Table 1 . Coating surface temperature is 4000 F, coating/metal interface temperature is 1500 F, and coolant-side temperature is 400 F. Thermal resistances of the coating and metal are 140 and 60 in.^{2}-sec-F/Btu, and a heat flux of 18.5 Btu/in.^{2}-sec is required to achieve these conditions. The heat flux, coolant-side temperature, and interface temperature are slightly different from the reference rocket engine values of 20 Btu/in.^{2}-sec, 0 F, and 1200 F because of the difference in the coolants used in the two cases, viz., water and liquid hydrogen. Nevertheless, test conditions are reasonably close to those of the reference rocket engine.

These conditions were not constant during testing because thermal resistance of the heat-barrier coatings varied. Thermal resistance of the coatings (thermal resistance = thickness ÷ thermal conductivity) varied because thermal conductivity of these experimental materials systems was not accurately known, and consequently the correct design thickness could not be calculated. Thermal resistance could have varied by a factor of at least two in some cases, from specimen to specimen. Thus, if the thermal

TABLE 1

CROSS-SECTION OF HEAT TRANSFER PARAMETERS ACROSS TEST SPECIMENS

HEAT FLUX:	18.5 Btu/in.^{2}-sec	<18.5 Btu/in.^{2}-sec	>18.5 Btu/in.^{2}-sec
	4000 F	4000 F	4000 F
COATING	(R = 140 in.^{2}-sec-F/Btu)	(R >140 in.^{2}-sec-F/Btu)	(R < 140 in.^{2}-sec-F/Btu)
	1500 F	$\lesssim$1500 F	$\gtrsim$1500 F
METAL	(R = 60 in.^{2}-sec-F/Btu)	(R = 60 in.^{2}-sec/Btu)	(R = 60 in.^{2}-sec-F/Btu)
	400 F	$\lesssim$400 F	$\gtrsim$400 F
	(a) Thermal resistance of coating equals reference value.	(B) Thermal resistance of coating is more than reference value.	(c) Thermal resistance of coating is less than reference value.

resistance of a coated specimen was considerably less than the design value, 140 in.^{2}-sec-F/Btu, the heat flux under the same arc-plasma jet operating parameters as used to obtain the conditions in Table 1 (a) would be >18.5 Btu/sec.-in.^{2}, and the surface temperature would be <4000 F. Such a test would be of little value because the coating would be subjected to relatively mild temperatures and temperature gradients.

On the other hand, the arc-plasma jet could be adjusted easily to produce whatever heat flux was required to drive the surface temperature to 4000 F. Because $Q/A = \Delta T/R$, and ΔT was kept constant at $4000 - 400 = 3600$ F, a heat flux greater than 18.5 Btu/in.^{2}-sec was required when the thermal resistance of the coating was less than 140 in.^{2}-sec-F/Btu, and conversely (Table 1 (b) and (c).

Because the coolant-side temperature was relatively stable, the temperature drop across the coating was also relatively consistent for coatings with a corresponding surface temperature. Temperature "gradient," however, was not necessarily consistent because coating thickness of the various systems may have been different. Several thicknesses of each coating material were tested, however, so that enough data were provided for qualified comparisons of the different coating materials.

Comparison of coated specimens in these tests, so long as differences in test conditions were recognized, was rationalized in this way: a coating that survived steady-state conditions and thermal shocks at surface temperatures of 4000 F at a heat flux level of 15 or 25 Btu/in.^{2}-sec would more than likely survive the same conditions at 20 Btu/in.^{2}-sec. Also, a coating that spalled repeatedly or melted when the surface temperature was 3500 F was more than likely to fail at a heat flux of 15, 20, or 25 Btu/in.^{2}-sec. Moreover, the large difference in test results made comparison of test results easy: one coating system (phosphate-bonded ZrO_2) performed far better under all test conditions than all of the other coatings that were tested. If all test conditions exactly matched the reference engine parameters, that is, if heat flux was precisely 18.5 Btu/in.^{2}-sec and the coating thickness was adjusted to drive surface temperature to exactly 4000 F in all cases, results and conclusions based on these tests would have been the same.

A description of the calibration tests and results is presented in Appendix C .

THE PHOSPHATE-BONDED ZrO_2 SYSTEM: RESULTS AND DISCUSSION

INTRODUCTION

The performance record of phosphate-bonded ZrO_2 coatings was outstanding in arc-plasma jet tests. Specimens with coating thicknesses of 5 mils or less did not fail at steady state or during thermal shock in more than 100 tests on about 30 different specimens.*

Each test, with a few exceptions where the purpose was calibration of the test rather than performance of the coating, included 5 minutes at temperature plus 25 thermal shocks from 70 F to the test temperature to 70 F. Surface temperature during these tests was up to 4100 F. Phosphate-bonded ZrO_2 coatings did not spall, erode, corrode, or even crack under design conditions. The fact that these coatings did not crack is particularly noteworthy, because arc-plasma sprayed, graded ZrO_2/Inconel heat-barrier coatings that were tested under similar conditions in another program failed by cracking (Ref. 1). Once those arc-plasma sprayed coatings cracked, melting started at the edges and the coating eventually spalled. Yet those same graded ZrO_2 coatings have demonstrated good performance in rocket engine tests (Ref. 2). Phosphate-bonded ZrO_2 coatings, in contrast, failed only when melting was induced above 4100 F, usually at ca. 4200 F or higher. Thus, based on arc-plasma jet tests, phosphate-bonded ZrO_2 coatings were the prime candidate from early in the program.

On the other hand, most of the other coating systems selected for evaluation failed far below the design thrust chamber conditions as simulated by the arc-plasma jet tests. Some coatings of other systems cracked or spalled below 4000 F (even during steady-state phases of testing), some melted at or below 4000 F, and some cementitiously bonded systems did not show enough promise even to be tested in the arc-plasma jet. One coating system that performed well was a specific formulation of phosphate-bonded ThO_2. But, as discussed in a later section, this material has many other disadvantages compared to the phosphate-bonded ZrO_2 system.

---

*One specimen, number 58-2, was an exception; the results are discussed later in this section of the report.

A small effort was undertaken to modify the phosphate-bonded ZrO_2 system for this program. The following studies, under the limited program scope, were not intended to be completely thorough. On the contrary, they were cursory and pursued only to the extent necessary to obtain a satisfactory coating system for evaluation in the arc-plasma jet test. Experiments are described in chronological order so that the logic of the sequential studies will be apparent.

FORMULATION STUDIES

State-of-the-Art Formulation

Monofluorophosphoric acid (H_2PO_3F) has been the binder for phosphate-bonded ZrO_2 systems in state-of-the-art formulations. The cemetitious phase, ZrP_2O_7, is formed by a three-step reaction (Ref. 3):

$$4HF + ZrO_2 \longrightarrow ZrF_4 + 2H_2O \ , \tag{1}$$

$$4H_3PO_4 \longrightarrow 2H_4P_2O_7 + 2H_2O \ , \tag{2}$$

$$ZrF_4 + H_4P_2O_7 \longrightarrow ZrP_2O_7 + 4HF \ ,$$

wherein HF and H_3PO_4 are hydrolysis products in the H_2PO_3F solution.

Use of H_2PO_3F as a binder requires an addition of another ingredient, a retarding agent. The reason for a retarding agent is that the reaction between ZrO_2 and H_2PO_3F is too rapid at room temperature to allow proper preparation of a slurry and application of the slurry on hardware. Reaction time can be increased by substituting a portion of the fluorophosphoric acid by ammonium dihydrogen phosphate ($NH_4H_2PO_4$). The manner in which

$NH_4H_2PO_4$ retards the bonding reaction was not specified by previous investigators. Two major disadvantages of the state-of-the-art formulation were the corrosive nature of the high HF content of the slurry and the complexity of the bonding reaction, which made control of the system and developmental studies difficult.

Complexity of the H_2PO_3F-ZrO_2 chemical system increases when excess water is added, as when a thin slurry for spray coating is made. Anhydrous commercial H_2PO_3F actually consists of:

$$70 \text{ w/o } H_2PO_3F; \quad 15 \text{ w/o } HPO_2F_2; \quad 15 \text{ w/o } H_3PO_4$$

New species, including HF and H_3PO_4, form as hydrolysis products when water is added to the solution. Also, the ratios of the original products change. Consequently, water does not serve simply as a diluent; in fact, it changes the chemistry of the solution drastically.

The chemistry of bonding becomes even more complicated when $NH_4H_2PO_4$ is added to the H_2PO_3F-H_2O system because numerous ammonium complexes form in addition to the abovementioned species. The chemistry of these complex systems is not understood well enough to predict how much of the various species are formed by the addition of the retarder and H_2O. It is likely that the effects of water and retarder additions are due to changes in the HF and H_3PO_4 activity.

The chemistry of the system could be simplified considerably by using combinations of HF and H_3PO_4, rather than H_2PO_3F. Independent control of the respective quantities of HF and H_3PO_4 are made possible, and use of a retarder should become unnecessary.

Modifications

Three modifications of the phosphate-bonded zirconia coating system were necessary: (1) elimination of the highly corrosive nature of the H_2PO_3F

binder system, (2) change in the particle size distribution and type of the ZrO_2 grains, and (3) change in the consistency of the slurry.

Corrosion. Corrosion of metal surfaces from the excessive amount of fluoride ion in state-of-the-art formulations is unacceptable for applications involving thin heat-barrier coatings. Existing phosphate-bonded ZrO_2 slurry coating systems, which used H_2PO_3F as the main source of the bonding agent, reacted with metal substrates in a way that precluded the formation of direct mechanical or chemical bonds between the coating and metal substrate. This deficiency had sometimes been compensated for by use of large metal reinforcements, such as tack-welded screens or sine-wave shaped strips that mechanically held the thick coatings, 1/4 to 1 inch, on the substrate. Use of reinforcements for attaching the coating to the substrate was not practical in the present program because the heat-barrier coatings were too thin, 3.5 mils. Thus, tenacious adherence at the interface of the coating and metal is mandatory for coating systems that will be used as thin heat-barrier coatings where metal reinforcements are not practical.

Corrosion is unacceptable for applications involving thin coatings for another reason also. Gases evolving from reactions at the coating-metal interface would result in high porosity and bloating in the resultant coating, and both of these factors would seriously impair coating performance due to loss in strength and in efficiency of thermal protectiveness.

The corrosion problem was eliminated early in the program by substituting a mixture of H_3PO_4* and a very small amount of HF for H_2PO_3F. The best H_3PO_4 to HF ratio was about 40:1 by volume (of commercial solutions). Because only this small amount of fluoride ion was required to promote phosphate bonding of the ZrO_2 grains, it was not corrosive to Hastelloy-X surfaces. Another benefit in avoiding the use of H_2PO_3F was that complexity of the chemical system was substantially reduced. Thus, interpretation of results of parametric studies was simplified.

---

*Ozark-Mahoning Co., Tulsa, Oklahoma

ZrO_2 Grain Size. Particle size distribution of ZrO_2 grains in state-of-the-art formulations had to be changed because the prior materials were far too coarse, up to 24 mils across. These grains would settle very rapidly in a thin slurry, they could not be sprayed through a standard spray-gun nozzle, and most significantly, they were almost 10 times larger than the thickness of the coatings in this program. For this reason, all powders used in this program were passed through a 325-mesh screen. A 325 mesh screen has 1.7 mil openings.

The purpose of coarse-grained ZrO_2 filler in prior formulations was to increase the bulk density of cementitiously bonded heat shields. Increased bulk density offers two significant advantages; viz., increased strength (other factors being equal) and decreased shrinkage during service.

At the beginning of this program, a study to increase density and strength of coatings was started using selected particle size distributions from the 1 micron to -200 mesh range (Appendix D). This study was stopped because -200 mesh powder was not suitable for standard spraying equipment and practices, and because significant advantages over as-received -325 mesh ZrO_2 powder were not shown. Controlling particle size distribution in the -325 mesh powder was not attempted, mainly because it was not necessary for improving coating performance. However, selectively altering the particle size range of the -325 mesh ZrO_2 powder is still possible for improving strength and decreasing shrinkage, should it become necessary.

Shrinkage at the hot surface of the coating was minimized by selecting a ZrO_2 powder that was prepared by a fusion process rather than by a sintering process. Fused powders shrink less on heating because they are more dense to begin with and because they have less surface energy. Excessive shrinkage was not a problem in arc-plasma jet tests. This does not necessarily ensure, however, that it will not be a problem in a full-scale thrust chamber where large areas will be heated to 4000 F. The estimated thickness of the coating that reaches appreciable sintering temperatures is less than one-half of the total thickness (refer to Fig. 11b). A disadvantage of fused powders is that the fused grains offer less total surface area for chemical bond formation and that this surface is less chemically active toward the phosphoric acid binding agent than is the case for grains derived from sintering processes.

A CaO-stabilized ZrO_2 raw material* was selected for slurry formulations because it met design requirements of this program, had been used in all similar programs reported in the literature, was readily available in the desired form (viz., fused and -325 mesh), and was economical. ZrO_2 stabilized with CaO is about 1/100 as costly as material stabilized by other oxides; and the physical, thermal, and chemical properties have been reported much more extensively.

Slurry Viscosity. Consistency of the slurries that were used for the cementitiously bonded coatings in previous programs was thick (i.e., viscous). Thick slurries were required for ramming and troweling thick layers into the openings provided by wire mesh or thin metal ribbon reinforcements. Viscous slurries could not be used in this program because applied coatings had to be uniform, very thin (3.5 mil), and applied by dip-coating, pour-coating, or preferably, spray-coating techniques. These coating techniques require a relatively thin slurry consistency.

Slurry consistencies are in general controlled by changing the solid-to-liquid ratio or by use of electrolytes. Use of electrolytes was considered impractical in this case because the ionic strength is already very high (H^+, $H_2PO_4^-$), and because most suitable salts would degrade the refractoriness of the cured coating. Use of excess water was, therefore, the only technique that was used to adjust slurry consistency. Excess water in modified slurry formulations was undesirable, but not so much so as in state-of-the-art formulations where the H_2PO_3F binder was used.

---

*Zirnorite grade I ZrO_2, 325 F, Norton Company, Refractories Division, Worcester, Massachusetts.

Initial Studies

Bonding. Purpose of the following experiment was to investigate whether a HF-H_3PO_4 solution would form a cementitious bond and, if so, what proportions of each acid were required. In these series of tests, ram mixes were made by combining 100 parts by weight of -325 mesh ZrO_2 with 5 parts of selected HF-H_3PO_2 mixtures. After mixing, the ram mix was pressed into bars, 5/16 inch by 2-1/2 inches, in a steel die at a pressure of 5000 psi. Specimens were dried for one hour at 150 F and cured for one hour at 600 F. Results were:

Specimen No.	Parts By Weight ZrO_2*	Parts By Volume HF*	Parts By Volume H_3PO_4*	Flexural Strength By 4-Point Loading, psi
1	100	2.50	2.50	18
2	100	1.15	3.85	36
3	100	0.25	4.75	1360
4	100	0.12	4.88	1060

*Unless otherwise stated all ZrO_2 is -325 mesh Zirnorite I, and HF and H_3PO_4 concentrations are 60 and 85 percent, respectively.

Bonding was clearly evident when the H_3PO_4:HF ratio was large; i.e., when only a small proportion of HF was present. In fact, the highest strength was obtained when the H_3PO_4:HF ratio was 19:1 (designated Solution A). This initial experiment demonstrated that strong bonds could indeed be formed in the H_3PO_4-HF-ZrO_2 system and that only a small portion of fluoride ion was needed.

Quantity of Binder Solution. Strength of the coating system was determined as a function of the amount of solution A added to -325 mesh zirconia. After mixing the appropriate amount of each ingredient, the mixtures were pressed into bars and cured as before. Results were as follows.

Specimen No.	Weight, grams		Flexural Strength of Cold-Pressed Specimens By 4-Point Loading, psi	Flexural Strength of Cast Specimens By 4-Point Loading, psi
	-325 ZrO	Solution A		
B3	10	0.52	1360	Not Determined
B5	10	1.05	4530	Not Determined
B6	10	1.57	4040	3820

Samples B5 and B6 could not be pressed immediately after mixing because they were too fluid. Fluidity was reduced sufficiently for pressing by air drying for about 1 hour. After pressing and curing, these two samples exhibited high strength compared with sample B3. Additional bars were made by casting slurry B6 in Teflon molds. Cast specimens had almost as much strength as the pressed specimen. Pressed bars were not stronger because much of the bonding reactions had set during the 1-hour drying period before the slurry was pressed. These formulations, as such, were not useful for slurry coating, however, because they were too thick.

Water Additions. Effects of adding water to mix B6 were investigated. Compositions were:

Specimen No.	Weight, grams			Slurry Consistency
	ZrO_2	Solution A	Water	
B6	10.0	1.57	0	Paste-like
B7	10.0	1.57	0.77	Lumpy and dry; reaction
B8	10.0	1.57	1.53	Creamy; slow reaction
B9	10.0	1.57	3.14	Creamy; reaction

In all cases, the water and solution A were mixed first and then added to the powder. Unusual results were found when the water content was increased. When B7 was mixed, the mixture dried into small lumps within seconds, and an exothermic reaction was indicated because heat was given off as the slurry dried. This result was contrasted to the paste-like consistency of slurry B6, particularly because B6 originally contained less fluid. The reaction of B7 suggested that a hydrate formed.

HF Concentration. The concentration of HF in B7 was decreased to determine whether this affected the initial reaction. Compositions were:

Specimen No.	Weight, grams					Reaction	Consistency
	ZrO_2	H_2PO_3F	HF	Added H_2O	H_3PO_4/HF		
B7	10.0	1.49	0.08	0.77	19/1	Rapid, Exothermic	Thick
B10	10.0	1.49	0.05	0.77	32/1	NR	Cream
B11	10.0	1.49	0.02	0.77	65/1	NR	Cream
B12	10.0	1.49	0.01	0.77	194/1	NR	Cream
B13	10.0	1.49	0.00	0.77	--	NR	Cream

Of the above, none except B7 exhibited a rapid reaction. All the rest had a creamy consistency and could easily be troweled into molds. Thus it appeared that the initial exothermic reaction involved HF and that a sufficient amount of HF must be present for the reaction to occur.

Fluoride Concentration

A small study, which was accomplished in three phases, was made to find a satisfactory HF addition that produced strong composites, yet that allowed sufficient working time for applying the slurry on test specimen substrates.

First Phase. Slurries containing a range of fluoride concentrations (0 to 100 percent by weight of the H_3PO_4 addition) were formulated without water and pressed into 1/4- by 1/4- by 2-inch bars at 10,000 psi. These bars were then cured 1 hour or more at room temperature, 1 hour at 150 F, and 1 hour at 600 F. Flexural strength was determined on one bar of each slurry formulation using 4-point loading. One measurement of flexural strength is not enough for any degree of confidence, and, moreover, cracks were suspected in the bars as a result of drying. Thus, the low flexural strength values are not considered necessarily indicative of the true flexural strength of these materails. To obtain more data, the longest fragment of each two-inch bar was broken using 3-point loading. Strength values are comparable to those obtained using 4-point loading. These data are presented in Table 2 as slurries B23 through B31.

Specimen B28, which had a H_3PO_4:HF ratio of 52:1 and was the same as the B5 formulation, was by far the strongest specimen of this group with a flexural strength of 1790 psi. Additional specimens with the same formulation as B28 were made by both pressing and casting. The one difference, however, was that water was added to these specimens, B30 and B31. All of the specimens that were made from slurries containing water cracked and broke into several pieces during drying. Consequently, slower drying schedules were used for bars in subsequent studies.

Second Phase. The second phase of this study consisted of preparing bars that were cast using slurries with a very fluid consistency (slurries B32 through B36 in Table 2). Thus, a large amount of water was added to each formulation. The total volume of liquid was held approximately constant so that the as-cast density of each bar would be similar. In other words, as more liquid binder was added, less water was added so that the total volume of liquid was always constant. The only variable in this series of specimens was HF content, which ranged from 0 to 0.50 parts by weight per 10 parts of ZrO_2.

The highest strength value, 1750 psi, was for formulation B35 which had the smallest HF addition greater than zero. Also, a relatively high value, 1160 psi, was obtained for specimen B36 which did not contain any fluoride.

Another important property of these slurries is shelf life; i.e., the time that the slurry is usable once the ingredients are mixed together. Approximate shelf life of selected slurry compositions is listed in Table 3. From the standpoint of shelf life, slurries with very little or no HF were

TABLE 2

FLEXURAL STRENGTH OF PHOSPHATE-BONDED ZIRCONIA AS A FUNCTION OF FLUORIDE CONTENT

Phase of Study	Slurry and Specimens Identification	Slurry Composition (Parts by Weight)						Density, g/cc	Flexural Strength, psi	
		ZrO_2	H_3PO_4 (85%)	HF(60%)	H_3PO_4/HF	H_2O	$NH_4H_2PO_4$		4-Point Loading	3-Point Loading
First	B23	10.00	0.50	0.021	24/1	--	--	4.26	500	404
	B24	10.00	0.51	0.009	57/1	--	--	3.85	760	393
	B25	10.00	0.52	--	--	--	--	3.77	270	180
	B26	10.00	0.51	0.009	57/1	0.823	--	3.98	600	614
	B27	10.00	0.51	0.009	57/1	2.17	--	--		
	B28 (B5)	10.00	1.03	0.02	52/1	--	--	4.00	1790	1100
	B30	10.00	1.03	0.02	52/1	2.3	--	--	(1)	(1)
	B31	10.00	1.03	0.02	52/1	1.05	--	--	(1)	(1)
Second	B32	10.00	0.50	0.50	1/1	1.00(2)	--	--	--	(1)
	B34	10.00	0.50	0.05	10/1	1.20(2)	--	3.39	--	1540(3)
	B35	10.00	0.50	0.013	38/1	1.20(2)	--	3.41	--	1750(3)
	B36	10.00	0.50	--	--	1.20(2)	--	3.59	--	1160(3)
Third	B37	10.00	0.488	0.013	38/1	(2)	0.011	3.39	--	1500(3)
	B38	10.00	0.456	0.05	9/1	(2)	0.43	3.27	--	608(3)
	B39	10.00	--	0.013	--	(2)	0.586	3.08	--	463(3)
	B40	10.00	--	0.05	--	(2)	0.586	3.15	--	390(3)
	B41	10.00	--	0.125	--	(2)	0.586	2.79	--	116(3)

(1) Broke during drying.

(2) Enough water was added to yield a pourable slurry and to maintain approximately constant volume of liquid content (water plus acid) in slurries B32 through B41.

(3) Highest value of two specimens.

TABLE 3

EFFECT OF FLUORIDE CONTENT ON THE SHELF LIFE OF PHOSPHATE-BONDED ZIRCONIA SLURRY COMPOSITIONS

Slurry	Parts By Weight of H_3PO_4 per 10 Parts ZrO_2	Weight Ratio of H_3PO_4 to HF	Degree of Chemical Reaction	Approximate Working Time, minutes
B30	1.03	52/1	Slight	5
B31	1.03	52/1	Slight	5
B32	0.50	1/1	Significant	0
B34	0.50	10/1	Slight	3
B35	0.50	38/1	Slight	10
B36	0.50	No HF	None	10 to 30
B37	0.50(1)	38/1	Slight	1-1/2
B38	0.50(2)	10/1	Slight	1-1/2
B39	0.50(3)	38/1	None	60
B40	0.50(3)	10/1	Slight	10
B41	0.50(3)	4/1	Slight	10

(1) 0.011 parts were added as $NH_4H_2PO_4$

(2) 0.043 parts were added as $NH_4H_2PO_4$

(3) An equivalent amount of phosphate was added as $NH_4H_2PO_4$

best. Slurry B36 without HF had a shelf life of 10 to 30 minutes, while slurry B35 with a 38:1 weight ratio of H_3PO_4 to HF had a shelf life of 10 minutes. After 10 minutes, the slurry emitted a small amount of heat and stiffened to a thick paste. Ten minutes working time is too short to be amenable to most production processes, but it was an adequate duration for preparing experimental specimens.

When it becomes necessary, there are several techniques that can be used to make this formulation usable in production processes. The third phase of this study explored one method of prolonging shelf life, with negative results.

It was concluded that a small amount of HF in the slurry formulation (about a 40-to-1 weight ratio of 85 percent concentration H_3PO_4 to 60 percent concentration HF) gave the best results from the standpoint of (1) shelf life of the slurry, and (2) ambient temperature flexural strength of the material after it was cured.

Third Phase. As was observed in Task I, a technique for increasing shelf life in the ZrO_2-H_2PO_3F system is to substitute a portion of $NH_4H_2PO_4$ for H_2PO_3F. This approach was studied in the H_3PO_4-HF-H_2O-ZrO_2 system by first replacing a small amount of H_3PO_4 with NH_4HPO_4 (slurries B39, B40, and B41). In each case, selected HF additions were used (Tables 2 and 3).

The only formulation that resulted in a cured bar with any appreciable strength was B37 (15,000 psi, Table 2) which had only a very small amount of $NH_4H_2PO_4$. But this slurry formulation was unsatisfactory because shelf life was shortened from 10 to 1-1/2 minutes (Table 3). Complete substitution of $NH_4H_2PO_4$ for H_3PO_4 did not result in any improvement either; in fact, it was deleterious because strength values were very low, less than 500 psi. Bars made with slurries B40 and B41 were soft, and bars made from slurry B39, although they were hard, were very porous because of gases that were given off during drying and curing. Thus, the use of $NH_4H_2PO_2$ offers no advantage in the H_3PO_4-HF-H_2O-ZrO_2 system.

Phosphate Concentration

General. Effect of phosphate binder solution concentration on selected properties of the coating was studied. Phosphate concentration is important because too little provides inadequate chemical bonding while too much impairs high-temperature strength. The range of phosphate binder additions studied included both extremes, 0.1 and 10.0 parts by weight of binder solution No. 4 (a 40:1 volume ratio of H_3PO_4 to HF) per 10.0 parts of ZrO_2 (Table 4).

In sum, the following studies showed that best phosphate additions were between 0.5 and 1.1 parts binder solution (BS) No. 4 and 10.0 parts ZrO_2. Bars and coatings made from slurries using this formulation were hard and strong. Strength and hardness was maintained after annealing at all temperatures with one key exception. Materials that were made from slurries containing 1.1 parts BS No. 4 per 10.0 parts ZrO_2 became friable after annealing at 2700 F for 5 minutes. Longer annealing time resulted in high strength once again because of sintering. The reason for the short-lived friable nature is caused by the phase change in the ZrO_2 grains. ZrO_2 is destabilized by the presence of phosphorous at ca. 2700 F.

Lowest phosphate addition (0.1 part BS No. 4 per 10.0 parts ZrO_2) produced materials after curing with low strength at room temperature. After annealing at temperatures above ca. 2700 F, however, sufficient strength was produced in these materials because of sintering. High-range phosphate additions (>1.1 parts BS No. 4 per 10.0 parts ZrO_2) produced weak materials because of high porosity. Bars made from slurries containing excess phosphate binder solution were slow to dry and cure. They were soft even after drying at room temperature for 3 days and curing at 240 F for another 3 days. After curing at 600 F for 1 hour, these materials became hard but strength was impaired by microcracks and high porosity. After annealing at high temperatures, $\gtrsim$3750 F, strength deteriorated and the materials became bloated and friable.

Evaluation of these slurries was based on the visual, microscopic, X-ray diffraction, and electron-beam microprobe X-ray analyses of bars that were subjected to three tests: (1) thermal stressing of bars using the arc-plasma jet, (2) annealing bars under isothermal conditions, and (3) flexural strength measurement at room temperature.

Test Bars: Fabrication and Evaluation. Test bars measuring 1/4 inch by 1/4 inch by 2 inches were made for evaluation of selected properties by casting thin (i.e., low-viscosity) slurries in Teflon molds. Thin slurries were used so that the chemical environment was the same as it would be in sprayed coatings. Unfortunately, when excessive amounts of fluids (either water, binder solution, or mixtures of both) were used, satisfactory test bars were very difficult to obtain. Shrinkage during drying and curing was so large that many micro and macrocracks formed in the bars.

Because only 1-inch, rather than 2-inch test bars were needed for testing, the 2-inch bars were notched in the center so that they cracked at the notch first during drying. However, too many other cracks also occurred for these bars to be useful for measuring strength. Slow drying and curing schedules reduced, but did not eliminate, the formation of cracks in the test bars. Bars were dried at least 1 day in an enclosed container where initial drying was very slow because of the high relative humidity; at least 1 day exposed to ambient air; 2 hours at 100 F, 2 hours at 180 F, 2 hours at 212 F, and 1 hour at 600 F. Bars made from formulations that contained excess binder solution (B47 and B48) were heated even more slowly, 4 days at room temperature, 3 days at 240 F, and 1 hour at 600 F.

Although strength could not be measured because all bars cracked, relative hardness did provide some useful information. Results are summarized on the following page.

Slurry No.	Parts By Weight Binder Solution No. 4 per 10 Parts ZrO_2	Relative Hardness
B43	0.1	Soft, easily scratched with fingernail.
B44	0.5	Bottom of bar: soft, scratched with fingernail. Top of bar: hard, barely scratched with knife blade.
B45	1.1	Hard, barely scratched with knife blade.
B46	1.25	Hard, barely scratched with knife blade.
B47	4.3	Hard, barely scratched with knife blade.
B48	10.0	Hard, barely scratched with knife blade.

Based on this information, 0.1 part binder solution per 10 parts ZrO_2 is too little, whereas 0.5 part is borderline in providing adequate bonding. Bars made from the slurry with 0.5 parts of binder solution (B44) were hard on the surface but soft inside because the binder solution migrated to the surface before it reacted with the ZrO_2 during drying and curing. Although segregation of the binder would be less likely in a 0.0035-inch-thick coating than in the 1/4-inch-thick test bar, the 0.5 part binder level was considered borderline. At the high end of the range, 4.3 and 10 parts binder solution constitute too much liquid. Slurries with this much liquid shrank excessively when cured and were excessively porous and susceptible to cracking. Thus, based on these results, the best binder concentration was between 0.5 and ca. 3 parts of binder solution No. 4 per 10 parts by weight of ZrO_2.

Thermal Stressing of Bars In the Arc-Plasma Jet. Test bars were subjected to a thermal stress test by placing them about 1 inch away from the front of the arc-plasma gun. Comparative analysis was not possible because the microcracks in the test bars caused premature thermal shock failure in most tests. Analysis of individual results, nonetheless, was informative. Results showed that these phosphate-bonded test bars made from slurries

B44 and B45 were refractory and resistant to thermal shock. Temperature in the molten area, which was measured with the optical pyrometer, was never less than 4100 F and more often about 4550 F.

The key point was that the test bars withstood the thermal stress which was severe because of the intensity of the arc-plasma jet and the low thermal conductivity of the zirconia-based material. As the material melted and formed a molten pool where the jet impinged on the surface of the bar, the molten material blew away from the center of the heated area. As it blew away, it solidified in the outer periphery of the test area. Thus, the test area looked like a floral cup with a diameter of about 1/4 inch, the outer petals being frozen droplets of zirconia (Fig. 3). The center of the flower eroded to a depth of as much as 1/8 inch before the bar broke as a result of the force of the arc-plasma gases. Most refractory ceramic hardware breaks immediately into many fragments when heated in this manner by the arc-plasma jet.

Thermal Stability.

Procedure. Thermal stability of the compositions listed in Table 4 was determined by annealing bars at selected temperatures and then examining the annealed bars by optical and X-ray diffraction techniques. Fragments of bars, about 1/4 to 1/2 inch long, were set on ZrO_2 bricks for annealing. Annealing at 1850 F and below was in an electrically heated muffle furnace, while annealing at higher temperatures was in a gas-fired ZrO_2 muffle furnace. The atmosphere in both cases was oxidizing. Annealing temperatures were selected at critical levels: 4000 and 3750 F because these were upper service temperatures; 2700 F because the cementitious phase was reported to change from ZrP_2O_7 to $(ZrO)_2P_2O_7$ + P_2O_5 (Ref. 4) and because CaO-stabilized ZrO_2 was reported to destabilize at this level (Ref. 5); 1850 and 1000 F because these were about equally spaced between the next higher temperature, 2700 F, and the curing temperature, 600 F. Annealing times were 5 and 30 minutes.

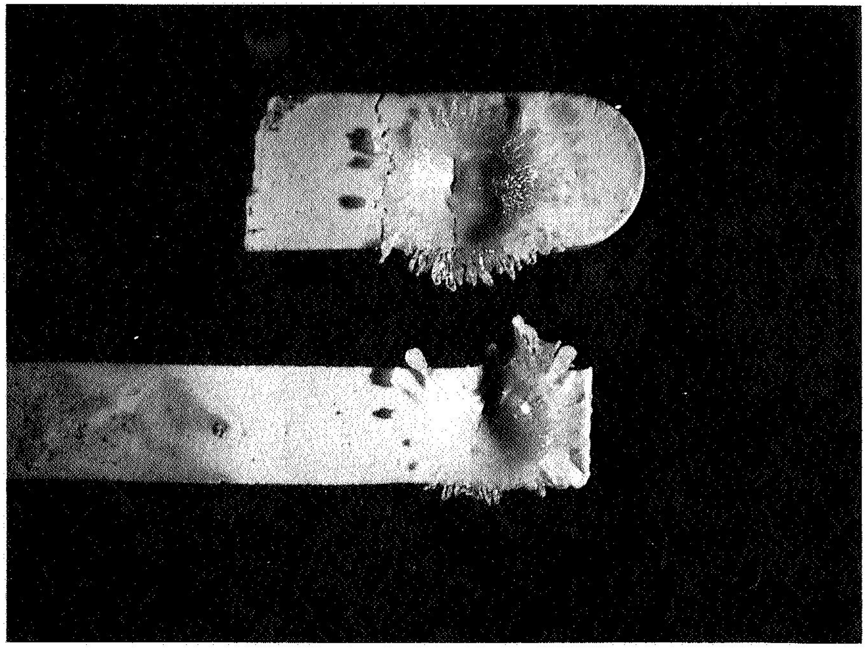

Figure 3. Specimens Melted in the Arc-Plasma Jet (Magnification X2.4)

TABLE 4

PHOSPHATE-BONDED ZrO_2 SLURRY FORMULATIONS

Slurry No.	Composition			Observations and Comments on Mixing the Slurry
	ZrO_2, g	Binder Solution No. 4, g	Volume of Binder Solution No. 4 Plus H_2O, cc	
B43	10.0	0.1	1.8	NSR*
B43-1	10.0	0.1	1.5	NSR
B44	10.0	0.5	1.8	NSR
B44-1	10.0	0.5	1.5	NSR
B45	10.0	1.1	1.5	Set to a paste consistency in 1-1/2 minutes
B46	10.0	1.25	1.6 (g of H_2O)	Set to heavy paste in 1-1/2 minutes; more water was added so that it could be poured
B47	10.0	4.3	No H_2O added	NSR; very thin consistency
B48	10.0	10.0	No H_2O added	NSR; very thin consistency

*NSR = No sensible reaction.

Results of the 30-minute anneal are listed in Table 5, and photomicrographs of mounted specimens are shown in Fig. 4a through d. Compositions of interest were B44 and B45. Specimens of B44 and B45 changed very little in appearance as a result of annealing. As in all specimens, color changed from light grey to light beige. Bars could not be scratched with a steel probe, and hardness did not change sensibly because of annealing. In fact, hardness probably increased because of sintering. A more sensitive yet meaningful hardness test was not available. Hardness testing instruments did not give useful data because the large indenters crushed test specimens, and a microhardness tester was not used because results would have varied considerably as a function of the location of the indenter.

Strength was high and probably increased with annealing temperature due to sintering. That these bars were strong and did not crack is significant. A small amount of glass formation was indicated at 3750 and 4000 F by the glassy appearance on the surface of the test bars. Formation of calcium phosphate or calcium zirconium phosphate glass is reasonable. Sharp edges on the bars remained sharp on the B44 bars but rounded at 4000 F on B45 bars. Edges on bars composed of B43, which had very little phosphate, also rounded.

Grain growth and sintering (Fig. 4a through d) were not evident at 2700 F, but were pronounced at 3750 F. Liquid-phase sintering due to the presence of a glassy phase, was not evident. Sintering and grain growth were of the same magnitude in bars that were made with excess and without any phosphate.

Strength and hardness of bars made from composition B43, which contained very little phosphate binder, increased with increasing annealing temperature. This was because of bonding and grain growth that resulted from sintering. Although strength was high after annealing at higher temperatures, this composition would be unsatisfactory for use in monolithic heat-barrier coatings because strength would not be developed in the moderate- and low-temperature strata where sintering did not occur.

TABLE 5

THE EFFECT OF RELATIVE STRENGTH AND HARDNESS OF SELECTED COMPOSITION OF PHOSPHATE-BONDED ZrO_2 AS A FUNCTION OF ANNEALING TEMPERATURE

Slurry No.	Binder Solution, No. 4 to ZrO_2 Weight Ratio	Description of Test Bars After:													
		Curing For 1 Hour at 600 F in Air		Annealing for 1/2 Hour at											
				1000 F		1850 F		2700 F		3750 F			4000 F		
		Relative Strength(2)	Hardness(1)	Relative Strength	Hardness	Relative Strength	Hardness	Relative Strength	Hardness	Relative Strength	Hardness	Comments	Relative Strength	Hardness	Comments
B43	0.1/10	Low	A	Low	A	Low	A	Moderate(3)	E	High(3)	E	Edges rounded	High(3)	E	Edges rounded
B44	0.5/10	High	E (On top) D (On sides)	High	E (On top) D (On sides)	High	E (On top) D (On sides)	High(3)	E	High(3)	E	Edges were sharp	(4)	E	Edges were sharp; surfaces glossy
B45	1.1/10	High	E	High	E	High(3)	E	Moderate(3)	D (On skin) C to D (On inside)	High(3)	E	Edges sharp; darker color	High(3)	E	Two edges were rounded; glossy surfaces
B46	1.25/10	Moderate	D to E	--	--	--	--	Moderate(3)	C to D	--	--	--	--	--	--
B49	2.5/10	Moderate	D	Moderate to high(3)	D to E	High	E	Low(3)	B to C	Low; friable	D	Stuck to support; bloated at surface	High(3)	D	Stuck to support; bloated at surfaces
B47	4.3/10	Moderate	D	Moderate	D	Moderate (3)	D	Low(3)	B	Low; friable	B	Stuck to support; bloated at surface	Low;(3) friable	D	Stuck to support; bloated at surfaces
B48	10/10	Moderate to low	B to C	--	--	--	--	Low(3)	B	Low	--	--	Low;(3) friable	D	Stuck to support; bloated at surfaces

NOTES: (1) Hardness

A = soft, rubs off
B = scratched with fingernail
C = scratched easily with steel blade
D = scratched with difficulty with steel blade
E = not scratched with steel blade

(2) Relative strength was determined by manually breaking the bars by bending.

(3) These specimens were too short to break manually. Relative strength was estimated by crushing.

(4) The small specimen appeared to be strong but it was easily broken manually. Possibly a crack existed in this specimen before annealing.

(a) B44

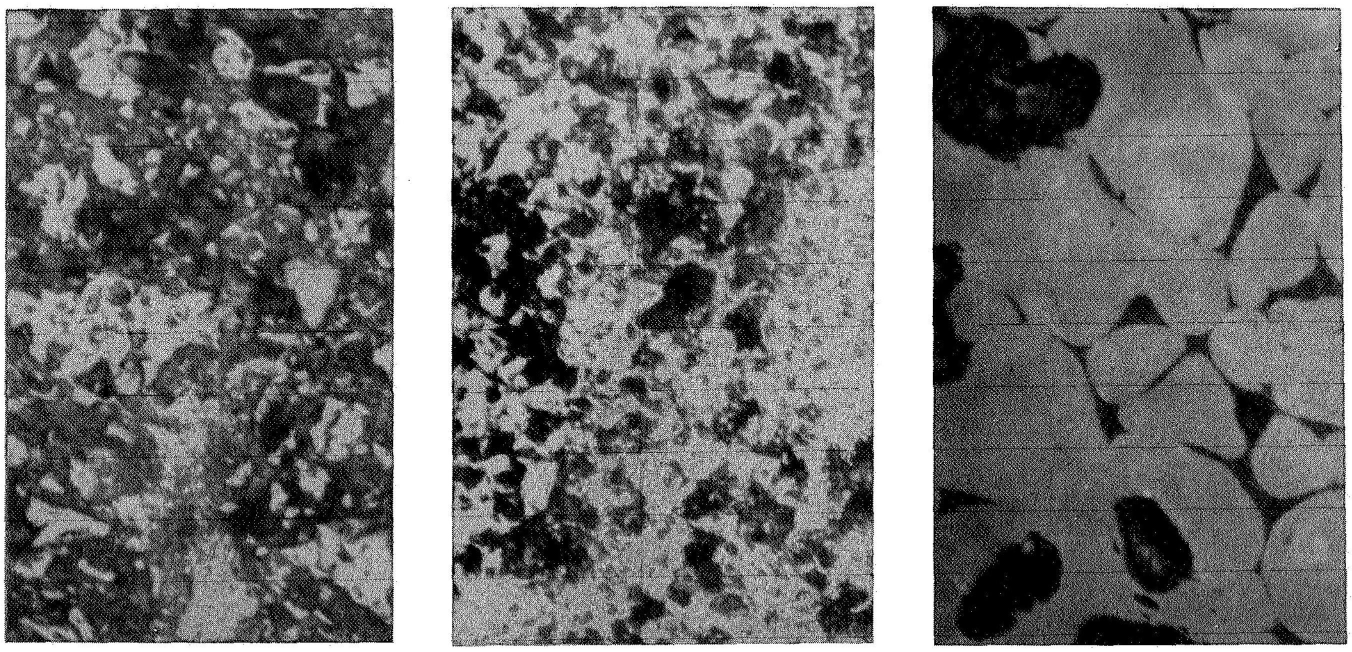

(b) B45

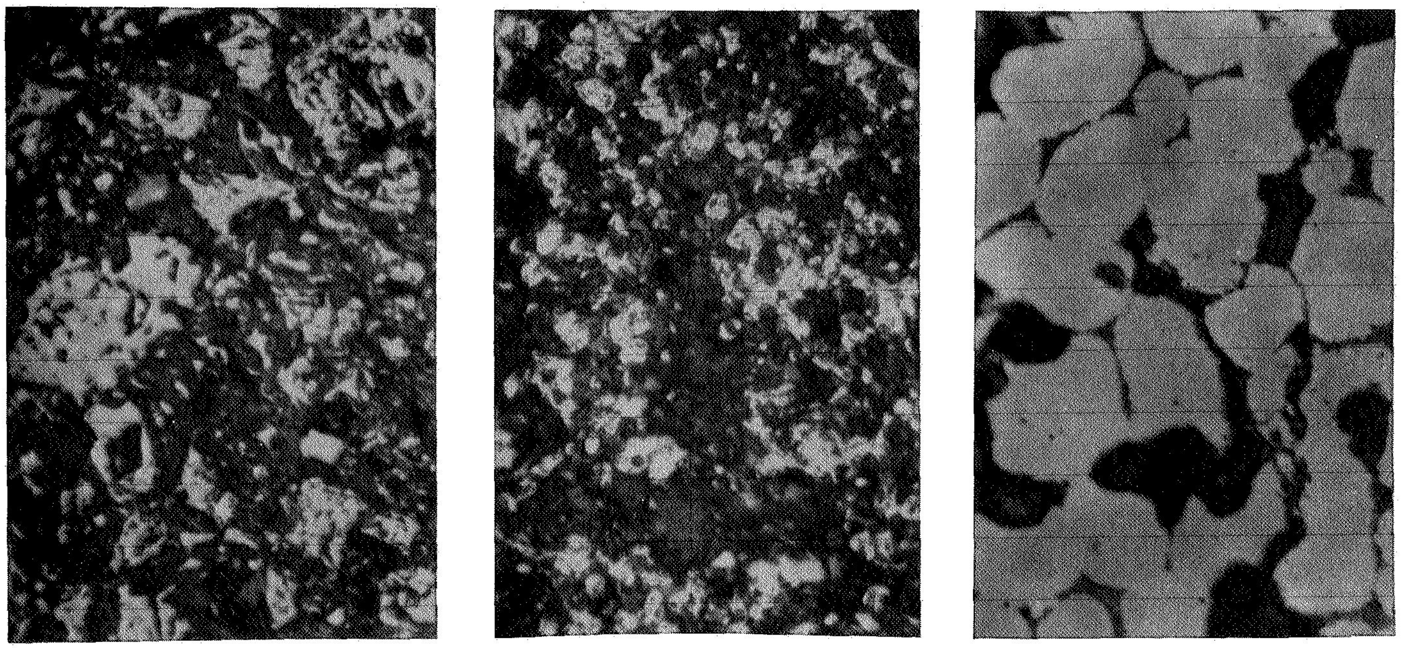

600 F 2700 F 3750 F

Figure 4a through d. Microstructure of Bars Composed of Formulations of B44, 45, 47, and 49 That Were Annealed for 1/2 Hour. (White areas are ZrO_2 grains; dark areas are mounting epoxy, cementitious phases, or voids. Magnification X400)

(c) B47

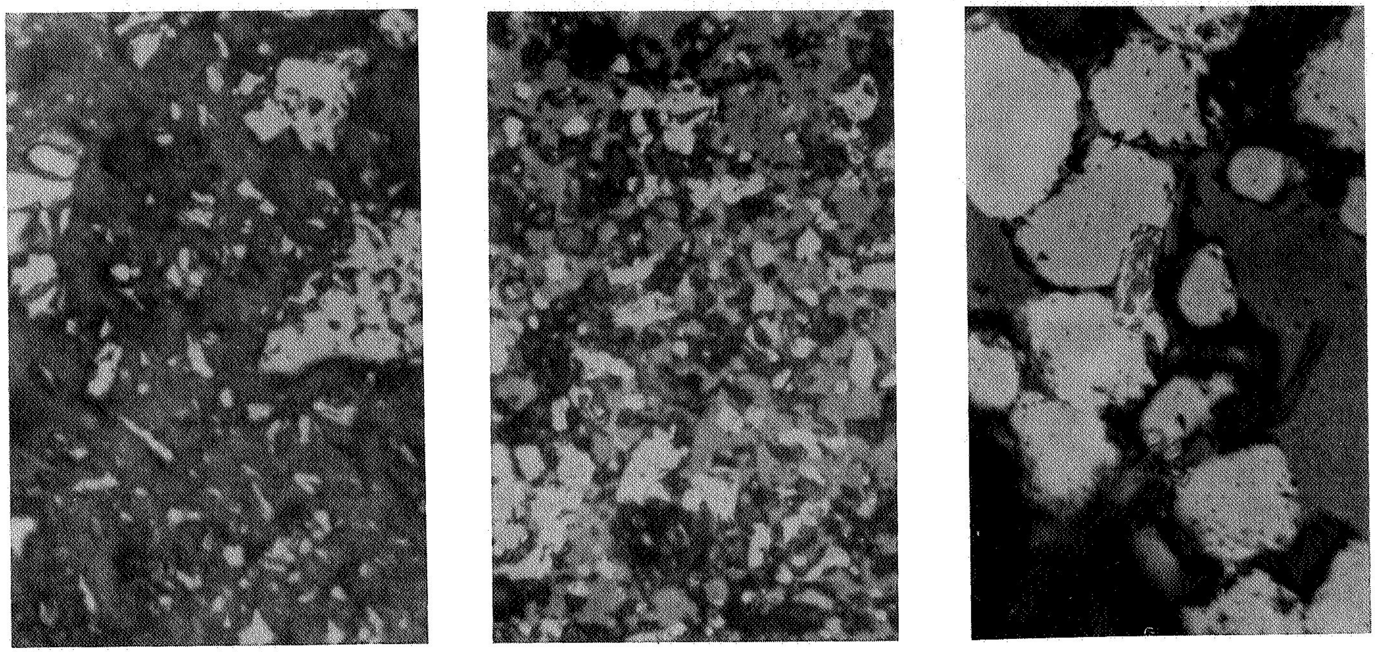

(d) B49

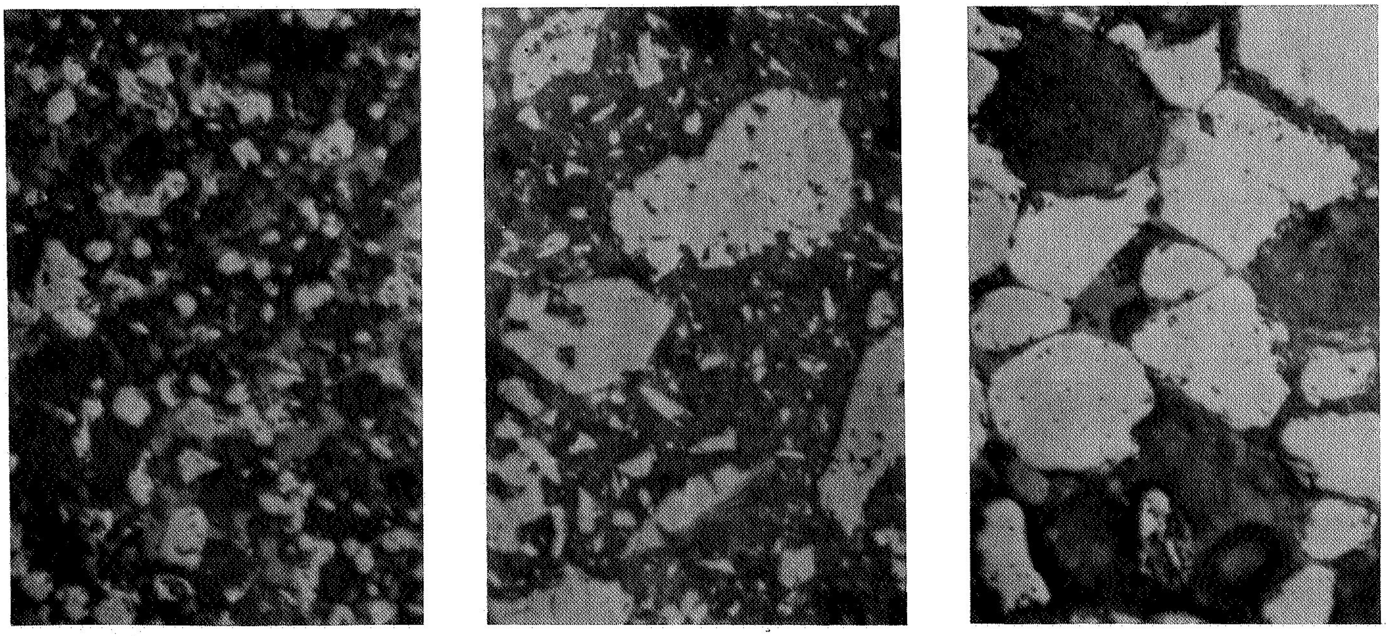

600 F 2700 F 3750 F

Figure 4a through d. (Concluded)

Conversely, for formulations containing higher concentrations of phosphate binder (B46 through B49), strength decreased with increasing annealing temperature. Strength decreased and the specimen became friable because of (1) increased porosity that resulted from bloating, (2) thermal strains caused by mismatched thermal properties of the ZrO_2 and the binder phases, and/or (3) phase changes in the binder or the ZrO_2. It should be pointed out that the nature of the binder phases in the system could change with increasing phosphate content. Excess H_3PO_4 and HF could shift the equilibrium of a particular reaction so that a given phase might reduce the resistance to thermal shock in the binder-rich formulations. It does not follow that it should do likewise in the binder-poor formulations.

Glass formation was clearly evident in those specimens that contained excess phosphate binder. Bars bloated, apparently the result of trapped gases in the viscous liquid. Bars also bonded to the support, due to the viscous phase that flowed from the specimen. Bonding by solid-state sintering was unlikely because similar specimens, but with less phosphate content, did not bond to the ZrO_2 supports.

Results of annealing bars for 5 minutes (Table 6) rather than for 1/2 hour were the same with one significant exception. Similar results were obtained in reference to hardness, strength, and microstructure. These results indicated that most of the sintering occurred within the first 5 minutes.

The important exception was that, whereas all other bars were strong after annealing for 5 and 30 minutes at all other temperatures, the bar of B45 was friable after annealing for 5 minutes at 2700 F. The reason for the friable nature of this one specimen was destabilization of the CaO-stabilized ZrO_2. This was proven by X-ray diffraction studies which are described below.

Significantly, the B45 bar that was destabilized by annealing at 2700 F for 1/2 hour was hard and strong. The reason for the improvement in strength and hardness over that of the bar annealed for only 5 minutes

TABLE 6

THE EFFECT ON STRENGTH AND HARDNESS OF SELECTED COMPOSITIONS OF PHOSPHATE-BONDED ZrO_2 AS A FUNCTION OF ANNEALING TEMPERATURE

Slurry No.	Binder Solution No. 4 to ZrO_2 Weight Ratio	Description of Test Bars After:					
		Curing for 1 Hour at 600 F		Annealing for 5 Minutes at 2700 F		Annealing for 5 Minutes at 4000 F	
		Relative Strength	Hardness(1)	Relative Strength	Hardness	Relative Strength	Hardness
B43	0.1/10	Low	A	Low	D	High	E
B44	0.5/10	High	E	High	E	High	E
B45	1.1/10	High	E	Friable	-	High (glassy)	E
B49	2.5/10	Moderate	D	Low	C	Low (bloated)	E (on skin) A (inside)
B47	4.3/10	Moderate	D	Low to moderate	B	None (bloated)	D (on skin) A (inside)
B48	10/10	Moderate to low	B to C	Low to moderate	B	None (bloated)	A

NOTES: (1) Hardness,
A = soft, rubs off
B = scratched with fingernail
C = scratched easily with steel blade
D = scratched with difficulty with steel blade
E = not scratched with steel blade

was probably bonding and grain growth due to sintering that occurred after the phase change. The bar annealed at 2700 F for only 5 minutes was probably still undergoing a phase change and, therefore, exhibited the friable nature of a material undergoing a large volume change.

X-Ray Diffraction Analysis. Powder X-ray diffraction analysis was performed on the B45 specimens annealed at 1000, 2700, 3750, and 4000 F and in the as-cured condition. Only phases of ZrO_2 were found; no phosphate or calcium compounds were detected. The only crystalline phase found in specimens annealed at 600 (as-cured), 1000, 1800, and 4000 F was cubic ZrO_2 (the stabilized phase). Cubic ZrO_2 was also the major phase found in the specimen annealed at 3750 F, while monoclinic ZrO_2 (the low-temperature, unstabilized phase) was found as a minor phase. On the other hand, the only phase found in the specimen annealed at 2700 F was monoclinic ZrO_2. It was surprising that no monoclinic ZrO_2 was detected in material that was annealed at 4000 F. The starting material, although advertized as being only 75-percent stabilized, is actually 100 percent stabilized in the as-received condition. It is designed to convert to 25 percent of the unstabilized form after annealing at 2500 F for 4 hours. A 25:75 ratio of monoclinic and cubic ZrO_2 is said to give the best thermal shock resistance to bodies made from this material. Destabilization of the ZrO_2, which is due to the formation of $CaZr(PO_4)_2$ at intermediate temperatures (Ref. 5 and 6), was unexpected based on prior work. Specimens studied in Ref. 5 and 6 had been annealed for several hours when the destabilization was observed (Ref. 7).

Because it is the phosphate that removes CaO (the stabilizing agent) out of solid solution in the ZrO_2 phase, the analysis was repeated on specimens that contained half as much phosphate content (formulation B44). These specimens, which were also annealed for 5 and 30 minutes, only partially destabilized. Thus, destabilization can be reduced, possibly to normal, by decreasing the phosphate content in the formulation.

Electron-Beam Microprobe Analysis. An electron-beam microprobe X-ray analysis substantiated the above results. The specimen (No. 72-4, test area 4) that was analyzed had been tested in the arc-plasma jet and mounted for analysis using a standard technique*. Consequently, the coating had been subjected to a temperature gradient across its 5 mil thickness with a hot-side surface temperature of 3750 F (optical pyrometer temperature). Three areas were analyzed at 220 and 880 magnification; they were located at the Hastelloy-X/coating interface, at the outer (hot-side) surface, and in the center of the coating (Fig. 5). The area shown in Fig. 5 was located about 50 mils laterally from the center of the arc-plasma jet. Because of the high magnification of the recorded images in the central stratum, they do not include the outside surface or the interface between the coating and Hastelloy-X substrate. Thus, the maximum temperature in the analyzed area was less than 3750 F; it was estimated to be about 3150 F.

Location of Zr, which is shown in the electron backscatter and Zr X-radiation images (Fig. 6a and c), corresponds with the ZrO_2 grains in the coating (Fig. 5). The electron backscatter image shows the location of the heavier elements in a material, in this case only Zr. Calcium is uniformly distributed in the ZrO_2 grains in the low-temperature zone (the lower half of Fig. 6d), but Ca is not found in the ZrO_2 grains in the high-temperature zone (the upper half of Fig. 6d). In the high-temperature zone, the location of Ca coincides with that of phosphorus. Phosphorus is located uniformly in the matrix surrounding the ZrO_2 grains and it is shown to be more dense in the high-temperature region (Fig. 6b).

These data concur with previous findings in that the CaO-stabilized ZrO_2 destabilizes at an intermediate temperature range around 2700 F. The CaO, which is originally in solid solution in the ZrO_2 grains, diffuses out of the ZrO_2 and reacts with the phosphate binder phases.

---

*The specimen was mounted for electron microprobe analysis using a standard procedure for nonconductive specimens. The specimen was mounted under 2400 psi at 325 F using Epiall epoxy which contained enough nickel powder to make it electrically conductive.

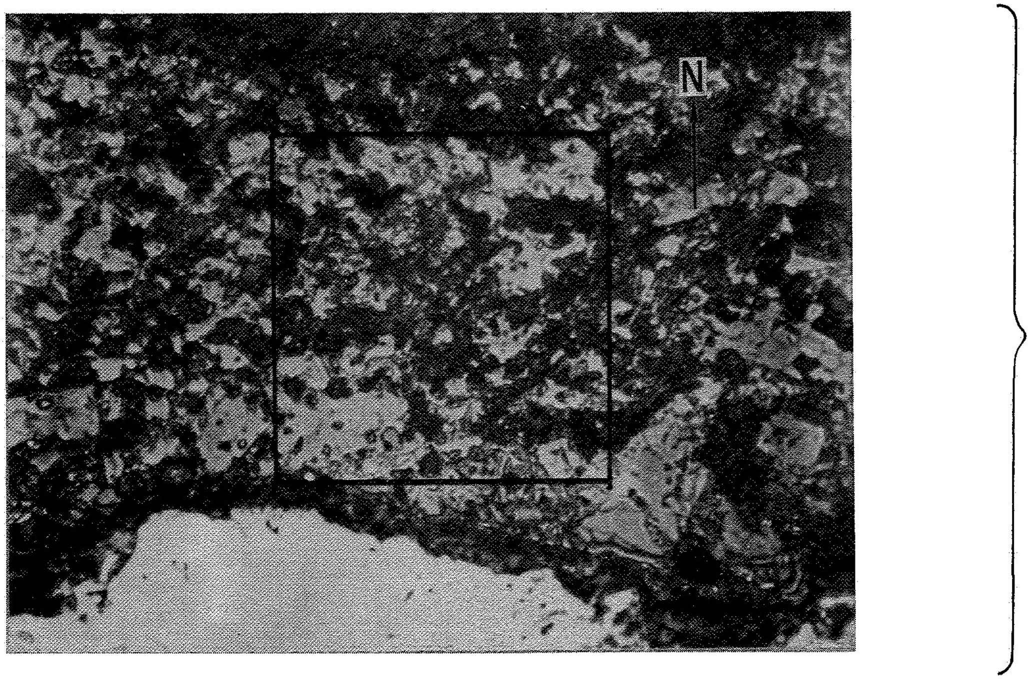

Phosphate-Bonded ZrO_2 Coating

(The outlined area is that scanned by the electron-beam microprobe.)

The white area at the bottom is the Hastelloy X Substrate

72-4-5

Figure 5. Photomicrograph of the Area That was Analyzed With the Electron-Beam Microprobe. (Magnification X400)

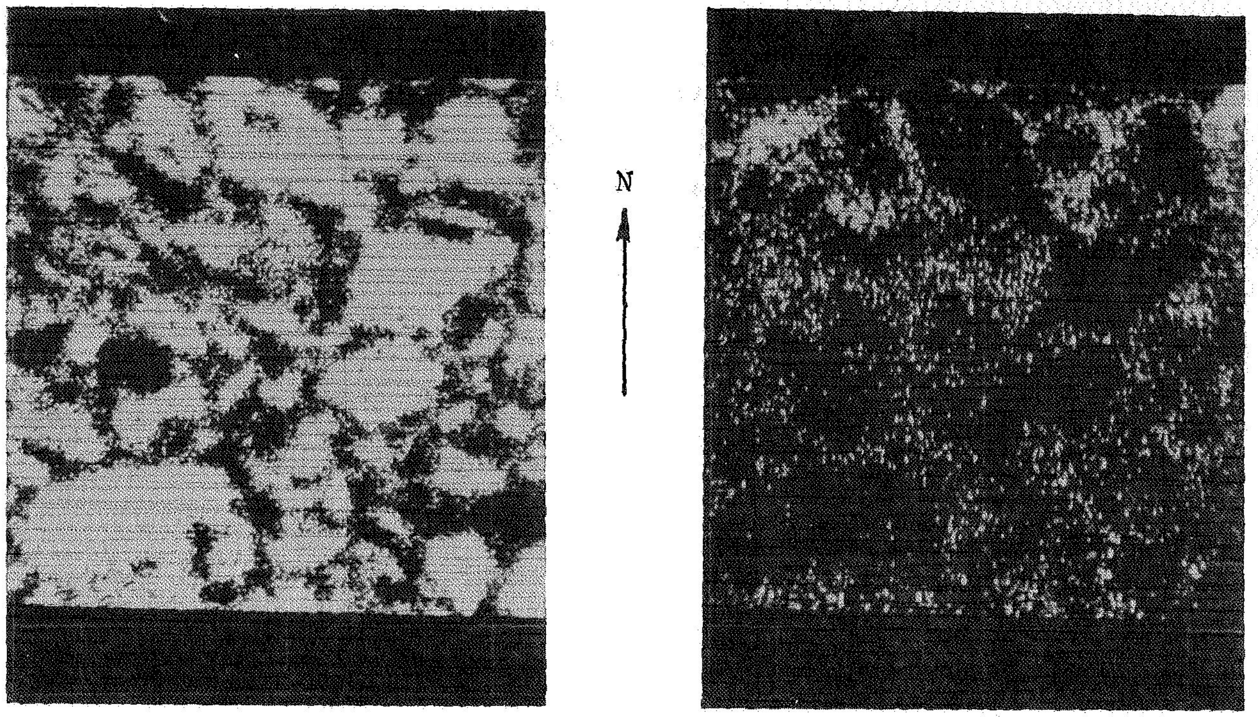

(a) Electron Backscatter Image

(b) Phosphorous X-Radiation Image

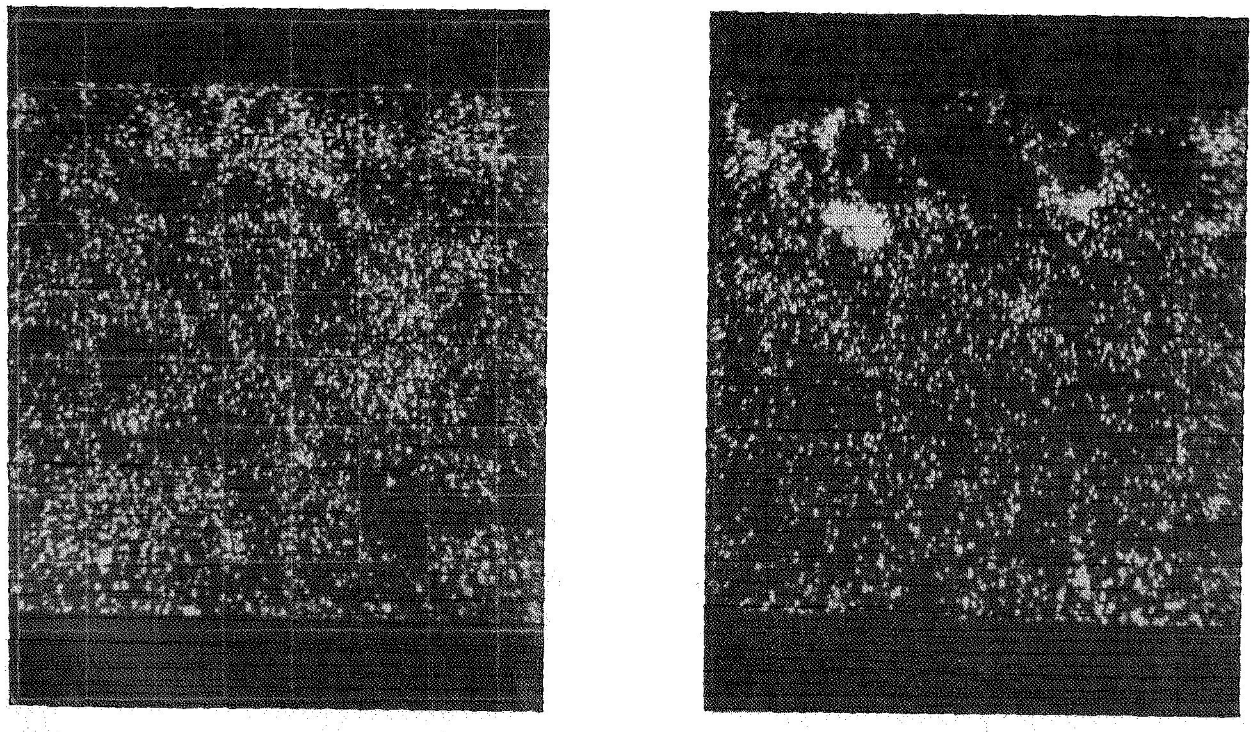

(c) Zirconium X-Radiation Image

(d) Calcium X-Radiation Image

Figure 6. Electron-Beam Microprobe Analysis of a Phosphate-Bonded ZrO_2 Coating That has Been Tested in an Arc-Plasma Jet. (Magnification X880. Power 25kw.)

Reason for the higher concentration of phosphorous in the high-temperature zone is unclear. It could be due to reinforcement of X-rays from Ca because both elements are relatively close in atomic number. The concentrated spots of Ca in the high-temperature zone can be explained because the same amount of Ca probably occupies a smaller volume after it diffuses from the ZrO_2 grain into the cementitious matrix.

Electron microprobe analyses in the outer (hot side) and inner (cold side) strata did not show the separation of Ca from Zr so clearly as was apparent in the central stratum. This indicated that Ca diffusion out of ZrO_2 and reaction with P_2O_5 occurred predominately in the middle-temperature range, near 2700 F.

Fluxing of the Phosphate Binder. Optical pyrometer melting temperature was obtained by melting test bars of selected compositions in the arc-plasma jet. The test was started at a low power setting and the power was gradually increased until surface melting was observed through the optical pyrometer. Results of this study (Fig. 7) are presented only as a guide for indicating the relative extent to which the phosphate content fluxed ZrO_2; they do not represent absolute melting temperatures because emittance of the surface and reflection of radiation from the arc-plasma jet were not considered. A reasonable curve can be faired through the data provided that one point is neglected. The atypical point is the lowest of the three data points (the open circle in Fig. 7) for the system with 5-percent binder content. Melting temperatures for compositions containing more binder than 10 percent were not obtained because satisfactory specimens were not available.

These data indicate that more than 10.1 parts binder solution No. 4 per 10 parts ZrO_2 would flux ZrO_2 near or below the acceptable limit for this program; ca. 4100 F. Note that 4100 F is the optical pyrometer temperature so that true melting temperature would be closer to 4200 F, or higher.

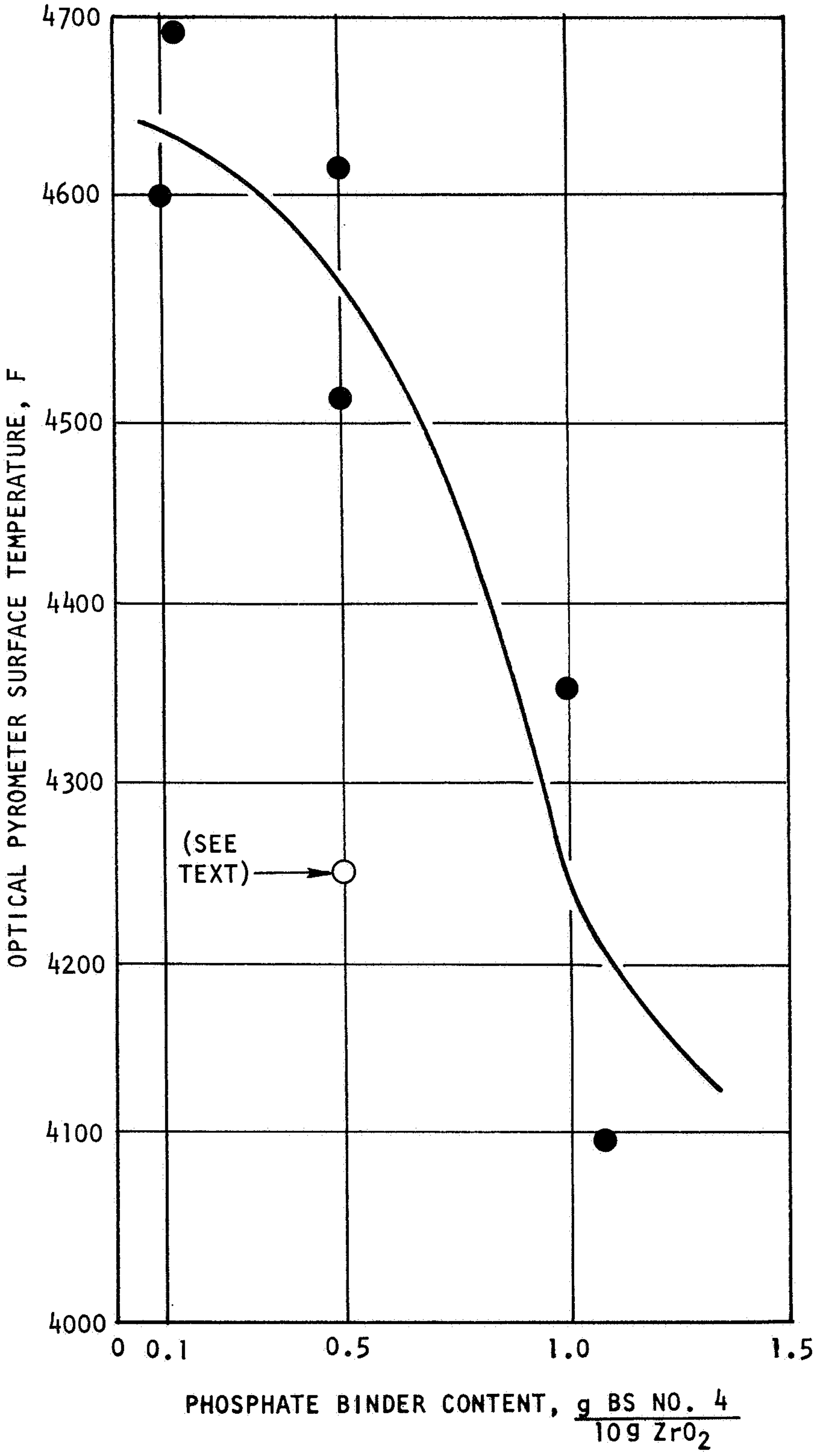

Figure 7. Melting Temperature of Phosphate-Bonded ZrO_2 as a Function of Binder Content

Alcohol Suspension Media

Use of an organic liquid rather than water offers two potential advantages; one, a liquid could be selected that is chemically inert and, therefore, does not complicate or accelerate bonding reactions; and two, the liquid would evaporate rapidly once the coating has been applied, thereby allowing shrinkage to occur before bonding occurred.

To evaluate this concept, several alcohol suspensions were made and tested in the arc-plasma jet. Coatings were hard, strong, and survived the arc-plasma jet test. This approach in formulation was not pursued at this time; however, it remains as a further potential process variable for development, should the slurry properties require alteration for uniform spraying on thrust chambers.

Summary

Optimum range of phosphate binder solution is between 0.5 and 1.1 parts by weight per 10 parts of ZrO_2. Less than 0.5 part binder solution is insufficient for producing high strength but 0.5 part provides adequate strength which increases because of sintering in the hotter strata of the coating. Destabilization of ZrO_2 has not been a problem when using the lower phosphate content. On the other hand, although more phosphate binder produces improved strength at lower temperatures and does not impair properties in the high-temperature strata of the coating, it leads to destabilization in the intermediate-temperature strata of the coating. Thus, it would seem that each service temperature level will require a different phosphate concentration for maximum reliability. A more thorough study of this system will be required to optimize the formulation for achieving the best coating for a particular service condition.

ADHERENCE

General

Tenacious adherence of the heat-barrier coating to the Hastelloy-X substrate is of primary importance to its ultimate usefulness in a rocket engine thrust chamber. Adherence has been quite adequate to survive conditions in the arc-plasma jet test; but it would be hazardous to conclude from this observation alone that the coating will survive the service environment in an actual thrust chamber where, in addition to the possibility of damage in field handling, operational stress conditions and shear forces are expected to be more severe than they have been in the arc-plasma jet tests. With this in mind, several design and process approaches to improving adherence were evaluated. These included: (1) chemical etching of the Hastelloy-X substrate, (2) preoxidation of the Hastelloy-X substrate, (3) use of a porous melt-sprayed metal base layer, and (4) use of a thin, refractory glass base layer. The thin glass base and melt-sprayed metal layers potentially offer the added advantage of accomodating and relieving strain between the coating system and the Hastelloy-X substrate under service conditions. And theoretically, the glass base layer should provide the best adherence possible: The glass can be chemically bonded to both materials, viz., the Hastelloy-X and the phosphate-bonded ZrO_2 coating; and chemical bonding can be expected to be of the order of 100 times stronger than the mechanical bonds depended upon on a Hastelloy-X substrate prepared simply by grit blasting.

Thermal Shock Test

A series of test specimens were prepared for comparing the above methods of improving adherence. Specimens with coating thicknesses of about 15 mils were prepared in exactly the same way, except for Hastelloy-X substrate preparation before coating. Methods of substrate preparation and results (Table 7 and Fig. 8) are discussed below.

TABLE 7

ADHERENCE DATA: THERMAL SHOCK TEST OF COATED HASTELLOY-X TABS THAT WERE PREPARED USING SELECTED TECHNIQUES

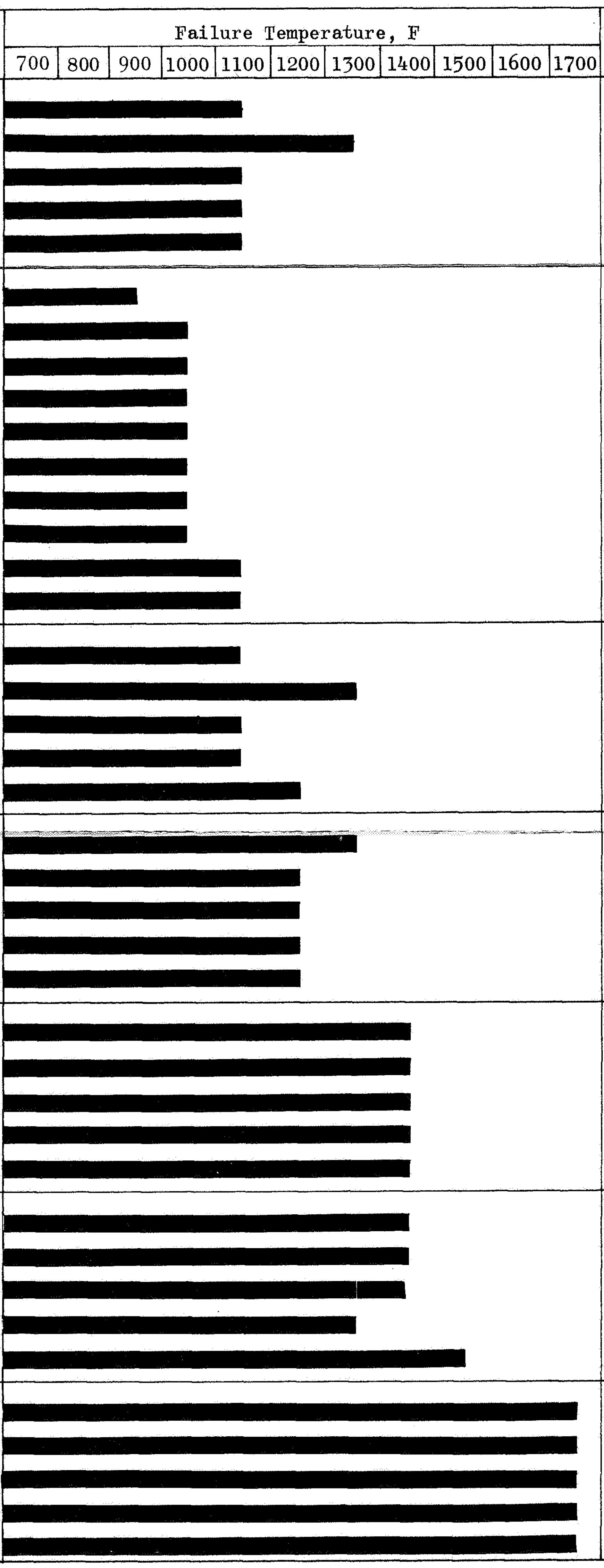

Specimen No.	Coating Thickness, mils	Surface Preparation	Comments
223	9.5	Plain	Adhesive Failure: The metal under the coating was clean and shiny.
224	11.4		
225	14.5		
227	13.4		
228	13.4		
233	10.8	Oxidized (1600 F)	Adhesive Failure: The exposed metal oxide layer under the coating contained some adherent fragments of coating; the coating surface contained some adherent fragments of metal oxide.
234	12.4		
235	12.4		
236	12.5		
237	10.4		
243	10.8	Oxidized (2000 F)	
244	9.3		
246	9.5		
247	9.8		
248	9.5		
162	15.2	Grit Blasted	Adhesive Failure: Adherent fragments of coating were uniformly distributed on the grit blasted metal surface.
163	15.2		
164	15.2		
165	15.2		
166	15.2		
A	12.0	Etched	Adhesive Failure: Same as the grit blasted metal surface except that fragments of coating were smaller.
B	12.0		
C	12.1		
D	12.0		
E	11.6		
196	16.2	Glass Coated and Grit Blasted	Cohesive Failure: The coating system spalled inside the glass layer.
197	16.3		
198	11.5		
199	17.5		
200	16.5		
K	16.0	Melt Sprayed, Inconel Coated	Cohesive Failure: The coating crushed; the metal was still completely covered with adherent fragments of coating.
L	15.0		
M	16.0		
N	15.5		
0	14.0		
214	17.0	Glass Coated and Fused	No Failure: The test was ended.
215	14.5		
217	15.5		
220	15.5		
221	15.5		

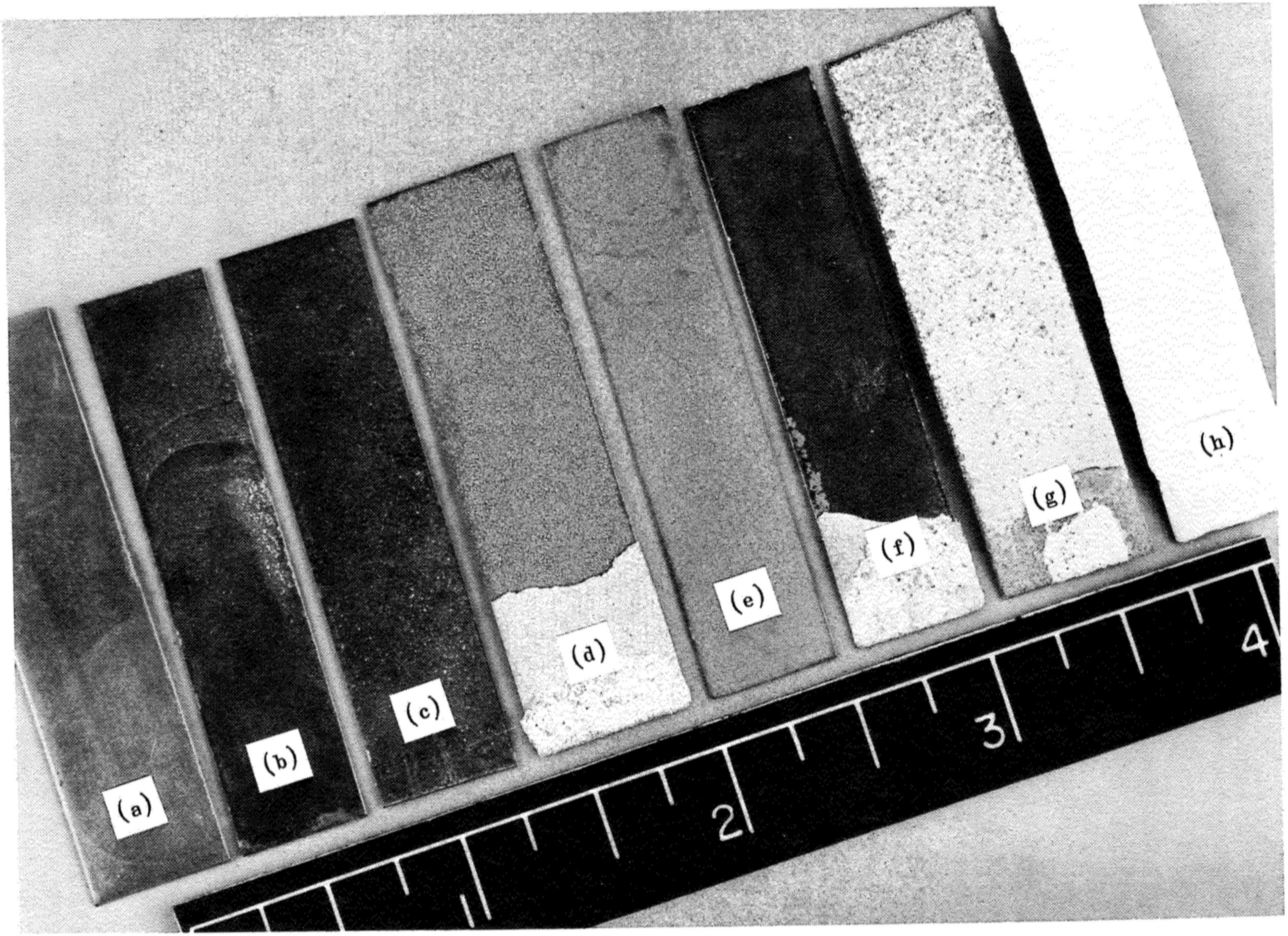

5AG16-1/17/69-C1

Figure 8. Specimens After the Thermal Shock Test. Substrate preparation was: (a) none, (b) oxidized at 1600 F for 1 hour, (c) oxidized at 2000 F for 1 hour, (d) grit blasted, (e) etched, (f) coated with glass (the glass coating was grit blasted with -120 mesh garnet), (g) coated with melt-sprayed Inconel, (h) and coated with glass which was fused to the phosphate-bonded ZrO_2 coating.

No Treatment. Specimen substrates were in the as-received condition except for the standard cleaning procedure. Coatings on substrates that had not been treated failed adhesively when cooled from an average temperature of 1100 F. The metal where the coating spalled was in the original condition, clean and shiny. The photograph of this specimen, Fig. 8a, does not show this clearly because of the nature of the reflected light. One specimen, number 224, indicated unusually good adherence for a coating that was applied to an untreated substrate. It failed when cooled from temperatures at least as high as those required to fail coatings that were applied on roughened substrates. This specimen indicated that some degree of chemical bonding between a phosphate-bonded ZrO_2 coating and Hastelloy-X substrate can be developed. The reason for the better adherence exhibited by this specimen was unknown because all specimens were supposedly prepared identically.

Oxidized. One group of substrate specimens was preoxidized in ambient air at 1600 F while another was preoxidized at 2000 F, both for 1 hour. Coatings that were applied on oxidized substrates failed adhesively when cooled from an average temperature of 1000 F (Fig. 8b and c). The 2000 F oxidation temperature gave slightly better adherence than that of 1600 F, but this method of substrate preparation did not show any improvement in promoting adherence over untreated substrates. Failure was at the metal oxide/phosphate-bonded ZrO_2 interface. Two specimens indicated, however, that improved adherence might be achieved by this approach with further development. A small portion of these specimens, about 10 percent, failed at the metal/metal oxide interface, indicating that the bond between the metal oxide and phosphate-bonded coating was stronger than the bond between the metal and the metal oxide layer. The bond of the oxide layer to the metal is very strong as evidenced by its superior oxidation resistance among metals.

Grit Blasted. Specimens were grit blasted by the standard procedure using -20 mesh Al_2O_3. Surface roughness varied between 150 and 200 microinches rms. Coatings on substrates that were grit blasted failed adhesively when cooled from an average temperature of 1160 F (Fig. 8d). They were surprisingly poor compared to previous results of one particular bend test (refer to Fig. 10). The coating on this specimen was crushed after many bends back and forth over progressively smaller mandrels, but even then, much of the substrate was still covered with adherent fragments of coating. This discrepancy points out the importance of quality control (and possibly cleanliness) of roughened surfaces.

Etched. Specimen substrates were macroetched in boiling aqua regia for about 1 minute before they were coated (see Appendix E). Coatings on etched substrates failed adhesively when cooled from an average temperature of 1200 F, which indicates that they were slightly more adherent than coatings that were applied on the grit blasted substrates. Proportionally as many adherent fragments remained on the substrate after the coating spalled as on grit blasted substrates, but the fragments were much smaller (Fig. 8e). That the adherent fragments were smaller is understandable, because the size (width) of the recessions of the etched grain boundaries was smaller than of those made by grit blasting.

Melt-Sprayed Inconel Coated. Specimens were grit blasted and then coated with 2 mils of arc-plasma sprayed Inconel. Coatings that were applied over the 2-mils of melt-sprayed Inconel failed cohesively rather than adhesively, and only when cooled from a much higher average temperature, 1400 F, than the previously described specimens. Both of these factors indicated strong adherence (and possibly strain relief). In fact, the Inconel substrate was still completely covered with strongly adherent fragments of phosphate-bonded ZrO_2 after testing (Fig. 8g). Strong mechanical adherence was promoted by this rough texture (to 280 microinches rms) of the melt-sprayed metal surface (Fig. 9a).

Glass Coated. Specimens were covered with 2 mils of a tenaciously adherent glass coating (Appendix E). The glass coating was roughened by grit blasting with -120 mesh garnet before the phosphate-bonded ZrO_2 was applied. Post-test microscopic examination of mounted specimens showed that grit blasting

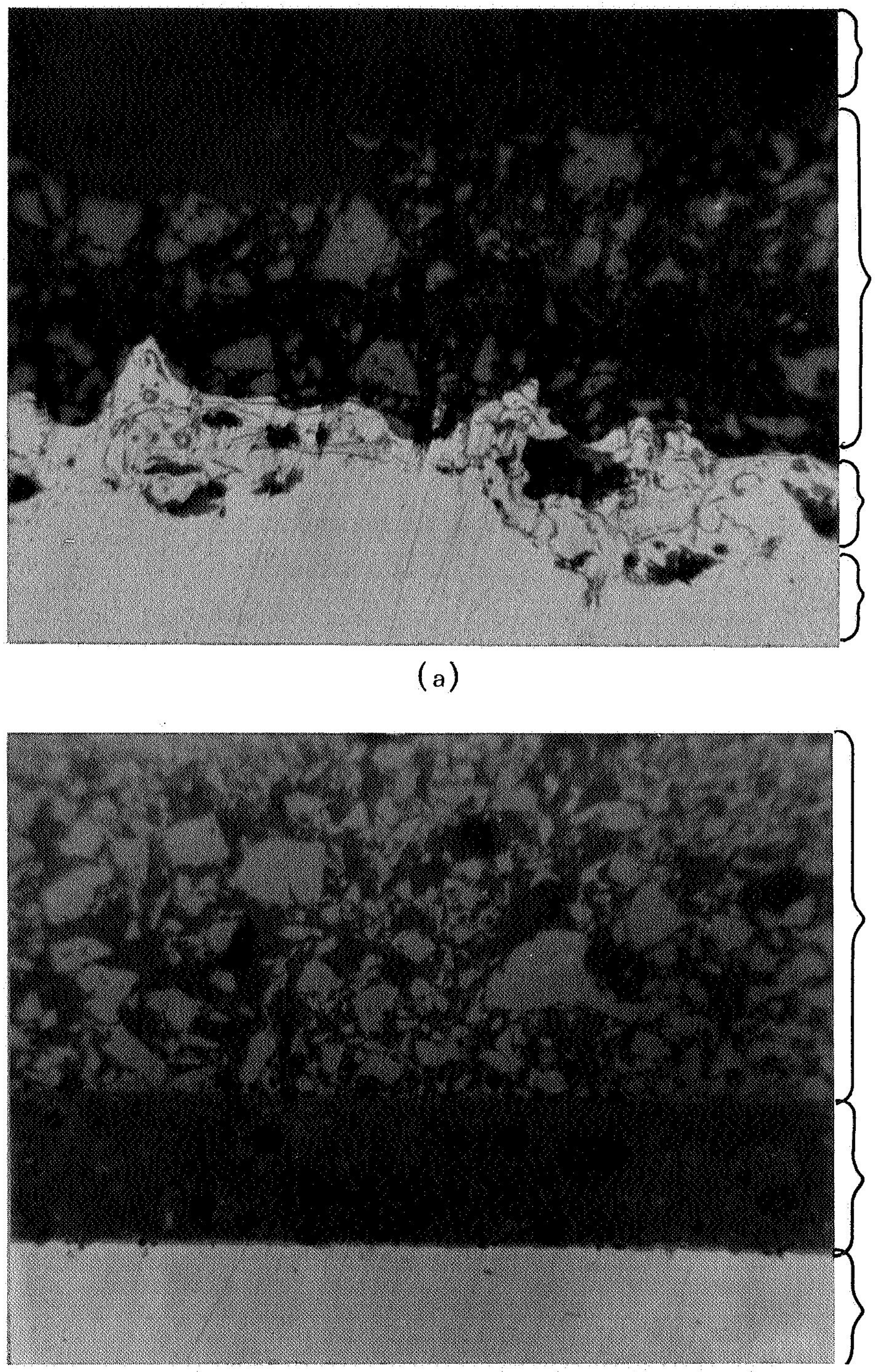

Mounting Material

Phosphate-Bonded ZrO_2 Coating

(Note: Although this coating had been crushed in adherence tests, the coating was still adherent at the inconel surface.)

Melt-Sprayed Inconel Base Layer

Hastelloy-X Substrate

(a)

Phosphate-Bonded ZrO_2 Coating

(Note: This coating was still adherent after thermal cycling from 1900 F.)

Glass Coating Base Layer

(Note the smooth boundaries on both sides.)

Hastelloy-X Substrate

(b)

Figure 9. Photomicrographs of Adherence Test Specimens That Have Special Adherence-Promoting Base Layers. (Magnification X400)

had seriously damaged the glass coating. Even though the glass was fractured, coatings applied over the grit blasted glass substrate showed improved adherence. In fact, the phosphate-bonded ZrO_2 coating did not fail; rather, the glass coating failed (Fig. 8f). A uniform layer of glass was still strongly attached to both the Hastelloy-X substrate and the phosphate-bonded ZrO_2 coating surface.

Glass Coated and Fused. Specimens were coated with glass exactly as in the above case, except that the grit blasting operation was omitted. After the phosphate-bonded ZrO_2 coating was applied and cured, it was fused to the glass coating at 1900 F for 1 minute. Coatings that were fused to the glass substrate showed by far the best adherence; in fact, they did not fail at all (Fig. 8h). The fact that these thick (14.5 to 17 mil) phosphate-bonded ZrO_2 coatings did not fail when thermally shocked from as high as 1900 F, the processing temperature, indicated that the glass was acting to relieve thermal strains between the phosphate-bonded ZrO_2 coating and the Hastelloy-X. Thermal strain above ca. 1300 F was probably negligible because the glass could deform plastically at this temperature. ZrO_2 grains in the heat-barrier coating were chemically bonded to the glass; they were not embedded in the glass and the glass surface was too smooth to promote any mechanical adherence (Fig. 9b).

An important sidelight of this study indicated that strong chemical bonds can be produced between the metal and the coating. The best example of this was shown on specimens in which the metal was in the as-received condition, although the same result was also observed on grit blasted specimens. When coated specimens were cooled from 1200 F or lower and the coating spalled or was broken off, the interface condition was as predicted: the metal was clean and the coating surface at the interface side was white. When coated specimens were cooled from 1300 F or higher, however, a different result occurred: the metal was clean where the coating spalled, but the interface side of the coating was covered with a bright metal finish. Failure was apparently within the metal, although very close to the surface.

Bend Test

Results of bend tests, types A and B, are summarized in Table 8 and 9. Specimens are listed in order of performance, with best adherence first. Ranking and comments as to mode of failure and to metal surface condition after the coating failed were the same as those that were given in the preceding section on thermal shock test results. Again, the glass-coated and Inconel-coated substrates promoted excellent adherence. In fact, adhesive failure was not achieved in these tests because the Hastelloy-X substrate crimped over the small-sized mandrels required to crush the phosphate-bonded ZrO_2 coating that was applied over the glass coating, and the coating crushed so badly before the metal substrate was exposed on the Inconel-coated specimen, that further testing was meaningless.

Results are noteworthy because of the extensive punishment that the phosphate-bonded ZrO_2 coatings took before they failed. Coatings applied on substrates that were Inconel coated or glass coated and fused to the phosphate-bonded ZrO_2 coatings survived all flexes in test A to the smallest mandrel, 3/4 inch in diameter; and they survived 10 flexes back and forth over 4-1/2, 3-1/2, 2-1/3, 2, and even in some cases 1-1/2 and 3/4-inch mandrels in test B.

Results using specimens prepared by grit blasting were again inconsistent. The coating spalled in test A when bent over 4-1/2- and 2-1/2-inch mandrels, and in test B when bent only twice (that is once in tension and once in compression) over a 4-1/2-inch mandrel. Earlier in a test to evaluate the validity of the bend test, a 5-mil-thick coating applied over a grit blasted substrate (specimen 116) survived:

1. Ten flexes back and forth over a 4-1/2- and 2-1/4-inch mandrel without any visible change in the coating
2. Ten flexes over a 1-1/2-inch mandrel, where 40 percent of the coating spalled after being crushed

TABLE 8

SUMMARY OF ADHERENCE DATA: BEND TEST TYPE A*

Substrate Preparation	Coating Thickness, mils	Mandrel Diameter Where 75 Percent of the Coating Spalled, inches	Coating Thickness Correction Factor***	Ranking In Order of Best Adherence
Glass Coated and Fused	6.0	NF**	-	1
Inconel Coated	4.6	NF	+	2
Glass Coated	5.5	1.5	0	3
Etched	5.2	1	+	3
Grit Blasted	6.9	3.5	-	4
Oxidized at 2000 F for 1 Hour	7.0	3.5	-	4
Oxidized at 1600 F for 1 Hour	6.0	3.0	-	4
None	5.5	3.5	0	5

*In this test, specimens were bent with the coating on the convex side once around progressively smaller mandrels, 4-1/2, 3-1/2, 2-1/2, 2, 1-1/2, 1, 3/4 inch diameters.

**NF = No failures

***0 = No correction was necessary; coating thickness was the same as that of the control specimens, 5.5 mils.

+ = Mandrel size at which the coating failed would have been larger had coating thickness been the same as the control specimens.

- = Mandrel size at which the coating failed would have been smaller had coating thickness been the same as the control specimens.

TABLE 9

SUMMARY OF ADHERENCE DATA: BEND TEST TYPE B

Substrate Preparation	Coating Thickness, mils	Number of Flexes*	Mandrel Diameter Where 75 Percent of the Coating Spalled, inches	Ranking In Order of Best Adherence
Glass Coated	18.0	6 1	2.5 1 (stopped because the Hastelloy-X crimped over the small mandrel)	1
Inconel Coated	4.5	7	0.75 (stopped because the coating was being crushed)	1
Glass Coated and Grit Blasted	4.1	2 2 3	4.5 4.5 4.5	2
Etched	6.0	2	4.5	2
Grit Blasted	6.3	2	4.5	2
Oxidized	--		(adherence was inadequate for this test)	3
None	--			3

*The coating was on the convex side during the first flex, on the concave side during the second flex, on the convex side during the third flex, etc.

3. Three flexes back and forth over a 3/4-inch mandrel without further damage to the coating.
4. One flex back and forth over 1/2-inch mandrel (Fig. 10).

Again, the only apparent reason for the diverse test results was inconsistency in degree of grit blasting.

Other reasons for scatter in adherence data are inherent in the bend tests. These include: (1) variations in coating thickness and surface condition, i.e., in coating strength, (2) edge effects, (3) bowing of the metal specimen across the width because of grit blasting or sectioning, (4) residual stresses in the metal because of grit blasting, and (5) residual stresses in the metal/coating system because of differences in the thermal expansion and conductivity of the metal and phosphate-bonded ZrO_2 coating.

Tensile Test

Tensile test data as such, were not obtained because of inability to make satisfactory specimens. Nevertheless, results did give useful information. The main problem in making specimens was that most of the thick coatings that were applied to the 1/4-inch-thick Hastelloy-X discs spalled after curing so that tensile tests were not possible. Thick coatings were required so that the epoxy would not penetrate to the coating/metal interface. One reason for spalling may have been the change in thermal stresses that were developed because of the slow cooling of the thick Hastelloy-X disc. Tensile tests of the specimens in which the coating did not spall were invalid because the epoxy cement penetrated under the coating and provided an indeterminate proportion of the tensile strength.

Only 12 specimens were made. Substrate preparation was: three untreated, three oxidized at 1950 F for 1-1/2 hours, three grit blasted, and three with glass. In this test, the glass was not further treated; i.e., either grit blasted or fused into the phosphate-bonded ZrO_2 coating.

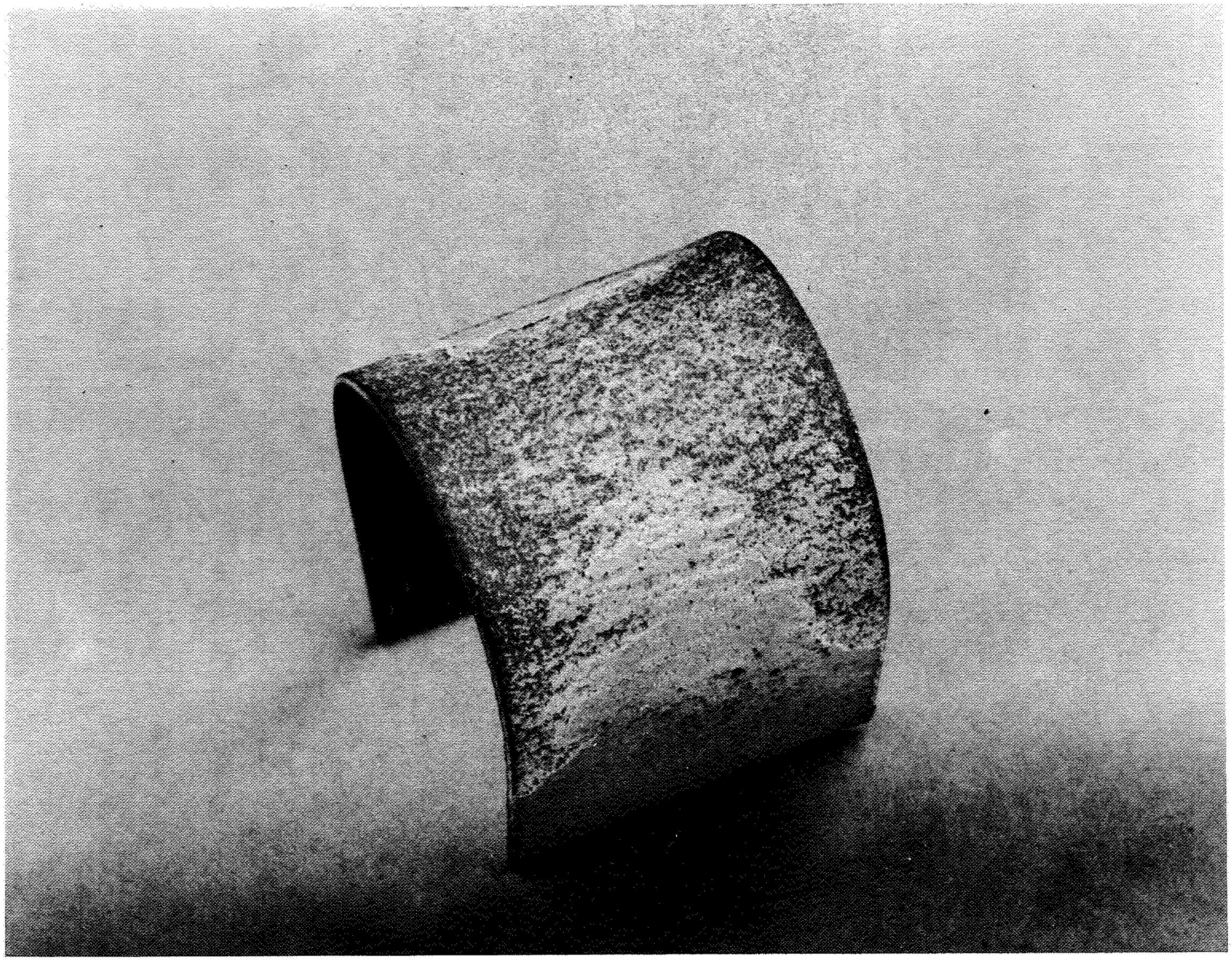

5AG13-12/10/68-C1A

Figure 10. Specimen 116 After Flexing Back and Forth Over Progressively Smaller Mandrels. (Substrate preparation: Grit blasting; Magnification X5)

Coatings on two of the untreated substrates spalled after curing, yet 80 percent of the metal discs were covered with adherent fragments of coating. These fragments could not be removed with a fingernail, but they could be with a sharp pointed steel blade. The third specimen, which was pulled apart in the tensile test machine, was 85 percent covered after testing with adherent fragments. This was even more, on the average, than the amount of coating fragments that adhered on the grit blasted substrates after the coating was pulled off. Again, chemical bonding to the metal substrate was indicated.

The coating on one of the specimens prepared by grit blasting spalled after curing, whereas coatings on the other two were pulled off in the tensile test. Portions of the metal substrate covered with adherent fragments were 100, 60, and 50 percent. Degree of bonding of the coating fragments was the same as for the untreated substrate; viz., they could not be removed with a finernail but they could with a sharp steel blade.

Coatings spalled off all three specimen substrates that were oxidized before coating. Proportions of adherent fragments were 10, 25, and 90 percent.

Coatings also spalled off the untreated glass surface after curing. Proportions of adherent fragments on the smooth glass surface were 10, 10, and 25 percent. The phosphate-bonded ZrO_2 coating bonded to untreated Hastelloy-X better than it did to untreated glass.

ARC-PLASMA JET TESTS

General

Performance of phosphate-bonded ZrO_2 coatings under the thermal and chemical conditions of the arc-plasma jet test was excellent. More than 30 test specimens in which the coating was 5-mils or less thick and applied to grit blasted substrates survived more than 100 different tests*. During these tests, coatings were exposed to surface temperatures as high as 4100 F**; to 25 thermal shocks from 70 F to the test temperature to 70 F; and to at least 5-minutes total test duration. Phosphate-bonded ZrO_2 coatings under these conditions did not melt, spall, corrode, erode, or crack. Coating and test variables included coating thickness, heat flux through the coating, arc-plasma gas composition (argon and argon-oxygen), phosphate-binder, fluorine (as HF), and water content. Special coated specimens included:

1. Specimen 54-2, a standard Hastelloy-X coupon which was coated in two successive, complete operations. The first layer of coating was cured before the second layer was applied and cured. (This specimen is discussed on pages 85 and 86.
2. Specimen 66-1, a standard Hastelloy-X coupon coated with an excessively thick coating (6 mils), in which special precaution was taken to avoid flexing the specimen before testing. The Hastelloy-X substrate was held rigid in the arc-plasma jet test fixture during coating, curing, and test operations. (This specimen is discussed on page 88.)
3. Specimen 73-T, a stainless-steel tube coated with a thick layer of coating. (This specimen is discussed on pages 86 and 87.)

All pertinent results are discussed in the following parts of this section, and the data plus photographs of specimens are presented in Appendix F. Description and evaluation of many specimens, particularly those tested early in the program, are omitted. Discussion of early data is of less importance and, in view of the newer data, would be repetitious. When evaluating these results, it is essential to note the complexity of the test and degree of accuracy of some measurements, such as of surface temperature. Meaningful evaluation of these tests must be based on consideration of all factors together, such as slurry composition (HF, H_3PO_4, H_2O, and ZrO_2 contents), special substrate preparation procedures, method of slurry application, coating thickness, test conditions, and purpose of test (e.g., heat flux calibration or coating performance).

---

*One exception out of more than 100 tests was specimen 58-2, test areas 3 and 4; this failure could be considered atypical because examination of the specimen showed that adherence was poor in this area.

**All reported temperatures are uncorrected optical pyrometer temperatures unless otherwise stated.

Appearance

Appearance of coatings that were tested below their fusion temperature changed little. In general, the only visible change was the color, which turned from light grey to light beige, Fig. F-1, of specimens 39-1 area 1, 39-2, 46-2, 55-2, 72-1 and 2. On one occasion when the argon plasma gas contained higher than normal oxygen impurity, oxides from the copper and tungsten electrodes were deposited in a ring around the test area, Fig. F-1, of specimen 38-2. Changes in hardness were sought by scratching with a steel probe, and changes in surface texture were sought at a magnification of 50 using a steromicroscope. When the coating fused it became transparent; see Fig. 3 of the test bars in previous section.

Oxidizing and Reducing Atmospheres

Specimen 38-2 was tested in neutral and oxidizing atmospheres without any difference in coating performance. The first two tests were performed using argon arc gas only. The coating survived the standard test sequence with surface temperature in both test areas of 3900 F. Oxygen was mixed with the argon arc gas in a 1:4 ratio during the next three tests by adding it through the powder-feed port of the arc-plasma gun. Power had to be increased substantially to drive the coating surface temperature to 3900 F because of the added heating requirement of the oxygen. No changes occurred in the first two tests at surface temperatures of 3500 and 3700 F. In the third test, however, burnout (i.e., backside coolant failure) occurred as the specimen was being centered during the test. The 600-ampere setting used to test this area was the highest power input of all tests performed during the program.

Specimen 39-2 was tested in neutral (argon) and reducing (argon/5% hydrogen) arc gases without apparent differences in coating stability. The principal effect of testing in the reducing atmosphere was the appearance of scattered, minute black flecks in the hot zone. Based on thermodynamic estimates, phosphate-bonded systems would not be expected to be stable in high concentrations of hydrogen at elevated temperatures; reduction to lower oxidation states and ultimately to elemental phosphorus, accompanied by vaporization of the products, appears energetically favored at roughly 2500 F and above under 1 atmosphere of hydrogen pressure.

Microstructural Changes

Microscopic examination of coatings after they had been tested in the arc-plasma jet provided very useful information as to the character of the coating system. Initial sintering temperature and degree of densification of the ZrO_2 grains were directly noted, while strength and resistance to thermal shock were correlatable. Of major note was the lack of gross cracking both parallel to the surface and perpendicular to the surface, even under extreme thermal conditions.

Even though coated specimens were vacuum infiltrated with epoxy for mounting, preparation of satisfactory ceramographic specimens was difficult. First, coatings were often damaged, although not visibly, when the large test specimen was cut into small pieces for mounting. The reason was that all cutting procedures flexed the Hastelloy-X four times each in a different direction because the squared specimen had to be cut on each side. The most satisfactory method of sectioning specimens was using a large paper cutter, but even so, the Hastelloy-X coupon was bent enough to damage the coating. The greatest advantage of the paper cutter was that the porous coating was not saturated with coolant water as was the case when using a diamond or SiC cutting wheel. Second, many of the ZrO_2 grains were broken out during grinding and polishing operations, even though care was taken to avoid this damage.

Direct observation of the cementitious phase was not possible because it was indistinguishable from the mounting epoxy. Special microscopy techniques were not attempted, such as use of polarized light, to distinguish between these two phases. One effort was made to do so by dyeing the epoxy black. Results were inconclusive, however, because the dye was not opaque at high magnification.

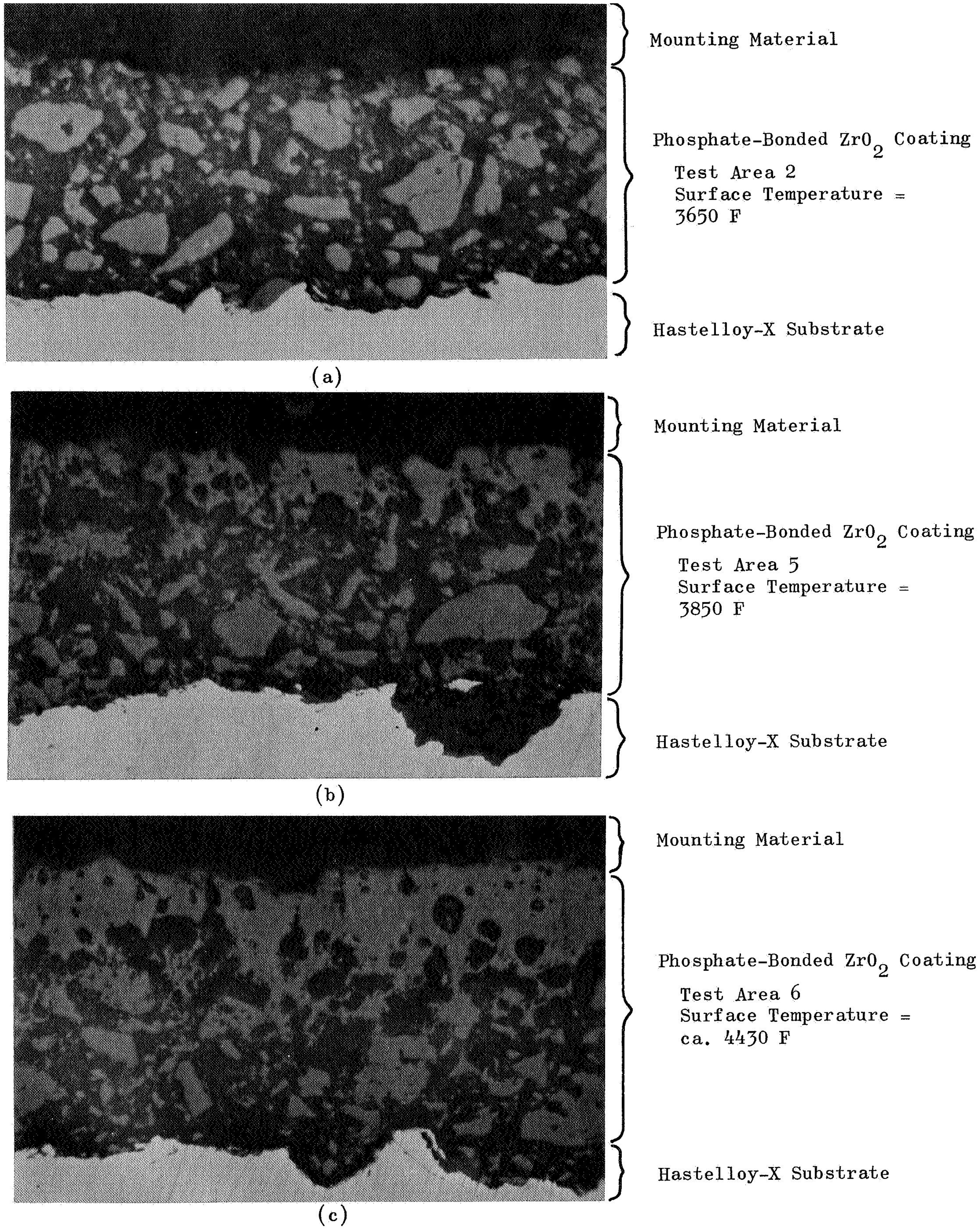
Mounting Material
Phosphate-Bonded ZrO_2 Coating
Test Area 2
Surface Temperature = 3650 F
Hastelloy-X Substrate
(a)
Mounting Material
Phosphate-Bonded ZrO_2 Coating
Test Area 5
Surface Temperature = 3850 F
Hastelloy-X Substrate
(b)
Mounting Material
Phosphate-Bonded ZrO_2 Coating
Test Area 6
Surface Temperature = ca. 4430 F
Hastelloy-X Substrate
(c)

Figure 11. Cross Sections of the Coating on Specimen 72-6 After Testing in the Arc-Plasma Jet. (The white areas in the coating are ZrO_2 grains; the dark areas include cementitious material, epoxy, and voids. Magnification X400)

No sensible changes in the coating system were apparent to ca. 3650 F (Fig. 11a). ZrO_2 grains at the surface still had sharp corners and had not sintered. At ca. 3850 F, ZrO_2 grains to a depth of about 1/4 the thickness of the coating sintered, but sintering was not accompanied by cracking or spalling of the coating (Fig. 11b).

Sintering and densification of the ZrO_2 grains was pronounced above 4000 F. Figure 11c is a photomicrograph of an area in which surface temperature reached ca. 4430 F, where the coating fused. The test was ended before the thermal cycling phase because the coating would have spalled. But at this stage, the coating was still adherent, free of gross cracks, and had not deteriorated.

Microscopic examinations of other test areas that were subjected to thermal conditions much higher than design requirements were also noteworthy. These coated areas were apparently more brittle or more weak than otherwise, because most of the coatings broke away during sectioning, mounting, grinding, and polishing operations. Surface temperature in the area shown in Fig. 12a reached ca. 4460 F before the test was ended. Although the ZrO_2 grains in the outer half of the coating thickness fused, and although the coating densified and microcracks were observed at 50X using a steromicroscope, the coating still did not spall. Possible microcracks are apparent in the photomicrograph perpendicular to the surface, but cracks parallel to the surface at the boundary between the uneffected and sintered layers of coating material, which could cause spalling, were not found. The test area that is shown in Fig. 12b was subjected to a surface temperature as high as ca. 4450 F before the end of the test. Although some deterioration is apparent in the outer one-fifth stratum, the coating was still intact in the area shown. This shows amazing durability under very harsh conditions.

Phosphate Binder Content

Formulations of phosphate-bonded ZrO_2 coatings that were tested in the arc-plasma jet contained either 0.5 or 1.1 parts by weight binder solution No. 4 per 10.0 parts ZrO_2 powder. Based on the results, no major difference in coating performance due to the phosphate content was noted. It should be pointed out, however, that the 1.1 parts per 10.0 parts ZrO_2 formulation

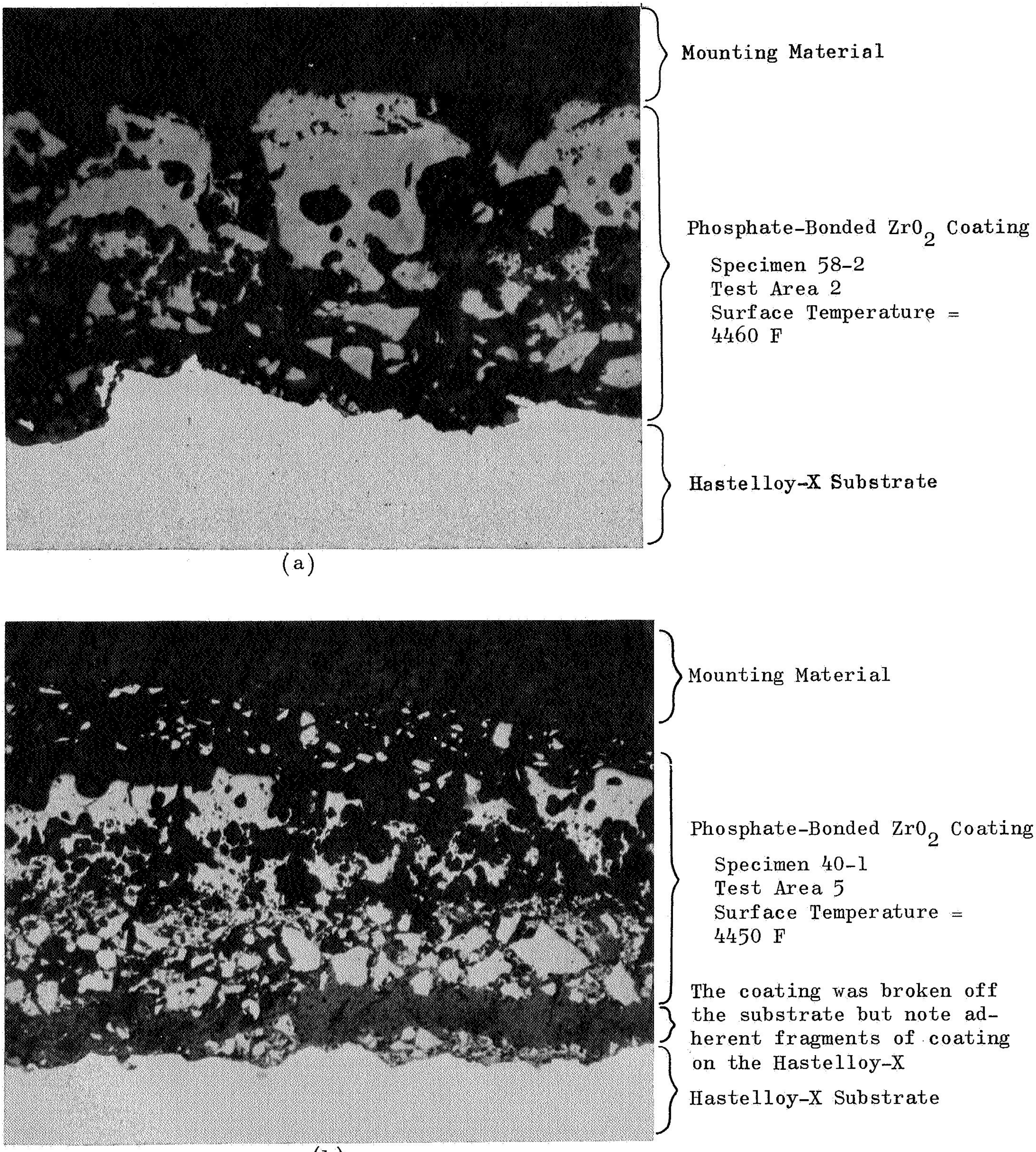
Mounting Material
Phosphate-Bonded ZrO_2 Coating
Hastelloy-X Substrate
Mounting Material
Phosphate-Bonded ZrO_2 Coating
Hastelloy-X Substrate

Specimen 58-2
Test Area 2
Surface Temperature =
4460 F

(a)

Specimen 40-1
Test Area 5
Surface Temperature =
4450 F

The coating was broken off the substrate but note adherent fragments of coating on the Hastelloy-X

(b)

Figure 12. Cross Sections of Coatings That Were Subjected to Thermal Conditions in the Arc-Plasma Jet Much More Severe Than Service Conditions in a Thrust Chamber (The white areas in the coating are ZrO_2 grains; the dark areas include cemetitious material, epoxy, and voids. Magnification X400).

was used on almost all of the specimens tested in the arc-plasma jet, whereas performance of the 0.5 parts is based on results from only one specimen (46-2). This coated specimen was tested in three areas. It survived all steady-state and cycling phases of testing with surface temperature of 3800 and 4000 F in two of the areas. No significant changes were noted at 3800 F in stereomicroscopic examination of the surface or in high-power microscopic examination of the mounted section. The only change that occurred as a result of the 4000 F test was incipient sintering of the ZrO_2 on the outer stratum of coating. In the third test, surface temperature in the center of the test area (Fig. F-1e, area 2 in Appendix F) was 4400 F. Because the coating fused on the surface, it was not thermally cycled. This particular test is irrelevant to the present discussion because the surface temperature was well over the design requirement.

It should also be pointed out that another specimen with this formulation, number 58-2, was the only specimen with a coating thickness less than 5 mils that failed in arc-plasma jet tests. The coating on this specimen failed in two areas after nine and seven thermal shocks. Test temperatures during the steady-state phase of testing in the two areas were 3850 and 3815 F, respectively. Microscopic examination after testing indicated that failure was caused by poor adherence, so this test should be discounted.

Fluoride and Water Content

Water content in slurry formulations varied between 1.3 and 2.0 parts by weight water per 10 parts ZrO_2 powder. No apparent difference in coating performance due to water content was noted in arc-plasma jet tests. Considering the large number of variables in these screening tests, water content was considered of minor importance, so that the testing was not specifically directed at studying this factor.

The only noticeable change in HF content (or more correctly, in HF to H_3PO_4 ratio) in slurry formulations was in specimen 40-2. The slurry that was used to prepare the specimen did not contain any fluoride in the binder solution. The binder was 1.05 parts H_3PO_4 per 10.0 parts

ZrO_2. This coating survived two tests in which surface temperatures were 3670 and 4000 F. Nothing unusual was observed in posttest examination other than that the ZrO_2 grains were packed closer together. Use of fluoride-free binder solutions was not pursued, however, because of inconsistency in coating hardness after curing. One-half of the cured coating on the specimen was hard, whereas the other half was soft enough to be scraped with a fingernail. Because of this inconsistency in hardness, slurries without a small amount of fluoride were not used. Testing was performed on the half that was hard.

Adherence

The coating in many of the specimens that were mounted for microscopic examination separated from the Hastelloy-X substrate. This was true of coated areas that had, and had not, been tested in the arc-plasma jet. These coatings most probably broke away from the substrate when the section to be mounted was cut from the larger test coupon. If the coatings had been separated from the substrate before testing in the arc-plasma jet, they could not have survived any of the tests. Surface temperature would have been above the melting temperature of ZrO_2 even in tests at low heat flux levels, because of the high thermal resistance across the gap between the coating and the Hastelloy-X substrate. Because all coatings survived, separation must have occurred after testing.

Many adherent fragments of coating were observed on the Hastelloy-X substrate after coatings broke off (Fig. 12b). This indicated that failure was not adhesive, but rather it was cohesive. The coatings broke cohesively at the stratum just across the peaks of the roughened Hastelloy-X substrate, where the stress was most concentrated and where the coating was weakest.

Double Coating Layer

The coating on specimen 54-2 was applied in two operations; i.e., the first layer was cured before the second was applied and cured. The coating failed during arc-plasma tests, but results were not clear. It could not be resolved whether the coating spalled during testing because the layers separated or because the coating was too thick. Other coatings as thick, ca. 7 mils, never survived testing even though they were applied as one layer. Microscopic examination did not resolve the question: the two layers were indistinguishable in some areas, whereas an interface or gap was visible in other areas.

Tubular Specimen

A tubular specimen (73-T) was coated with the phosphate-bonded ZrO_2 coating (formulation B45) and tested in the arc-plasma jet. The purpose of this test was to gain an indication whether difficulties would arise in applying and curing the coating on a convex shape and whether the coating would stay on a convex surface during testing. Hastelloy-X tubing was not available, so type 347 stainless-steel tubing with a 0.012-inch wall and 0.450-inch OD was substituted. The substrate was distorted by grit blasting with -20 mesh Al_2O_3. Distortion of the tubing occurred, probably because of the comparatively large diameter. Smaller tubing, particularly if it is brazed together, such as in a thrust chamber wall, does not ordinarily distort when grit blasted. The slurry coating was sprayed on while the tube was rotated slowly in a drill chuck. Thickness, which was measured after testing, varied from 5 to 8 mils. About 40 percent of the coating spalled in long, wide strips running axially along the tube after cooling from curing at 600 F. The coating that remained was adherent, without visible cracks, and satisfactory for arc-plasma testing. Spalling was not unexpected because the coating was applied on 347 stainless steel rather than Hastelloy-X and the coating was excessively thick. This coating was designed for use on Hastelloy-X which has a lower expansion coefficient than the stainless steel.

The procedure for arc-plasma testing was the same as it was for flat specimens. The specimen was cooled internally with water, and the coated area was swung in and out of the arc-plasma jet as usual. The actual test sequence is listed below:

Amperage	Duration, seconds	Coating Thickness, mils	Surface Temperature, F	Comments
280	180	5.0	3410	No change
285	180	7.7	3450	No change
305	180	6.3	3700	No change
	(25 thermal shocks)			No change
	180			No change
358	180	8.0	4000	No change
	(20 thermal shocks)		(>>4000)	Started to melt

The coating finally melted substantially above 4000 F; it apparently separated from the metal first and then melted because it was no longer cooled on the back side.

Although this was a cursory test, it did indicate that the coating system can be applied to the outside surface of tubes, and it can survive severe thermal shocks on a convex surface. More significant results would be expected using Hastelloy-X tubing.

A significant observation regarding adherence was made on this specimen. After testing in the arc-plasma jet, the tubular specimen was heated with an oxyacetylene torch without cooling water flowing on the inside of the tube. On cooling, all of the coating spalled except where it had been subjected to the arc-plasma jet. The coating in these areas was still adherent. Apparently, adherence had been improved under plasma-jet test conditions.

Thick Coatings

Coatings applied in excess of 5 mils thick, on flat substrates, did not survive 25 thermal shocks at elevated temperatures, i.e., between 3500 and 4000 F. Results of several specimens with thick (5 to 10 mils) coatings tested early in the program are not reported because the coatings cracked and spalled, in some cases, when mounted in the holding fixture. The reason for this was that the thick coating crimped when the distorted substrates were straightened by clamping in the holder. Distortion, as described earlier, was caused by gritblasting.

Specimen 66-1, on the other hand, was coated and cured while it was mounted in the arc-plasma jet test holder. Through this procedure, the coating was preserved undamaged after curing. Results were no different, however: the coating survived only 12 and 18 thermal shocks at 3600 F and 4065 F, respectively.

DISQUALIFIED COATING SYSTEMS: RESULTS AND DISCUSSION

FLUOROSILICIC ACID-BONDED SYSTEMS

Introduction

Oxide systems bonded with fluorosilicic acid (H_2SiF_6) were prime candidates in this program because they were reported to be better than oxides bonded with phosphoric acid (Ref. 8 and 9). Reasons for being better were (1) working time of the slurry before any reactions occurred was longer, and (2) coated specimens were found to perform better during thermal tests. Of the oxide systems reported, best composition was (by weight):

70 parts ZrO_2
7 parts H_2SiF_6
1 part $NH_4H_2PO_4$

The resulting amount of SiO_2 by weight would be 1.4 percent. Bars made from water-free ram mixes yielded flexural strengths between 700 and 940 psi. $NH_4H_2PO_4$ was added to retard the bonding reaction rate, as it did in systems bonded with H_2PO_3F. The retarding mechanism was not stated.

A literature search for identification of the reactions of H_2SiF_6 with ZrO_2 or other refractory oxides was unsucessful. A search for the character and properties of H_2SiF_6, however, showed that H_2SiF_6 evaporates at 105 F without leaving any residue (Ref.10), and this was subsequently verified by experiment.

Because H_2SiF_6 evaporates without residue, cementitious bonds will not form unless it reacts with ZrO_2 or SiO_2 is precipitated. Thus, initial studies were pointed at determining the bonding mechanism between ZrO_2 and H_2SiF_6.

Bonding Studies

Five slurries were formulated (Table 10). Slurry C7 was the state-of-art formulation, C8 was the same but without the retarding agent, $NH_4H_2PO_4$, and C9 and C10 were the same as C7 and C8, respectively, except that twice the amount of H_2SiF_6 and $NH_4H_2PO_4$ was added. Slurry C11 contained $NH_4H_2PO_4$ but no H_2SiF_6. No water was added. Slurries were cast into 1/4- by 1/4- by 1-inch bars, and bars of each formulation were cured to 400 F by three different heating schedules.

TABLE 10

COMPOSITION AND PROPERTIES OF SELECTED ZrO_2 SYSTEMS CONTAINING H_2SiF_6 AND $NH_4H_2PO_4$

Slurry Identity	Composition (parts by weight)			Bulk Density, g/cc	Flexural Strength in 3-Point Loading, psi	Weight Loss (parts by weight)
	ZrO_2	H_2SiF_6	$NH_4H_2PO_4$			
C7	70	7	1	3.4	405	-
C8	70	7	-	3.3	81	7
C9	70	14	2	3.1	360	-
C10	70	14	-	2.9	96	14
C11	70	-	2	-	371	-

Results clearly showed that bonding was not due to H_2SiF_6 but to the $NH_4H_2PO_4$ addition. Bars made from the state-of-the-art formulation (C7) had a maximum strength of 405 psi compared to the 900 psi reported in the literature. In contrast, bars made from the slurry (C8) with the same amount of H_2SiF_6 but without the phosphate addition, had only a nominal maximum strength, 81 psi. The same result was obtained with bars made from slurries (C9 and C10) which contained double the amount of additives.

Higher strength was not obtained when the phosphate additive was doubled because porosity was high due to the large liquid content and evolution of reaction gases. Studies of material composed of formulations C8 and C10 showed that total weight loss was equal to the original amount of H_2SiF_6.

To demonstrate further that H_2SiF_6 did not contribute to bonding, slurry C11 was formulated. This slurry contained $NH_4H_2PO_4$ and water but it did not contain H_2SiF_6. Flexural strength of bars made of slurry C11 had the same strength as the equivalent slurry formulation containing both H_2SiF_6 and $NH_4H_2PO_4$.

Conclusion

Strength of H_2SiF_6-bonded ZrO_2 systems reported in the literature was due, not to the H_2SiF_6, but to a phosphate compound, $NH_4H_2PO_4$, which was also used in the formulation.

The use of H_2SiF_6 was discontinued in this program. This is not to mean that silica or silicate binders would not be good bonding agents; they may well be. However, simply mixing H_2SiF_6 with a filler material will not produce cementitious bonds. Silica would have to be precipitated from the H_2SiF_6 solution or added in another form.

POTASSIUM SILICATE-BONDED ZrO_2

Three formulations of potassium silicate-bonded zirconia slurries were initially prepared for evaluation. Before evaluation in the arc-plasma jet, 1/4- by 1/4- by 2-1/2-inch bars were cast in Teflon molds for determining flexural strength. Composition of the slurries is listed on the following page. Slurry D1 is the state-of-the-art formulation (Ref. 9).

Material	Slurry D1, g	Slurry D2, g	Slurry D3, g
ZrO_2 (-200 mesh blend)	40.0	40.0	40.0
Kasil No. 1*	2.0	2.0	7.0
K_3PO_4	0.21	---	---
Water	3.0	3.0	---

*Philadelphia Quartz Co.

A curing cycle was selected based on suggested curing schedules by the vendor and by weight-loss studies. Weight loss was not sensible above 200 F for these compositions, and the vendor recommended slow heating to 210 F and a final cure between 300 and 400 F. Two bars of each composition were also heated to 1800 F to determine whether the material would be affected by heating above the softening point of the potassium silicate binder. The softening point (viscosity = 4×10^{17} poise) is ca. 1300 F and the flow point (viscosity = 10^5 poise) is 1660 F. Results are summed below:

Slurry Formulation	Final Cure Temperature, F	Density, g/cc	Modulus of Rupture, psi
D1	400	3.4	1900
D1	1800	3.4	1615
D2	400	3.3	698
D2	1800	3.4	860
D3	400	3.2	2217
D3	1800	3.3	2290

Bars which were formulated without the setting agent, K_3PO_4, were soft on the bottom because the water-soluble binder migrated upward during drying. The setting agent was henceforth used, although a phosphate compound could be harmful by fluxing the silicate binder phase. Room temperature strength values of these materials were adequate and further studies, were directed toward improving high-temperature properties.

An arc-plasma test specimen was prepared using the state-of-the-art formulation (D1), except that water was added so that the slurry could be applied as a uniform, thin coating. The resultant formulation was:

10.0-g ZrO_2

0.5-g Kasil No. 1

0.04-g K_3PO_4

1.36-g water

After curing, the coating was weak and porous. Even so, it was tested in the arc-plasma jet. Surprisingly, the coating survived a steady-state test in which surface temperature was 3650 F, but it failed instantly on the first thermal cycle. Lack of strength was related, evidently, to the excess water content added to obtain a usable slurry consistency that would be tractable for spray coating equipment.

Because of this lack of strength in the cured coating, two more formulations that contained 5 and 10 times the amount of binder of the state-of-the-art formulation were prepared. The setting agent was increased proportionally, and sufficient water was added to make a thin slurry consistency. Increasing the binder content by this amount was reasonable, because the state-of-the-art formulation only contained 1.45 percent by weight of potassium silicate. Slurry compositions were:

Slurry Identity	D1	D6	D5
ZrO_2	10.0	10.0	10.0
Kasil No. 1	0.5	2.5	5.0
K_3PO_4	0.04	0.2	0.4

The slurries were applied to metal substrates as thin coatings and cured as before, without difficulty. Cured coatings made from slurry D1 again were so soft that they could be scraped off with a finger nail. Coatings made from slurries D5 and D6, in contrast, were hard and strong. Coating thickness was 3 to 4 mils.

Coating performance in ar-plasma jet tests was inconsistent and, in general, poor. Although each specimen that was tested survived at least one test out of an average of four, these results were very poor because surface temperature, and hence heat flux, was very low in each case. Best performance was shown by specimen 32-6 which survived 25 thermal shocks from 3700 F. However, this same specimen failed three subsequent tests at temperatures of 3100 and 3400 F. Highest surface temperature reached in all of the tests was 4000 F where the coating fused (specimen 32-2, area 5). All other specimens showed poor resistance to thermal shock. Table 11 presents a summary of test results and Fig. 13 shows the specimens after testing.

Summary

Potassium-silicate-bonded ZrO_2 coating systems were dropped from contention because performance was much inferior to phosphate-bonded ZrO_2 systems, and they showed little indication that they could be improved sufficiently to meet the objectives of this program.

BARIUM ZIRCONATE SYSTEMS

Silicate Bonded

Cementitiously bonded $BaZrO_3$ systems had not been studied previously. Because there were no criteria for formulating these systems, the same slurry formulations as for ZrO_2 systems were used. Formulations for silicate-bonded systems were (parts by weight):

Slurry Identity	H1	H2	H3
$BaZrO_3$ (Zircoa, -325 mesh)	10.0	10.0	10.0
Kasil No. 1	0.5	2.5	5.0
K_3PO_4	0.04	0.2	0.4

TABLE 11

ARC-PLASMA TEST RESULTS OF SPECIMENS COATED WITH SILICATE-BONDED ZrO_2: A SUMMARY

Specimen	Slurry	Surface Temperature, F	Results
14	D1	3600	Spalled on first thermal shock
		3600	Spalled on second thermal shock
30-1	D1	3400 (Hot Spot 3700)	Survived 25 thermal shocks
		3635	Survived 25 thermal shocks but hot-spot temperature increased to 4350 F
		3600	Spalled on first thermal shock
		3700 ⟶ 4500	Spalled on first thermal shock
30-3	D1	3200	Spalled on first thermal shock
		3350-3450	Spalled on first thermal shock
		3850	Spalled on first thermal shock
		4000	Spalled after 50 seconds of steady-state phase of test
32-2	D6	3450 (Hot Spot 3725)	Survived 25 thermal shocks
		3400-3500	Spalled on sixth thermal shock
		3500	Spalled on fourteenth thermal shock
		3850	Spalled on second thermal shock
		4000	Surface fused; not thermally cycled
32-6	D6	2840	Survived 25 thermal shocks
		3000-3100	Spalled on seventeenth thermal shock
		3200 ⟶ 3400	Spalled on thirteenth thermal shock
		3360	Spalled on thirteenth thermal shock
		3600 ⟶ 3700	Survived 25 thermal shocks

⟶ = Changed during test

TABLE 11

(Concluded)

Specimen	Slurry	Surface Temperature, F	Results
31-1	D5	3350	Survived 25 thermal shocks
		3450-3550	Spalled in one small area during thermal cycling; remainder of test area survived 25 thermal shocks
		3700-3800	Blistered and spalled during steady-state phase of testing

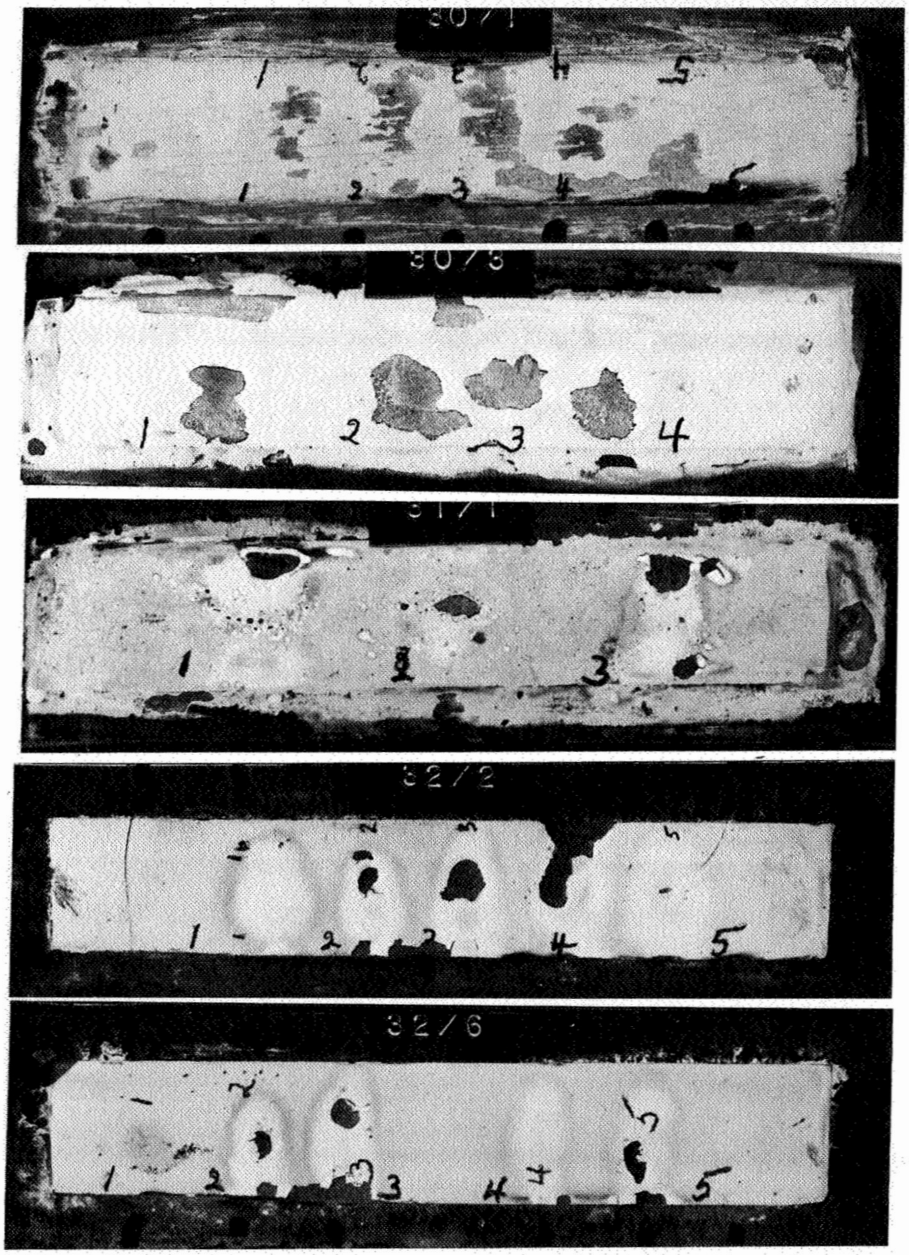
30/1
30/3
31/1
32/2
32/6

Figure 13. Silicate-Bonded ZrO_2 Specimens After Arc-Plasma Jet Tests (Specimen Size is 1.5 by 4.5 Inches)

After enough water was added to make a paint-like consistency, these slurries were easily applied as thin coatings by brushing. Curing was the same as for silicate-bonded ZrO_2 coatings. Thickness of coatings that were prepared for arc-plasma jet tests was 1-1/2 to 4 mils.

Slurries H2 and H3 resulted in uniform, hard coatings whereas slurry H1 resulted in a very soft coating. This was consistent with the potassium-silicate-bonded ZrO_2 systems.

Results of arc-plasma jet tests (Table 12, Fig. 14) showed that this coating system was better than the potassium-silicate-bonded ZrO_2 system but that it was still much inferior to the phosphate-bonded ZrO_2 system. Although the coating survived a few tests, coating performance was poor and erratic.

Phosphate Bonded

Formulations of phosphate-bonded $BaZrO_3$ systems were also based on experience with phosphate-bonded ZrO_2 systems. Use of HF with the H_3PO_4 binder was not necessary, however. In fact, mixtures of H_3PO_4 and HF reacted violently with $BaZrO_3$. Enough heat was evolved in one case to melt the container, a polyethylene beaker. HF additions were eliminated and H_3PO_4 alone produced good bonding. A satisfactory coating was applied to an arc-plasma jet test specimen (33) using 2.0 parts by weight H_3PO_4 per 10 parts $BaZrO_3$ plus enough water to make a trowelable slurry. Curing cycle was the same as for phosphate-bonded ZrO_2 systems. Coatings were hard but they contained many pit defects. Although of poor quality, this coating formulation was tested in the arc-plasma jet.

Performance in the arc-plasma jet test was poor. The coating failed by spalling in every test in which surface temperatures of 3000 to 4000 F were reached (Fig. 14 and Table 12).

TABLE 12

ARC-PLASMA TEST RESULTS OF SPECIMENS COATED WITH CEMENTITIOUSLY BONDED $BaZrO_3$: A SUMMARY

Coating System	Specimen No.	Slurry Identity	Surface Temperature, F	Results
Potassium Silicate-Bonded $BaZrO_3$	36-1	H2	3750 to 3900	Survived 25 thermal shocks
			3900 to 4000	Spalled and melted on forth thermal shock
			4000	Spalled on second thermal shock
			3700	(Oxygen was added to the test gases.) Spalled on tenth thermal shock
Silicate-Bonded $BaZrO_3$	37-2	H3	3400	Spalled on eighth thermal shock
			3540	Spalled on sixth thermal shock
			3540	Spalled on fifteenth thermal shock
			3800	Spalled on fifteenth thermal shock
			4000	Survived 25 thermal shocks
			4000	Spalled on fifteenth thermal shock
Phosphate-Bonded $BaZrO_3$	33	F4	3600	Partial spalling during 25 thermal shocks
			3760	Spalling gradually increased; complete failure after 7 thermal shocks
			3870	Spalled on second thermal shock
			3920	Spalled on forth thermal shock
			4000*	Temperature increased to 4450; specimen was not thermally cycled

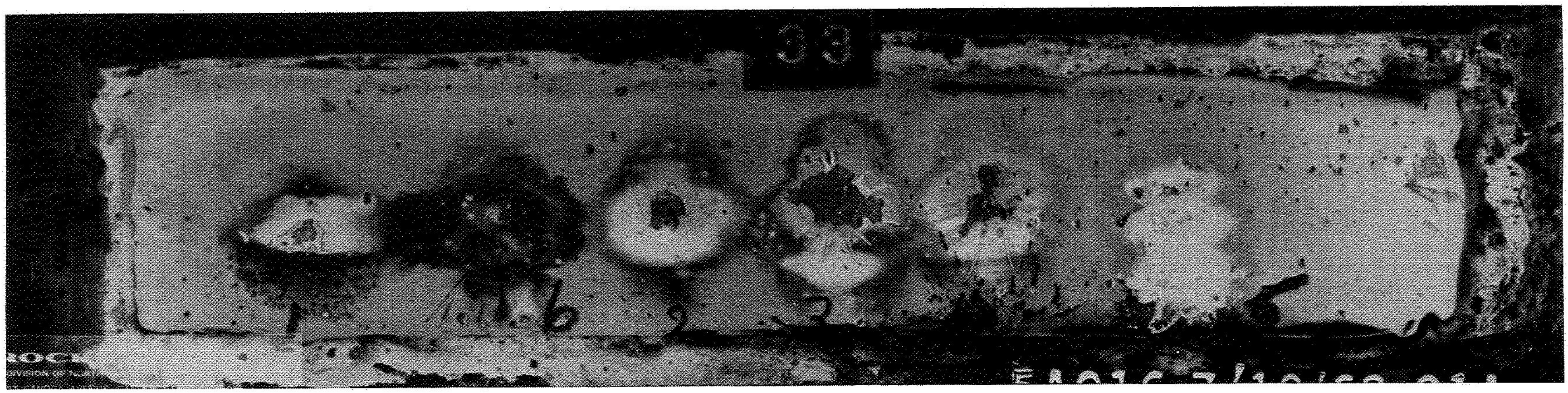

Phosphate-Bonded $BaZrO_3$

Potassium-Silicate-Bonded $BaZrO_3$

Figure 14. Cementitiously Bonded $BaZrO_3$ Specimens After Testing in the Arc-Plasma Jet (Magnification X1-1/2)

Summary

Use of $BaZrO_3$ as a filler in cementitiously bonded coating systems was discontinued because of the poor quality of resultant coatings and their poor performance in arc-plasma jet tests.

HAFNIA-RICH MIXED OXIDE SYSTEMS

Monolithic Coatings

Cementitiously bonded hafnia-rich mixed oxide (HRMO) systems had not been studied previously, so no criterion for formulating coatings existed. However, because HRMO material is mostly HfO_2 and ZrO_2 and both of these oxides are the same chemically, formulations were based on experience in this program with phosphate-bonded ZrO_2 systems. By the time this material was evaluated in Task II, experience was that one binder, H_3PO_4, was superior to the others that were selected for evaluation. For this reason, only phosphate-containing bonding agents were used to prepare cementitiously bonded HRMO systems.

First, a systematic study was made by preparing 10-gram batches of slurries containing selected binder concentrations. Results showed that a small amount of HF in the binder solution was required to promote bonding. Therefore, binder solution No. 4 was selected for all further studies. Binder slurries containing selected amounts of binder solution No. 4 were cast into bars and cured using the slow schedule that was used for bars made of phosphate-bonded ZrO_2. The best formulation was 10.0-g HRMO, 1.1-g BS No. 4, plus 1-g water. This formulation was selected as best based on hardness, strength, and visual observation. Bars made from this formulation were hard, yet they were weak. This was contrary to results in the phosphate-bonded ZrO_2 system where hardness was proportional to strength at room temperature. Even though it was weak, this phosphate-bonded HRMO material was used to prepare arc-plasma jet test specimens.

Slurries of the above formulation were sprayed on two arc-plasma jet test specimens, and both specimens were cured while clamped flat in the test fixtures. This was done so that the specimens would not have to be flexed after curing, because all substrates were bowed due to grit blasting. Coating thickness averaged 3-1/2 and 4 mils in the two specimens.

The cured coatings spalled from the substrate, apparently because of low strength of the coating material plus a large mismatch in thermal expansion between the coating and Hastelloy-X substrate. The metal substrate has an expansion coefficient almost triple that of the coating. The HRMO was accordingly dropped from consideration in this program for a monolithic coating design.

Graded Coating

Two more specimens were prepared, using the graded coating concept. The first layer was phosphate-bonded ZrO_2 (B45), while the second (outer) layer was phosphate-bonded HRMO. This system represented a progressive decrease of thermal expansion across the thickness of the coated system. The HRMO material did not spall when it was cured. Average thickness of the individual layers was about 3-1/2 to 4 mils, for a total coating thickness of about 7 to 8 mils.

These graded coatings performed poorly in the arc-plasma jet tests. They spalled immediately when tested under a high flux condition, and failed gradually when tested under low heat flux conditions where surface temperatures were 3500 F or less at the start of the test.

Summary

Use of the phosphate-bonded hafnia-rich mixture of oxides was not pursued because of its poor strength and poor performance in arc-plasma jet tests.

THORIA-BASED SYSTEMS

General

ThO_2-based cementitiously bonded systems, which were one of the two major candidate systems for this program, were reported in the literature to have been successfully tested as 1/4 to 1 inch thick heat shields in oxyacetylene torch tests. These thick layers, which were radiation cooled on the back side during testing, survived both steady-state and thermal cycling tests to 4000 F. Potentially, then, ThO_2-based systems could be even more attractive than ZrO_2-based systems because ThO_2 is more thermally and chemically stable and it does not undergo a phase change on heating. ThO_2-based systems have not been studied and evaluated as extensively as ZrO_2-based systems, however. Bonding agents previously investigated included H_2PO_3F, potassium silicate, and $Th(NO_3)_4$.

ThO_2 systems bonded with H_2SiF_6 and the water-soluble potassium-silicate were not evaluated in arc-plasma jet tests, because neither of these bonding agents showed any promise in previous studies performed in this program on ZrO_2-based systems. Two bonding agents thus remained to be evaluated in this series of tests, $Th(NO_3)_4$ and the phosphate binder solution that was successful in ZrO_2-based systems.

Thorium Nitrate Binder

Thorium nitrate was unsatisfactory as a bonding agent. Slurries containing 5, 10, 15, and 20 percent by weight of $Th(NO_3)_4 \cdot 4H_2O$ plus enough water to yield a pourable slurry consistency were applied on metal substrates, air dried, and cured slowly to 1000 F. All coatings were soft and chalky, and the coatings containing 15- and 20-percent $Th(NO_3)_4 \cdot 4H_2O$ cracked and spalled in several areas.

In situ formation of nitrate bonds was attempted by adding 5 percent by weight of concentrated nitric acid to ThO_2 powder. The mixture was aged overnight at room temperature before water was added to yield the desired consistency. The slurry was applied as a thin coating on metal substrates, dried at 200 F for 2 hours, and cured by slowly heating to 1000 F.

Cured coatings did not crack or spall, but strength of the coating and adherence to the metal substrate were poor. Coatings bonded with HNO_3 were only slightly better than those bonded with $Th(NO_3)_4$. Based on this result, use of nitrates as a bonding agent was abandoned.

Phosphate Binder

Although at least one phosphate-bonded ThO_2 coating system showed much promise for fulfilling program objectives, further development of this coating system was not pursued. It was not evaluated further because of several major disadvantages inherent with ThO_2 and because of the concurrent, highly successful performance of phosphate-bonded ZrO_2 coating systems.

Initial studies of phosphate-bonded ThO_2 systems were conducted using a ThO_2 powder with very small grain size and very narrow size distribution 1 to 4 microns (American Potash Co.). H_3PO_4 with and without HF additions was used as the bonding agent, and water was used as the suspension medium. Coatings were air dried, then cured by heating slowly to a maximum of 1000 F. None of these coating systems had sufficient strength or adherence to metal substrates, and consequently they failed immediately in arc-plasma jet tests.

Because of the poor results in the above study, three different ThO_2 raw materials were next compared in an attempt to develop satisfactory chemical bonding. Coated specimens were prepared and cured as described above. Composition of each slurry was 10.0-g ThO_2, 1-ml 85-percent H_3PO_4, plus 5-ml water.

Source of ThO_2, hardness of the coating, and adherence to the metal substrate are shown on the following page.

Slurry Identity	Thoria Powder	Hardness	Adherence
T19	-325 Mesh, Fused (Cerac)	Hard	Fair
T20	-325 Mesh, Calcined (Zircoa-f 2274)	Hardest	Best
T21	1-4 Micron, 99.9 Percent Pure (American Potash)	Soft	Poor

The ThO_2 raw material that produced the best coating (T20) was a -325 mesh calcined powder. This material was used subsequently in preparing specimens for testing the arc-plasma jet.

Results of arc-plasma jet tests were encouraging but inconclusive. They were inconclusive particularly from the standpoint that only three specimens were tested and two of these had very thin coatings, <2 mils.

Specimen 59-1 (Table 13A and Fig. 15a), which had only a 3/4-mil thick coating, survived all tests in the arc-plasma jet. Test temperatures were as high as 4170 F with hot spots to 4450 F. Specimen 59-2 (Table 13B, Fig. 15b), which had only a 1-3/4-mil thick coating, survived all tests to 4000 F but failed the last one by burnout from the back (i.e., coolant failure). Heat flux through the coated system had to be very high, much greater than 20 Btu/in.^{2}-sec, to drive the surface temperature to above 4000 F in these specimens. This is evidenced by the burnout in the last test for specimen 59-2.

Uniform coating thickness of 3-1/2 mils was difficult to obtain using this slurry, because the ThO_2 settled rapidly during coating operations. One satisfactory specimen was prepared with a coating thickness of 3-1/2 to 4 mils, however, and it was tested in the arc-plasma jet (Table 13C, Fig. 15c). Coating performance was considered to be good, although the coating spalled at the edge on all but the least severe test. Spalling in each case originated at the edge of the coated area where the gasket material was located. Interpretation of the reason for spalling is complicated by edge effects of the coated surface and by hot spots which developed at the edge of the gasket as the specimen was swung in and out of the arc-plasma jet.

True surface temperature in these tests was difficult to estimate. Total normal emittance* increases rapidly from .25 at 3000 F to .65 at 3500 F (Ref. 10). Data at higher temperaters were not available. Another interference with temperature estimation was the formation of many hot spots, which appeared and disappeared during testing. Temperature readings in the test on specimen 60-1 were unusual because temperature remained at about 3800 F for each test, even though power input and coating thickness were both increased in each new test area. Hot-spot temperature, on the other hand, increased to 4550 F in the test area and 5500 F near the gasket. The reason for increase in hot-spot temperature (or more accurately, increase in brightness) is not known, but perhaps hot-spot temperature is closer to true temperature in these tests than is 3800 F. If this is true, these test results are even more noteworthy.

Summary

One formulation of phosphate-bonded ThO_2 showed promise, but this system was dropped in favor of phosphate-bonded ZrO_2 systems because it was still inferior to the ZrO_2-based coatings and it needed further development. Use of ThO_2-based systems also offer the disadvantages of hazard from radioactivity and toxicity, high cost (at least 10 times that of ZrO_2), and apparent limitations on reactivity to the bonding agent related to the grade of powder used.

---

*Spectral emittance at 0.65 microns, which is the wavelength that the optical pyrometer detects, was not available

TABLE 13

ARC-PLASMA TEST RESULTS FOR SPECIMENS COATED WITH PHOSPHATE-BONDED ThO_2

A. Arc-Plasma Jet Test Specimen No. 59-1 Date: 29 July 1968

Purpose or Special Notes: The coating was very thin. Thus, very high heat flux levels were required to drive the surface temperature to ca. 4000 F, and resistance to thermal shock would be expected to be better than for thicker coatings

Water Flowrate: 27.5 lb/min

Test Area	Coating Thickness, mils	Amperes	ΔT_{water}, F	Test Phase	Surface Temperature, F	Comments
1	0.7	300	–	A	–	The arc was unstable; no data collected
2	0.7	350	4.6	A	3860	NC(1)
				B	–	NC
				C	3860	NC, except test area appeared darker
3	0.7	400	5.1	A	4060	Hot spots(4250 F) formed immediately and then slowly disappeared
				B	–	Hot spots formed
				C	4060	Hot spots (4450 F)
4	1.1	425	5.5	A	4100	Hot spots formed and then slowly (within 10 seconds) disappeared
				B	–	NC, except two very small hot spots formed
				C	4170	
5	0.6	450	6.1	A	4160	NC
				B	–	NC, except two very small hot spots formed and then disappeared
				C	4160	NC

(1) NC = no change

B. Arc-Plasma Jet Test Specimen No. 59-2 Date: 30 July 1968

Purpose or Special Notes: The coating was very thin (see comments for specimen 59-1)

Test Area	Thickness, mils	Amperes	ΔT_{water}, F	Test Phase	Surface Temperature, F	Comments
1	1-3/4	300	4.5	A	3275	NC
		350	4.6	A	3630	25 very small hot spots
				B	-	NC
				C	3630	NC
2	1-3/4	400	5.3	A	3815	50 very small hot spots (4550 F) formed; temperature of hot spots decreased to 4000 F
				B		NC
				C	4080	Temperature increased
3	1-3/4	425	5.7	A	4000	50 hot spots (4700 F) formed; hot spot temperature decreased to 4175 F
				B		Hot spots got bright again (4700 F)
				C	4000	Hot spot (4700 F)
4	1-3/4	450	-	A	-	Spalled
5	1-3/4	450	-	A	-	Burnout occurred at edge of gasket

C. Arc-Plasma Jet Test Specimen No. 60-1 Date: 9 August 1968

Water Flowrate: 27 lb/min

Test Area	Coating Thickness, mils	Amperes	ΔT_{water} F	Test Phase	Surface Temperature, F	Comments
1	3.5	275	2.6	A	3700	NC
				B	–	NC
				C	3700	NC
2	3.7	300	3.2	A	3780	Hot spots (4300 F) formed in 10 seconds; and then decreased to 4100 F in 2 minutes. Spalled at edge as it was swung out of the arc-plasma jet
3	3.8	300	3.4	A	3800	6 hot spots (4100 F) formed in 10 seconds
				B	–	17 large hot spots formed at edge of coated area near the gasket. NC in test area
4	4.6	325	3.7	A	3930	Many hot spots (4350 F) all over
				B	–	Spalled at edge
				C	3890	Hot spots (4350 to 4500 F)
5	4.6	350	4.1	A	3820	Edge is 5500 F
				B	–	Edges spalled after 13 thermal shocks

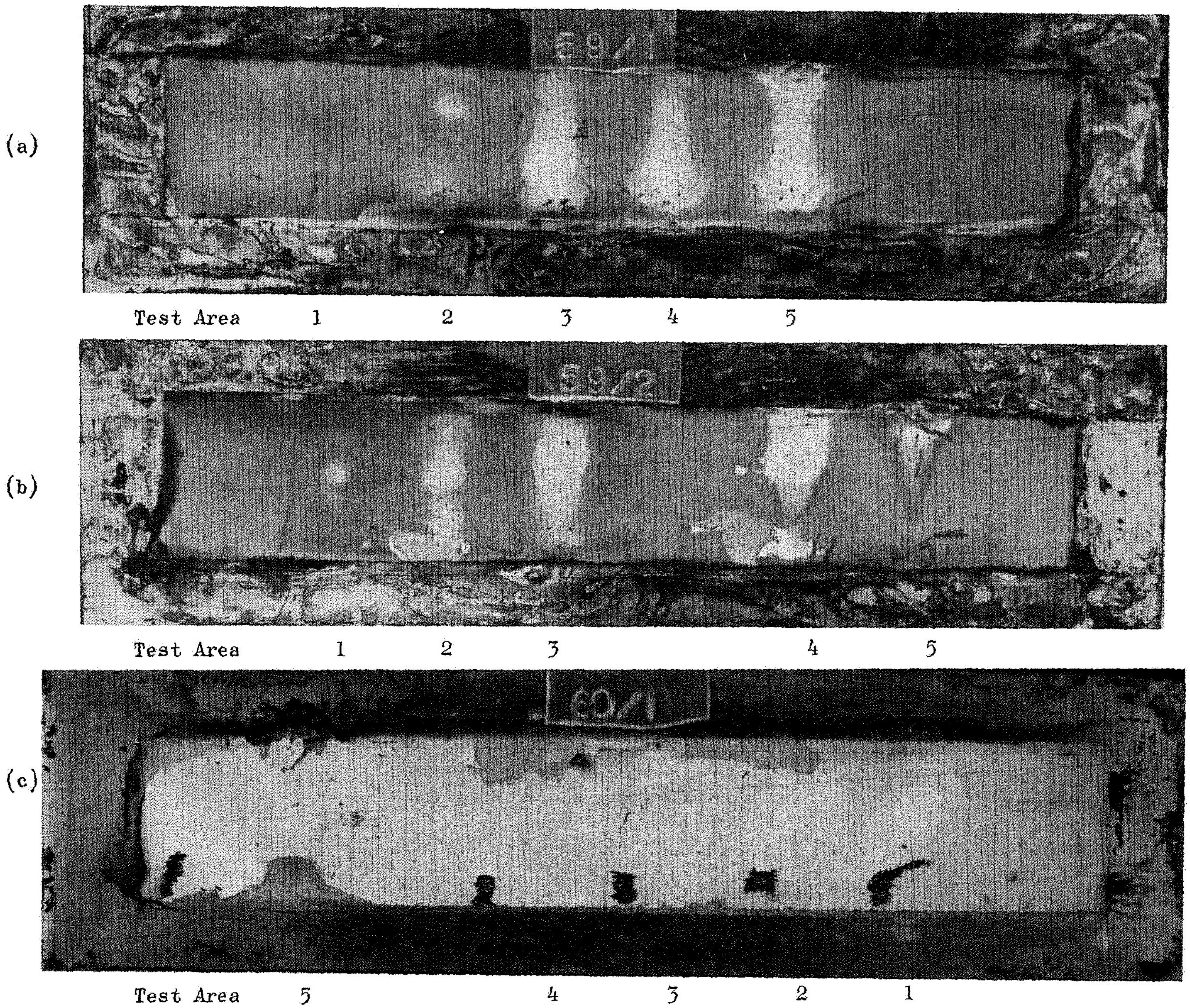
(a)
59/1
Test Area 1 2 3 4 5
(b)
59/2
Test Area 1 2 3 4 5
(c)
60/1
Test Area 5 4 3 2 1

Figure 15. Phosphate-Bonded ThO_2-Coated Specimens After Testing in the Arc-Plasma Jet (Magnification X1-1/2: all specimens are 1-1/2 inch by 4-1/2 inch)

CONCLUSIONS AND RECOMMENDATIONS

CONCLUSIONS

Accomplishments

Goals of the program within the scope of Tasks I and II were accomplished. A heat-barrier coating system was designed and tested that survived all phases of testing in the arc-plasma jet under the reference conditions; viz., surface temperatures to at least 4000 F, multiple thermal shocks, and severe temperature gradients at a heat flux of approximately 20 Btu/in.^{2}-sec. This coating appears capable of reducing the heat flux through the thrust chamber walls in the reference engine from 50 to 20 Btu/in.^{2}-sec, and of reducing the metal surface temperature to below 1600 F. The coating system is a cementitiously bonded material that can be applied by slurry coating techniques, and it requires only a 600 F curing treatment before service at 4000 F. Inexpensive commercial materials are all that are required to prepare the coating and to apply it to small hardware. Coating of large hardware appears entirely feasible but was not demonstrated.

In Task II, a number of cementitiously bonded refractory oxide systems which were selected in Task I were modified as necessary and evaluated in arc-plasma jet tests that simulated the thermal conditions of a rocket engine firing. All appropriate combinations of filler oxides and bonding agents were evaluated for potential use as heat-barrier coatings under the reference rocket engine conditions. One coating system was developed, based on test results, to a point of readiness for further evaluation in tests more closely related to an actual rocket engine firing. All other candidate material systems were significantly inferior to the one selected.

Coating System

The coating system that was developed for further evaluation is phosphate-bonded ZrO_2. The preferred slurry formulation consists of 10.0 grams, -325 mesh, as-received ZrO_2 powder, 1.1 grams binder solution No. 4 (40 parts by volume of 85-percent H_3PO_4 to 1 part of 60-percent HF), and about 1.5 grams of distilled water depending on the desired slurry consistency. Coatings can be readily applied by pour-coating, dipping, spraying, and even troweling if the water content is lowered. Advantages of this slurry coating include:

1. Low thermal conductivity, similar to that of phosphate-free ZrO_2
2. Thermal and chemical stability in oxidizing to slightly reducing atmospheres
3. Resistance to thermal shock
4. Simplicity in slurry preparation
5. Ease and flexibility in coating application techniques
6. Ability to coat large or small, inside or outside, regular or irregular surfaces
7. Low-temperature curing (600 F) for use to 4000 F
8. Low-cost of coating material and application

Disqualified Coating Systems

Coating constituents that were disqualified included the filler oxides ThO_2, $BaZrO_3$, and a HfO_2-rich mixture of oxides, plus the bonding agents H_2SiF_6, potassium silicate, $Th(NO_3)_4$, and H_3PO_4.

RECOMMENDATIONS

Final Qualification for Full-Scale Rocket Engine Test

The phosphate-bonded ZrO_2 coating system has met all program goals to date, but it is still not completely qualified for a full-scale rocket engine test. Arc-plasma tests have been a meaningful and a very severe test that has screened one promising coating system from at least eight different candidate coating systems. Moreover, experimental results have shown ways in which the coating system can be modified, under appropriate guidance, to give fuller assurance of performance in a full-scale rocket engine. On the other hand, the arc-plasma jet has two major limitations. It does not simulate the high shear forces of the combustion gases under engine conditions, nor does it heat a large area of coated specimen. High shear forces of the gases could affect the performance of the coating considerably. Sonic and supersonic gases at high pressures could (1) remove loosely bonded ZrO_2 at the coating surface, (2) get under and spall sections of the coating if cracks had formed and if the coating was poorly bonded to the thrust chamber wall, (3) wash the coating down the wall if too much glass phase forms in the cementitious material in the higher-temperature strata, and (4) possibly increase the effective thermal conductivity of the coated system enough to reduce its degree of thermal protection. The resultant effect of heating larger areas of coated metal could lead to a different stress distribution in the coated system. Designs that survive small-scale arc-plasma jet tests could be affected differently in large areas, requiring design changes to reduce this thermal stress.

The logical next step in qualifying the coating system for a full-scale test is to test it in a small, economical rocket engine simulator. Such an engine will simulate effects of high pressure, shear forces, chemistry, vibration, stress, as well as thermal conditions produced in a large engine, but at a very substantial cost saving. At the same time, because it is cheaper and more flexible, it will allow evaluation of many important coating material and process variables that would not be possible in a full-scale test. Optimization of these variables will be essential for achieving top reliability of the coating system in any full-scale test or actual duty cycle. Such a test and optimization program is recommended.

Study of the Coating Material System and Coating Process

Bonding and Hydration Control. More studies are required to better understand chemical bonding reactions. Strongly developed chemical bonds are vital to successful coating performance. Development of these bonds must be controlled, however, to achieve best coating properties. That is, bonds must be set when the ZrO_2 grains are most densely packed; they must not be allowed to set while water separates the ZrO_2 grains.

Also, premature or side reactions must be prevented in the slurry system so that shelf life of the slurry is prolonged and so that less water is needed to adequately suspend the ZrO_2 grains. Presence of less water means that the ZrO_2 grains will probably be closer together when bonding reactions occur.

Better knowledge of the catalytic role of HF is required to control formation of phosphate bonds and eliminate hydration reactions. Also, other sources of phosphorus in developing phosphate bonding should be explored.

Advanced Application Methods. Unique methods of applying slurrries to thrust chambers may be a solution to existing problems. For example, shelf life of the slurry is presently less than 10 minutes. This could cause production problems in coating larger thrust chambers where large quantities of slurry were needed. One way of eliminating the problem would be to apply a binderless ZrO_2 suspension to the chamber and dry it first. The dried film of ZrO_2 grains would then be sprayed with the binder solution which would saturate the film of ZrO_2. Bonds, hence, would form after the coating was in place and after ZrO_2 grains were closely packed. Another way would be to provide two slurry feed systems to a mixing tank just prior to spraying on the thrust chamber wall. One slurry would be the binderless ZrO_2 suspension and the other would be the binder solution. Thus, shelf life of the slurry would be unimportant because the cementitious slurry would be mixed as it was being applied. Other potential problems to be met by application technology include that of ensuring (and monitoring) the deposition of a uniform coating thickness, within design limits at all points (see further below).

Different Stabilizing Agents. Use of ZrO_2 that is stabilized with oxides other than CaO should be investigated. Use of MgO and particularly Y_2O_3-stabilized ZrO_2 could offer at least one major advantage. These other stabilized zirconia powders may not be subject to destabilization by phosphates at moderately high temperatures as is the case with CaO-stabilized ZrO_2. Also, these stabilizing agents are reported to offer better resistances to thermal shock under certain conditions.

Use of stabilized HfO_2 rather than ZrO_2 should also be explored. The melting temperature of HfO_2 is higher and the phase change, should it destabilize, is slower and occurs at higher temperatures than is the case for ZrO_2.

Thickness Control. Methods of accurately controlling thickness of coatings should be developed. Accurate thickness control of heat-barrier coatings is critical to successful performance in rocket engine thrust chambers, particularly in the reference thrust chamber where heat flux through the chamber wall is at such a high level. In one way this high heat flux is an advantage when designing coatings because only very thin heat barriers are required. But in another sense, it imposes a stringent requirement for coating thickness. Coatings that are too thin, say 3 mils rather than 3-1/2 mils, would be about 14 percent less effective as a heat barrier. Allowing 14 percent more heat to the coolant would lead to reduced engine efficiency or harmful overheating in another area of the engine because of the increase in heat content of the coolant. On the other hand, coatings that are too thick will have surface temperatures and temperature gradients during service that are beyond reliable operational limits of the coating. Result of this condition could be complete failure of the heat-barrier coating, and failure of the coating would mean that heat flux through the chamber wall would increase a disastrous 150 percent.

Control of thickness when the slurry is sprayed is largely dependent on the experience of the technician. One way in which thickness can be controlled accurately and reproducibly, on the other hand, is by dip coating in the same way that paint is applied to some automobile bodies. In dip-coating processes, thickness can be controlled by knowledge of the rheology of the slurry system. Such factors as solid-to-liquid ratio, nature of the solid particle surface, and use of electrolytes can be used to adjust the slurry rheology and, hence, resultant coating thickness.

REFERENCES

1. Carpenter, H. W., "Design and Testing of Protective Coatings for the J-2X Film-Coolant Ring," Rocketdyne Research Report No. 66-31, September 1966.
2. Carpenter, H. W., "Heat-Barrier Coatings for Rocket Engines," p. 380, Summary of the Thirteenth Refractory Composites Working Group Meeting, AFML-TR-68-84, May 1968.
3. Greszczuk, L. B., and H. Leggett, "Development of a System for Prestressing Brittle Materials," Douglas Aircraft Corp. Report 92200, NASA Contract No. NAS 7-429, August 1967.
4. Harrison, E. E., H. A. McKinstry, and F. A. Hummel, "High Temperature Zirconium Phosphates," Jour. Amer. Ceramic Soc., 37 (6) pp 277-80, 1954.
5. Bremser, A. H., and J. A. Nelson, "Phosphate Bonding of Zirconia," Jour. Amer. Ceramic Soc., 46 (3) pp 280-2, 1967.
6. Bremser, A. H., "Thermal Decompositions and Phase Identification in the ZrO_2-CaO-P_2O_5 System," Ph.D. Thesis, Dept. Ceramic Engineering, University of Illinois, Urbana, Illinois, 1967.
7. Bremser, A. H., Personal communication 8 May 1968.
8. Kallup, C., Jr., S. Skalrew, and S. V. Castner, "Application and Evaluation of Reinforced Refractory Ceramic Coatings," ML-TRD-64-84, Contract AF33(616)-8209, June 1964.
9. Kummer, D. L., et al., "Shielded Ceramic Composite Structure," AFML-TR-65-331, Contract AF33(657)-10996, October 1965.
10. Encyclopedia of Chemical Technology, Vol. 6, p. 726, Interscience Encyclopedia, Inc., New York, N. Y., 1951.
11. "The Thermal Properties of Twenty-Six Solid Materials to 5000 F or Their Destruction Temperatures," ASD-TDR-62-765, p. 165, January 1963.

12. Jen, W. H., and P. A. Lottas, ANL 4627, 1 May 1957.

13. McAdams, W. H., Heat Transmission, 3rd Edition, McGraw-Hill, p. 392, 1954.

14. Kreith, F., Principles of Heat Transfer, 2nd Edition, Internation Textbook Co., Scranton, Pa., p. 436, 1967.

APPENDIX A

TASK I FINAL REPORT

PREFACE

The Task I Final Report, issued as Rocketdyne Report R-7273, dated 21 November 1967, is reproduced here as originally written. It is presented as such because it points out the major problems that had to be approached before Task II could be undertaken, and it outlines the logic that was used to approach these problems and the information on which decisions were based which gave Task II its essential direction. Furthermore, several coating design features are discussed in it that were not developed in Task II, and these features should be preserved in the record for reference, should they be needed later when the coating system is tested under the more severe conditions of actual rocket engine service or when being redesigned for other applications.

A few comments in retrospect about the technical discussions in the Task I report are appropriate:

1. It was stated in Task I that monolithic coating designs probably would not survive the thermal stresses produced by the arc-plasma jet test. This prediction, which was based on elastic thermal stress analyses using best estimates for thermal and mechanical properties, has been shown in Task II to be over-conservative. Certain monolithic coatings survived the arc-plasma jet test so well that testing of only one graded coating design was attempted. Monolithic coating designs probably survived the severe thermal stress conditions better than anticipated because (1) their elastic moduli and the micromechanics of their response were largely affected by their high porosity, (2) strains

were relieved by anelastic and plastic deformation due to the presence of phosphate phases in the structure, and (3) coatings were thin and supported by the substrate in a manner not presently capable of adequate description for stress analysis.

2. Because wetting and bonding of the coating to the metal substrate had been unsuccessful in past programs, it was predicted in Task I that special surface treatment of the metal would be mandatory. The principal method recommended was to form a thin film of oxide on the metal before applying the coating. But the work of Task II showed that phosphate-bonded ZrO_2 did wet untreated Hastelloy-X surfaces, and satisfactory bonding was obtained on unoxidized (but roughened) substrates. It was further indicated in Task II that chemical bonding between smooth Hastelloy-X and phosphate-bonded ZrO_2 slurry coatings would be feasible with additional development. Also, the design feature of interposing a layer of glass between the Hastelloy-X substrate and the cementitiously bonded coating to promote very strong chemical bonding was demonstrated. Although all of the adherence studies of Task II were preliminary in nature, it appeared that simple preoxidation of the substrate did not produce the most effective transition layer between the metal and the oxide (or, phosphatic) coating.

3. Although reinforcements were not required for satisfactory performance in Task II, the discussion of reinforcement methods is preserved in the Task I report for reference should these be required when the phosphate-bonded zirconia coating system is evaluated under more severe conditions of test or application.

4. The design feature of using a strain-accommodation layer between the Hastelloy-X substrate and the heat-barrier coating, discussed in Task I, was not required to achieve successful coating performance in Task II.

Results of thermal shock tests for evaluating coating adherence did demonstrate, however, that this design feature probably has merit. Coatings that were applied over a thin layer of glass could not be failed when thermally cycled from room temperature to 1900 F and back to room temperature under isothermal heating conditions. Preliminary work with a flame-sprayed metal undercoat also indicated some promise. Although it is not possible to sort out causes with precision, it is felt that a part of the effect seen in each of these cases was due to strain accommodation provided by the underlayer.

APPENDIX A

NASA CR-
R-7273

PROTECTIVE COATING SYSTEM FOR A REGENERATIVELY COOLED THRUST CHAMBER

TASK I--Final Report

(1 July 1967 through 31 October 1967)

By

H. W. Carpenter
G. Y. Onoda, Jr.
S. D. Brown

Prepared For

National Aeronautics and Space Administration

21 November 1967

Contract NAS3-11187

Technical Management
NASA Lewis Research Center
Cleveland, Ohio
Chemical and Nuclear Rocket Division
Mr. Charles Zalabak

Rocketdyne
A Division of North American Rockwell Corporation
Canoga Park, California

FOREWORD

The effort described herein was performed under Contract NAS3-11187 from 1 July 1967 through 31 October 1967, and is the completion of the first of two consecutive tasks. The technical manager was Mr. Charles Zalabak, Chemical and Nuclear Rocket Division, National Aeronautics and Space Administration, Lewis Research Center, Cleveland, Ohio 44135.

The contribution of Mr. George S. Osugi to the technical effort is gratefully acknowledged.

ABSTRACT

The results of a theoretical study of cementitiously bonded coatings are reported. These coatings are designed for the thermal protection of high-performance, liquid hydrogen- and oxygen-fueled, regeneratively cooled rocket engines. Four filler materials (zirconia, thoria, barium zirconate, and a hafnia-rich mixture of oxides) and four bonding agents (H_2PO_3F, H_2SiF_6, K_2SiO_3, and $Th(NO_3)_4$) were selected for the systems to be evaluated in arc-plasma tests during Task II of this program. The selection of coating systems and designs was based on the following:

1. The state-of-the-art of cementitiously bonded materials described in the literature
2. Steady-state and transient heat transfer analyses of a specified, but hypothetical, rocket engine
3. Steady-state and transient thermal stress analyses of the chamber wall-coating system
4. Important design factors expected to influence the performance of the coating under service conditions

CONTENTS

Foreword A-5

Abstract A-6

A Literature Review of Heat-Barrier, Slurry-Applied Coating Systems and Designs A-12

Aluminum Phosphate Coatings [National Bureau of Standards, 1959 (Ref. 1)] A-12

Reinforced Alumina and Zirconia Coatings [Marquardt Corporation, 1957 Through 1962] A-13

Reinforced Thoria Coatings for Tungsten [Solar, 1964 (Ref. 5)] A-16

Review of Cementitious Bonding in Ceramics A-18

The Cementitious Bond A-18

Important Fabrication Considerations A-19

Properties of Cementitiously Bonded Ceramics in General . . . A-25

Factors Influencing the Performance of Slurry-Type, Heat-Barrier Coating Systems A-30

Thermal Analyses A-30

Thermal Stress Analyses A-40

Properties of the Coating System A-57

Analyses and Selection of Materials Systems A-72

Substrate Alloy A-72

Filler Materials for 4000 F Service A-72

Binders for Candidate Filler Materials A-78

Intermediate Layers and Reinforcements A-87

Coating Design A-89

Appendix A-A

Stress-Free Curvature for a Coating Having a Linear Temperature Distribution Across Its Thickness A-100

Appendix A-B

Adhesive Forces Between the Coating and Substrate A-104

Appendix A-C

Thermal Stresses in a Two-Dimensionally Infinite, Planar Coating-Substrate System with Temperature and Material Properties Varying Through the Thickness Only A-110

Appendix A-D

Graded Distribution Having the Condition That $\alpha(T-T_e)$ is Constant Throughout the Coating A-114

References A-120

Bibliography A-126

ILLUSTRATIONS

1. Illustrations of the Two General Types of Cementitious-Bonding Reactions 14
2. Modulus of Rupture of (A) Phosphate Bonded Calcia-Stabilized Zirconia, and (B) Phosphate Bonded Unstabilized Zirconia as a Function of Temperature 23
3. Schematic of Heat Transfer Across Coated Chamber Wall . . . 26
4. Steady-State Temperature Distribution Across Metal-Coating System 30
5. Wall Temperature Distribution vs Time 34
6. Illustration of the Origin of Thermal Stresses in Coatings 39
7. Purely Elastic, Restrained, Coating-Metal System at Steady-State Heating Conditions 45
8. Coating Gradation Yielding Zero Bending Moments 49
9. Thermal Conductivity: Zirconium Oxide + Calcium Oxide . . . 92
10. Thermal Conductivity: Thorium Oxide 93

A LITERATURE REVIEW OF HEAT-BARRIER, SLURRY-APPLIED COATING SYSTEMS AND DESIGNS

Although numerous papers and patents relating to slurry coating processes have been written, few of them pertain to materials systems for use at temperatures above 3000 F. Thus, because high-temperature coatings applied by slurry techniques are in their early stages, considerable research and development effort will be required to improve these coatings to a level of wide applicability in rocket engine environments. A review and discussion of the state-of-the-art of slurry coatings for heat barrier applications is presented in this chapter.

ALUMINUM PHOSPHATE COATINGS [NATIONAL BUREAU OF STANDARDS, 1959 (REF. 1)]

Heat-barrier coatings for type 321 stainless steel were developed in which ceramic oxide powders were bonded with monoaluminum phosphate. The oxides used included various combinations of Cr_2O_3, Al_2O_3, asbestos, CeO_2, fluorspar, National Bureau of Standards (NBS) frit (powdered glass), mica, and talc with and without metal reinforcements. These coatings, which could be cured at 400 F, were found to have softening points in the range 2800 to 3150 F. For several of the better coating systems, measurements were made of hardness, moisture resistance, thermal conductivity, thermal expansion, density, oxidation resistance, and emittance.

The slurries were applied to sandblasted type 321 stainless steel by dipping, spraying, or brushing. Coating thicknesses varied from 1.5 to 200 mils. The heavier coatings were reinforced with expanded-mesh type SAE 1020 carbon steel spot-welded to the base metal.

Thermal shock resistance of the coatings was measured in the following manner. Test coupons of coated metal were inserted in a hot furnace at a temperature (T_s). When the coupon reached the temperature of the furnace, it was removed and cooled in static air or quenched in water. If the coating survived this treatment without spalling, the procedure was repeated up to 10 cycles. The parameter used to compare the thermal shock resistance of different coatings was the maximum furnace temperature to which the coating could be cycled 10 times from room temperature without failure (spalling or flaking).

None of the coatings survived cycling conditions at furnace temperatures above 1400 F, and thick coatings (i.e., 200 mils) were less resistant to thermal shock than thin ones. All reinforced coatings cracked and spalled from the metal substrate at T_s values of 1200 F and higher, even though the reinforcement system remained anchored to the metal at the spot weld to T_s values as high as 1800 F. Thin coatings (1 to 3 mils) were resistant to thermal shocks at T_s values as high as 1400 F (200 F higher than the thicker coatings). The coatings most resistant to thermal shock contained quartz as the predominant filler material. When Al_2O_3 was used as the filler, coatings failed at a T_s value of 800 F.

REINFORCED ALUMINA AND ZIRCONIA COATINGS
[MARQUARDT CORPORATION, 1957 THROUGH 1962]

An extensive 5-year program was conducted by Marquardt Corporation on insulative, slurry coatings, or more descriptively, heat shields. During the first and second years of the investigation, a broad approach to the field of refractory ceramic materials for use as metal-reinforced coatings resulted in the elimination of many inferior compositions and the selection of a limited number of promising ceramic materials for further investigation. During the third year (Ref. 2), a phosphate-bonded alumina coating that was reinforced with corrugated strips of stainless steel was developed to successfully withstand temperatures to 3500 F. In the fourth year (Ref. 3), reinforced coatings containing zirconia instead of alumina were developed to withstand temperatures above 4000 F. After considering a variety of binder candidates, the best coating, based on thermal shock studies, was found to be a metal-reinforced coating of zirconia bonded by monofluorophosphoric acid. The development of zirconia coatings was extended in the fifth year by evaluating more binders and reinforcement systems (Ref. 4). Hydrofluosilicic acid was determined to be equal, if not superior to, monofluorophosphoric acid, for bonding zirconia. The use of refractory metal reinforcements was not possible because of oxidation. Neither the coatings developed during these programs nor conventional oxidation protective coatings afforded sufficient protection from oxidation. Therefore, reinforcements were fabricated from a conventional stainless-steel alloy, and submerged in the insulative coating for thermal protection.

The thermal shock test for evaluating the coatings throughout the research effort, which was called a "thermal drop" test, consisted of a large oxyacetylene torch that heated the coated surface of a suspended test panel. Approximately 1 minute was required to reach equilibrium temperature, and the specimen was only cooled by radiation from the back face of the panel. The temperature of the surface exposed to the flame was measured with an optical pyrometer, while the back surface temperature was measured with a thermocouple. The difference between the temperature of the front and back face was defined as the "thermal drop." Generally, the specimen was heated in such a manner that the front surface reached a preselected temperature. After a steady-state condition was attained, the test cycle was completed either by allowing the specimen to air cool or by quenching it in a blast of cool air. Then, after the specimen cooled to room temperature, it was recycled. The specimen was cycled until failure of the coating became visually apparent. At steady-state heating, temperature gradients were in the range 6 to 12 F/mil of coating thickness, and during any of the tests the maximum heat flux was only 3.2 Btu/in.^{2}-sec.

The earlier work on alumina coatings involved studies on improving phosphoric acid-bonded systems. Although the orthophosphoric acid strongly bonded the alumina composite, a major problem was that the acid attacked the metal substrate and caused bloating in the coating because of the evolution of hydrogen gas. The problem of bloating in the coating was reduced by using an acid inhibitor (Euthane No. 11). One of the better slurry coatings, designated P-150, contained 50 percent (by weight) -48 mesh, 25 percent -325 mesh, and 20 percent -600 mesh alumina powder (Alcoa T61 grade), 2 percent magnesium trisilicate, 3 percent Red Label clay (Ferro Corporation), 11 percent of 85 percent H_3PO_4, and 8 percent water. Coating P-150 sustained four cycles in the thermal drop test at a test temperature of 2680 F on the surface exposed to the flame. Although fine cracks developed in the coating after the first cycle, the coating remained intact during the following three cycles.

Successful zirconia coatings were developed, but only after an extensive evaluation of a wide variety of binder-filler systems. Binders that were studied included orthophosphoric acid, monofluorophosphoric acid, hexafluorophosphoric acid, combinations of dolomite and calcium hydroxide, fluosulphonic acid, hydrofluosilicic acid, various mixtures of these acids, magnesium zirconate, calcium zirconate, and magnesium zirconium silicate with ammonium dihydrogen phosphate.

The best binders for zirconia systems were monofluorophosphoric acid and hydrofluosilicic acid, and the best coating system consisted of 40 parts of -30 mesh ZrO_2, 30 parts of -325 mesh ZrO_2, 1 part $NH_4H_2PO_4$, and either 5 parts of H_2PO_3F with 2 parts water or 2 parts H_2SiF_6 with 4 parts water. The presence of $NH_4H_2PO_4$ apparently improved the workable life of the slurry. Coatings were troweled as a paste onto N-155 alloy sheets (40 mils thick) with type 321 stainless-steel corrugated reinforcements spot-welded to the substrate. Coating thicknesses were approximately 0.29 inch (280 mils).

The best monofluorophosphoric and hydrofluosilicic acid-bonded coatings survived one cycle (5-minute run time) in the thermal drop test with a front-face temperature of approximately 4000 F. No cracks were observed but a slight glaze formed on the front surface. No attempts were made to thermally cycle these coatings.

REINFORCED THORIA COATINGS FOR TUNGSTEN

[SOLAR, 1964 (REF. 5)]

A heat barrier coating, developed for the ASSET glide re-entry vehicle, was designed to reduce the temperature and to reduce the oxidation of a tungsten substrate in an oxidizing, low-pressure environment. The only cooling was by radiation. Screening tests and final ground tests on this heat-shield system were performed under the following conditions:

1. Heat flux levels between 1 and 4.3 Btu/in.^{2}-sec
2. Coating surface temperatures between 4000 and 5000 F
3. Test duration of less than 10 minutes
4. Temperature drop across the coating thickness of less than 1000 F
5. Coating thicknesses between 0.2 and 0.3 inch

ThO_2 was selected early in the program over ZrO_2 and HfO_2 as the matrix coating material based primarily on two factors: (1) state-of-the-art arc-plasma sprayed coatings of ZrO_2 on tungsten performed better than coatings of ThO_2 and HfO_2 in oxidation protection tests, (2) state-of-the-art slurry coatings of ThO_2 performed better than coatings of ZrO_2 and HfO_2 during thermal shock tests.

Various bonding agents for ThO_2 that were studied during this program included colloidal ThO_2, phosphoric acid, an organo-zirconium compound, and $Th(NO_3)_4$. Of these, $Th(NO_3)_4$ was selected as best because the nitrate radical decomposed and volatilized, so that no eutectic compositions could be formed, as they were when other binders were used. Thorium nitrate provided low-temperature strength for the coating system,but high-temperature strength was developed by sintering of the powdered ThO_2 rather than by chemical reaction with the bonding agent because the nitrate decomposed and volatilized at temperatures far below the use temperature. Thus, proper sizing of the ThO_2 powders was essential to reduce shrinkage and to increase the final density which was proportional to strength. Mixtures of different size fractions of ThO_2, bonded by from 5 to 10 weight percent $Th(NO_3)_4$ shrunk linearly less than 1 percent when heated at approximately 4300 F.

Because no bond was developed between the substrate and the coating, reinforcements were essential to maintain the coating. The best reinforcements were (1) sine-wave-shaped tungsten ribbons that were spot welded on the tungsten substrate with tungsten wire coils wound through the tungsten ribbons, or (2) a tungsten mesh held to the substrate by tungsten pins.

REVIEW OF CEMENTITIOUS BONDING IN CERAMICS

THE CEMENTITIOUS BOND

A cement can be defined (Ref.6), as a bonding material that forms by reaction and that imparts strength to an aggregate in which the bonding material is present in minor proportions. For the purpose of this program, only cements that set by chemical reaction and that bond ceramic materials are of interest. Specifically, individual cements discussed in the latter part of this section are bonding agents for those filler materials considered to be appropriate for the present heat-barrier coating program.

In cementitious bonding processes, powdered ceramic material (the "filler") is mixed and reacted ("cured") with a liquid phase (the "binder system"*). The reaction occurs at a relatively low temperature, always below 1800 F, usually below 1200 F, and occasionally at room temperature. During curing, individual particles of the filler become cemented together at locations of contact as a result of the formation of cementitious material on the particle surface.

For the most part, cementitious chemical reactions can be grouped into two general types of reactions, illustrated in Fig. 1. Figure 1a illustrates the formation of a cement, referred to as Type I, that contains constituents that originate from the liquid phase only; the filler C is not a reactant. Type I cements form by a reaction where chemical species in the fluid phase combine at the surface of the ceramic particle to form a precipitated product, or where sols or colloidal particles in the liquid phase precipitate on the particle surface. The reactants may, or may not, include the carrier fluid (e g., water) An example of a reaction where a Type I cement is formed is:

$$\underset{\text{Reactant in solution}}{n\,[Si(OH)_4]} \longrightarrow \underset{\text{Cement}}{[SiO(OH)_2]_n} + nH_2O$$

---

*A binder system is a solution, usually aqueous, containing some or all of the reactants that form the cement.

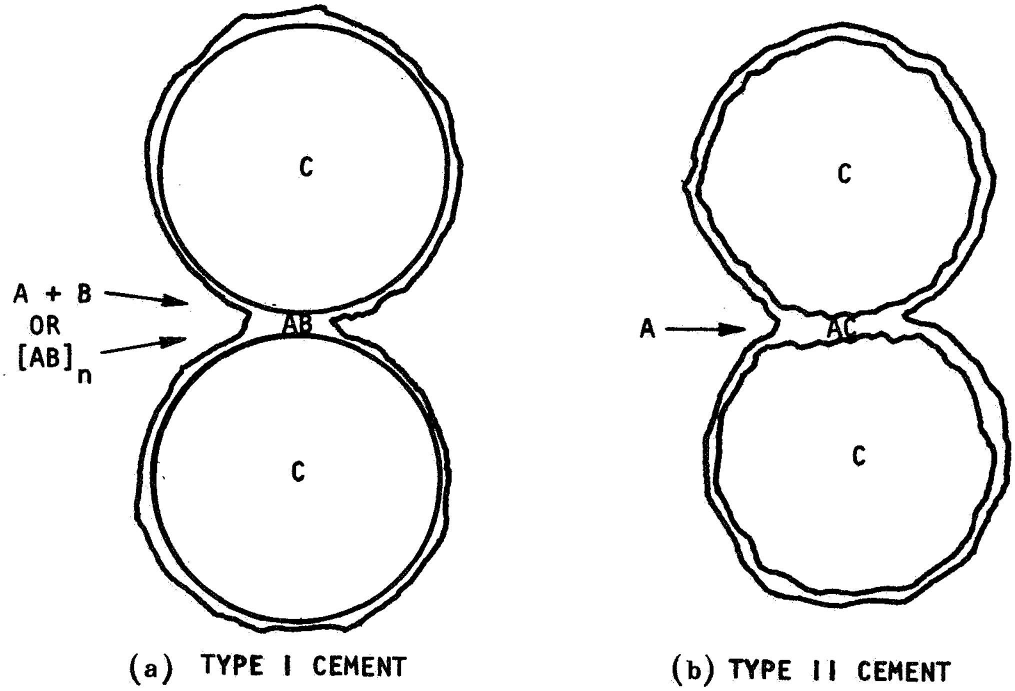
C
A + B
OR
[AB]n
AB
C
(a) TYPE I CEMENT
C
A
AC
C
(b) TYPE II CEMENT

Figure 1. Illustrations of the Two General Types of Cementitious-Bonding Reactions

Type II cements (Fig. 1b) are more common than those of Type I. A well-known example of a Type II reaction is the one between phosphoric acid and certain metal oxides:

$$\underset{\text{Filler}}{MO} \quad + \quad \underset{\text{Acid}}{H_3PO_4} \longrightarrow \underset{\text{Cement}}{M(HPO_4)} \quad + H_2O$$

To be considered a cement, the reaction product must produce a strong bridge between the filler particles. That is, both the cohesive strength of the cement and the adhesive strength of the cement to the filler material must be sufficient to impart reasonable strength to the overall aggregate. With rare exceptions, cements are comprised of glass-forming components. Wygant (Ref. 6) has suggested that a random structure is a practical necessity for cements. Crystalline materials do not easily form dense, homogeneous structures when deposited by reaction because the crystal growth habit tends to produce porous structures. Random strucures, however, more easily form dense materials because growth is random and relatively unaffected by impurities and nonstoichiometry. Also, many residual force fields exist in a random structure which contribute to the adhesive bond.

IMPORTANT FABRICATION CONSIDERATIONS

General

Regardless of the type of binder used, the procedures for most cementitious processes are similar. The filler material is carefully sized, and suitable quantities of the size fractions necessary to yield the desired packing density are blended. The filler is then mixed with the liquid containing the cement and whatever additives that may be required (e.g., reaction retardants, mold release agents, lubricants, wetting agents, etc). The consistency of the mixture is adjusted by dilution or by electrolytes to provide the necessary properties for the forming process. Care must be exercised in those cases where the quantity of diluent used may affect the properties of the product. Excessive diluent can result in excessive porosity. The suspension is then formed into shape by pressing, casting, molding or troweling, and in the case of coatings, the suspension (called "slip" or "slurry") is sprayed, troweled, dip-coated, or pour-coated on the substrate. The body or coating is then air dried to develop sufficient strength for handling. A few bonding agents cure completely at room temperature, but the majority require a curing operation at a moderately elevated temperature which is never above 1800 F (980 C) and generally much lower. The time-temperature relationship during the curing operation can be critical in promoting a bond having optimum properties, in controlling residual stresses and in preventing bloating. The curing cycle should be adjusted to provide maximum strength of the aggregate, but even when maximum strength is achieved, the temperature at which the bonds "set" can be important with respect to residual strains. For example, a lattice that is chemically formed at 900 F (480 C) will result in less residual strain when cooled to room temperature, than the same lattice that is formed at 1800 F (980 C) and similarly cooled.

Strength

The strength of the cemented aggregate depends in part on the number of cemented particle-to-particle contact points per unit volume which increases with increasing packing density. The strength of the aggregate also depends on the bulk density because a dense solid is usually stronger than a porous one. Thus, to obtain maximum strength, the particles must be sized to provide maximum packing efficiency and sufficient cement must be used to just fill the voids.

Packing of the filler material will be close to maximum if a trimodal particle size distribution is used with the mean particle sizes of the modes approximately an order of magnitude apart. Usually very little is gained by using more than three fractions of particle size ranges. However, if permeability is desired in the finished product, particles are sized to pack more loosely and only that amount of cement is used that is necessary to bond the particles together at their points of contact. Articles made from filler powders having narrow particle size distributions usually will have a void volume of approximately 50 percent, whereas those made from powders having size distributions that give efficient packing will have a void volume of approximately 70 percent.

Strength is also dependent on the ratio of cement to filler material. Sufficient cement must be present to weld together the contact points between filler particles. Generally, the strength can be improved further if sufficient cement is available to completely fill the pores in a densely-packed blend of powders. Care must be taken, however, that an excess amount of cement is not used because the excess may have a detrimental effect on strength as well as other properties of the aggregate by preventing the powders from becoming densely packed, thereby forming a weak matrix.

Rheology

The rheological characteristics of the slurry are important in forming the aggregate before curing. The viscosity of the slurry must be appropriate for the forming method. It must have the viscosity of paint (approximately 2.0 poise or less) if it is to be sprayed or brushed, or it must have a somewhat thicker consistency if it is to be trowelled. The powder also must have a slow settling rate so that uniformly dispersed slurries can be retained during the forming process. Preferably, the powder should not settle appreciably within 8 hours, or one working day, and certainly they should not settle appreciably within 1 hour, or whatever time would be required to coat the hardware, such as a thrust chamber.

The rheology of slurries is not a simple function of either the fluid or the ratio of the components. Rather, it depends on complex physicochemical processes.* Chemical aspects of the rheology of aqueous slurries involve the properties of the interface between the liquid and the solid phases. The surface of the solid absorbs ions from solution to produce an electric charge (i.e., an electric double layer), the nature of which depends on the chemistry of the aqueous phase. The type of interactions that occur between individual particles depends extensively on the nature of the electrical double layers and, consequently, on the solution chemistry.

---

*Excellent reviews on the rheology of oxide suspensions (Ref. 7 and 8) exist; therefore, only a brief discussion is presented in this report.

To form a stable suspension (one in which the particles do not separate from the fluid matrix at a sensible rate because of gravity), the individual filler particles must be very small and must not flocculate. In water base suspensions of oxide powders, suspension stability is a function of pH. At a certain pH, called the Zero-Point-of-Charge (ZPC), the particles contain no electric charge. The value of the ZPC depends on the specific oxide involved. At pH values above and below the ZPC, the oxide has a surface charge because of the electrochemical nature of the system. At pH values below the ZPC (acidic side) the oxide is positively charged and at pH values above the ZPC (basic side) the oxide is negatively charged. At the ZPC, oxide particles tend to flocculate because of the absence of electric forces that tend to maintain their separation. Thus, the suspension is unstable at the ZPC and is not suitable for slurry coating methods. For example, the ZPC for Al_2O_3 and ZrO_2 occurs at pH values of 8 and 4, respectively (Ref. 9). Acid solutions, except at the ZPC, create positively charged surfaces on oxides that lead to deflocculation and stable suspensions.

Also, the viscosity of the slurry depends on the interaction of individual particles, and, consequently, on the chemistry of the liquid phase. The effect of ions and of pH on viscosity is, at present, not well understood. Conflicting theories are evident in the literature (Ref. 8). Additional complications arise because behavior such as dilatancy and thixotropy are frequently encountered.

Setting Rate

The rate at which the cementing material reacts with the filler is another important consideration. Time must be available, after the cement and filler are combined, for adequate mixing and for the handling required to apply the slurry to a substrate. Reactions with gaseous products cause bloating when the reaction is too rapid to allow the gases to escape harmlessly; and furthermore, excessively rapid exothermic reactions cause localized temperature increases that can lead to deformation of the article during curing and to undesirable residual stresses in the final product. Hence, reaction retarding additives and/or special techniques are often required to control the reaction rate.

Thermal Expansion

Thermal expansion properties of the cement and filler are also important, especially if the product is intended for high-temperature service. If the mismatch in thermal expansion coefficients is too great, the mismatch will cause stresses in the aggregate during heating and/or cooling sufficiently to cause cracking and failure. However, differences in the thermal expansion properties of the cement and filler could be used to advantage in some instances. For example, if thermal expansion differences can be used to place residual compressive stresses in the surface regions of a body, its strength will be enhanced.

Sometimes, cementitiously bonded structures are made with the supposition that the cement will serve only to hold the filler material together until it is bonded by sintering processes during actual service. In these cases, it is particularly important that measures be taken to minimize the shrinkage that will occur during the in-service sintering.

PROPERTIES OF CEMENTITIOUSLY BONDED CERAMICS IN GENERAL

Materials produced by cementitiously bonded slurry methods generally have certain features in common. First, the grains in the aggregate have essentially the same size distribution and shapes as those of the starting grains. Little or no reaction that would alter particle size or shape occurs during processing. Secondly, there is a binder phase. It may or may not fill the interstices of the aggregate particles, depending on the specific case. In the strongest cementitiously bonded ceramics, the binder will just fill essentially all the void space and form a continuous matrix. Thirdly, while strength at ordinary temperatures may be affected considerably by the properties of the ceramic filler, high-temperature strength and dimensional stability are almost always determined by the character of the cement and the cement-filler bond. This is true unless sintering occurs during use at high temperatures to convert the cementitious bond to the more stable sintered bond. Fourthly, the thermal stability of the cement (which is invariably much less than that of the filler material) will limit the maximum use temperature of the material unless some reaction occurs to convert the cement into a substance at least as refractory as the filler ceramic.

Data concerning the properties of the cementitiously bonded materials described in the literature are in general inadequate; and, in many cases when property data are presented, the process and composition of the test specimens are not adequately characterized. In general, optimizing any cementitious bonding process is an engineering problem involving mixture ratios, curing cycles, mixing methods, reaction-controlling methods, etc. Thus, the making and using of cementitiously bonded materials is to a large extent an "art." This should be considered when evaluating and comparing property data in the literature.

Density

Density is controlled by the packing density of the ceramic filler and the quantity of binder in the system. Densities in excess of 80 percent theoretical are difficult to obtain under ordinary conditions when small amounts of cement are used. The binder may fill pore volume to some extent, but it also must separate the centers of the particles to some extent to bond them together. However, when large amounts of cement (20 to 40 percent of the volume) are used to form a skeletal matrix, higher densities are achievable. Porosities as low as 1 percent have been reported (Ref. 10 and 11).

Mechanical Strength

High mechanical strength is sacrificed in cementitiously bonded hardware for the processing advantages associated with the slurry fabrication technique. Typical strength values reported in the literature are shown in Table 1.

Limited data on strength as a function of temperature are available and there is no general rule for temperature dependency because strength will depend on the thermal,chemical, and mechanical stability of the binder and on the proportion of binder in the aggregate. Figure 2 shows the effect of temperature on the strength of phosphate-bonded-zirconia bodies.

Strength can be improved by incorporating a reinforcement in the body. This technique has been used to increase strength and thermal shock resistance for slurry-type heat-barrier coatings (Ref. 5 and 12) and radomes (Ref. 13 through 15). Modulus of rupture values for reinforced, phosphate-bonded alumina radomes are as high as 30,000 psi. Reinforcement materials that have been used are silicon carbide and alumina fibers, superalloy and refractory alloy wires, honeycomb structures, and meshes.

TABLE 1

TYPICAL STRENGTH VALUES FOR CEMENTITIOUSLY BONDED OXIDE BODIES

Maximum Strength Value, psi	Type of Test	Material	Bonding Agent	Reference
1,150	MOR(1)(2)	ThO_2	$Th(NO_3)_4$	5
2,000	MOR (3)	ZrO_2 (unstabilized)	Phosphate	16
3,600	MOR (3)	ZrO_2 (stabilized)	Phosphate	16
8,000	Compression	ZrO_2	Phosphate	17
4,300	MOR (4)	Al_2O_3	Phosphate	51

(1) MOR = Modulus of rupture

(2) Number of loading points were not stated

(3) Three-point loading

(4) ASTM C-133-49 (1952)

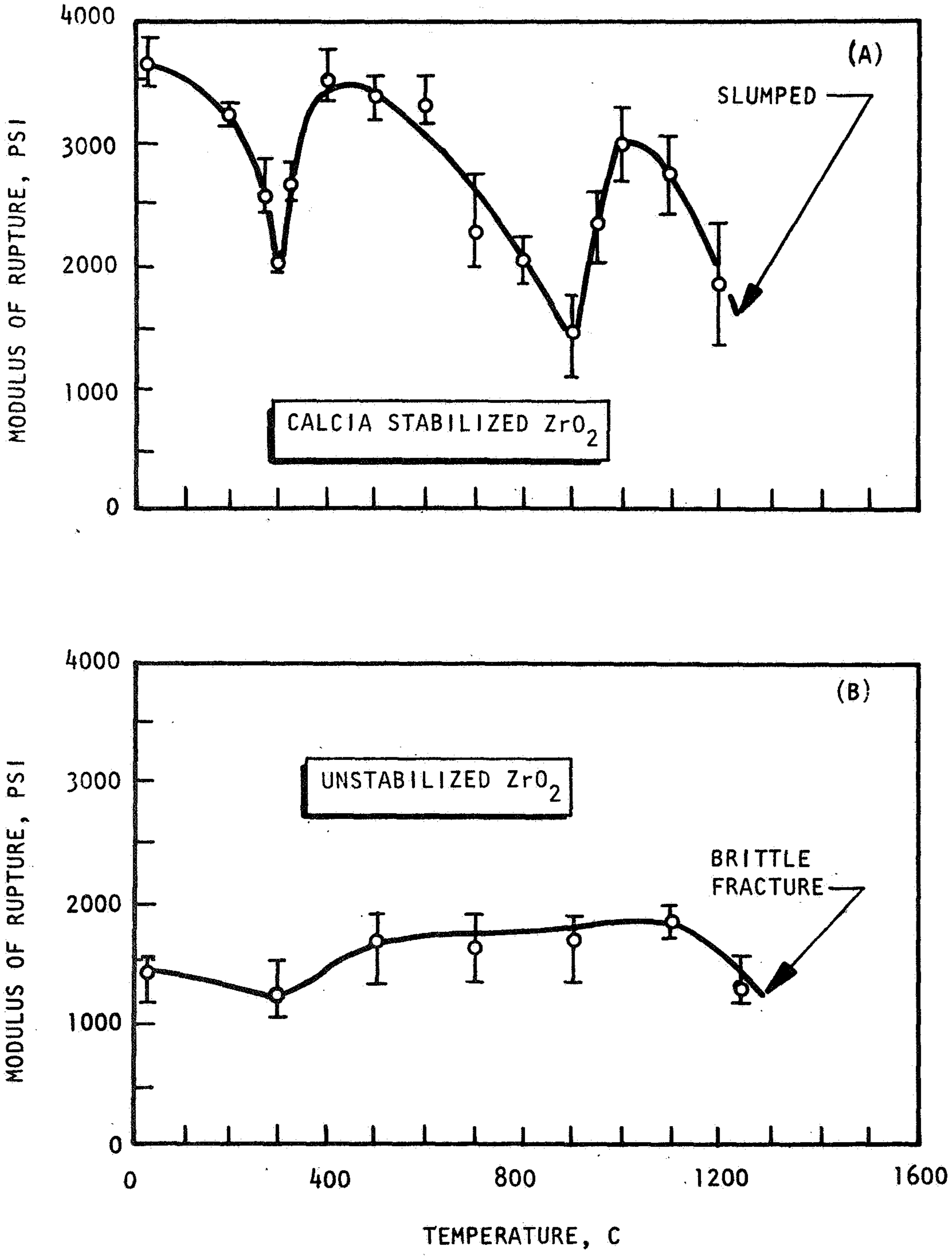

Figure 2 . Modulus of Rupture of (A) Phosphate-Bonded Calcia-stabilized Zirconia, and (B) Phosphate Bonded Unstabilized Zirconia As A Function of Temperature. Lines Indicate Data Spread and Open Circles Give Average Strength Value. (Modulus of rupture determined by loading the center of a 5-inch span)

Thermal Stability

Thermal stability of a cementitiously bonded aggregate depends principally on two factors: (1) the melting point of the filler material, and (2) the type and amount of binder. The limit of the use temperature can be predicted by an analysis of phase diagrams and a knowledge of use conditions. Interpretation of phase diagrams can be used to determine temperatures where eutectics will form and it can be used as an aid to determine where glassy phases will form. In general, phosphate-bonded alumina and zirconia materials are the most refractory and these are limited to continuous use temperatures of less than 2500 and 3500 F, respectively. Use temperature can be raised in some systems by using fugitive binders that do not flux the oxide filler. High-temperature strength is produced by in situ sintering in these cases.

Thermal Shock Resistance

Thermal shock resistance of cementitiously bonded materials is usually inferior to ceramics produced by sintering because of the low strength and low thermal conductivity of the porous structures.

FACTORS INFLUENCING THE PERFORMANCE OF SLURRY-TYPE HEAT-BARRIER COATING SYSTEMS

THERMAL ANALYSES

Introduction

Before a coating system can be designed, the thermal conditions under which it will be used must be known. If the exposed surface of the coating must withstand temperatures in excess of 4000 F, for example, the requirements which the coating must meet are substantially different from those which must be met by a coating which is never to be exposed to temperatures in excess of 3000 F. Such facts impose important constraints upon the selection of materials for any coating system. If the coating has a large temperature gradient, the coating must be designed carefully to accommodate for thermal stresses. Thus, the object of thermal analyses in this program is to determine service thermal conditions for the heat-barrier coating that are required to accomplish the program goals. These analyses include both steady-state and transient conditions.

An adequate thermal analysis of the heat-barrier coating system can be conducted by utilizing a theoretical model based on a one-dimensional analysis. The coating-metal system is assumed to be flat, infinite in length and width, homogeneous along the plane of the system, and the net heat flow occurs only along a direction perpendicular to the plane of the system. A gas boundary layer exists at the hot side of the coating and on the cold side between the metal and the bulk coolant (Fig. 3). For this program, the flame temperature is 6000 F and the bulk coolant temperature varies between -410 and 40 F. An intermediate value of -200 F was used for the coolant temperature in the following calculations. The steady-state heat flux $\dot{Q}$ is to be by design no more than 20 Btu/in.^{2}-sec.

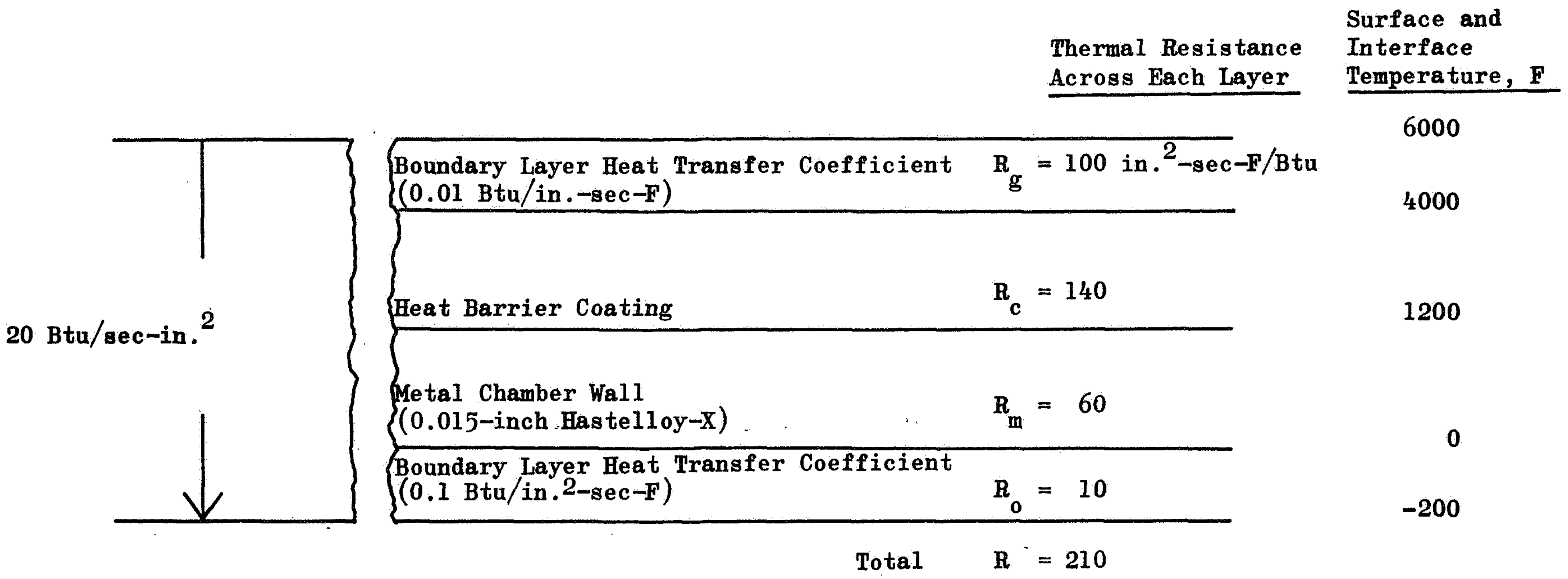
Thermal Resistance Across Each Layer
Surface and Interface Temperature, F
20 Btu/sec-in.^{2}
Boundary Layer Heat Transfer Coefficient (0.01 Btu/in.-sec-F)
R_g = 100 in.^{2}-sec-F/Btu
Heat Barrier Coating
R_c = 140
Metal Chamber Wall (0.015-inch Hastelloy-X)
R_m = 60
Boundary Layer Heat Transfer Coefficient (0.1 Btu/in.^{2}-sec-F)
R_o = 10
Total R = 210
6000
4000
1200
0
-200

Figure 3. Schematic of Heat Transfer Across Coated Chamber Wall

Required Thermal Resistance for the Coating

A specific, or at least a minimum, design thermal resistance for a heat-barrier coating applied on the inside of a metal chamber wall is required to reduce heat flux through the wall and to reduce metal wall temperatures to within the design limits. The required resistance of the coating can be calculated by considering the entire system. The effective total resistance, R_t, of the overall system with a steady-state heat flux of 20 Btu/in.^{2}-sec is given by

$$R_t = \frac{\Delta T}{\dot{Q}} = \frac{6200\ \text{F}}{20\ \text{Btu/in.}^2\text{-sec}}$$

$$= 310\ \text{in.}^2\text{-sec-F/Btu}$$

Because the theoretical model is a series of thermal resistances, the total resistance of the system is the sum of the individual resistance values. These resistances are (1) R_g, for the hot-gas boundary layer, (2) R_c, for the coating, (3) R_{cm}, for the interface between the coating and the metal substrate, (4) R_m, for the metal substrate, and (5) R_o, for the boundary layer between the metal and the coolant, so that

$$R_t = R_g + R_c + R_{cm} + R_m + R_o \tag{1}$$

The resistance of the hot-gas boundary layer, R_g, is 100 in.^{2}-sec-F/Btu for the system under consideration. This value is implied from the original information (Ref. 18) that the gas side surface temperature of the coating will be in the range of 4000 F when the steady-state flux is 20 Btu/in.^{2}-sec ($R_g = \frac{\Delta T}{\dot{Q}} = \frac{6000-4000}{20} = 100$).

The resistance of the cold wall boundary layer, R_o, was estimated to be small, approximately 10 in.^{2}-sec-F/Btu, based on calculations made previously at Rocketdyne on similar, high-performance engines. This estimate is satisfactory because the absolute value is small compared with the other values for thermal resistance in the system.

The resistance of the metal wall, R_m, depends on the thermal conductivity, k, of the metal and on the wall thickness. For many structural metals, such as Hastelloy-X, k is approximately 2.5×10^{-4} Btu/in.-sec F. A wall thickness of 15×10^{-3} inches is a satisfactory thickness for design purposes in rocket engines (Ref. 19). Thus, the thermal resistance, which is the ratio of the thickness to the thermal conductivity, is equal to 60 in.^{2}-sec-F/Btu.

The resistance of the coating-metal interface R_{cm}, depends on the efficiency of contact between the two phases. This resistance cannot be calculated theoretically, but is believed to be very small in most cases; consequently, R_{cm} shall be considered as being negligible.

The resistance of the coating, R_c, can be calculated from Eq. 1 because R_t and all other resistances are known, thus

$$R_c = R_t - R_g - R_{cm} - R_m - R_o$$

$$= 310 - 100 - 0 - 60 - 10$$

$$R_c = 140 \text{ in.}^2\text{-sec-F/Btu}$$

In the following paragraphs, it will be shown that coating designs having a fixed resistance, viz., 140 in.^{2}-sec-F/Btu, can have different thicknesses, depending on the magnitude of the thermal conductivity parameters of the coating materials.

Temperature Distribution and Coating Thickness for a Homogeneous Coating When k is Independent of Temperature

When the coating is a homogeneous material and, for simplicity, when the thermal conductivity of the material, k, is independent of temperature, the thermal resistance of the coating, R_c, is related directly to its thickness, t_c

$$t_c = kR_c$$

Thus, for a fixed resistance (e.g., 140 in.^{2}-sec-F/Btu), the thickness of the required coating is directly proportional to its conductivity. As an example, if the conductivity of the coating is between 2 and 5 x 10^{-5} Btu/in.-sec-F, which is typical for many insulative ceramics, a coating thickness of 3 x 10^{-3} to 7 x 10^{-3} inches is required.

The temperature distribution across the coated system is shown in Fig. 4. The temperature of the coating surface is 4000 F, and the temperature of the coating-metal interface is 1200 F, which is 400 F within the design requirement. The temperature drop, for this case, is linear through the coating and the metal.

Coating Thickness for a Homogeneous Coating When k Varies With Temperature

If the thermal conductivity k(T) for a homogeneous coating is temperature dependent, the thickness is given by

$$t_c = R_c \bar{k}$$

and

$$\bar{k} = \frac{1}{(T_s - T_i)} \int_{T_i}^{T_s} k(T)\, dT$$

where $\bar{k}$ = average thermal conductivity, T_s = surface temperature and T_i = metal-coating interface temperature. The solution to the integral is generally easy when the function k(T) is known. For the materials used in this program, the scatter is so great in the limited thermal conductivity data available that a precise calculation is not possible.

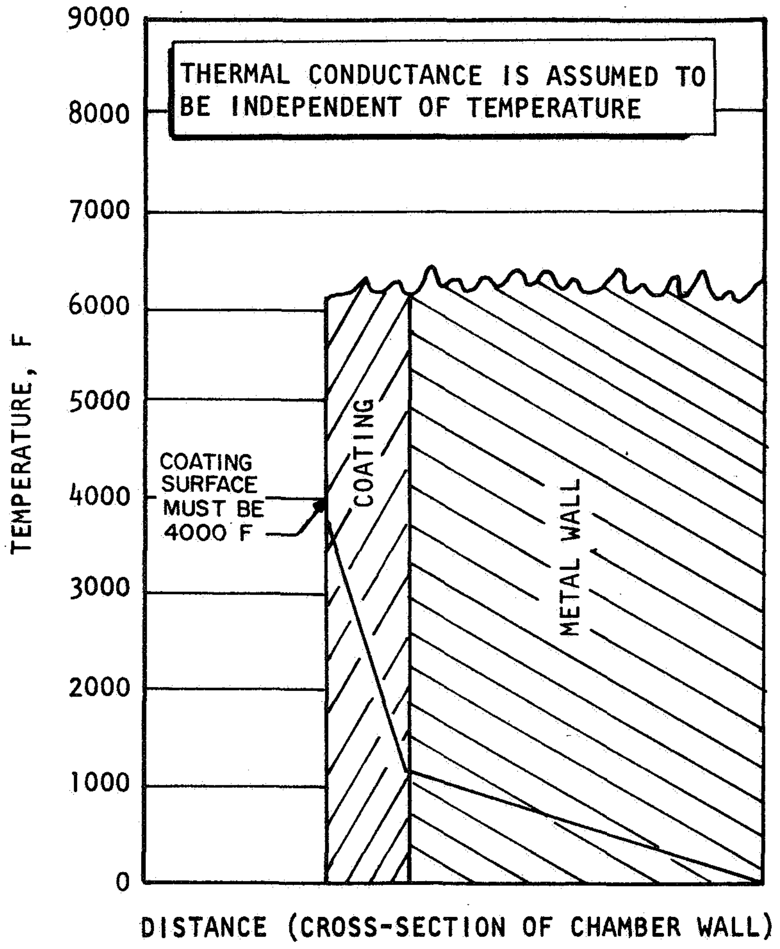

Figure 4 . Steady-State Temperature Distribution Across Metal-Coating System

Coating Thickness for Graded Coatings

For graded coatings, where $k(z)$ is the conductivity as a function of position through the coating and it is assumed to be temperature independent,

$$R_c = \int_0^{t_c} \frac{1}{k(z)} dz$$

The thickness required can be obtained by a graphical solution if the function $k(z)$ is known.

The case in which k varies across the thickness of the coating as a function of composition and also of temperature, need not be resolved for the purposes of this program. One reason is that the effect of temperature on k can be neglected for materials selected for this program because the data scatter of the limited available data is greater than the effect of temperature on k. And most importantly, the effect of composition is far more significant. Whereas k might change less than 1 unit over the specified temperature range (for example, k for zirconia varies between 1.8×10^{-5} and 2.5×10^{-5} Btu/in.-sec-F from 1200 to 4000 F; Ref. 20), $\bar{k}$ will change one or two orders of magnitude across the graded coating thickness because of compositional change (for example, $\bar{k}$ for zirconia is 2×10^{-5} Btu/in.-sec-F while $\bar{k}$ for Hastelloy-X is 4×10^{-4} Btu/in.-sec-F.)

Temperature Distribution for Transient Conditions

An analysis was conducted to determine the temperature response of a ceramic-coated thin-walled Hastelloy-X tube. It was assumed that the flow of heat from the gas-side to the coolant-side could be represented by a one-dimensional model.

The computer program which was used to make this analysis utilizes a finite difference approach to solve the transient conduction equations. The geometry is divided into small elemental volumes that are designated as nodes. An elemental mass corresponds to each node so that each element is capable of absorbing heat to raise its temperature. A temperature (T) is associated with each node, which is generally located at the center of the node. Heat is conducted between nodes by heat flow paths which incorporate the material resistance to the flow and the resistance associated with the heat transfer to a surface by convection or radiation. The heat flow network is formed by nodes and the interconnecting heat flow paths. A typical network is as follows:

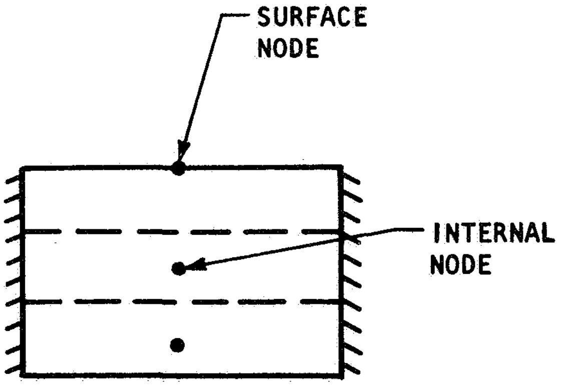

MATERIAL DIVIDED INTO ELEMENTS

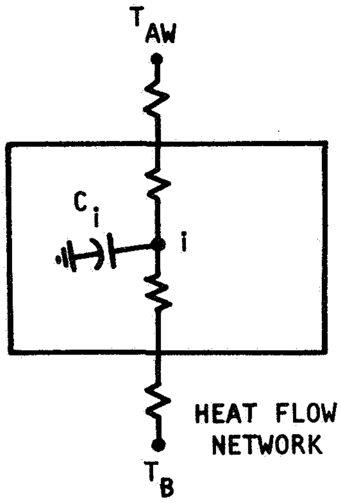

HEAT FLOW NETWORK

The heat flow network is directly analogous to an electrical network, both physically and mathematically, where temperature is analogous to the rate of heat flow, and thermal capacitance and resistance are similar to electrical capacitance and resistance.

The program computes the temperature at all nodes at each time (i.e., θ) increment. The partial differential equation describing the transient equation is:

$$\frac{\partial}{\partial z}\left[K_z \frac{\partial T}{\partial z}\right] + q\,(z, \theta) = C_z \frac{\partial T}{\partial \theta}$$

The numerical solution of the preceding equation is:

$$T_j\ (\tau + \Delta\theta) = T_j\ (\theta) + \frac{\Delta\theta}{C_j} \left\{ \sum_i {}_jK_i \left[T_i\ (\theta) - T_j\ (\theta) \right] + Q_j\ (\theta) \right\}$$

To ensure convergence, the convergence criterion

$$\Delta\tau \leqq \left[\frac{C_j}{\sum_i {}_jK_i} \right]$$

must be satisfied.

Figure 5 shows the wall temperature response for the ceramic coated, thin-walled Hastelloy-X tube. The tube wall thickness was 0.015 inch with a 0.0035-inch-thick ceramic coating. The tube was exposed to a gas temperature of 6460 R and heat transfer coefficient of 0.01 Btu/in.^{2}-sec-F. The coolant side heat transfer coefficient was 0.05* Btu/in.^{2}-sec-F and the bulk temperature was 260 R.

It was assumed that the initial tube temperature was 530 R. At time 0^+, the tube experienced the previously mentioned environment. Within the first millisecond, the gas-side surface temperature increased rapidly; the coolant-side wall temperature decreased below the initial temperature; and the bulk of the wall material remained at the initial temperature level. The wall temperature, in general, increased until a steady-state operation occurred at approximately 50 milliseconds for all practical purposes.

In the physical situation, the tube surfaces do not experience a step-type function in terms of the heat transfer coefficients. Consequently, the predicted transient temperature behavior which is shown does not accurately describe the physical case for short times. The predicted initial temperature gradients are higher.

---

*This value is a factor of two smaller than the one originally used in this model to calculate the thermal resistance of the heat-barrier coating. The effect of either of these two values on the result of either calculation is small.

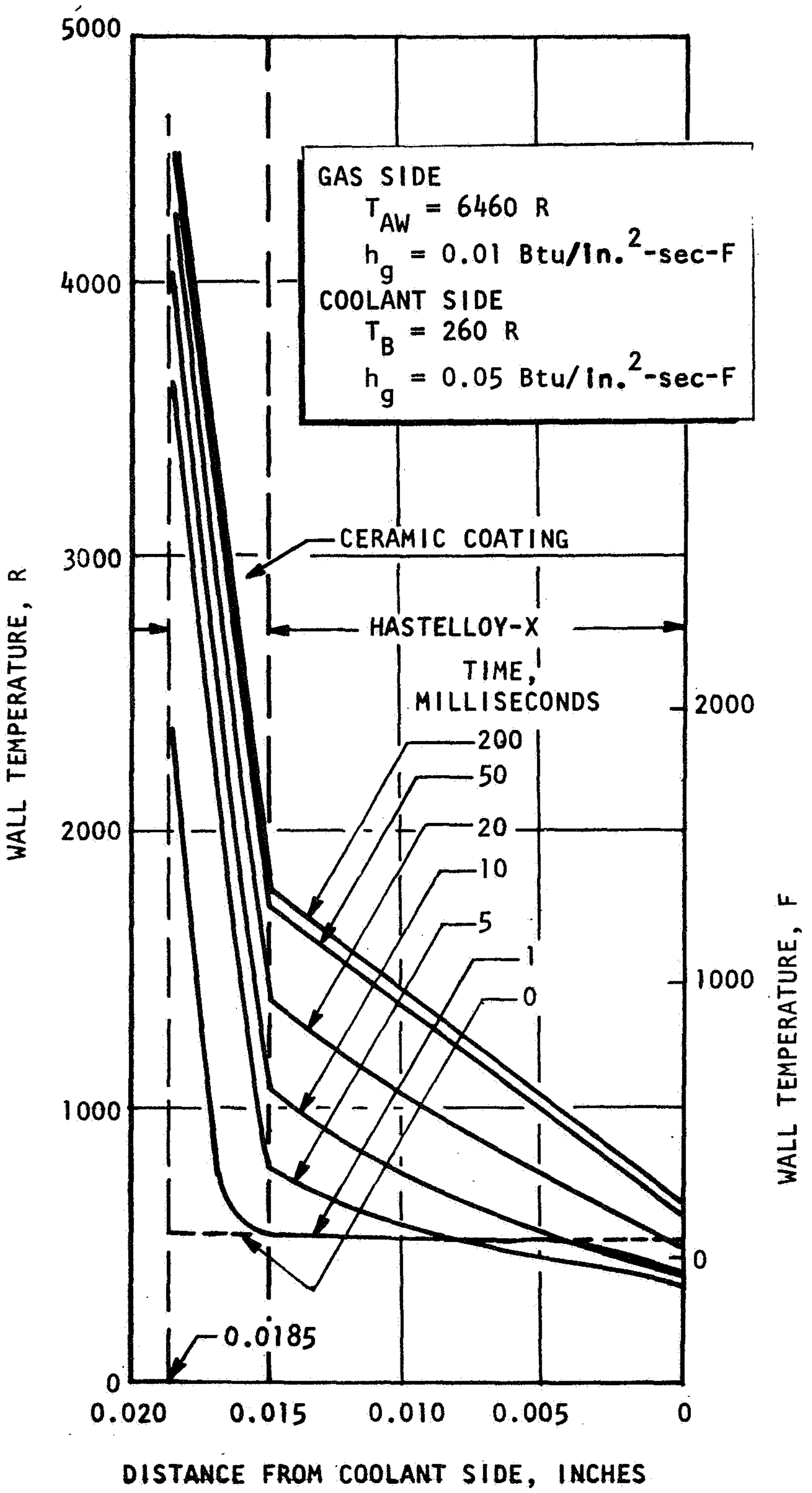

Figure 5. Wall Temperature Distribution vs Time

Conclusion

The coating system for the present application must have a thermal resistance of 140 in.^{2}-sec-F/Btu to reduce the heat flux to 20 Btu/sec-in.^{2}. The coating surface temperature will be 4000 F, the metal-coating interface temperature will be 1200 F, and steady state will be attained in approximately 50 milliseconds. The thickness of the coating will depend on the thermal conductance properties of the coating. Coating thickness for typical ceramic insulative materials will be between 3 and 7 mils.

THERMAL STRESS ANALYSES

Introduction

Success of heat barrier coatings will depend, in part, on their ability to withstand thermal stresses that develop during service. Large thermal stresses will be produced by severe temperature gradients across the thickness of the coating systems and by extremely rapid heating and cooling rates. As shown by the heat transfer analysis, these temperature gradients will be between 10^5 and 10^6 F/in. and the heating rate will be approximately 10^5 F/sec. If the thermal stresses are too severe, even the strongest and most adherent coating will fail mechanically. In designing a new coating system, therefore, the relationships between thermal stresses and coating design must be understood. The results of a theoretical study of thermal stresses in heat barrier coatings are presented in this section.

Unless otherwise specified, coating and substrate materials will be assumed to be homogenous and to have the following properties which are considered typical for the first generation coating systems of the present program.

Property	Symbol	Typical Value
Elastic modulus of coating	E_c	14×10^6 psi
Elastic modulus of metal	E_m	26×10^6 psi
Poisson's ratio of coating	μ_c	0.34
Poisson's ratio of metal	μ_m	0.32
Expansion coefficient of coating	α_c	4.82×10^{-6} F^{-1}
Expansion coefficient of metal	α_m	8.0×10^{-6} F^{-1}
Thickness of coating	t_c	3.5×10^{-3} inch
Thickness of metal	t_m	15.0×10^{-3} inch
Thermal conductivity of coating	k_c	2.5×10^{-5} Btu/in.-sec-F
Thermal conductivity of metal	k_m	25.0×10^{-5} Btu/in.-sec-F

Also, it is assumed that at steady state the heat flux ($\dot{Q}$) is 20 Btu/in.^{2}-sec, the hot surface of the coating is at a temperature (T_s) of 4000 F, the coating-metal temperature (T_i) is 1200 F, and the cold side temperature (T_o) of the metal is 0 F.

Origin of Thermal Stresses in Coatings

The origin of thermal stresses in coatings is perhaps best visualized by conducting a free-body examination of a perfectly elastic coating, without considering the influence of the substrate. The coating is assumed to be a flat sheet of thickness h that is (1) stress free at room temperature (T_e), (2) comprised of an isotropic material and (3) characterized by an expansion coefficient (α_c) and a thermal conductivity (k_c). If the coating is subjected to a steady-state heat flux ($\dot{Q}$) across its thickness, a linear temperature gradient arises in the coating. The temperature gradient produces differences in thermal expansion at different depths below the surface of the coating. Consequently, the coating will tend to curve, and, if there are no external restraint forces present, will assume a curved, stress-free condition. The radius of curvature (ρ) for the stress-free state is given by the equation (Appendix A-A):

$$\rho = \frac{k_c}{\alpha_c \dot{Q}} \tag{2}$$

For purposes of illustration, consider a coating comprised of a hypothetical material possessing the properties listed on Page A-41. With a steady-state heat flux of 20 Btu/sec in.^{2}, the radius of curvature for the stress-free state, as calculated by Eq. 2 will be 0.26 inch.

Large stresses will arise in the coating if external restraint forces do not allow the coating to assume the very high curvature required for stress-free conditions. Because heat-barrier coatings, in general, are restrained to varying degrees by the metal substrate and by other external sources, the restraint forces impose moments on the coating that oppose the thermally induced bending tendency of the coating. The force distribution in thermally stressed bodies can often be estimated by the principle of superimposition, using a two-step process where the body is first allowed to deform freely and then, secondly, the external restraint forces are applied until the actual strain configuration is realized. Thus, if the coating in the actual case is prevented completely from bending, the stresses in the coating are equivalent and opposite to those produced by external moment forces that can flatten curved coatings of radius of curvature (ρ). In general, large compressive stresses will exist on the outer surface of the coating and large tensile stresses will exist on the inner surface. In addition to moments, other restraint forces can be present, as for example, those that produce pure tensile or compressive stresses along the plane of the coating.

Because the stress distribution in the coating depends on the exact nature of the external restraint forces, specific analysis is necessary for any set of restraint forces. Subsequently, specific cases will be examined in detail.

Adhesion

An assumption made in the subsequent thermal stress analyses is that the coating and substrate remain in intimate contact and that there is no discontinuity in the strains acting parallel to the interface across the coating-substrate interface. This condition is satisfied only if there is sufficient coating-substrate adhesion.

In general, two types of stresses can contribute to the failure at solid-solid interfaces: (1) stresses acting normal to the interface, tending to pull the two solids apart, and (2) shear stresses tending to disrupt bonds by a sliding action. To illustrate why these stresses exist, consider the diagrams in Fig. 6 . Let Fig. 6a represent the condition before any heat is applied to the coating system. When heat flows through the coating, the coating will tend to bend into a stress-free state, and, if the coating is not adherent to the substrate, the situation depicted in Fig. 6b would result. For simplicity, the substrate will be assumed to be very thick compared with the coating and to not distort appreciably. If the coating is to be adherent, stresses must be imposed on it by the substrate to return the situation to that depicted on the left of Fig. 6c, To accomplish this, normal stresses at the interface provide the necessary moment forces required to straighten the coating (Fig. 6c, right side). Also, because the coating has expanded, interface shear stresses compress the coating to match it with the substrate (Fig. 6d).

A precise analysis for determining the magnitude of normal and shear stresses at the interface would be very complex and is not within the scope of the present study. These stresses can be easily estimated, however, using a somewhat simplified approach. Although the calculations can be considered only as rough estimates, important qualitative features are revealed by the analysis.

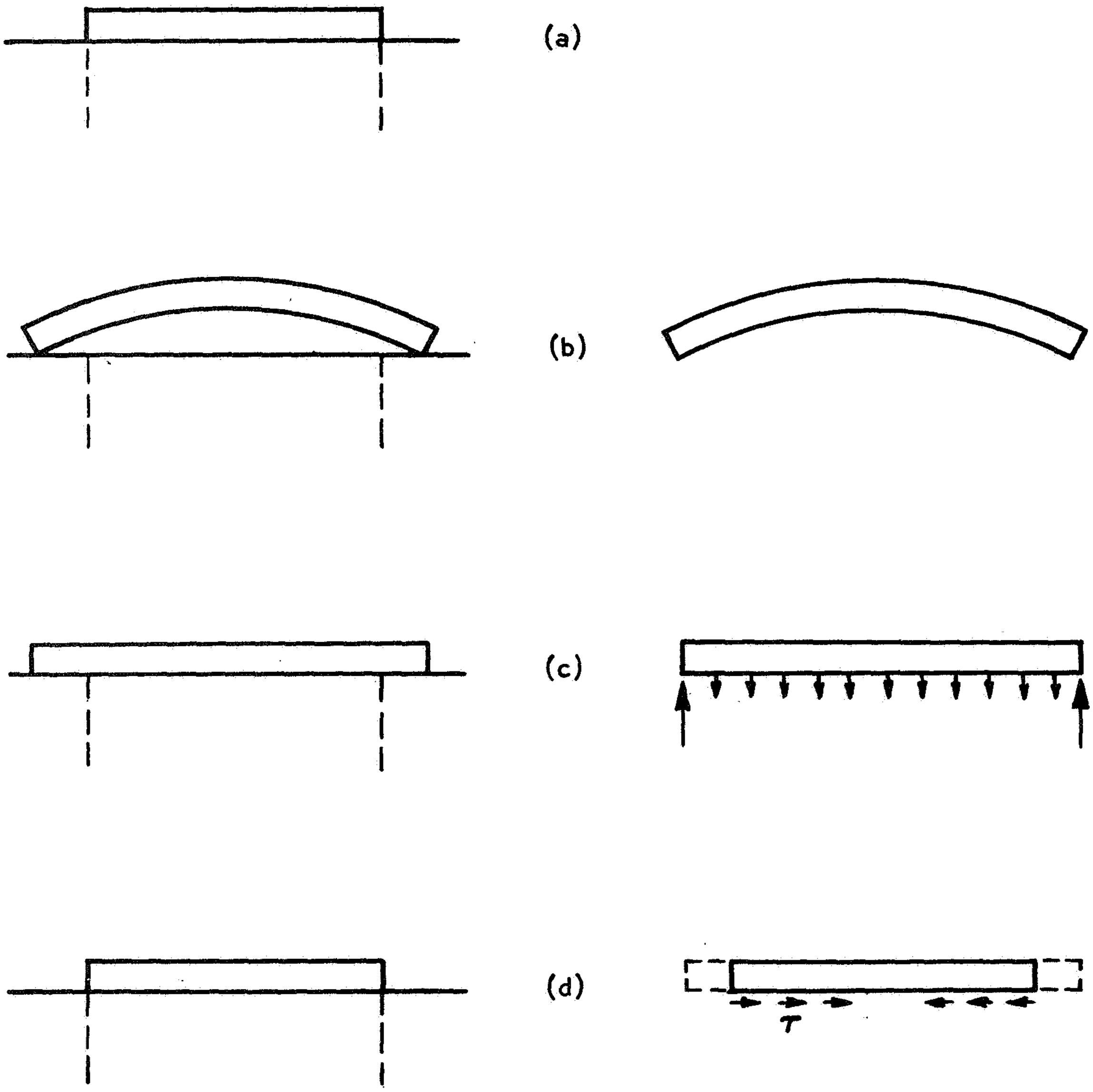

Figure 6. Illustration of the Origin of Thermal Stresses in Coatings (refer to text for description)

According to the analysis presented in Appendix B, the normal stress σ_N and maximum shear stress τ_{max} at the interface are given approximately by the following equations:

$$\sigma_N = \frac{2}{3}\frac{t_c^3}{L^2}\frac{E_c \alpha_c \dot{Q}}{k_c(1-\mu_c)} \qquad (3)$$

$$\tau_{max} = 4\,\frac{t_c}{L}\left[\frac{\alpha m(\bar{T}_m - T_e) - \alpha_c(\bar{T}_c - T_e}{\dfrac{(1-\mu_c)}{E_c} + \dfrac{t_c}{t_m}\,\dfrac{(1-\mu_m)}{E_m}}\right] \qquad (4)$$

These equations apply to a coating of finite length L, of unit width, and of thickness t_c. Both σ_n and τ_{max} are seen to decrease with increasing size (L).

Using values on p. A-41 for t_c, E, α, $\dot{Q}$, k, and u, the equation for the normal stress becomes

$$\sigma_N = \frac{2.3}{L^2}\ \text{(psi)}$$

Thus, for all practical values of L, σ_N is very small. Compared with the stresses in the coating system, σ_N will be negligible.

The shear stress, using the data on Page A-41, is given by

$$\tau = \frac{3.34 \times 10^3}{L}\ \text{(psi)}$$

Thus, the interfacial shear stress can be very appreciable, especially for small values of L. For example, if L is 1 inch τ is 3,340 psi, while if L is 1/4-inch, τ is 13,360 psi. In practical terms, the preceding results mean that coatings applied as small patches would have high interfacial shear stresses. The same applies to coatings that have become cracked into individual segments. Interfacial shear stresses are minimized when the area of contact between an unbroken unit of coating and the substrate is the largest possible.

Thermal Stress Distribution in Restrained Elastic Coating-Substrate

General Solution. Consider a system composed of a coating on a metal substrate, with a steady-state heat flux ($\dot{Q}$) flowing perpendicular to the surface. This system is illustrated in Fig. 4.

The general problem is to determine the stresses in the system under the condition that the system is not free to relieve stresses by bending. To generalize the problem, the properties of the coating and the metal are assumed to be variable along the z direction. The derivation of the solution to this problem is presented in Appendix A-B. The general equation representing the solution is presented below. The stress $\sigma(z)$, which is that in the plane of an element dz a distance from the cold wall, is given by

$$\sigma(z) = \frac{E(z)}{[1-\mu(z)]} \left\{ e_T - \alpha(z) \left[T(z) - T_e \right] \right\} \qquad (5)$$

where

$E(z)$ = elastic modulus at position z

$\mu(z)$ = Poisson's ratio at position z

$\alpha(z)$ = expansion coefficient at position z

$T(z)$ = temperature at position z

T_e = room temperature, where the system is assumed to be stress free

and

e_T = actual net strain produced in the system,

or,

$$e_T = \frac{\displaystyle\int_0^{t_m+t_c} \frac{E(z)\,\alpha(z)}{[1-\mu(z)]}\,[T(z) - T_e]\,dz}{\displaystyle\int_0^{t_m+t_c} \frac{E(z)}{[1-\mu(z)]}\,dz}$$

Stresses When the Coating and Substrate are Each Homogeneous. The simplest application of Eq. 5 is the case where both the coating and the substrate have homogeneous properties (independent of z). That is, E, α, and k are uniform within each material. Let the subscripts c and m denote that a particular parameter corresponds to that for the coating and the metal, respectively. Because $\dot{Q}$ and k are constant through each layer, the temperature gradient is linear across each layer. By making use of these facts, Eq. 5 becomes

$$\sigma(z) = \frac{E(z)}{[1-\mu(z)]}\left\{e_T - \alpha(z)\,[T(z)-T_e]\right\}$$

where now

$$e_T = \frac{B_m\alpha_m\left[\bar{T}_m - T_e\right] + B_c\alpha_c\left[\bar{T}_c - T_e\right]}{B_m + B_c}$$

and

$$B_m \equiv \frac{E_m t_m}{[1-\mu_m]}$$

$$B_c \equiv \frac{E_c t_c}{[1-\mu_c]}$$

$\bar{T}_m = \dfrac{T_i + T_o}{2}$ = average temperature of the metal

$\bar{T}_c = \dfrac{T_s + T_i}{2}$ = average temperature of the coating also

$$\left.\begin{aligned} E(z) &= E_m \\ \alpha(z) &= \alpha_m \\ \mu(z) &= \mu_m \end{aligned}\right\} \quad \text{from } 0 < z < t_m$$

$$\left.\begin{aligned} E(z) &= E_c \\ \alpha(z) &= \alpha_c \\ \mu(z) &= \mu_c \end{aligned}\right\} \quad \text{from } t_m < z < \left(t_m + t_c\right)$$

As a numerical example, the properties for the materials listed on Page A-39 shall be used to calculate stresses in the system.

Then

$$R_m = \frac{E_m t_m}{1-\mu_m} = \frac{(26 \times 10^6)(15 \times 10^{-3})}{0.680} = 5.73 \times 10^5$$

$$R_c = \frac{E_c t_c}{1\mu_c} = \frac{(14.2 \times 10^5)(3.5 \times 10^{-3})}{0.663} = 0.75 \times 10^5$$

$$\bar{T}_m = \frac{1200+0}{2} = 600, \quad Te = 100$$

$$\bar{T}_c = \frac{4000 + 1200}{2} = 2600$$

$$e_T = \frac{5.73 \times 10^5\ (8.05 \times 10^{-6})(600-100) + 0.75 \times 10^5\ (4.8 \times 10^{-6})(2600 - 100)}{5.73 \times 10^5 + 0.75 \times 10^5}$$

$$= 4.95 \times 10^{-3}$$

Thus, in the coating

$$\sigma(z) = 116{,}000 - 102\ T(z) \tag{6a}$$

and in the metal

$$\sigma(z) = 220{,}000 - 308\ T(z) \tag{6b}$$

The stresses are plotted as a function of z in Fig. 7 . As expected, the stresses are compressive at the hot surface and tensile at the cold surface. The abrupt change in stress at the interface is caused by the thermal expansion mismatch between the ceramic and the metal.

It is important to consider that the stresses in Fig. 7 are calculated from a purely elastic analysis. Extremely large stresses are predicted for this coating. These stresses will arise in a real situation only if the elastic limits (yield points) of the coating and/or substrate materials are higher than the maximum stresses in the coating and if the materials have sufficient strength to withstand these stresses.

If one or both materials yield plastically, the overall stresses will be somewhat lower. For example, if the metal substrate yields at a stress σ_y without subsequent work hardening, the maximum stresses in the metal will be $\pm\ \sigma_y$. The compressive restraint on the coating produced by the metal will be much lower than if the metal were perfectly elastic, thereby reducing the compressive stresses in the coating. The same stress gradient across the coating will be maintained, however, because the coating is still restrained from bending. Consequently, the effect of plastic flow in the metal will be to change all the stresses in the coating by a constant amount in the positive direction. Thus, there will still remain a difference in stress of nearly 300,000 psi between the inner and outer surfaces of the coating.

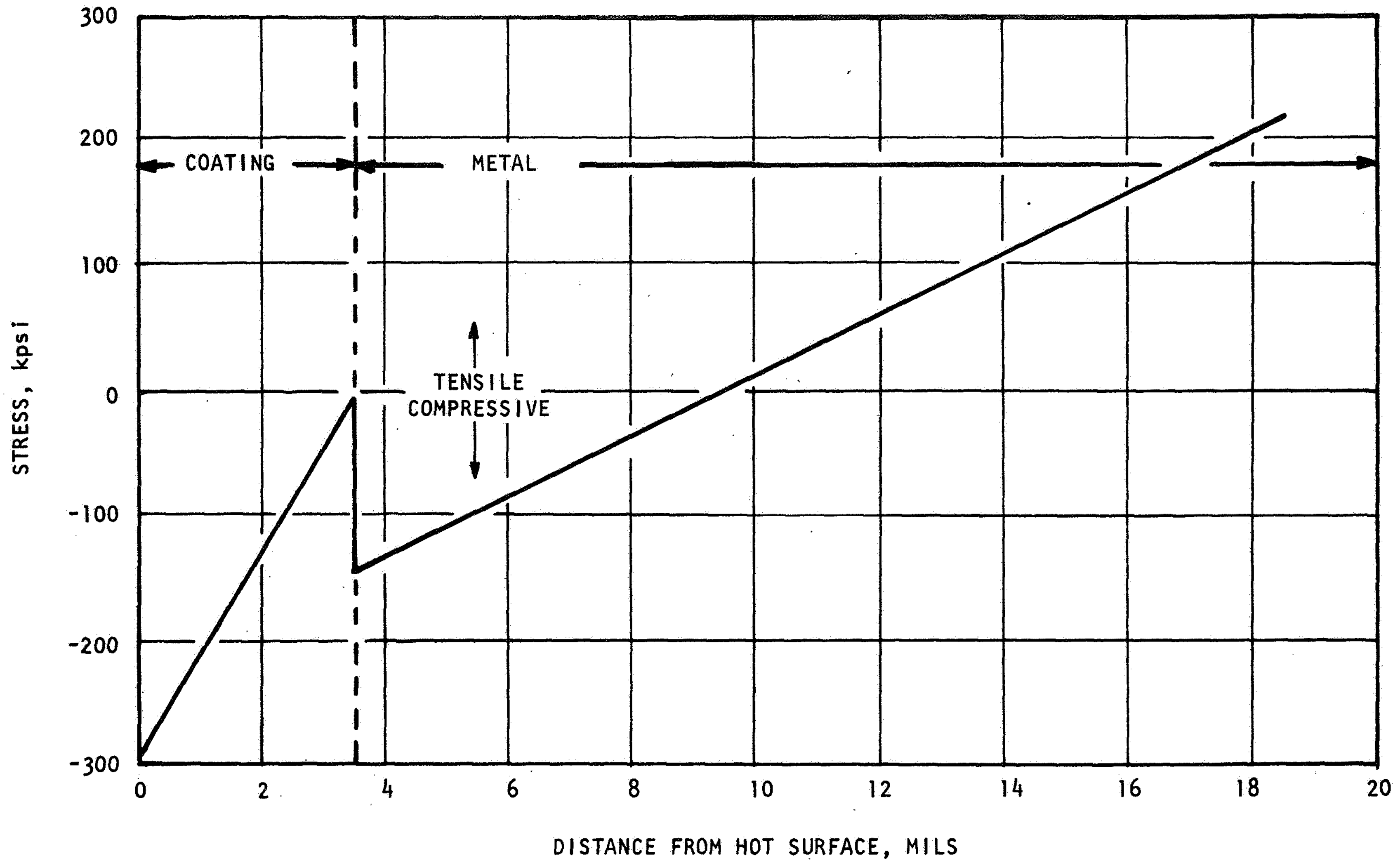

Figure 7, Purely Elastic, Restrained, Coating-Metal System at Steady-State Heating Conditions

From the preceding results, it is apparent that severe stresses are predicted for a completely elastic coating of homogeneous composition on a substrate that does not allow bending. Ceramic materials, with few exceptions, cannot sustain stresses on the order of several hundred thousand psi and mechanical failures must be expected. Alternative designs, therefore, will be considered next.

Nonhomogeneous (Graded) Coatings. The thermally induced bending tendency of uniform coatings can be eliminated, in principle, if the expansion coefficient varies through the coating in a manner such that the product $\alpha(z)\,[T(z)-T_e]$ is constant. In this way, every element dz will tend to expand equally.

If the coating is composed of a mixture of two materials (e.g., metal plus ceramic), and if the proportion of each varies through the coating, the coating is said to be graded. A graded coating gives a graded distribution of properties such as E, α, k, and μ. To analyze the effects of grading, it is necessary to know the extent k and α vary with V_m, the volume fraction of metal at position z. To simplify the problem, k and α will be assumed to be temperature independent. In general, α and k are much more sensitive to variations in V_m than to temperature variations, so the simplification is reasonable to a first order approximation. Expressing these dependences as

$$\alpha = \alpha(V_m)$$

$$k = k(V_m)$$

as shown in Appendix A-D the gradation (V_m vs z) required for constant thermal strain in the coating when the metal substrate is perfectly elastic must follow the relation

$$z' = \frac{\alpha_m [T_i - T_e]}{\dot{Q}} \int_0^{V_m} \frac{k(V_m)}{\left[\alpha(V_m)\right]^2} \, d\,[(\alpha V_m)] \qquad (7)$$

where z' is the distance below the hot coating surface. The integral is evaluated by graphical integration when the functions $k(V_m)$ and $\alpha(V_m)$ are known, leading to a relation between z and V_m.

For purposes of illustration, specific k vs V_m and α vs V_m relationships will be assumed. The Lichtenecker formula (Ref. 21) was found to represent fairly well the dependence of k on V_m for zirconia-metal mixtures (Ref. 22). This formula is

$$k = k_c \exp\left[V_m \ln (k_m/k_c)\right] \tag{8}$$

where k is the conductivity of a mixture whose metal volume fraction is V_m, k_c is the conductivity of the pure ceramic, and k_m is that of the pure metal. The expansion coefficient of the mixture shall be estimated by the rule of simple mixtures:

$$\alpha = (\alpha_m - \alpha_c)\, V_m + \alpha_c \tag{9}$$

Because the literature contains very little information on thermal expansion data for ceramic-metal mixtures, theoretical estimates must be used.

Substituting Eq. 8 and 9 in Eq. 7

$$z' = \frac{\alpha_m[T_i - T_e]\, k_c b_2}{\dot{Q}} \int_o^{V_m} \frac{\exp(b_1 V_m)}{[b_2 V_m + \alpha_c]^2}\, dV_m$$

where $b_1 \equiv \ln (k_m/k_c)$ and $b_2 \equiv (\alpha_m - \alpha_c)$;

The equation can be made dimensionless because $z' = t_c$ when $V_m = 1$. Thus

$$\frac{z'}{t_c} = \frac{\displaystyle\int_o^{V_m} \frac{\exp(b_1 V_m)}{[b_2 V_m + \alpha_c]^2}\, dV_m}{\displaystyle\int_o^{1} \frac{\exp(b_1 V_m)}{[b_2 V_m + \alpha_c]^2}\, dV_m}$$

For zirconia-Inconel mixtures, using reasonable values for the parameters b_1, b_2, and α_c, values of V_m vs z'/t_c are obtained in Appendix A-D and are represented in Fig. 8. The gradation required for uniform thermal expansion in the coating is steeper near the hot surface than near the metal-coating interface.

The gradation profile calculated above serves as an example of how it may be obtained theoretically and to show that uniform thermal expansion can be obtained in principle. In actual cases, the relationship between k and V_m and between α and V_m may not be in the form represented by Eq. 8 and 9. More complex relationships may exist, and very little experimental data are available for systems of interest in the present program to establish the correct relationships.

The graded coatings of the type cited previously are well suited for substrates that are restrained in such a manner that very little bending can occur. In that event, the substrate will have little tendency to bend the coating, and, consequently, stresses in the coating caused by applied moments will be small.

Although, in theory, continuously graded coatings appear best suited for restrained systems, in practice these coatings may be difficult to fabricate by slurry methods, particularly because the coatings will be extremely thin.

Stress Relief by Nonelastic Deformation

Qualitatively, the effect of plastic deformation in the metal substrate on thermal stresses has been previously discussed. In this section, the effects of nonelastic behavior of components other than the substrate will be considered.

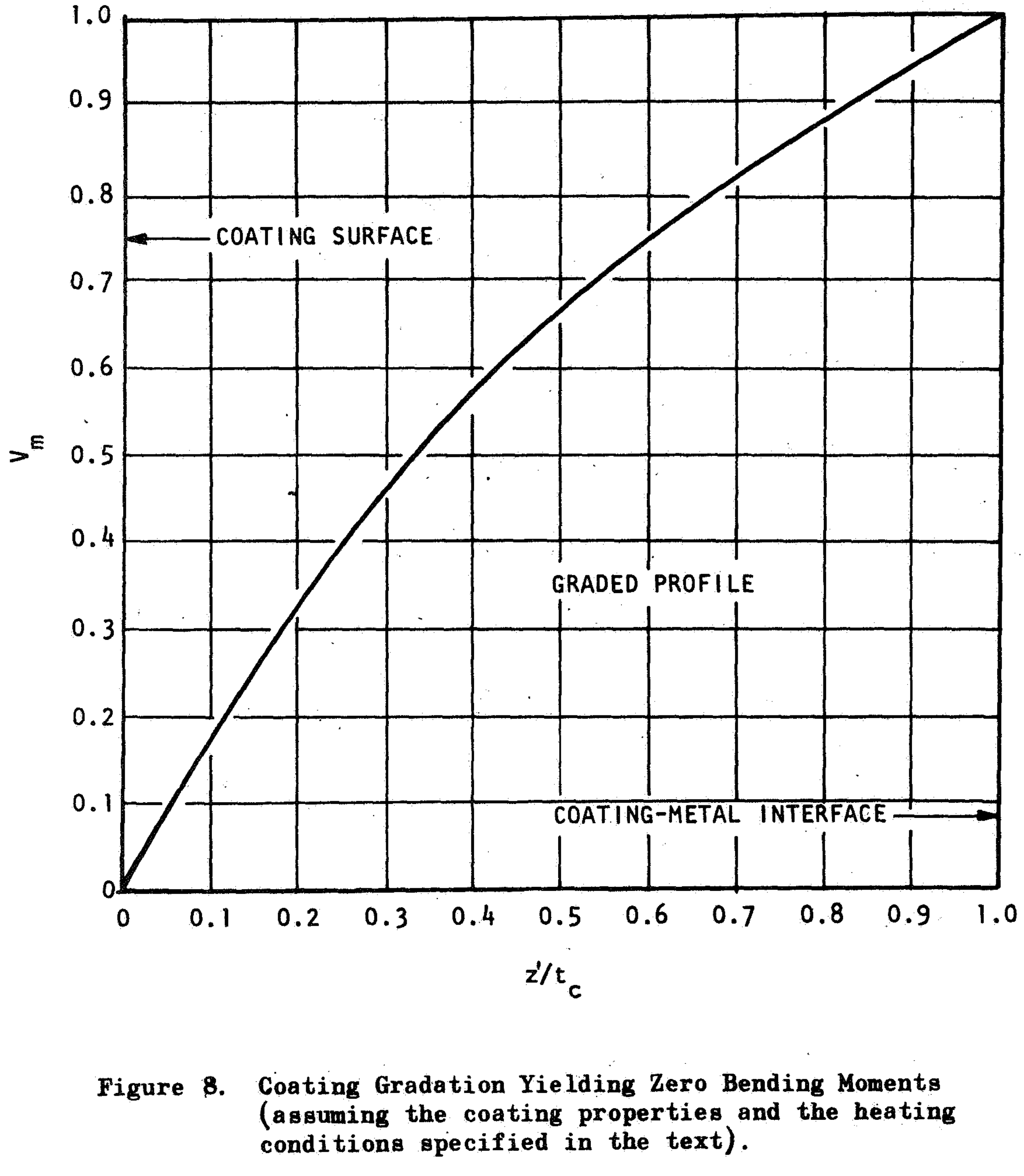

Figure 8. Coating Gradation Yielding Zero Bending Moments (assuming the coating properties and the heating conditions specified in the text).

Coatings With High-Temperature Deformability. If the coating contains glass as a binding agent, there will exist a softening temperature T_{sf} above which the coating will deform viscously at low stress levels. Only small stresses exist in the coating if its temperature is above the softening point. The major stresses that arise in these coatings are those formed on cooling after the coating material hardens. Because of expansion coefficient differences between the coating and substrate, residual stresses develop on cooling.

Lauchner and Bennett (Ref. 23) give an equation for residual stresses in coatings for the situation where the metal-coating system undergoes uniform cooling (the temperature being the same in the coating and substrate at any given instant). This equation is:

$$\bar{\sigma}_c = \frac{(\alpha_c - \alpha_m)(T_{sf} - T_e)}{\frac{1-\mu_c}{E_c} + \frac{t_c}{t_m}\frac{(1-\mu_m)}{\epsilon_m}}$$

Where $\bar{\sigma}_c$ is the average compressive stress in the coating at ambient temperature T_e, and T_{sf} is the softening temperature of the coating. If α_c is 5×10^{-6} F^{-1}, α_m is 8×10^{-6} F^{-1}, E_c is 14.2×10^6 psi, E_m is 26×10^6 psi, μ_c is 0.337 and μ_m is 4320, then

$$\bar{\sigma}_c = 56.7\ (T_{sf} - T_e)$$

If T_{sf} is 1900 F, $\bar{\sigma}$ is approximately 100×10^3 psi, and if T_{sf} is 1000 F, $\bar{\sigma}_c$ is approximately 50×10^3 psi. Thus, large stresses develop throughout the expected range of softening points (1000 to 1900 F).

In actual heat-barrier applications, the preceding analysis does not strictly apply because uniform cooling does not occur. Actual cooling occurs somewhat in reverse to that depicted for heating in Fig. 5 . Contraction of the metal during cooling is much less than supposed for the uniform cooling model, and consequently the compressive stresses arising in the coating may be much less severe.

To a first approximation, the actual cooling situation can be depicted as a system where the average temperature in the metal is T_x when the coating temperature is at the softening point T_{sf}. In this case

$$\bar{\sigma}_c = \frac{\alpha_c(T_{sf}-T_e) - \alpha_m(T_x-T_e)}{(1-\mu_a) + \frac{t_c}{t_m}\frac{(1-\mu_m)}{T_m}}$$

The coating is approximately stress free when

$$\alpha_c(T_{sf}-T_e) = \alpha_m(T_x-T_e)$$

Thus, if T_{sf} is 1900 F, T_x must be 1200 F if the coating is stress free. The coating will have compressive residual stresses if, in the actual case, T_x is above 1200 F and will have tensile residual stresses if T_x is below 1200 F. Inspection of Fig. 5 suggests that T_x will be below 1200 F, and consequently the coating will experience tensile forces. Because an analysis of the cooling situation has not been carried out, an estimate of the magnitude of the residual stress cannot be calculated.

Strain Accommodation Layer. Large stresses arise in coatings because their natural tendency for expanding when heated is restrained by the substrate. As discussed previously, the coating would expand and bend if unrestrained. The presence of a very ductile metal layer placed between the coating and the substrate would relieve some of the restraints imposed on the coating by the substrate. To be effective, the ductile metal must have a yield strength considerably below the ultimate strength of the ceramic coating. In this way, plastic strain can occur in the ductile layer to relieve stresses in the coating before the coating stresses build up to fracture levels.

A theoretical analysis of thermal stresses in coating systems having a strain accommodation layer was not conducted because such an analysis would involve complex elastoplastic considerations which are beyond the scope of the present program.

Qualitatively, however, it is clear that a reduction in stresses in the coating will result by using a strain accommodation layer because the restraint conditions on the coating are somewhat relieved.

PROPERTIES OF THE COATING SYSTEM

Chemical and Physical Stability

The properties that the coating must possess to withstand the thermal and chemical environment of the present heat-barrier application are discussed in this section. Mechanical aspects, such as thermal shock were discussed in greater detail in the previous section.

Melting Point. The surface temperature of the coating will be 4000 F, whereas subsurface temperature will be proportionately lower. Material systems selected for any strata in the coating should not melt at the use temperature. Also, the melting point should be higher than the use temperature to provide a margin of safety because of possible fluctuations in the heat flux of experimental rocket engines. Molten phases should be avoided because they are corrosive, unstable, and cause a significant reduction in strength. However, the selection of cementitiously bonded materials systems that do not have any liquid, or viscous, phases at temperatures of approximately 4000 F may not be practical, yet the preceding criteria must at least be met in regard to the filler materials.

Destructive Phase Changes. Materials must be selected that do not undergo large volume changes over a small temperature range. Large internal stresses that are caused by the sudden change in volume can cause mechanical failure, or at least cause weaknesses in the coating system.

Otherwise useful materials that undergo harmful phase transformations, such as ZrO_2, are usually stabilized in one phase to render them usable.

Chemical Reactions. Materials must be chemically inert in the environment so as not to change properties during use. All materials should be stable in hydrogen, oxygen, and water atmospheres because cementitiously bonded coating systems will be pervious to the combustion gases to some extent. Moreover, adjacent materials of different composition (for example, the first layer of coating and the metal substrate, and a bonded layer of zirconia over a bonded sublayer of alumina) must be compatible.

Erosion. The outer layer of coating must be sufficiently strong and hard to ensure that the erosion rate is negligible. Because these coatings will be relatively thin, and because the heat flux is relatively high, even small changes in thickness (which is proportional to thermal resistance) could result in a large reduction in thermal protection.

Cohesive Strength of the Coating

Cohesive strength of a given cementitiously bonded system is closely related to packing density and size distribution of the filler oxide powder because these factors govern the number of point-to-point contacts between the filler powder, the ratio of cement to filler, and size distribution of pores. These topics are discussed in the following paragraphs.

Density. Theoretical density of the composite can be obtained by completely filling the voids (30 percent of volume or greater) between the grains of the filler oxide with the binder material; nevertheless, theortetical density is not possible in most cases, nor is it desirable in any case. It is not desirable because the binder invariably will be less thermally and chemically stable than the filler. Thus, the use of only a small amount of binder (approximately 10 percent by volume) will yield optimum thermal and chemical stability of the composite at high temperatures, especially at 4000 F. Moreover, it is not desirable because the best resistance to thermal shock is not usually achieved at theoretical density. Thermal strains are usually better accommodated when a small amount of porosity is present.

Completely filling the voids is not generally possible because most binder compounds decompose during setting, losing water molecules or other molecules that were chemically or mechanically combined with the basic cementing compound. The cured cement generally occupies less volume than the original bonding agent. Also, all slurry coatings are suspended in a liquid, usually water, that is removed after the coating is applied. Unless particles are rearranged by unconventional procedures, the density of the dried composite will be less than that of the as-applied slurry.

At any rate, best results will be obtained in this program by using only sufficient binder to adequately cement the grains of the filler together. Voids formed between the grains of the filler will not be completely filled with any material (unless of course, special techniques are used to add more filler in liquid form and to precipitate it inside the voids). In fact, the grains of the filler oxide will be separated to some extent by the cement that bonds them together.

The density of the composite will be governed by the packing efficiency of the grains of the filler oxide and best results will be achieved by obtaining maximum packing density. The maximum packing density obtained by usual procedures is approximately 80 percent of theoretical.

Particle Size and Other Raw Material Characteristics. Maximum packing density of particles is generally obtained by mixing three size fractions, each at least one order of magnitude different in size. This general rule was not always followed in development programs reported in the literature, but increased density (or strength) for cementitiously bonded materials is generally obtained by combining at least two, and usually three, different size fractions of powder although not always a factor of 10 different in size. Most programs reported in the literature also used a fraction of large-sized grog, approximately 50 mesh, to improve the properties of the composite. The use of large-size fractions also allows the use of smaller size fractions that are a factor of 10 smaller. But using such large grains will not be possible in this program because these particles are considerably larger in diameter than the thickness of the coating. Particles used in this program must be -200 mesh to exclude particles with diameters (or at least a minimum axis) of 2.9 mils because coating thicknesses will be as small as 3.5 mils.

Being limited to such a small particle size is a disadvantage. Small particles do not pack as efficiently as large ones. This is mainly because, physically, handling and mixing are difficult, because the absorbed layers of impurities represent a large fraction of the total volume, and because clustering results due to electrostatic forces which become prevalent on small particles. Another reason is that three particle size fractions an order of magnitude apart in size, cannot be used for obtaining maximum density. The smaller of the fractions would consist of submicron size particles with chemical, physical and mechanical characteristics resulting from the large surface-area-to mass ratio that would make the powder too difficult to handle. Such particles would easily become airborne, hydrate, absorb impurities, and agglomerate.

Thus, particle sizes and particle size fractions used in coatings for this program must be determined by experiment. Two, and even three, different fractions may be used to obtain maximum density, but there will not be any large size gap between the fractions. For example, -200, +325 mesh powder would be mixed with -325 powder to obtain a high packing density. The -325 mesh fraction could be further divided into two fractions although this procedure would have disadvantages. Particle size separation in this range is expensive and it requires elaborate quality control procedures to ensure reproducibility. The use of one -325 mesh fraction with a specified particle size distribution, such as commonly used for melt-sprayed coatings, would be more practical.

Another factor must be considered in selecting powders for development of cementitiously bonded slurry coatings, viz., the surface area of fine powders causes a rapid chemical bonding reaction rate, and rapid bonding reactions usually result in bloating and a low coating strength. The reaction rate can be controlled in two ways, however. One is by the use of special additives, such as retardants, buffering agents, sequestering agents, etc. This method is not always possible, however, and when it is, its effectiveness is limited. The second method for controlling reaction rate is to change the available surface area of the solid reactant, i.e., the filler oxide powder. Surface area can be adjusted by interchanging powder derived from either fusion or sintering processes. Sintered powders generally have a higher surface area and porosity, whereas fused powders have lower surface area, are more dense, and are more irregular in shape with sharp edges. In general, sintered powders of equivalent size would react faster than fused ones and would produce stronger composites provided the reaction is not too rapid.

In summation, the proper combination of available raw materials in regard to particle sizes, or size distributions, must be determined experimentally for this program because the technology involving the use of the small grain sizes demanded by the design requirements of this program does not exist. Moreover, the dense, strong,cementitiously bonded coatings will be difficult to develop when restricted to the use of such small grain-sized powders.

Adherence

State-of-the-Art. Adherence of slurry coatings to metal substrates was not obtained in any of the coating-metal systems reported in the literature. Without exception the coating systems were held to the metal substrate with metal reinforcements. There are several possible reasons for this lack of bonding between the two materials. For one, most of the cementitiously bonded coated systems included an acid bonding agent that readily reacted with metals. In fact, this reaction caused problems in the use of the metal reinforcements because the reaction corroded the metal and gaseous products caused bloating in the coating. These acid bonding agents must have also reacted similarly, but less noticeably, with the metal substrate. Therefore, any reaction at the metal substrate-coating interface was detrimental to both materials, and it was not conducive to bonding between the two materials. Another reason for poor adherence could have been that the coating did not wet the metal substrate. Wetting properties of the slurry coating systems on the metal substrates are not reported in the literature, but the existence of wetting problems is inferred because wetting agents were occasionally used. Wetting is essential for adherence to occur whether it occurs by the sharing of electrons across the interface, by Van der Waals-type bonds across the interface, or by mechanical interlocking into holes, grooves, or undercuts in the metal surface. In other words, the coating must make intimate contact with the surface of the metal to become adherent.

Mechanical Adherence. To achieve good mechanical adherence of the coating to the metal substrate, therefore, several conditions must be met. First, the substrate must be very rough, preferably with deep undercuttings in which the coating can fit into so as to attach itself to the metal substrate. These undercuttings must be formed by grit blasting with grit that will produce pits larger than the particles which must fit into the pits, and by grit blasting at an angle so as to form the undercuttings. Obtaining such a surface that is conducive to good mechanical adherence is not easy, however, because the grit blasting closes as many undercuts as it forms on the metal surface by peening over the edges, and much of the abrasive grit imbeds into the surface. Imbedded grit not only reduces the possible number of holes that the powder in the coating can fill, but it can lead to other problems because of surface contamination. Another method of roughening the surface is to chemically etch the grain boundaries of the metal substrate (Ref. 24). Because grain boundaries usually meet at 120-degree dihedral angles, the majority of the etched holes will be oblique to the surface, that is, they will be undercuts rather than tapered holes with the largest diameter at the surface.

The second criterion for good mechanical adherence is that the slurry must wet the metal so that it will enter the undercuts. Wetting can be achieved by adjusting the pH, by adding minute quantities of wetting agents, and by changing the surface energy of the metal substrate. Metal surfaces have high surface energies because of the nature of the uniform atomic size of all constituents. That is, a large proportion of the surface atoms are not shielded by larger atoms as they are in oxides, Conversely, the slurry has a low surface energy because atoms are not equisized, and they are sufficiently mobil that they can present the lowest surface energy for the system. Therefore, the slurry will not wet the metal because of the large difference in surface energies of the two systems.

Wetting can be increased appreciably, however, by changing the surface composition, and therefore, surface energy, of the metal surface. The surface composition of the metal surface can be changed by the formation of a very thin layer of adherent oxide on the metal surface. Moreover, this oxide layer offers other benefits: it protects the metal from corrosion from acid binders, and reduces bloating in the coating by eliminating the formation of gaseous reaction products.

Chemical Adherence. Achieving a chemical bond between the metal substrate and the cementitiously bonded coating will be more difficult; in fact it might be beyond the scope of this program. The state-of-the-art of cementitious bonding only includes ceramic-to-ceramic bonding, not ceramic-to-metal bonding. An extensive program to develop chemical adherence by creating ceramic-to-metal cementitious bonds is not expected to be necessary in this program. The bonding agents used in the slurry coatings should chemically bond to the preoxidized surface of the metal, thus avoiding the metal-ceramic bonding problem. In fact, because the metal should be preoxidized to promote wetting, the slurry coating should never be applied on a clean metal surface.

Two other methods of promoting a chemical bond, although neither has been attempted, is to interpose a thin layer of a semiconductor, such as silicon, or a glass between the metal substrate and the cementitiously bonded coating. The layer of silicon would be a strong link between substrate and cementitiously bonded coating. It would be diffusion bonded to the metal substrate and it would form Si-O bonds with the coating when the coating is applied and cured.

For the other method, producing strong chemical bonds between the glass and the metal substrate would be accomplished using standard practices (Ref. 27). Chemical bonding is promoted by either of two mechanisms but this is only academic because the laboratory procedure for producing adherence is identical for both. Basically, chemical adherence is produced between a glass coating and its metal substrate when the glass coating is saturated with oxide(s) of the substrate metal. One proposed mechanism is that electrons are shared across the interface because of a balance of bond energies and a continuous electronic structure (Ref. 26 and 27). That is, the transition across the interface is from metal A, to metal A oxide, to metal A oxide-saturated glass, to the glass coating. The other proposed mechanism is that Van der Waals forces sufficient to cause strong chemical bonding are created by allowing a high ratio of atoms on both surfaces (the glass and the metal in this case) to come in contact with each other (Ref. 28 and 29). In any case, however, the most practical way to achieve chemical bonding, by either of the two mechanisms, is to preoxidize the metal surface before, or during, application of the glass coating. An oxidized surface is required in the second theory to promote the complete wetting that is mandatory for a high ratio of atom-to-atom contacts, and an oxidized surface is required in the first theory to promote wetting and to promote the transitional electronic lattice structure. The oxide layer should not be too thick or it will weaken the composite structure, but it should be sufficiently thick to ensure that sufficient oxide(s) dissolve and saturate the adjacent stratum of glass.

The cementitiously bonded, heat-barrier coating would then be applied to the glass substrate by the same techniques used to apply it to a metal substrate. Then, a short firing (heating) operation would cause the cementitiously bonded coating to become imbedded in the glass. Thus, the heat-barrier coating would be both chemically bonded to, and mechanically held by, the glass which, in turn, would be chemically bonded to the metal chamber wall.

The glass will be designed to survive thermal shock in this system through the selection of a glass with the following properties. First, the glass must fuse at 1800 F, or less, so that the properties of the Hastelloy-X substrate are not impaired when the glass is fired (fused to the substrate). Glasses applied as subsieve-size powders fuse into dense coatings well below their smelting temperatures (the temperature required to melt and to pour the glass from a crucible). Second, the glass should not soften at 1200 F (the service temperature) so that shear forces during rocket engine firing could cause sufficient movement to cause failure of the coating system. Third, the glass should have a coefficient of thermal expansion between that of the metal substrate and that of the heat-barrier coating.

An added advantage in using this intermediate layer of glass would be that the glass will be annealed at the service temperature, thus relieving thermal stresses created by the difference in properties between the metal substrate on one side and the cementitiously bonded coating on the other.

In summary, the procedure for using an intermediate layer of glass would be to first form an adherent, uniformly thick layer of oxide on the metal substrate. The use of Hastelloy-X is extremely advantageous here because its tenaciously adherent, strong oxide layer promotes excellent adherence of glass coatings. Next, the glass coating would be fused into a dense, uniform coating at the optimum time-temperature relationship that results in saturation of the glass with the substrate oxide. The next operation would be to apply the cementitiously bonded, slurry coating over the glass and to refuse the glass by heating it at a lower temperature and for a shorter time than was used in the first operation.

A principal disadvantage of this technique for obtaining strong adherence of the heat barrier coating to the chamber wall is that the chamber must be heated to a relatively high temperature to apply the glass coating. This disadvantage should not prevent the investigation of this method because, should this method be useful, this problem can be reduced by several techniques if necessary. For example, a new glass can be formulated to have a lower application temperature and still meet all of the design critera, or the glass could be applied by new, low-temperature techniques (Ref. 30).

Although this technique has not been attempted it appears theoretically sound and practical. It should produce exceptionally strong attachment of the heat barrier coating to the chamber wall, and it could increase thermal stress resistance of the entire system by annealing during service.

Composite Design for Improving Resistance to Failure

Reinforcement. In all of the slurry heat-barrier coatings programs reported in the literature, reinforcements were required to hold the coating systems to the substrate and to maintain the structure in one piece when the coatings cracked. Because, as reported previously, many differences of design requirements between this program and past programs exist, reinforcements may not necessarily be required in this program. The most important factor in this case is the difference in coating thickness. Coatings reported in the literature were so thick (from 1/4 to more than 1 inch) that, in comparison with this program, they are better described as heat shields. Because both thickness and shape are important factors relative to the resistance of a body to thermal stress, it is probable that the thin coatings (3-1/2 mils, for example), will be less prone to cracking and spalling than the thick heat shields. In fact, it may be possible to bond the coating to the substrate without using reinforcements by using one of the techniques described in the preceding section of this report.

If unreinforced coatings prove unsatisfactory, reinforcements substantially different from those used with thick coatings may be required. Employing a scaled-down version of the type of reinforcements used in thick coatings (e.g., spot-welded, corrugated strips) may be impractical because of the small size. Furthermore, the mechanism for failure in thin coatings may be different from that of thick coatings, and the reinforcement may have to serve a different function.

Because an exact thermal stress analysis for predicting the mode of failure in coatings was not possible, an appropriate reinforcement cannot be selected until a better appreciation can be gained from failure analysis of actual test specimens. For instance, if the coating cannot be made to adhere to the substrate in arc-plasma tests, reinforcements must be used to hold the heat barrier in place. If the coating cracks because of tensile stresses, then a reinforcement must be used to strengthen the coating and to hold it together. If the coating fails because of compressive forces, then a ductile, or crushable, reinforcement must be used. If the reinforcement must be used in the cooler strata, then Hastelloy-X, or stainless steel can be used. If the reinforcement must be used in the hottest strata of the heat barrier, then it must be made of ceramic material. Refractory metals cannot be protected from oxidation for appreciable time at temperatures as high as 4000 F. Many methods of protecting refractory metal reinforcements have been reported, but all were unsuccessful (Ref. 3 through 5, 31, and 32).

Many methods of reinforcing the thin coating designs of this program are feasible, but the use of the majority of them will require some developmental effort because methods of reinforcing such thin coatings have not been studied previously. This is another reason for not designing the reinforcement system until more is known concerning the design requirements.

Concepts for various types of reinforcements for attaching the heat barrier coating to the substrate are as follows:

1. Prefabricated fine wire screens attached at all contact points or at the end of barbed wires that stick out of the screen. The screens would be attached to the chamber wall by one of the following techniques:
    a. Electrical-resistance spot welding
    b. Brazing
    c. Diffusion
    d. Fusion of the metal screen into a glass coating that is itself chemically bonded to the substrate
    e. Electroforming
2. Screen-like structures fabricated in place by one of the following techniques:
    a. Melt spraying on metal in such a manner that it splashes as it freezes, or simply melt spraying a very porous layer of metal
    b.. Cold spraying short wires or coils on a hot substrate coated with a braze or glass

   c. Electroforming before the heat-barrier coating is applied by plating over a pyrolyzable fabric or by plating a mixture having one constituent that could be preferentially dissolved or etched
   d. Electroforming a metal after the heat-barrier coating is applied to the chamber wall in the continuous pore network of the heat barrier coating

3. Fibers or coils protruding from the substrate attached by any of the preceding methods

Reinforcements for strengthening the coating could consist of any of the preceding ideas but without the problem of attachment to the substrate. The problem in this case would be obtaining uniform distribution in the coating, preferred orientation, and adherence between the reinforcement and the heat-barrier coatings.

One potential method for attaching fibers to a metal substrate has been studied during a Rocketdyne-funded program. Metal fibers were oriented parallel to the surface and held in place with a magnetic field. Attachment to the substrate was then accomplished by electroplating techniques. Orienting fibers perpendicular to the substrate, like hair, was also demonstrated, but they were not attached to the substrate in this manner because this was not an objective. But attachment by the same electroforming techniques is possible. Nonmagnetic fibers were also attached using this method by first plating with a layer of a magnetic metal, such as nickel. Vapor deposition, electroless deposition, or electrodeposition are methods of plating the nonmagnetic fiber with a magnetic film.

Intermediate Layers. Use within a coating of interstratified layers of materials having thermal property values (particularly with regard to coefficient of thermal expansion) intermediate between those of the chamber wall and those of the outer layer of heat-barrier coating is a most practical method of reducing thermal stresses. Thermal properties of such layers can be adjusted in two ways: (1) other coating systems, different from the basic protective coating system in the outer layer, can be used, or (2) mixtures of the end member materials, Hastelloy-X and ZrO_2 for example, can be used to produce composite coating materials with graded properties. Graded coating designs have been used successfully in melt-sprayed coating systems where controlled alteration of the composition across the thickness of melt-sprayed coatings is very easy because of the nature of the melt-spraying process. Graded coating designs have never been utilized in cementitiously bonded, slurry systems, however, and their use may be difficult. Chemical reactions between metals (especially when they are in the form of subsieve-sized powders) and acid-type bonding agents, which represent some of the better candidate bonding agents for this program, will probably not result in satisfactory composite materials. Rather, the reactions will corrode the metal and cause bloating in the coating. Bonding, however, might be produced by forming a thin film of oxide on the metal grains so that the bonding reaction is between oxides (the oxidized metal and the filler oxide) and not between metal and oxide. It would be necessary to control oxidation of -200 mesh metal powder very carefully to ensure that the oxide film would be adherent and thin. If excessive oxidation of the powders occurred, the metal grains would be consumed and the "graded" mixture would not be a graded mixture of the coating and of the substrate alloy. Using graded coating systems in cementitiously bonded coating designs, therefore, requires a developmental effort in which no state-of-the-art is presently available for guidance. Also, it would be necessary to maintain the temperature of these layers below 2400 F by proper design of the coating system. Higher temperatures would result in melting of the alloy phase which would weaken the coating and which could result in undesirable changes in the properties of the coating system.

The other method of changing properties to reduce thermal stress is to use sublayers composed of different materials systems. The choice of materials systems is not limited to those for 4000 F service because the sublayer materials will be protected by the outer layer(s) of the heat-barrier system. Selection of filler materials must be based on several considerations. Filler materials should (1) have melting points above 2600 F, and preferably above 3000 F, (2) be compatible with the metal substrate and with the oxides in the outer layers of the coating system, (3) have thermal expansion coefficients intermediate between that of the coating and that of the metal substrate (refer to Thermal Stress Analysis section); and (4) be stable in oxygen gas and water vapor. The selection of these materials is also limited to oxide materials for the same reasons as presented for the outer layer materials in another section of the report. Although the coefficient of thermal expansion should be between that of the chamber wall alloy and that of the outer layer of heat barrier material system, this criterion should not be limiting. Other desirable properties of cementitiously bonded oxide systems could off-set the thermal expansion coefficient criterion by providing improved resistance to thermal shock by other means. For example, other advantageous properties include plasticity and high strength. Some of the candidate systems for less than 3000 F service are reported to deform plastically (Ref. 33) and to be 10 times stronger than cementitiously bonded systems composed of the more refractory oxide systems (Ref. 1 and 56). Also, compositions containing viscous silica glasses should result in thermal stress relief during service.

Another, and a most important criterion, is that these cementitiously bonded materials systems must be selected from state-of-the-art systems because developing new, low-temperature (melting point ≤ 2500 F) materials is beyond the scope of this program.

ANALYSES AND SELECTION OF MATERIALS SYSTEMS

SUBSTRATE ALLOY

The work statement of this contract specified that the substrate material for the coating (the chamber wall material) was to be selected from either Hastelloy-X or stainless steel (type 347). Hastelloy-X was selected because of several important advantages. Hastelloy-X has a 20 percent lower thermal expansion coefficient than type 347 stainless steel, and it forms a more protective, more tenacious oxide coating when heated in air. The lower expansion coefficient will cause less thermal stress in the coating, the protective oxide will reduce corrosion under service conditions, and it will be a more satisfactory substrate for coatings. Because slurry coatings will wet oxidized substrates better than unoxidized metal substrates, better coverage and better bonding will occur on a properly oxidized chamber wall.

Disadvantages of using Hastelloy-X are that it is not stocked in as many shapes and sizes and that it costs more than type 347 stainless steel. Usually a 6-month lead time is required when buying stock of special sizes, and the cost of Hastelloy-X can be as much as 10 times higher than that of stainless steel. However, the technical advantages far outweigh the logistical disadvantages: the price difference and long lead time in ordering are not crucial when manufacturing rocket engines because the cost increase due to the better alloy represents a small portion of the entire manufacturing cost, and 6-month lead times are not unusual for large orders of special shapes and sizes.

FILLER MATERIALS FOR 4000 F SERVICE

Survey

To meet the design requirements of this program, coating materials must be stable for a long duration at 4000 F in a stream of subsonic, sonic, then supersonic, oxidizing gases. Because of these conditions, the list of candidate materials is comparatively small. First, only refractory oxide materials are sufficiently stable under these conditions. Refractory borides, carbides, silicides, sulfides, and intermetallics will oxidize too rapidly in a highly oxidizing environment of 4000 F, particularly for any appreciable duration. These materials must be also rejected for another reason. No state-of-the-art exists for these materials in cementitiously bonded systems and this program is to be based primarily on existing technology and information. The list of candidate oxides is also limited because only those with a melting point above 4000 F are useful for 4000 F service. The criterion was arbitrarily set at a minimum melting point of 4300 F as a safety precaution and so that the coating would not melt under even small fluctuations normally expected during service. Further, several otherwise useful oxides must be eliminated because of high vapor pressures or reactions with water vapor. Even small vapor pressures or reaction rates can become important when the reaction products are continually swept away from the surface. Erosion is also an important factor in material performance but it was not taken into consideration in selecting the oxides. The inherent or potential, resistance to erosion is not important because the resistance to erosion of all of the state-of-the-art materials will be much lower than the inherent value.

Oxide materials with melting points above 4300 F (Table 2) are discussed individually in the following paragraphs with respect to their possible use as a filler material. The discussions in large part are taken from previous analyses (Ref. 5 and 34 through 38).

Beryllium Oxide. Beryllium oxide is chemically stable in contact with metals at high temperature and exhibits no tendency toward reduction in hydrogen up to 4250 F. However, beryllia reacts with water to form a volatile hydroxide above 3000 F, and it undergoes a phase transformation at 3810 F sufficient to cause cracking and spalling (Ref. 39). Also, beryllia is highly toxic and must be handled inside glove boxes.

TABLE 2

SELECTED PROPERTIES OF CANDIDATE COATING MATERIALS(1) (Ref. 40)

Material	Formula	Melting Point, F	Thermal Expansion Coefficient at 2500 F (x 10^6/F)	Thermal Conductivity at 2500 F, Btu/in.-sec-F x 10^5	Phase Transformation Temperature, F	Specific Gravity, gm/cm^3
Thoria	ThO_2	5400	5.6	3.0	--	9.69
Hafnia	HfO_2	5100	3.4	(3.5)(2)	3100	9.68
Magnesia	MgO	5100	7.8	7.0	--	3.58
Thorium Zirconate	$ThO_2 \cdot ZrO_2$	>5070	—	--	--	—
Strontium Zirconate	$SrO \cdot ZrO_2$	5070	>5	--	--	5.48
Barium Zirconate	$BrO \cdot ZrO_2$	4870	~5 (3.5 in Ref. 41)	--	--	6.26
Zirconia(3)	ZrO_2	4700	4.5	3.5	1900	5.7
Ceria	CeO_2	4700	5 (at 1800 F)	--	--	7.13
Calcia	CaO	4700	7.8	5.6	--	3.32
Beryllium Zirconate	$3BeO \cdot 2ZrO_2$	4600	—	--	--	—
Beryllia	BeO	4550	5.5	20	~3700	3.03
Strontia	SrO	4380	8.0	--	--	4.70
Hafnia-Rich Mixture	**(4)	4000 to 4400	0	--	2700	—
Yttria	Y_2O_3	4300	—	7	--	4.84
Calcium Zirconate	$CaO \cdot ZrO_2$	4250	6.5	--	--	—
Lanthia	La_2O_3	4180	--	--	2700	6.51
Urania	UO_2	4140	6.7	4.5	--	10.8
Chromia	Cr_2O_3	4110	4.1	--	--	5.21
Alumina	Al_2O_3	3600	5	7	--	3.98
Zircon	$ZrO_2 \cdot SiO_2$	3400(5)	5.5	5.3	--	4.6
Mullite	$3Al_2O_3 \cdot 2SiO_2$	3250	2.8	5	--	2.78

(1) These property data are presented for comparison only. The properties of a particular compound must be carefully evaluated when using that compound in a coating design. Properties for the same composition can change drastically with temperature, purity, density, grain size, etc.

(2) Ref. 42

(3) 80 weight percent is CaO stabilized

(4) Proprietary to Rocketdyne Division of North American Rockwell Corporation

(5) Decomposes

Consequently, the use of beryllia drastically reduces the amount of flexibility on work that can be accomplished. For the preceding reasons, beryllia is not an attractive candidate.

Calcium Oxide and Strontium Oxide. These materials are members of the alkaline earth group, and are not attractive in view of their chemical instability, especially with regard to water (hydration) and carbon dioxide (carbonation).

Cerium Dioxide, Cerium dioxide is easily reduced to lower oxides in hydrogen atmospheres at increasing temperatures, forming several "ordered" intermediate phases. The reduction with hydrogen occurs to an appreciable degree at 932 F, and is considerable at 1200 F. Possibly the reduced oxides represent a series of solid solutions of cerous oxide (Ce_2O_3) in ceric oxide (CeO_2).

Hafnium Oxide. This material, in most respects, is similar to zirconium oxide. Hafnium oxide has a monoclinic form at room temperature which inverts to a tetragonal form at approximately 3100 F. Pure hafnia is scarce because it is difficult to separate from the zirconia-containing minerals with which it is generally found. Because of its very high cost and few advantages compared to zirconia, pure hafnia has not been used and studied extensively in ceramic bodies.

Hafnia-Rich Mixtures of Oxides. These mixtures can be formulated to produce a composite having an extremely low coefficient of thermal-expansion. The formulation of the particular mixtures considered for this program is proprietary to Rocketdyne. The material melts at approximately 4200F and it would be cementitiously bonded with the same binder systems that are used in cementitiously bonded zirconia systems.

Magnesium Oxide. Magnesium oxide has no phase inversions up to its melting point of 5070 F. However, it is not useful in neutral or reducing atmospheres above 3100 F. Magnesia is easily reduced and has a high vapor pressure at high temperatures. Also, because the strength of magnesia bodies is low because of its distinct cubic cleavage and because it hydrates easily when not in a dense form, this material is not a promising candidate for heat-barrier coatings.

Thorium Oxide. Thorium oxide has the highest melting point of all the oxides, 5800 F. It has a very low vapor pressure at high temperatures and it is the most chemically stable oxide. Thorium oxide has a cubic structure, with no phase inversions occurring to its melting temperature. The major deterrents to its use include its high specific gravity of 9.9 gm/cm^3, high cost, and slight radioactivity. Thoria coatings have already been used as heat shields for super-orbital, lifting re-entry leading edges and nose caps at 4000 F.

Yttrium Oxide. Yttrium oxide has no phase inversions from room temperature to its melting point of 4300 F. Its high cost and slight tendency to hydrate and form a carbonate at low temperature limit its use. Yttria is similar to alumina in respect to thermal expansion and thermal conduction.

Zirconium Oxide. Zirconium oxide normally has a monoclinic structure below 2160 F and a tetragonal structure above 2160 F. This phase transformation can be very destructive mechanically because of the large associated volume change (9 percent). Zirconia can be "stabilized" by adding 3 to 15 percent CaO, CeO_2, Y_2O_3, or MgO. These compounds form a solid solution of cubic structure which is stable at high temperatures and metastable at low temperatures. Zirconia coatings that are applied by flame or plasma spray methods have been developed by numerous investigators. These have exhibited excellent thermal stability but frequently are subject to thermal stress failures under severe conditions. Cementitiously bonded zirconia coatings have also been developed for certain applications. The zirconia phase of the cementitiously bonded coating system apparently suffers no deteriation, whereas the binder phase exhibits poor resistance to thermal shock and high-temperature service.

Zirconates. Zirconates of barium, beryllium, strontium, and thorium have high melting points, but in general very little information on their properties is available.

Selected Filler Materials

Based on available data from the literature, as described and discussed in the preceding sections, the two candidate filler materials, zirconia and thoria, qualify far above any others. These oxides, used with various binders, were successfully used at 4000 F or higher for the intended application, and all other materials were reported to be inferior. One exception was a cementitiously bonded hafnia system that was abandoned when the particular raw material source became unavailable and other sources of hafnia powder did not produce identical results. The use of hafnia instead of zirconia, however, is not warranted in this program.

Several other oxides are potential candidates for this program but selection of these oxides cannot be based on available literature because their use in cementitiously bonded systems has not been reported.

Two of these untested materials are also selected for evaluation in this program; the materials are barium zirconate and a hafnium-rich mixture of oxides*. Barium zirconate has not been evaluated in cementitiously bonded systems, nor has it been evaluated to a large extent as a coating material. However, its melting point is above 4300 F, the criterion for selection in this program, and its coefficient of thermal expansion in the melt-sprayed form is reported to be less than that of stabilized zirconia, 3.5×10^{-6} compared with 5.2×10^{-6} (Ref. 41) This latter property is the basis for its selection because using a material with a lower expansion coefficient than zirconia may become very important as a means for reducing thermal stresses, and the list of candidate materials with lower expansion coefficients is limited. The low expansion coefficient is the same reason for selecting the hafnia-rich mixture. Because this material can be formulated to have a negligible expansion coefficient, it could become invaluable for reducing thermal stresses in coating design. The melting point of the hafnia-rich mixture is slightly below the arbitrary limit of 4300 F, but it is not so low that it cannot be used in this program.

---

*The formulation is proprietary to Rocketdyne

In summary, filler materials selected for this program are:

1. Zirconia
2. Thoria
3. Barium zirconate
4. Mixture of hafnia-rich oxides (MHRO)

BINDERS FOR CANDIDATE FILLER MATERIALS

Survey

The only filler materials that were satisfactory for service to 4000 F and that were reported in the literature were ZrO_2, HfO_2, and ThO_2. Binder systems used to cementitiously bond these oxides into useful products are described in the following paragraphs.

Binders for Zirconia

Orthophosphoric Acid (H_3PO_4). Orthophosphoric acid has been used as a binder for several refractory oxides, some of which set at room temperature. Bonding of zirconia with H_3PO_4 does not occur at room temperature (Ref. 43), but it does occur when the system is heated between 800 F and 1000 F (Ref. 3 and 17). The cementitious product is believed to be either ZrP_2O_7 or $Zr_3(PO_4)_4$ (Ref. 3). A zirconia body bonded by H_3PO_4 and cured at 800 F (and having a porosity of 25 percent) was found to have a modulus of rupture of 1890 psi. The same material applied as a coating to an N-155 alloy substrate with type 304 stainless-steel reinforcements was found to be very friable after being subjected to a "thermal drop (gradient)" test at 2800 F. From the observation of strength deterioration and from weight loss studies, it was concluded that this cement is not stable at 2800 F (Ref. 3).

Ammonium Dihydrogen Phosphate ($NH_4H_2PO_4$). Ammonium dihydrogen phosphate bonds zirconia, when cured at 1000 F, presumably by the formation of $Zr_3(PO_4)_4$. Bodies formed with this binder had a modulus of rupture of 1500 psi, but the bond deteriorated at high temperature (Ref. 3).

Fluophosphoric Acids. Monofluophosphoric acid (H_2PO_3F) bonds zirconia at room temperature to produce a hard, dense product (Ref. 3 , 16, 44, and 45). When H_2PO_3F was reacted with mixtures of zirconia and $NH_4H_2PO_4$ and cured at approximately 300 F, a modulus of rupture of 3800 psi was obtained at room temperature (Ref. 3). Ammonium dihydrogen phosphate served to retard the reaction rate. Hexafluophosphoric acid additions to zirconia, however, react immediately,making coating operations difficult or impossible.

From chemical reaction and X-ray diffraction studies, Bremser and Nelson (Ref. 16) concluded that the mechanism for bonding between H_2PO_3F and zirconia at 260 C (500 F) proceeds as follows. The fluorine from the dissociated H_2PO_3F leads to the formation of an intermediate zirconium fluoride which then reacts with the phosphate ions to form zirconium pyrophosphate (ZrP_2O_7). The presence of an intermediate fluoride compound, $ZrF_4 \cdot 3H_2O$, was also indicated by Edlin et al. from differential thermal analysis studies (Ref. 44). The dependence of strength on temperature for monoclinic (unstabilized) and cubic (calcia-stabilized) zirconia as determined by Bremser and Nelson (Ref. 16) is shown in Fig. 2 .

The irregular dependence of strength on temperature for the calcia-stabilized body was believed to result from the formation of one or more calcium compounds which undergo changes with increasing temperature. For the calcia-stabilized body, softening and plastic deformation occurred at 1200 C (2200 F). At 1240 C (2270 F), the presence of a fluid phase was indicated because the specimens deformed under their own weight. For the unstabilized body, there was some decrease in strength at 1240 C, but the specimens showed brittle fracture. After prolonged heating at 2800 F, the stabilized zirconia converted to unstabilized zirconia; this should be expected because the calcia stabilizing agent is no longer in solid solution in the zirconia lattice.

Hydrofluosilicic Acid (H_2SiF_6). Hydrofluosilicic acid bonded calcia-stabilized zirconia, but the strength (modulus at rupture) at room temperature was only 600 to 950 psi. Nevertheless, this binder was judged as good as or better than, monofluorophosphoric acid by the investigators (Ref. 4).

Hydrofluosulfonic Acid (HSO_3F). Hydrofluosulfonic acid bonds zirconia, but these bodies are very difficult to prepare (Ref. 4). Noxious fumes evolve, the slurry is thixotropic, and the composite bloats during curing. Because of these difficulties, very little work has been performed with this binder. The only information reported describes an extremely hard body when cured at 450 F that could not be scratched with steel.

Alkali Silicates. Alkali silicates bond zirconia, yielding bodies with high cured strength, good thermal shock resistance and use-temperature as high as 4000 F (Ref. 17). Zirconia bodies bonded with K_2SiO_3* appeared to have somewhat higher cured strength and more refractoriness than those bonded with Na_2SiO_3. Bodies bonded by K_2SiO_3 were fabricated by combining zirconia powder with an aqueous solution of KaSil88 (Philadelphia Quartz Co.) which undergoes a "water glass" type reaction to produce the K_2SiO_3 cement.

Sulfuric Acid and Nitric Acid. These acids bond zirconia when cured at temperatures of at least 600 F. Bodies cured at 800 F could not be scratched with a steel knife blade and sulphate-bonded zirconia has been used at temperatures as high as 4300 F (Ref. 31) but the bonding mechanism was not reported.

Astroceran. Astroceran is a commercial proprietary cement (American Thermocatalytic Corp.) which is claimed to have a maximum service temperature of 4400 F, to bond zirconia, and to withstand severe thermal shock (Ref. 46). Furthermore, it is reported as having a tensile strength of 10,000 to 15,000 psi, a compressure strength from 80,000 to 150,000, and a modulus of rupture close to 23,000 psi.

Other Materials. Other materials that were reported as unsatisfactory binders for zirconia include:

1. Dolomite and calcium hydroxide
2. Magnesium zirconate, calcium zirconate, and magnesium zirconium silicate with ammonium dihydrogen phosphate
3. Sodium carbonate
4. Aluminum sulphate
5. Tannic acid

---

*The molecular constitution of potassium and sodium silicates is not exactly K_2SiO_3 and Na_2SiO_3, but these symbols were used for convenience.

6. Oxalic acid
7. Butyric acid
8. Sodium tetrapyrophosphate
9. Aluminum chloride
10. Aluminum phosphate
11. Ammonium phosphate
12. Ammonium tartrate
13. Bentonite
14. Hydrochloric Acid
15. Calgon
16. Mono-DiN butylan butylamine
17. Silicic acid
18. Ammonium sulfate
19. Aluminum sulfate
20. Boron phosphate
21. Sodium borate
22. Citric acid
23. Sebacic acid
24. Monochloracetic acid
25. Sulfamilic acid
26. Chromic acid
27. Toluene sulfonic acid
28. Aluminum acetate
29. Ammonium fluoroborate
30. Ammonium molybdate
31. Ammonium oxalate

32. Ammonium fluoride

33. Ammonium thiocyanate

34. Ammonium vanadate

35. Magnesium perchloride

36. Glacial acetic acid

37. Oleic acid

38. Urea

39. Stearic acid

40. Boric acid

41. Lauric acid

42. Strontium hydroxide

Binders for Hafnia-Rich Mixtures

A hafnia-rich mixture of oxides* (proprietary to Rocketdyne) is another candidate filler material. The advantages of this material is its low, almost negligible, thermal expansion coefficient, and its high melting point. The major portion of this oxide mixture consists of hafnia and zirconia. Because these oxides are identical from a chemical standpoint, the mixture of oxides should behave similarly to commercial zirconia. Hence, the information on binder systems discussed previously for zirconia should apply to hafnia-zirconia mixtures as well.

This is a prediction, however, because cementitious bonding of the particular hafnia-rich systems referred to here has never been studied.

---

*All zirconia, except reactor-grade zirconia, contains between 2 and 4 weight percent hafnia.

Only one reference in the literature (Ref. 47), includes pertinent information on the cementitious bonding of hafnia. In this study, a particular grade of hafnia was found to be superior to cementitiously bonded zirconia. This conclusion was based on hardness-after-curing data and on erosion-oxidation during 4000 F tests. When that specific source of hafnia became unavailable, however, cementitiously bonded hafnia bodies made with hafnia from other sources was found to be inferior to cementitiously bonded zirconia bodies. Reasons for the decrease in performance of cementitiously bonded hafnia bodies was attributed to impurities in the available hafnia powders rather than to reasons inherent to the cementitious bonding reactions.

Binders for Thoria

Orthophosphoric Acid (H_3PO_4). Thoria bonded with H_3PO_4 was found to produce weak bonds compared with oxides having smaller cationic radii, namely beryllia, alumina, iron oxide, and magnesia (Ref. 43). Another investigation (Ref. 17) reported that H_3PO_4-bonded thoria had good thermal shock resistance, low shrinkage, and a crushing strength of 8000 psi. Another binder was selected for thoria bodies as being better, however, because of a bloating problem at elevated temperatures. Orthophosphoric acid was eliminated as a binder for thoria bodies in another program because H_3PO_4-bonded thoria bodies deformed under a load at elevated temperature; zero percent deformation was observed at 2500 F, 20 percent at 3000 F, and 60 percent at 3500 and 4000 F under a load of 14 psi. A binder ($Th(NO_3)_4$) that did not form any liquid phases was selected in this program.

Potassium Silicate (K_2SiO_3). Potassium silicate was found to be the best binder for cementitiously bonded thoria heat shields developed for reentry vehicles (Ref. 48). Potassium silicate bonded thoria bodies had a crushing strength of 6500 psi, low shrinkage, good thermal shock resistance, and adequate refractoriness. No apparent change (melting) was observed in bodies heated to 4600 F.

Five grams of K_2SiO_3 (plus 0.3 gram of a setting agent, Na_2SiF_6) was the minimum amount that gave adequate cured strength. The curing cycle was overnight at ambient conditions, 24 hours at 150 F, 2 hours at 200 F, and 2 hours at 300 F.

Sodium Silicate (Na_2SiO_3) Plus Colloidal Zirconia. Thoria bodies bonded with Na_2SiO_3 (grade "K", Philadelphia Quartz Co.) and colloidal zirconia were reported in screening-type studies to be weaker than thoria bodies bonded with $Th(NO_3)_4$ (Ref. 17). This binder system was, thus, eliminated from further study and not reported in detail.

Thorium Nitrate ($Th(NO_3)_4$). Reference 48 reported the use of $Th(NO_3)_4$ as a binder for thoria bodies used as re-entry heat shields. Screening test results were not reported in detail, but $Th(NO_3)_4$-bonded bodies were reported as being weaker than H_3PO_4-bonded thoria bodies and that K_2SiO_3-bonded ThO_2 bodies were better than H_3PO_4-bonded ThO_2 bodies. Thus, $Th(NO_3)_4$ was not found to be the best binder, nor even the second best binder, for ThO_2 bodies. The curing cycle was 24 hours overnight, 2 hours each at 200 and 300 F, 6 hours at 450 and 600 F, and 2 hours at 1000 F.

Conversely, in an earlier program, in which a thoria oxidation protective coating was developed for a tungsten substrate, $Th(NO_3)_4$- bonded thoria was selected as the best binder system for that application (Ref. 5). $Th(NO_3)_4$ was determined to be the best binder for thoria because no liquid phases formed due to the presence of the binder to the melting point of thoria. The thoria powder sintered during service conditions but shrinkage was restricted to less than 1 percent by proper selection of particle size fractions. The best composition contained 5 percent $Th(NO_3)_4$ and had an average modulus of rupture of 1050 psi after annealing 2 hours at 2200 F. The curing cycle was 2 hours each at 200, 300, 400, 400, and 600 F.

Colloidal Zirconia and Colloidal Alumina. Colloidal zirconia and alumina were studied as binders for thoria bodies in Ref. 5. These materials were not found to act as binders because the composite bodies lacked strength and shrank considerably.

Selected Binders

Based on the literature, one specific binder for each filler cannot be selected. This does not mean that the literature is necessarily contradictory; it means that meaningful comparisons of filler-binder systems are not possible. Various binder systems were either not compared in the same program, or they cannot be compared in different programs because they were prepared by different techniques, prepared using different raw materials, and tested in different ways. Another factor when evaluating binders by comparing products developed in different programs is that the development of these products is to some extent an art because of the complexity of the systems. These systems involve so many important variables* that comparisons of different coating systems developed by different, and even by the same, investigators are not clearly defined.

Thus, the selection of binders can only be reduced to four, and each of these must be evaluated through tests especially designed for this program.

The best binders that are selected for evaluation in this program for each of the four oxides are:

1. H_2PO_3F
2. H_2SiF_6

---

*Important variables include: (1) filler composition, impurity content, grain size, grain size distribution, grain shape, grain surface energy; (2) filler-to-binder ratio and water content; (3) binder chemistry, concentration, curing temperature, thermal stability; (4) effects of additives, such as mold release agents, chemical reaction inhibitors, setting agents, deflocculation agents; (5) system rheology; (6) mixing and coating techniques; (7) time-temperature-atmospheric relationships under curing and service conditions; (8) stress levels due to geometry and testing procedures.

3. K_2SiO_3
4. $Th(NO_3)_4$ - for ThO_2 systems only
5. Proprietary binders that have not been evaluated previously, and that meet the requirements of this program.

INTERMEDIATE LAYERS AND REINFORCEMENTS

Intermediate Oxide Layers

Potentially useful filler oxides for the intermediate layers include most of those listed in Table 2. When the criteria outlined in the previous sections, except for melting temperature, are applied, however, the list is reduced to just three: alumina, mullite, and zircon. The rest of the oxides are eliminated, among other reasons, because cementitiously-bonded composites have not been studied and developed, whereas several cementitiously bonded systems have been developed using alumina, mullite, and zircon (Ref. 1, 12 through 15, 17, 33, 43, and 49 through 58). A complete description and analysis of these systems is not justified at this stage of the program, however, because they will be considered for use only if it becomes necessary based on the failure analyses of the first series of arc-plasma tests.

Glass Adherence Layer

A special layer of glass for attaching the heat barrier coating to the substrate and for relieving thermal stresses was discussed in an earlier section of this report. This special layer of coating will not be investigated, however, until there is proof for its need. The purpose of the first series of arc-plasma tests is to evaluate existing materials and to determine by failure analysis what changes in design and what improvements in materials are required. Thus, the use of a special adherence layer will not be investigated until the lack of adherence is shown to actually be a problem.

Should the arc-plasma tests demonstrate that the lack of adherence is a major problem in the development of a heat barrier coating, then glass adherence coatings will be evaluated during the second series of arc-plasma tests. The properties of this glass will be based on the criteria specified in a discussion earlier in this report. Careful attention in selecting a glass coating will be given to adherence to Hastelloy-X, thermal expansion coefficient (which should be approximately between that of the heat-barrier coating and Hastelloy-X), softening temperature range, and application temperature. This glass will not be developed in this program; one of several commercial porcelain enamel formulations should be satisfactory for evaluation of the glass adherence layer theory. Examples of useful formulations are NBS 418 and the Solaramic series (Solar, Division of International Harvester, Inc.). These will be selected at the appropriate time based on vendor specifications.

Strain Accommodation Layer

A ductile base layer (strain accommodation layer) for relieving stresses in the coating was discussed in the section of this report on thermal stress analyses. The layer must have a low yield strength, must not melt or become exceptionally weak to 1600 F and must be compatible with the coating material and the metal chamber wall.

For initial tests to evaluate the usefulness of stress accommodating sublayers, copper and nickel will be used because they are readily available and inexpensive, have been studied extensively, are easy to apply, melt above 1600 F, and have a low yield strength at 1200 F, the service temperature of this layer.

The metal layer can be applied by electroplating, brazing, or melt spraying. Melt-spraying will be used to make initial specimens because of the convenience and low cost of this coating technique. Coating thickness will approximate the thickness of the so called "adherence" layer commonly used under melt-sprayed heat barrier coatings. This thickness is approximately 3 mils and will not present a significant resistance to heat flow through the metal wall-heat barrier system.

Reinforcements

As discussed under this subject in a previous section of this report, reinforcements cannot be designed, nor can potential materials be selected until after the failure analyses of the first series of test specimens tested in the arc-plasma.

If metal reinforcements are required to improve failure resistance of the heat-barrier coating, it is likely that they will be welded, melt sprayed or electroformed in place on the metal substrate. Metal reinforcements for welding or for melt spraying will probably be made of type 347 stainless steel, Inconel, or Hastelloy-X. Refractory metals and alloys cannot be used because they cannot be protected sufficiently from oxidation. Electroformed reinforcements must be made from pure metals rather than from alloys, and chromium will probably be best because it is strong and has a high melting point.

If fibrous ceramic reinforcements are required to improve failure resistance of the heat-barrier coating, alumina fibers will probably be used. It is doubtful that other fibers will meet the design requirements. Design requirements for ceramic fibers include: (1) a high-melting point (3000 F or higher), (2) stability in oxygen (they must be oxides), (3) high tensile strength (polycrystalline fibers will be too weak), and (4) availability at reasonable cost.

COATING DESIGN

General

Whereas the literature was useful in the selection of filler-binder systems, the literature is of little value in guiding coating design. Only four programs reported in the literature describe the design and development of slurry-type heat-barrier coatings (or heat shields) for use at or above 4000 F (Ref. 3 , 5 , 12, and 21). And because the purposes and the objectives of these past programs were vastly different from those of this program, the design factors were also vastly different from those of this program. For example, differences in design include:

1. Heat fluxes that were a factor of 10 smaller. Maximum heat flux values reported in the literature were less than 4 Btu/in.^{2}-sec, with 2 Btu/in.^{2}-sec being more typical. The heat flux through the coating in this program will be 20 Btu/in.^{2}-sec.
2. Heating rates that were a factor of 10^3 slower. Typical time to reach equilibrium temperature was approximately 60 seconds, or an average heating rate of 100 F/sec. Heating rates for the thrust chamber wall in a high-performance rocket engine will be approximately 100,000 F/sec.
3. Temperature gradients that were a factor of 30 lower. The highest temperature gradients reported in the literature were approximately 10 F/mil, or 10,000 F/inch. Gradients across the coating in this program will be on the order of 300,000 F/inch.
4. Thickness values that were up to a factor of 10^4 times higher. Thicknesses of heat-barrier coatings ranged between 1/4 and 3/4 inch. Thicknesses for coatings in this program could be as low as 0.0035 inch.
5. Geometry that was different. Coatings and shields reported in the literature were developed for the outer surfaces of leading edges, or for convex surfaces with relatively large radii of curvatures which were measured in inches. Coatings developed in this program will be initially tested on flat surfaces but they will be eventually designed for the inside surface of a thrust chamber. These surfaces are both concave

and convex depending on which way a plane is passed through the chamber. Moreover, on a smaller scale and assuming the coating is applied in a tubular chamber wall, surfaces change from concave (cuspids) to convex (crowns) every tube diameter, which is measured in fractions of an inch in this case.

6. The substrate properties were different. One of the most important design considerations in minimizing thermal stress is the matching of thermal expansion coefficients and of elastic modulii between the substrate and the coating. Because a specific coating performs well on tungsten, does not necessarily mean that it will perform well on Hastelloy-X, for example. Because substrate materials for coatings reported in the literature were not the same as that for this program, the design factors for coatings reported in the literature were vastly different from those in this program.

Another point is pertinent in comparing state-of-the-art coatings with coatings required for this program. That is, because of the complexity in the design and materials development factors, state-of-the-art coatings were, at best, borderline in performance under the conditions for which they were developed. Coating systems were reported as being promising and adequate for the specific purpose that they were designed for, but none were reported as being a satisfactory or superior material. One coating system only had a modulus of rupture of 1000 psi at room temperature, and other systems were not much, if any, stronger. None of the systems survived more than one, or at most, a few thermal shocks, and none adhered to the substrate; all coating systems were held together, and to the substrate with metal reinforcements. Also, because coating design was limited in the extent that all coating systems were monolithic in structure, thermal stresses were not reduced by grading material properties across coating thickness.

Coatings designed and developed in this program for the extremely hostile environment of a rocket engine, therefore, must show a very large improvement in the state-of-the-art, and they must be developed for the specific intended service conditions to be successful.

Coating Constitution

First generation coating designs for the first series of arc-plasma tests will consist of single layers of each of the four filler-binder systems applied directly on the Hastelloy-X substrate. Because these materials have not been evaluated under the conditions of this program, the use of simplified, ungraded coatings is a logical starting point.

When graded and multilayer coatings are evaluated later during arc-plasma laboratory tests, there must be a basis for comparison. Results from the first series of testing will act, therefore, as a reference for subsequent test results of more complex coating designs.

Also, inasmuch as these complex coating designs must be based on the most important factors leading to failure of the particular materials systems involved, for efficiency, second generation coating systems and designs must be based on the failure analysis of first generation coating systems and designs.

Coating Thickness

Calculation. The thickness for ungraded layers of cementitiously bonded zirconia, thoria, HRMO*, and barium zirconate was calculated to be 3.5 mils. The calculation was made using the equation

$$t_c = R_c \bar{k},$$

where t_c = coating thickness in inches, R = a coating thermal resistance of 140 in.^{2}-sec-F/Btu, and $\bar{k}$ = an average value for coating thermal conductance of 2.5 x 10^{-5} Btu/in.-sec-F.

---

*HRMO = hafnia-rich mixture of oxides.

Thermal Resistance Value. The design value for the thermal resistance of the coating has varied during the Task I effort between 130 and 150 $in.^2$-sec-F/Btu, depending on the parameters that were selected as being most accurate at the time. Because many of the variables used in this calculation are best estimates, such as average bulk coolant temperature, and gas boundary layer heat transfer coefficients on both the hot and cold sides, the required value of coating thermal resistance is also essentially a best estimate. Thus, a coating thermal resistance of 140 $in.^2$-sec-F/Btu was used in these calculations even though this value may not be precisely consistent with other heat transfer calculations made in Task I.

Thermal Conductance Value. It was necessary to estimate the average values for thermal conductance of the cementitiously bonded composite because these data are unavailable for the composite materials. The thermal conductance values for the cementitiously bonded materials must be calculated by adjusting thermal conductivity values for the pure filler materials for (1) porosity, (2) concentrations of other phases (liquid and/or solid), and (3) effects caused by coating thickness and substrate emittance relationships.

A porosity of 30 percent can be assumed to be a good approximation for first generation coatings. Thirty percent porosity is slightly less than the porosity of most of the stronger cementitiously bonded materials reported in the literature. A low-side value was selected because surface effects of a very thin coating will cause the apparent porosity to be higher than that for a thick body prepared with the same material. The effect of such a high amount of porosity usually decreases thermal conductivity as compared to a completely dense body of the same materials. However, the selection of a precise thermal conductivity value must be treated sceptically because reported thermal conductivity values can vary considerably due to impurities, specimen history, and measurement techniques. Also, the pore size will have a large effect on conductivity. When pore size is too small for convection to occur, conductivity is reduced; but when pore size is large, effective thermal conductivity can be actually increased because of the dominance of heat transfer by radiation, or by presence of a high conductivity gas such as H_2.

Thus, adjusting thermal conductivity to account for porosity and even selecting specific values from reported literature is not possible with a high degree of confidence. In this case, however, the effect of porosity will probably be to reduce the effective thermal conductance because pores will be small and they will be continuous.

Adjusting the thermal conductance of the composite coating for concentrations of other phases is a complex procedure. First, the exact concentration and composition of these phases must be known. But in the initial portion of this program the binder content will vary in both concentration and composition. Moreover, for many filler-binder systems, the exact composition and the exact concentration after and during heating is not known with certainty because of variations in compound volatility and in chemical reactions which depend on specimen history. Second, the effect of the location of the second-phase in the composite is difficult to determine when calculating effective thermal conductance. This system differs from standard models that are used to develop thermal conductance equations. In a cementitiously bonded composite, the bonding agent will most likely be a continuous phase because it will cover all of the grains of the filler; yet the concentration of the bonding agent will probably be less than 10 volume percent. Thus, there is a continuous phase which is present at a concentration of less than 10 volume percent, and equations for this model are not known as well as for models having the continuous phase concentration larger than 10 volume percent. Therefore, although the binder should have a proportionally large influence on the effective thermal conductance of the composite, the extent of this effect cannot be calculated accurately. This influence should be toward increasing the thermal conductance of the composite, however, because the filler materials already have the lowest thermal conductivity values of all oxides in this temperature range.

Effective thermal conductance of the coating will also be higher than that of reported values for the pure oxides because of the effect of thickness. Thermal conductivity values reported in the literature were obtained using relatively large, thick specimens, whereas thermal conductivity values required for this program are to apply to very thin layers of material. These thin layers are orders of magnitude thinner than the specimens used to measure bulk thermal conductivity. This thin layer of coating might be thought of as the skin of the large bulk thermal, and any abnormal effect on thermal conductivity due to this skin (at steady-state) would be so inconsequential that it would be unnoticed. Thus, it is possible that the effective thermal conductivity of material in the form of a thin layer, i.e., a coating, could be significantly different from that of the equivalent material in the bulk form.

The effective thermal conductivity of a thin layer also could be different from that of the bulk material if the material were semitransparent to infrared radiation. Although the largest portion of heat is probably transferred to the coating by conduction and convection, a substantial proportion is probably transferred through the porous coating at high temperatures by radiation. Most bulk oxides are thought of as being opaque, but in reality, many of them are not; they are semiopaque or more familiarly, semitransparent. Therefore, if the material is thin and semitransparent, radiant heat can pass through the material more easily. Thus, the effective thermal conductivity of thin semitransparent layers could be higher than reported values obtained from measurements on large, thick specimens.

The degree of transparency for the design materials in this program is unknown, but, some insight to the degree can be gained from an example of a similar material. A coating of alumina was found to be semitransparent to radiation at 1600 F until the thickness of that coating was increased to more than 40 mils, approximately factor of 10 thicker than first generation coatings in this program (Ref. 59).

In summary, factors influence the effective thermal conductivity of candidate materials in the following way:

Factor	Influence
Porosity	Decreases but can increase
Presence of Binder Materials	Increases
Semitransparency and Short Transmission Path	Increases
Small Number of Reported Data	Decreases degree of confidence

It is, therefore, apparent that selecting a precise value for the average effective thermal conductance of the composite for a temperature range is not possible. Rather, an estimation must be made based on the estimated range of thermal conductivity values that are possible. These estimates were made as follows. The thermal conductivity of zirconia at 3150 F (the average temperature across the coating) is approximately 1.4×10^{-5} Btu/in.-sec-F (Fig. 9). Because the majority of the other factors influencing effective thermal conductance indicate that the value will be on the high side, the value of 2.5×10^{-5} Btu/in.-sec-F was arbitrarily selected as the effective thermal conductance of the composite material.

Even less data are available to aid in selecting the effective thermal conductivity value for thoria (Fig.10), barium zirconate, and HRMO. The value of 2.5×10^{-5} Btu/in.-sec-F was also selected for these materials also because this value is logical based on the small amount of available data.

The accuracy of this effective thermal conductance of these materials will be improved based on calorimetric measurements that will be made during the first phase of the testing program. The thermal resistance, and hence, effective thermal conductance, of the coating systems can be

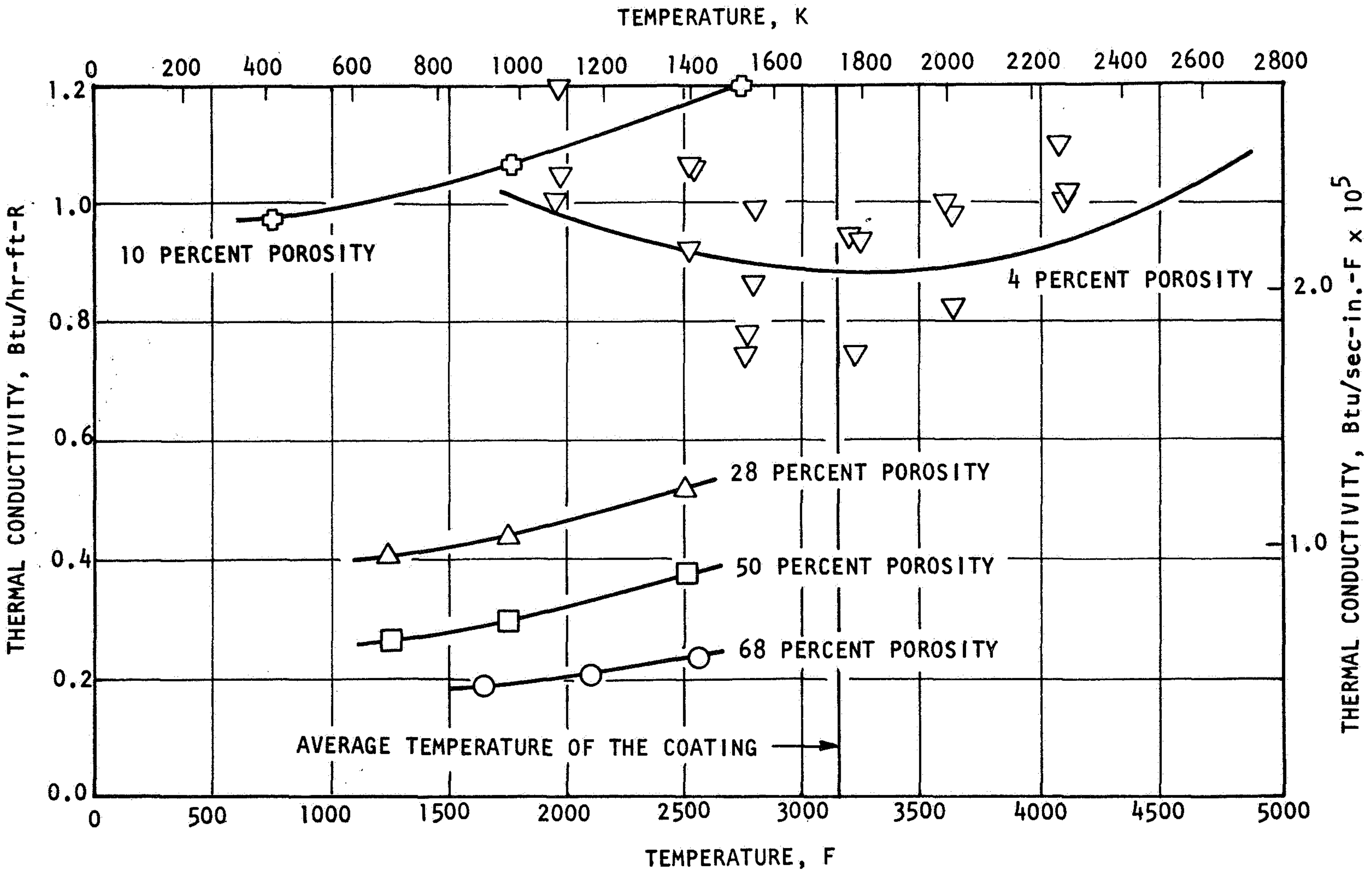

Figure 9 . Thermal Conductivity: Zirconium Oxide + Calcium Oxide (Ref. 42 and 60)

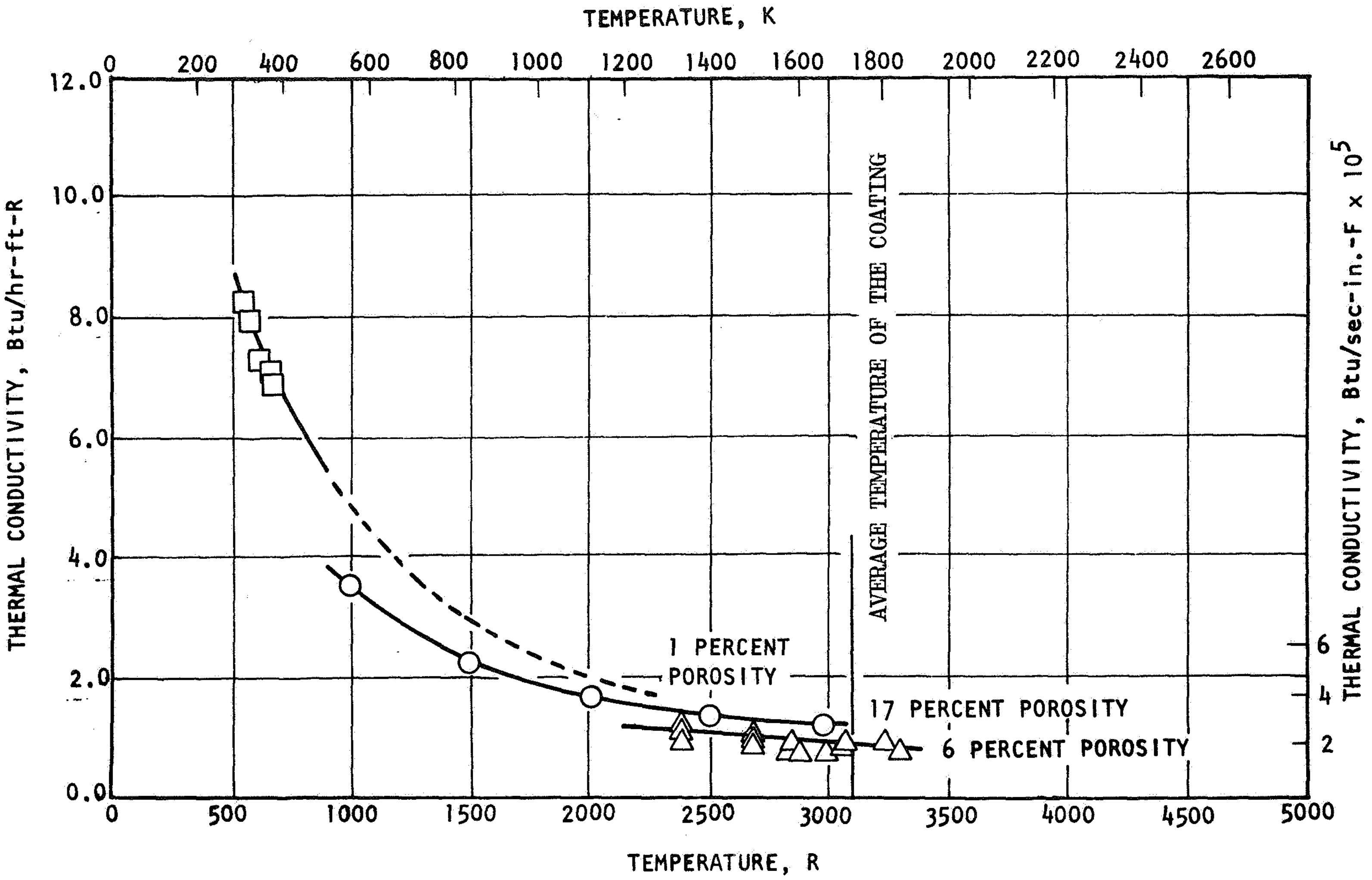

Figure 10. Thermal Conductivity: Thorium Oxide (Ref. 42 and 60)

roughly calculated from calorimetric data obtained from arc-plasma testing using the relationship

$$\dot{Q}/A = \frac{(T_h - T_c)}{R_m + R_c}$$

where

$\dot{Q}$ = heat flow through the coating (obtained from the water flowrate and the change in water temperature)

A = heated area (estimated from the known arc-plasma jet diameter and from the appearance of tested coating)

T_h = surface temperature of the coating (obtained from the corrected optical pyrometer reading)

T_c = cold-side temperature (estimated from the known water saturation temperature)

R_m = thermal resistance of the metal (calculated from $R = t_m/k_m$)

R_c = thermal resistance of the coating (where $R_c = t_c/k_c$, and t_c = coating thickness, and k_c = the effective thermal conductance of the coating.)

APPENDIX A-A

STRESS-FREE CURVATURE FOR A COATING HAVING A LINEAR TEMPERATURE DISTRIBUTION ACROSS ITS THICKNESS

Initially, a homogeneous coating of thickness t_c is assumed to be planar when a uniform temperature, T_e, exists throughout. Heat is then allowed to flow through the coating, where, at steady state, a linear temperature distribution develops across the coating. A planar element, dz, located a distance, z, from the cooler (back) surface, will undergo thermal expansion as a result of the increase in temperature from T_e. Letting L represent the original length of the coating, every element dz will increase in length to a value $\ell(z)$ given by

$$\ell(z) = L\left[1 + \alpha\,(T-T_e)\right] \tag{A-1}$$

where α is the expansion coefficient and T is the temperature at z. The temperature T is a function of z under steady-state conditions according to the equation

$$T = T_i + \frac{\dot{Q}}{k} z \tag{A-2}$$

where T_i is the temperature at the coating-metal interface.

Thus

$$\ell(z) = L\left[1 + \alpha(T_i - T_e + \frac{\dot{Q}}{k} z)\right] \tag{A-3}$$

The strains in the coating can be related to the curvature of the coating by considering the diagram on the following page.

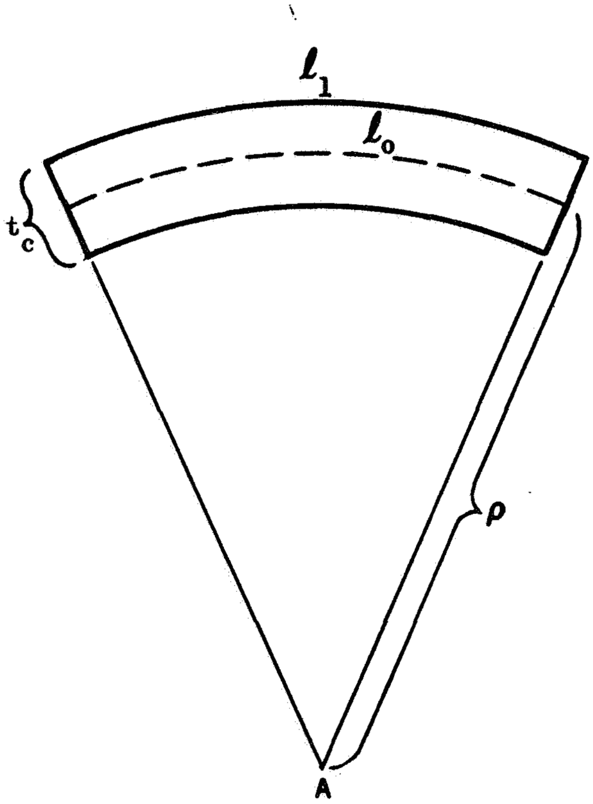

The length of any element dz is directly proportional to its distance from the center of curvature A. Thus

$$\frac{\ell_1}{\ell_o} = \frac{\rho + t_c/2}{\rho} \qquad \text{(A-4)}$$

where ℓ_1 and ℓ_o are the lengths of elements at the hot surface and at the central element, and ρ is the radius of curvature of the central element. Substituting Eq. A-1 into A-4 yields

$$\frac{\rho + t_c/2}{\rho} = \frac{1 + \alpha\,(T_1 - T_e)}{1 + \alpha\,(T_o - T_e)} \qquad \text{(A-5)}$$

Where T_o and T_i are the temperatures at Stations 0 and 1, respectively (see above sketch).

Rearranging gives

$$\rho = \frac{t_c/2\left[1 + \alpha(T_o - T_e)\right]}{\alpha\left(T_1 - T_o\right)} \tag{A-6}$$

and because $\alpha\left(T_o - T_e\right) \ll 1$,

$$\rho = \frac{t_c}{2\,\alpha\left(T_1 - T_o\right)} \tag{A-7}$$

Now, because $T_1 = T_i + \frac{\dot{Q}}{k}\left(t_c\right)$, and $T_o = T_i + \frac{\dot{Q}}{k}\left(\frac{t_c}{2}\right)$,

$$\rho = \frac{k}{\alpha\dot{Q}} \tag{A-8}$$

APPENDIX A-B

ADHESIVE FORCES BETWEEN THE COATING AND SUBSTRATE

STRESSES NORMAL TO THE INTERFACE

Stresses acting normal to the interface between the coating and the substrate may cause the coating to pull away from the substrate if these stresses are sufficiently severe. The magnitude of these stresses can be estimated from simplified considerations.

The coating is represented as a flat sheet of thickness t_c. The coating is subjected to a linear temperature variation through its thickness, decreasing from the exposed surface to the coating-substrate boundary. The bending tendency of the coating is restrained by an external moment M such that the coating remains flat. Consider a planar element in the X-Y plane of thickness dz, a distance z above the colder surface of the coating:

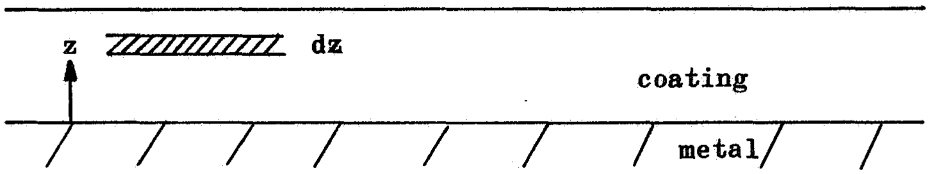

The actual strain along the plane of the element, which shall be designated as (z), is related to the thermal and mechanical strain components by the equation

$$\epsilon(z) = \epsilon_{\text{mechanical}} + \epsilon_{\text{thermal}}$$

$$= \sigma(z)\frac{[1-\mu]}{E} + \alpha\left[T(z)-T_e\right]$$

where

$\sigma(z)$ = the stress in an element located a distance z above the colder surface of the coating

μ = Poisson's ratio

α = expansion coefficient

$T(z)$ = temperature at position z

T_e = temperature where no thermal strains are present in the coating

Because the coating is completely restrained, the actual strains of every element are all equivalent. Thus

$$\epsilon(z) = \epsilon(z = 0)$$

and

$$\sigma(z)\frac{[1-\mu]}{E} + \alpha[T(z) - T_e] = \sigma(z = 0)\frac{[1-\mu]}{E} + \alpha[T(z = 0) - T_e]$$

or, rearranging

$$\sigma(z) = \sigma(z = 0) + \frac{E\alpha}{(1-\mu)}\left[T(z = 0) - T(z)\right]$$

Now

$$T(z) = T(z = 0) + \frac{\dot{Q}}{k} z$$

Thus

$$\sigma(z) = \sigma(z = 0) - \frac{E\alpha\dot{Q}}{(1-\mu)k} z \qquad \text{(B-1)}$$

A condition of equilibrium of forces requires that

$$\int_0^{t_c} \sigma(z)\, dz = 0$$

Then

$$\int_0^{t_c}\left[\sigma(z = 0) - \frac{E\alpha\dot{Q}}{(1-\mu)k} z\right] dz = 0$$

Integrating and rearranging gives

$$\sigma(z = 0) = \frac{E\alpha\dot{Q}t_c}{2(1-\mu)k}$$

Thus, from Eq. B-1.

$$\sigma(z) = \frac{E\,\alpha\,\dot{Q}}{(1-\mu)k}\left[\frac{t_c}{2} - z\right]$$

The moment in the coating that is equivalent to the external moment force is given by

$$M = \int_0^{t_c} z\,\sigma(z)\,dz$$

$$= \frac{E\alpha\dot{Q}}{(1-\mu)k}\int_0^{t_c} z\left(\frac{t_c}{2} - z\right) dz$$

$$= -\frac{1}{12}\,\frac{E\alpha\dot{Q}}{(1-\mu)k}\,t_c^{\,3}$$

The preceding expression gives, then, the moment that must be applied to flatten a curved coating in the stress-free state. This moment is supplied to the coating by the substrate through normal stresses at the coating-substrate interface. Consider the following diagram. The

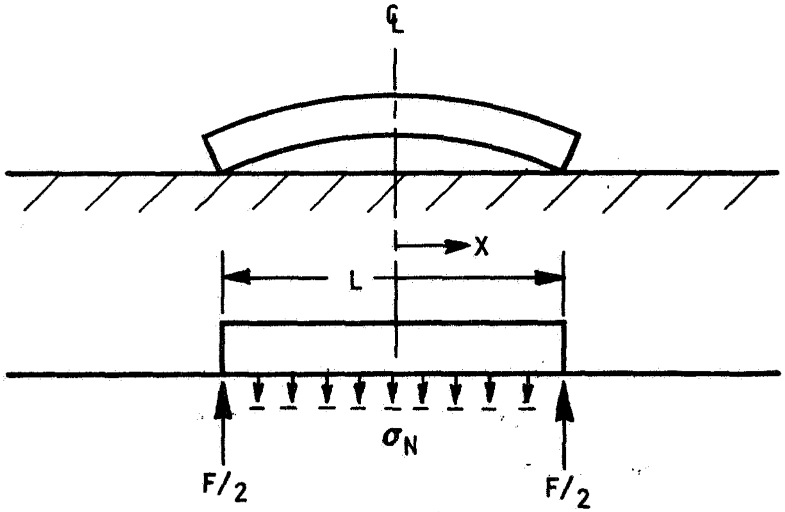

coating, without interfacial forces, would bend as shown above. Normal forces, σ_N, at the interface provide the moment required to keep the coating flat. If the normal stresses are assumed to be uniformly distributed, the moment at the centerline for a coating of unit width is given by

$$M = +\int_{o}^{L/2} x\,\sigma_N\,dx - \left(\frac{L}{2}\right)\left(\frac{F}{2}\right)$$

Because

$$F = L\,\sigma_N$$

then

$$M = +\left[\sigma_N \frac{x^2}{2}\right]_{o}^{L/2} + \frac{L^2\,\sigma_N}{4}$$

$$= -\frac{1}{8} L^2\,\sigma_N$$

Thus

$$\frac{1}{8} L^2\,\sigma_N = \frac{1}{12}\,\frac{E\alpha\dot{Q}}{(1-\mu)k}\,t_c^{\,3}$$

or

$$\sigma_N = \frac{2}{3}\,\frac{E\alpha\dot{Q}}{(1-\mu)k}\,\frac{t_c^{\,3}}{L^2} \qquad \text{(B-2)}$$

SHEAR STRESSES AT THE INTERFACE

The shear stress at the coating-substrate interface depends on the relative mismatch in thermal expansion between the metal substrate and the coating and the ductility of the boundary zone between the coating and substrate. If the average temperature of the coating (located at the midpoint within the coating for the case of a linear temperature distribution) is $\bar{T}_c$ and of the metal (located at the midpoint within the metal wall for the case of a linear temperature distribution) is $\bar{T}_m$, the average thermal strain of the coating and of the metal are

$$\bar{\epsilon}_c = \alpha_c (\bar{T}_c - T_e)$$

$$\bar{\epsilon}_m = \alpha_m (\bar{T}_m - T_e)$$

The actual (total) strain is the same in the coating and in the metal. Thus

$$\alpha_c(\bar{T}_c - T_e) + \sigma_c \frac{[1-\mu_c]}{E_c} = \alpha_m(\bar{T}_m - T_e) + \sigma_m \frac{[1-\mu_m]}{E_m} \qquad \text{(B-3)}$$

For equilibrium of forces (assume unit width)

$$t_m \sigma_m = - t_c \sigma_c \qquad \text{(B-4)}$$

where t_m and t_c are the thicknesses of the metal wall and coating,respectively.

Thus, combining Eq. B-3 and B-4, and rearranging,

$$\sigma_c = \frac{\alpha_m(\bar{T}_m - T_e) - \alpha_c(\bar{T}_c - T_e)}{\frac{1-\mu_c}{E_c} + \frac{t_c}{t_m}\frac{1-\mu_m}{E_m}} \qquad \text{(B-5)}$$

The average force in the coating is

$$F = t_c \sigma_c \qquad \text{(B-6)}$$

This force must be counteracted by the shear forces at the interface. If the shear stress τ, which is zero at the center of a slab of coating, increases linearly to a maximum τ_{max} at the ends of the slab a distance L/2 from the center, then at any position x from the center

$$\tau = \tau_{max} \left(\frac{x}{L/2} \right)$$

The force transmitted by the shear stresses is

$$F = \int_0^{L/2} \tau dx$$

$$= \int_0^{L/2} \tau_{max} \left(\frac{x}{L/2}\right) dx$$

$$= \frac{\tau_{max}}{4} L \qquad \text{(B-7)}$$

Equating Eq. B-5 through B-7 and rearranging gives

$$\tau_{max} = \frac{4t_c}{L} \frac{\alpha_m(\bar{T}_m - T_e) - \alpha_c(\bar{T}_c - T_e)}{\frac{1 - \mu_c}{E_c} + \frac{t_c}{t_m} \frac{1 - \mu_m}{E_m}} \qquad \text{(B-8)}$$

APPENDIX A-C

THERMAL STRESSES IN A TWO-DIMENSIONALLY INFINITE, PLANAR COATING-SUBSTRATE SYSTEM WITH TEMPERATURE AND MATERIAL PROPERTIES VARYING THROUGH THE THICKNESS ONLY

Consider a completely elastic, plane coating-substrate system of infinite extent along the plane subject to a temperature variation through the thickness. The ends of the plate (at infinity) are appropriately constrained so that the plate remains flat at all times.

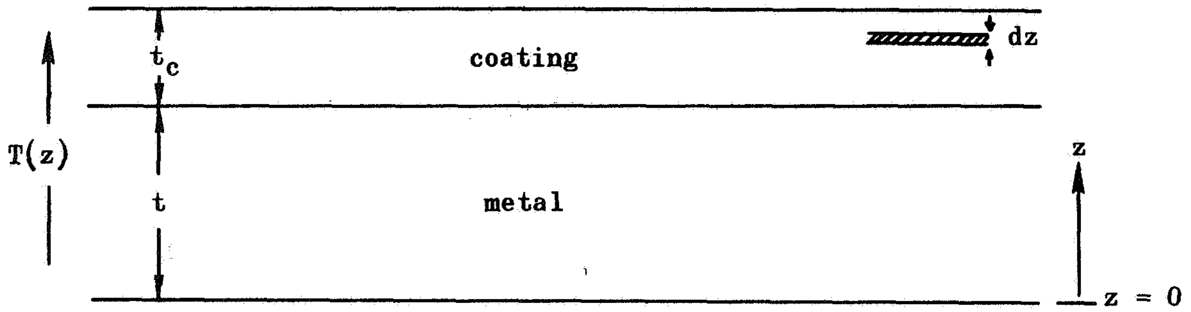

Consider a planar element in the x-y plane of thickness dz, a distance z above the origin (z = 0). The strain at z parallel to the element (namely, ϵ_{xx} and ϵ_{yy} which are designated simply as ϵ, or $\epsilon(z)$ at a distance z above the origin) is related to the thermal and mechanical strain components by the equation

$$\epsilon(z) = \epsilon_{\text{mechanical}} + \epsilon_{\text{thermal}}$$

$$= \sigma(z) \frac{[1-\mu(z)]}{E(z)} + \alpha(z) \left[T(z) - T_e\right] \qquad \text{(C-1)}$$

where

(z) = the value of the accompanying parameter at the position z

σ = σ_{xx} and σ_{yy}, which are equal

E = elastic modulus

μ = Poisson's ratio

α = linear expansion coefficient

T = temperature

T_e = the temperature at which no thermal strains are present in the body

Because E, μ, and α may be temperature dependent and because $T = T(z)$, these parameters are a function of z also.

At the cold metal wall ($z = 0$),

$$\epsilon(o) = \sigma(o) \frac{[1-\mu(o)]}{E(o)} + \alpha(o) \left[T(o) - T_e\right]$$

Because the original condition imposed was that the plate always remains planer, then a necessary condition is that

$\epsilon(z)$ = the same value at all z positions.

Thus

$$\epsilon(z) = \epsilon(o)$$

and

$$\sigma(z) \frac{[1-\mu(z)]}{E(z)} + \alpha(z) \left[T(z) - T_e\right] = \sigma(o) \frac{[1-\mu(o)]}{E(o)} + \alpha(o) \left[T(o) - T_e\right]$$

Rearranging yields

$$\sigma(z) = \frac{E(z)}{[1-\mu(z)]} \left\{\sigma(o) \frac{[1-\mu(o)]}{E(o)} + \alpha(o) \left[T(o) - T_e\right] - \alpha(z) \left[T(z) - T_e\right]\right\} \tag{C-2}$$

A force balance in the x or y direction requires that

$$\int_0^{t_m+t_c} \sigma(z)\, dz = 0$$

Thus

$$\left\{\sigma(o)\,\frac{[1-\mu(o)]}{E(o)} + \alpha(o)\left[T(o) - T_e\right]\right\}\int_o^{t_m+t_c} \frac{E(z)}{[1-\mu(z)]}\,dz -$$

$$\int_o^{t_m+t_c} \frac{E(z)\alpha(z)}{[1-\mu(z)]}\left[T(z) - T_e\right] dz = 0$$

Rearranging gives

$$\sigma(o) = \frac{E(0)}{[1-\mu(o)]}\left\{\frac{\displaystyle\int_o^{t_m+t_c} \frac{E(z)\alpha(z)}{1-\mu(z)}\left[T(z) - T_e\right] dz}{\displaystyle\int_o^{t_m+t_c} \frac{E(z)}{[1-\mu(z)]}\,dz} - \alpha(o)\left[T(o) - T_e\right]\right\}$$

$$\text{Let } I \equiv \frac{\displaystyle\int_o^{t_m+t_c} \frac{E(z)\alpha(z)}{[1-\mu(z)]}\left[T(z) - T_e\right] dz}{\displaystyle\int_o^{t_m+t_c} \frac{E(z)}{[1-\mu(z)]}\,dz}$$

Then

$$\sigma(o) = \frac{E(0)}{[1-\mu(o)]}\left\{I - \alpha(o)\left[T(o) - T_e\right]\right\} \qquad \text{(C-3)}$$

Substituting the expression for $\sigma(o)$ from Eq. C-3 into Eq. C-2 yields

$$\sigma(z) = \frac{E(z)}{[1-\mu(z)]}\left\{I - \alpha(z)\left[T(z) - T_e\right]\right\} \qquad \text{(C-4)}$$

By comparison of Eq. C-4 with Eq. C-1, it can be seen that I is equivalent to $\epsilon(z)$, the total strain undergone by each planar element.

APPENDIX A-D

GRADED DISTRIBUTION HAVING THE CONDITION THAT $\alpha(T-T_e)$ IS CONSTANT THROUGHOUT THE COATING

GENERAL DERIVATION

Inspection of Eq. C-1 or C-4 reveals that the mechanical strain component ($\epsilon_{\text{mechanical}}$) would be constant across the coating if the term $\alpha(z)\,[T(z) - T_e]$ is invariant with z. The variation in $\sigma(z)$ would be small, depending only on how E(z) and $\mu(z)$ vary across the coating. Thus, the net moment in the coating will be small.

The condition that $\alpha(z)\left[T(z) - T_e\right]$ be constant can be met if α can be varied through the coating to compensate for the change in T(z). The value of α can be made variable by using a graded coating. For a two-phase graded system such as a metal dispersed with a ceramic, the composition at any location z will be represented by V_m, the volume fraction of the metal phase.

The general condition sought is

$$\alpha(z)\left[T(z) - T_e\right] = C$$

where C is a constant. Differentiating gives

$$dT(z) = -C\frac{d\alpha}{\alpha^2} \tag{D-1}$$

The steady-state heat flux equation gives

$$dT = -\dot{Q}\frac{dz'}{k} \tag{D-2}$$

where z′ is measured from the hot surface of the coating, and k is the average thermal conductivity over the temperatures involved.

Equating Eq. D-1 and D-2:

$$C \frac{d\alpha}{\alpha^2} = \dot{Q} \frac{dz'}{k} \tag{D-3}$$

Now α and k are a function of V_m. This shall be expressed as

$$k = k(V_m)$$

$$\alpha = \alpha(V_m)$$

Then substituting into Eq. D-3, and rearranging:

$$dz' = \frac{C}{\dot{Q}} \frac{k(V_m)}{\left[\alpha(V_m)\right]^2} d\left[\alpha(V_m)\right]$$

If the metal used for grading is the same as the substrate metal,

$$C = \alpha_m(T_i - T_e)$$

where T_i is the temperature at the coating-substrate interface under steady-state conditions. Then

$$dz' = \frac{\alpha_m(T_i - T_e)}{\dot{Q}} \frac{k(V_m)}{\left[\alpha(V_m)\right]^2} d\left[\alpha(V_m)\right]$$

Integrating gives

$$z' = \frac{\alpha_m(T_i - T_e)}{\dot{Q}} \int_0^{V_m} \frac{k(V_m)}{\left[\alpha(V_m)\right]^2} d\left[\alpha(V_m)\right]$$

To solve this integral, the relations $k(V_m)$ and $\alpha(V_m)$ must be known. An example of a solution where $k(V_m)$ and $\alpha(V_m)$ are assumed to be known will be presented next.

EXAMPLE

Using the form expressed in the text,

$$k = k(V_m) = k_c \exp(b_1 V_m)$$

$$\alpha = \alpha(V_m) = b_2 V_m + \alpha_c$$

where

k_c = thermal conductivity of the pure ceramic coating

α_c = thermal expansion of the pure ceramic coating

b_1, b_2 = constants

Then

$$z' = \frac{\alpha_m (T_i - T_e)}{\dot{Q}} \int_0^{V_m} \frac{k_c \exp(b_1 V_m)}{\left[b_2 V_m + \alpha_c\right]^2} \, d\left[b_2 V_m + \alpha_c\right]$$

$$= \frac{\alpha_m (T_i - T_e) \, k_c b_2}{\dot{Q}} \int_0^{V_m} \frac{\exp(b_1 V_m)}{\left[b_2 V_m + \alpha_c\right]^2} \, d \, V_m$$

This integral can be evaluated for different values of V_m by graphical integration, where

$$\frac{\exp(b_1 V_m)}{\left[b_2 V_m + \alpha_c\right]^2} \text{ is plotted vs } V_m$$

and the area under the curve is evaluated.

For a numerical example, let

$\dot{Q} = 20$ Btu/in.^{2} sec

$k_c = 2 \times 10^{-5}$ Btu/in.-sec-F

$k_m = 4 \times 10^{-4}$ Btu/in.-sec-F

$\alpha_c = 4 \times 10^{-6}$ F^{-1}

$\alpha_m = 9 \times 10^{-6}$ F^{-1}

$T_i = 1200$ F = 1660 R

$T_e = 0$ F = 460 R

Now

$$b_1 = \ln \frac{k_m}{k_c} = 3.00$$

$$b_2 = \alpha_m - \alpha_c = 5 \times 10^{-6} \text{ F}^{-1}$$

Then

$$z' = \frac{(9\text{x}10^{-6})(1600-460)\ (2\text{x}10^{-5})(5\text{x}10^{-6})}{(20)} \int_0^{V_m} \frac{\exp\ (3\ V_m)}{\left[5\text{x}10^{-6} V_m + 4\text{x}10^{-6}\right]^2}\, d\ V_m$$

$$z' = 5.11 \times 10^{-2} \int_0^{V_m} \frac{\exp\ (3V_m)}{(5V_m + 4)^2}\, d\ V_m$$

At $V_m = 1$, $z' = t_c$; thus

$$t_c = 5.11 \times 10^{-2} \int_0^{1} \frac{\exp\ (3V_m)}{(5V_m + 4)^2}\, d\ V_m$$

and the grading therefore can be made dimensionless by using the ratio z'/t_c to yield

$$\frac{z'}{t_c} = \frac{\displaystyle\int_o^{V_m} \frac{\exp(3V_m)}{(5V_m + 4)^2}\, d\, V_m}{\displaystyle\int_o^{1} \frac{\exp(3V_m)}{(5V_m + 4)^2}\, d\, V_m}$$

The integrals were evaluated graphically, yielding the plot given in Fig. 8 . of the test. The value for t_c was found to be 6.25×10^{-3} inches.

REFERENCES

1. Eubanks, A. G. and D. G. Moore, Investigation of Aluminum Phosphate Coatings for Thermal Insulation of Airframes, NASA TN D-106, November 1959.
2. Blocker, E. W., et al., Development and Evaluation of Insulating Type Ceramic Coatings,WADC TR 59-102, Contract AF33(616)-5441, November 1959.
3. Leggett, H., R. L. Johnson, E. W. Blocker and E. D. Weisert, Development and Evaluation of Insulating Type Ceramic Coatings, Wright Air Development Division, Wright-Patterson Air Force Base, Ohio, Report No. WADC-TR-59-102, Part II; Contract No. AF33(616)-5441, Project No. 7350; 172 pp., October 1960.
4. Kallup, Jr., C., S. Skalrew, and S. V. Castner, Application and Evaluation of Reinforced Refractory Ceramic Coatings, ML-TRD-64-81, Contract AF33(616)-8209, June 1964.
5. Licciardello, M. R., et.al., Development of Frontal Section for Super-Orbital, Lifting, Re-entry Vehicle, Tech. Doc. Reprt. No. FDC-TDR-64-59, Vol. II, 29 May 1964.
6. Wygant, J. F., "Cementitious Bonding in Ceramic Fabrication," Ceramic Fabrication Processes, p. 171-188, W. D. Kingery, John Wiley & Sons, New York, 1960.
7. Hauth, W. E., "Behavior of the Alumina-Water Systems," J. Phys. & Colloid Chem., 54, 142-156 (1950).
8. St Pierre, P.D.S., "Slip Coating Non-clay Ceramics," Ceramic Fabrication Processes, Kingery, W. D. edition, The Technology Press of M.I.T., Wiley and Sons, N. Y. (1958).
9. Parks, G. A., and P. L. de Bruyn, J. Phys. Chem. 66, 967, 1962.
10. Filippi, F. J., Composite Ceramic Radome Manufacture by Mosaic Techniques, AD401053, January 1963, Contract No. AF33(657)-10111.

11. Philipp, W. H., Chemical Reactions of Carbides, Nitrides, and Diborides of Titanium and Zirconium and Chemical Bonding in These Compounds, NASA TN D-3533, August 1966.

12. Kallup, J. C., et.al., Application and Evaluation of Reinforced Refractory Ceramic Coatings, ML-TDR-64-81, Contract No. 33(616)-8209, June 1964.

13. Filamentized Ceramic Radome Techniques, Interim Report for 1 May - 31 July 1961, AD 272112, Contract No. AF33(616)-7872.

14. Plant, H. T. and P. P. Keenan, Research on Binder Techniques for High Temperature Radome Structures, Iterim Report for 1961, AD 261856, Contract No. AF33(616-8176).

15. Chase, V. A. and R. L. Copeland, Development of a 1200 F Radome, Interim Report March 1964, Contract No. AF33(657)11469.

16. Bremser, A. H., and J. A. Nelson, "Phosphate Bonding of Zirconia," Bull. Amer. Ceram. Soc., 46 (3), 281-3, 1967.

17. Kummer, D. L., Shielded Ceramic Composite Structure, Interim Engineering Progress Report 1 June 1963 - 31 August 1963, AD 417116, ASD Proj. NR7-997, Contract AF33(657)-10996.

18. Work Statement for Contract NAS3-11187, 30 June 1967.

19. Zalabak, C., Personal communication 18 July 1967.

20. Hague, J. R., et al., Refractory Ceramics of Interest in Aerospace Structural Applications—A Materials Selection Handbook," ASD-TR-63-4102, October 1963.

21. J. B. Austin, Flow of Heat in Metals, American Society for Metals, Cleveland, Ohio, 1942.

22. Refractory Thermal Barriers for Regeneratively Cooled Liquid Rocket Engine Thrust Chambers, Appendix C, Report No. LRP 298, 21, Aerojet-General Corporation, February 1963.

23. Lauchner, J. H., and D. G. Bennet, "Thermal Fracture Resistance of Ceramic Coatings Applied to Metal: I, Elastic Deformation," Jour Amer Ceram. Soc., 42 (3), 146-50, 1959.

24. Laszlo, R. S., "Mechanical Adherence of Flame-Sprayed Coatings," Bull. Amer. Ceram. Soc., 40 (12), 751-55, December 1961.

25. King, B. W., H. P. Tripp, and W. H. Duckworth, "Nature of Adherence of Porcelain Enamels to Metals," Jour. Amer. Ceram. Soc., 42 (11), 504-25, (1959).

26. Borom, M. P., and J. A. Pask, "Role of "Adherence Oxides" in the Development of Chemical Bonding at Glass-Metal Interfaces," Jour. Amer. Ceram. Soc., 49 (1), 1-6, (1966).

27. Pask, J. A., and R. M. Fulrath, "Fundamentals of Glass-to-Metal Bonding: VIII Jour, Amer. Ceram. Soc., 45 (12), 592-96 (1962).

28. Sharpe, L. H., "Adhesives," Int. Sci. and Tech, 26-37, April 1964.

29. O'Brien, W. J. and G. Ryge, "Relation Between Molecular Force Calculations and Observed Strengths of Enamel Metal Interfaces," Jour. Amer. Ceram. Soc., 47 (1), 5-8, (1964).

30. Carpenter, H. W., S. D. Brown, et al., "Cementitious Bonding," from Critical Evaluation of Ceramic Processing at Subconventional Temperatures, Contract AF33(615)-5124, AFML-TR-67-194, 1967.

31. Vogan, J. W. and J. L. Trumbull, Metal-Ceramic Structural Composite Materials, ML-TDR-64-83, Contract AF33(616)-7815.

32. Styskal, L. M., et al., Development of Reinforced Ceramic Materials Systems, WADD TR60-491, AD 259930, January 1961.

33. Wehr, A. G., J. H. Lauchner, J. Montgomery, Plastic Behavior in Inorganic Oxide-Phosphate Bonded Materials, ASD-TDR-62-775, Contract AF33(616)-8134, August 1962.

34. Penetecost, J. L., "Coating Materials and Coating Systems," High-Temperature Inorganic Coatings, edited by J. Huminik, Jr., Reinhold Publishing Corp., New York, pp 10-109. 1963.

35. Boland, P. and J. D. Walton, Jr., Aerospace Ceramics-Characteristics and Design Principles, AMFL-TR-65-171, June 1965.

36. Krier, C. A., Coatings for the Protection of Refractory Metals From Oxidation," DMIC Report 162, 24 November 1961.

37. Campbell, I. E., High Temperature Technology, John Wiley and Sons, New York (1957).

38. Ryshkewitch, E., Oxide Ceramics, Academic Press, New York, 1960.

39. Advanced Development Program, Atomics International, Canoga Park, California, Report No. NAA-SR-7400, 15 November 1962.

40. Shaffer, P. T. B., Materials Index: High-Temperature Materiale, Plenum Press, New York, 1964.

41. Wheildon, W.M., "Properties of Thermally Sprayed Zirconate Coatings," paper presented at the Thirteenth Meeting of the Refractories Composite Working Group," Seattle, Washington, July 1967.

42. Pears, C. P., and S. Oglesby, The Thermal Properties of 26 Solid Materials to 5000 F or to Their Destruction Temperature, ASD-TDR-62-765, January 1963.

43. Kingery, W. D., "Fundamental Study of Phosphate Bonding in Refractories: I," J. Am. Ceram. Soc. 33 (8) 239-41, 1950; "II" ibid., 242-47.

44. Edlin, V. H., "Bonding Reaction and Mechanism in Chemically Bonded Zirconia," Scientific and Technical Aerospace Reports, 2 (11) 1384, 1964.

45. Greszczuk, L. B., and H. Leggett, "Development of a System for Prestressing Brittle Materials," DAC-92200, Contract NAS 7-429, August 1967.

46. Cornely, K. W., "New Cements Prove Suitable for Applications Above 4,000 F," Ceramic Age, pp 52-3, January 1962.

47. Stepskal, L. M., et al., Development of Reinforced Ceramic Material Systems, AD 259930, WADD TR 60-491, Contract No. AF33(616)-6511, Project No. 3048, January 1961.

48. Kummer, D. L., et al., Shielded Ceramic Composite Structure, AFML-TR-65-331, Contract AF33(657)-10996, October 1965.

49. Boulle, Andre and F. B. Yvoire, "Thermal Evolution of Aluminum Phosphates of the Group P_2O_5/Al_2O_3," Compt. Rend. 245, 531-34, 1957.

50. Bearer, L. C., "Process for Manufacturing Mullite-Containing Refractories," U.S. Patent 2,641,044, June 1953.

51. Gitzen, W. H., et al., "Phosphate-Bonded Alumina Castables: Some Properties and Applications," Bull. Amer. Ceram. Soc. 35 (6), 217, 1956.

52. Plunket, J. D., NASA Contribution to the Technology of Inorganic Coatings, NASA S.P-5014, 1964.

53. Ott, E. and E. R. Allen, Aluminum Phosphate Coatings, ASTIA 268779, May 1961, Contract No. AF33(616)6160.

54. Lyon, J. E., T. U. Fox and J. W. Lyons, "An Inhibited Phosphoric Acid for Use in High-Alumina Refractories," Bull. Amer. Ceram. Soc. 45 (7), 661-5, 1966.

55. Bearer, L. C., "Process for Manufacturing Mullite-Containing Refractories," U.S. Patent 2,641,044, 24 October 1949.

56. Kelsey, R. H. and B. C. Raynes, Filamentized Ceramic Randome Techniques, ASD-TDR-62-721, August 1962.

57. Vondrack, C. H., L. E. Moberly, O. E. Sestrich, Fiber Reinforced Boron Phosphate Structural Composites, AFML-TR-65-38, Contract AF33(657)-7587, February 1965.

58. Tauchner, J. H., W. B. Hall, and J. M. Fields, Jr., Composite Materials, ASD-TDR-62-202, Contract AF33(616)-7765, November 1962.

59. Lewis, B. W., et al., "The Thermal Radiation Characteristics of Some High-Emittance Coatings for Space Applications," paper presented at the 1966 National Metals Congress, Chicago, Illinois, TR No. C6-4.3, 31 October - 3 November 1966.

60. Goldsmith, et al., Thermophysical Properties of Solid Materials: Volume III-Ceramics, WADC TR 58-476, Vol. III, AD265597, November 1960

61. Carpenter, H. W., G. Y. Onoda, Jr., and S. D. Brown, Program Plan for Task II--Protective Coating Systems for Regeneratively Cooled Thrust Chambers, Contract NAS8-11187, November 1967.

BIBLIOGRAPHY

1. Lyons, J. W., G. J. McEwan and C. D. Siebenthal; Highway Research Board Bulletin No. 318. Highway Research Board, National Academy of Sciences-National Research Council, Washington, D.C., 1962.

2. Beller, W. S., "Silicate Paints Proving Thermal Stability," Technology Week, 31 October, pp 24-25.

3. Licciardello, M. R., et al., Development of Frontal Section for Super-Orbital, Lifting, Re-entry Vehicle, Tech. Doc. Reprt. No. FDC-TDR-64-59, Vol. III, May 1964.

4. Seidel, J. et al., High Temperature Inorganic Binders for Magnetic "C" Cores, Final Report 27 November 1960, AD 253091.

5. NASA Tech Brief 65-1035-7, Air-Cured Ceramics Coating Insulates Against High Heat Fluxes, November 1965.

6. Zimmerman, W. F., "Development of a Foamed Alumina Castable Cement," Indus. Heating, pp 2330-4, November 1958.

7. Wehr, A. G., W. B. Hall, J. H. Lauchner, High Temperature Inorganic Structural Composite Materials, ASD-TDR-62-202, Part II, Contract AF33(616)-7765, January 1963.

8. Clausen, E. M., et al., Synthesis of Fiber Reinforced Inorganic Laminates, WADD TR 60-299, Part II, Contract AF33(616)-6283, June 1962.

9. Frolov, A. S., et al., "Seminar Po Zharostoy-kim Pokrytiyam," Leningrad, 1965. Vysokotemperaturnyye Pokrytiya (High-Temperature Coatings); Trudz Seminara, Moscow, Izd-vo "Nauka," 1967, 153-161.

10. Protective Coatings for Refractory Metals in Rocket Engines, IITRI-B237-12, Contract NAS7-113, October 1963.

11. Powers, C. T. "Improvement of Chemically Bonded Castable Zirconia," R&D Report SM-44672, Missile & Space System Division, Douglas Aircraft Co., Inc., 29 May 1964.

APPENDIX B

EVALUATION OF THE THERMAL SHOCK TEST FOR ADHERENCE

A series of specimens were made and tested to evaluate the usefulness of the thermal shock test to this program. The test was easy and it seemingly gave meaningful data. The phosphate-bonded ZrO_2 coating (B45) was used to prepare all specimens. Variables that were evaluated included as-received and grit blasted metal surface conditions, coating thickness, and cooling rate. Specimens in the first series of tests were cooled in still air. Results (Table B-1and Fig.B-1) were meaningful because of the wide separation in the failure temperature, 400 F, between coatings of the same thickness that were applied on as-received and roughened substrates. Coatings spalled at 1400 and 1800 to 1900 F, respectively. From a test point of view, 1800 F was too high because the coating-metal interface could conceivably oxidize enough to influence failure. This would be an unrealistic evaluation because the service temperature is theoretically only 1200 F, where oxidation does not occur in the short duty cycles of this program (less than 1 hour). Failure, therefore, should be induced near 1200 F in this test so that oxidation, and other factors, do not complicate interpretation of results.

From the viewpoint of coating performance, test results were impressive. Three- to 4-mil thick coatings did not fail until cooled from 1800 and 1900 F, and 2-mil thick coatings only started to spall at 2000 F. And most important, failure was mainly cohesive rather than adhesive. Even after the coating spalled, the metal was still 80 percent covered with adhering fragments of the coating. Because failure was not of an adhesive mode, this adherence test as such, was not meaningful for evaluating degree of bonding of the coating to the metal substrate.

To induce failure at lower temperatures, specimens were cooled faster after removal from the furnace by placing them in front of a large fan. Results (Table B-2), when adjusted for thickness, showed that faster cooling caused failure to occur about 200 F lower for coatings applied on smooth substrates and 300 F lower for coatings applied on grit blasted substrates. Once again, however, failure of thin coatings, 3 to 4 mils thick, was cohesive, not adhesive. Coatings between 12.9 and 27.7 mils thick, however, were found to fail by an adhesive mode.

The effect of coating thickness is shown in Fig. B-1. Failure temperature dropped rapidly until coating thickness was about 3 mils, and then it dropped slowly with increased coating thickness. For a meaningful test in which the test was not too sensitive to coating thickness, then, coating thickness had to be more than 3 mils. As it turned out, however, coating thickness had to be 10 mils or greater to induce failure at the coating-metal interface (adhesive failure).

A following series of specimens was tested to evaluate reproducibility of test data. Significant data is shown by the open triangles which represent coated specimens that failed adhesively (Fig. B-2). These data show that all specimens with a coating thickness greater than 12 mils failed when cooled from 1200 or 1300 F, and they failed by an adhesive mode. Specimens with coating thicknesses less than 10 mils failed cohesively, and cohesive failure does not represent a useful index of degree of adherence. Most specimens with coating thicknesses less than 4 mils failed by a combination of both modes. These data were not meaningful because failure could have been influenced by oxidation of the metal at the interface, and oxidation at the interface is not representative of real service conditions where interface temperature should never rise above 1600 F, and only for short periods.

Based on these initial studies, this technique for testing adherence did provide meaningful data for evaluating selected methods of improving adherence. More evaluation of the test itself is necessary, however, before a high degree of confidence could be placed in the unqualified meaning of results. Nevertheless, it was useful within the scope of this program.

TABLE B-1

THERMAL SHOCK ADHERENCE TEST DATA FOR SPECIMENS COOLED BY FREE CONVECTION

Specimen No.	Metal Surface Condition	Coating Thickness, mils	Percent of Coating That Spalled When Cooled to Room Temperature (F) From:							
			1300	1400	1500	1600	1700	1800	1900	2000
28	As-received	4.2	0	50A(1)						
32	↓	3.9	↓	50A(1)						
33	↓	3.8	↓	100A(1)						
34	↓	3.7	↓	100A(1)						
35	↓	3.4	↓	100A(1)						
1	Grit blasted with -20 mesh Al_2O_3(3)	3.8	0	0	0	0	0	100C(2)		
4		4.2	↓	↓	↓	↓	↓	0	100C(2)	
5		4.0	↓	↓	↓	↓	↓	0	100C(2)	
6	↓	3.6	↓	↓	↓	↓	↓	100C(2)	—	
8	↓	4.2	↓	↓	↓	↓	↓	100C(2)		
12	↓	2.2	0	0	0	0	0	0	0	5 to 20
15	↓	2.4	↓	↓	↓	↓	↓	↓	↓	↓
16	↓	2.5	↓	↓	↓	↓	↓	↓	↓	↓
17	↓	2.4	↓	↓	↓	↓	↓	↓	↓	↓
18	↓	2.4	↓	↓	↓	↓	↓	↓	↓	↓
96	↓	6.8	0	0	0	0	100C(2)	—		
97	↓	6.5	↓	↓	↓	↓	0	100C(2)		
98	↓	5.9	↓	↓	↓	↓	0	100C(2)		
99	↓	6.8	↓	50	—	—	—	—		
100	↓	6.5	↓	0	0	0	0	100C(2)		

(1) Adhesive failure; metal shiny where coating spalled.

(2) Cohesive failure; surface 80- to 90-percent covered with adherent fragments from the coating.

(3) Grit blasing in general was not satisfactory; the surface was not roughened as much as standard practice.

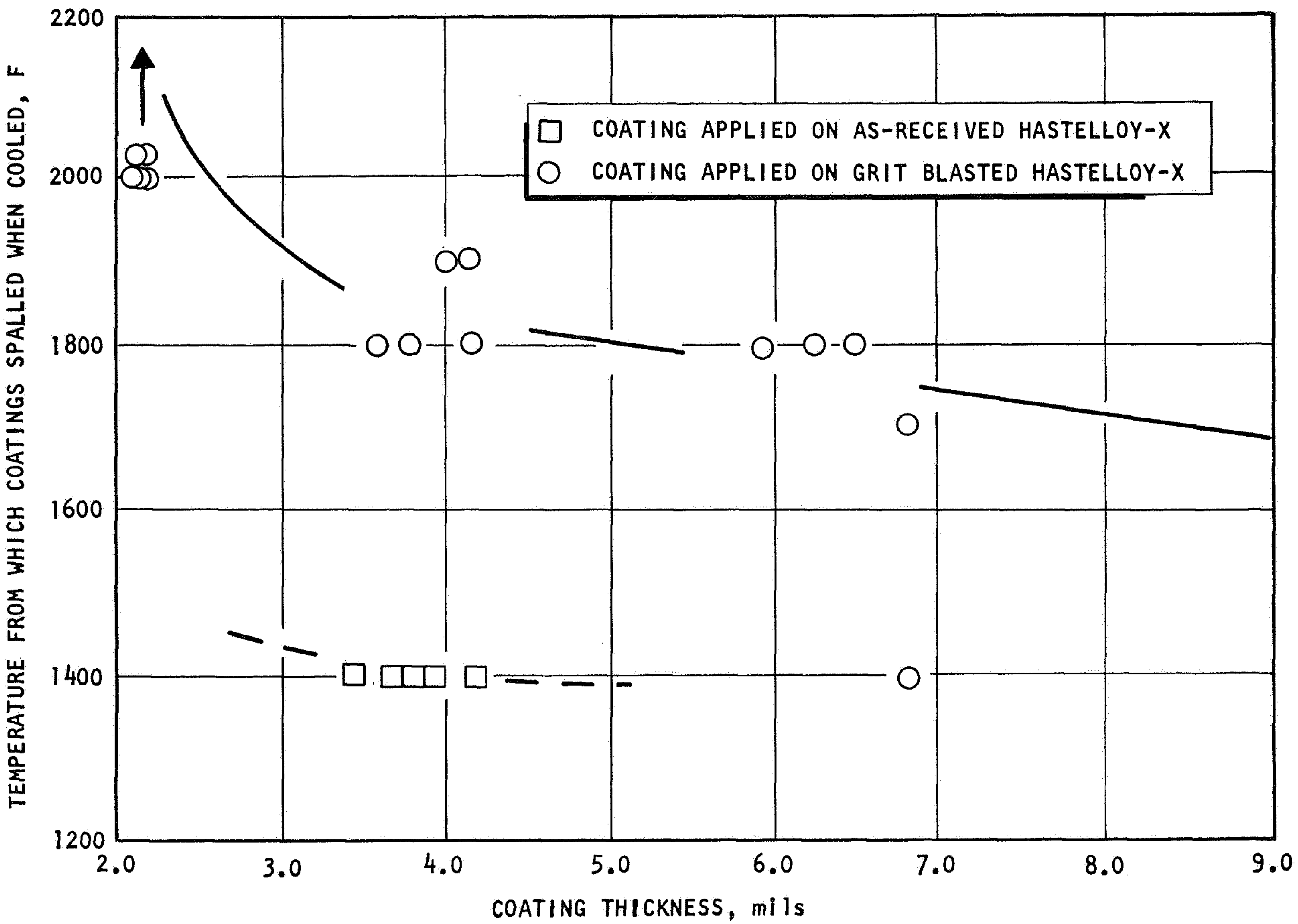

Figure B-1. Adherence Test Results: Thermal Shock Test

TABLE B-2

THERMAL SHOCK ADHERENCE TEST DATA FOR SPECIMENS COOLED BY FORCED CONVECTION

Specimen No.	Metal Surface Condition	Thickness, mils	Percent of Coating That Spalled When Cooled to Room Temperature (F) From:							
			1200	1300	1400	1500	1600	1700	1800	1900
21	As received	2.4	0	100A(1)						
22	↓	2.3	↓	↓						
23	↓	2.5	↓	↓						
26	↓	2.9	↓	↓						
3	Grit blasted with -20 mesh Al_2O_3(5)	3.2	0	0	0	0	100C(2)			
9	↓	3.2	↓	↓	↓	100C(2)	—	—	—	—
2	↓	3.5	↓	↓	↓	0	0	0	0	95A(3)
7	↓	3.0	↓	↓	↓	0	0	0	0	95A
43	↓	27.7	100A(4)	—						
68	↓	18.4	0	80A(6)						
83	↓	13.6	0	100A(6)						
84	↓	12.9	100A(7)	—						
36(8)	↓	4.2	0	0	0	80C(2)				
37(8)	↓	4.1	↓	↓	↓	50C(2)				
38(8)	↓	3.4	↓	↓	↓	60C(2)				
39(8)	↓	3.3	↓	↓	↓	100C(2)				

NOTES:

(1) Adhesive failure; metal shiny where coating spalled

(2) Cohesive failure; surface 80- to 90-percent covered with adherent fragments from one coating

(3) Adhesive failure; metal surface was dark grey where coating spalled

(4) Adhesive failure; no visible coating remained

(5) Grit blasting in general was not satisfactory; the surface was not roughened as much as standard practice

(6) Adhesive failure; 10 percent of coating remained

(7) Adhesive failure; 5 percent of coating remained

(8) Hastelloy-X was 40 mils thick

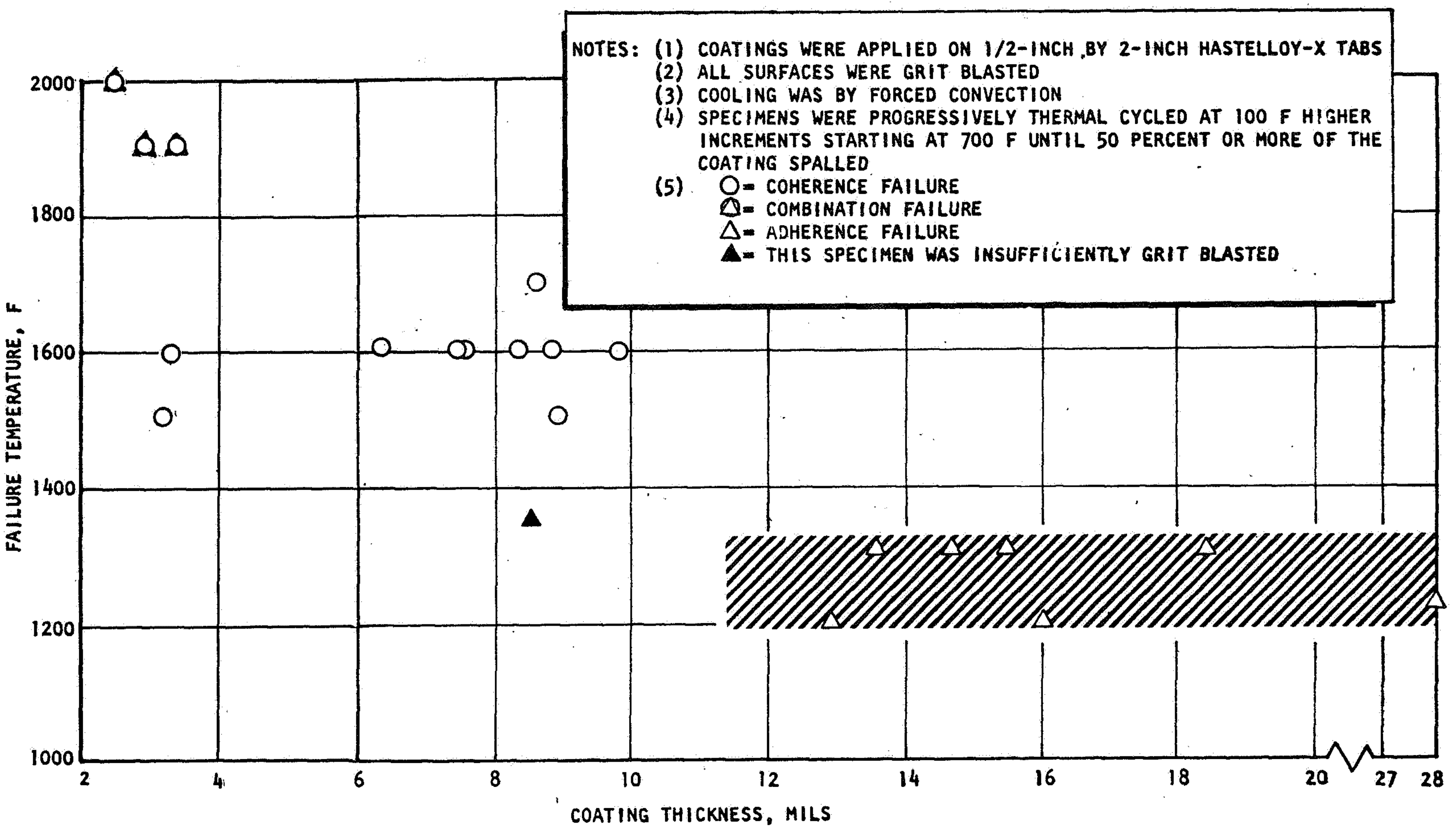

NOTES: (1) COATINGS WERE APPLIED ON 1/2-INCH BY 2-INCH HASTELLOY-X TABS
(2) ALL SURFACES WERE GRIT BLASTED
(3) COOLING WAS BY FORCED CONVECTION
(4) SPECIMENS WERE PROGRESSIVELY THERMAL CYCLED AT 100 F HIGHER INCREMENTS STARTING AT 700 F UNTIL 50 PERCENT OR MORE OF THE COATING SPALLED
(5) ○ = COHERENCE FAILURE
Ô = COMBINATION FAILURE
△ = ADHERENCE FAILURE
▲ = THIS SPECIMEN WAS INSUFFICIENTLY GRIT BLASTED

Figure B-2. Adherence Data Using the Thermal Cycling Technique

APPENDIX C

HEAT FLUX CALIBRATION OF THE ARC-PLASMA JET TEST

INTRODUCTION

Measurement of heat flux under the arc-plasma jet test conditions was important for: (1) verifying that the coated specimens were actually being tested at a heat flux of 20 Btu/in.^{2}-sec, and (2) calculating the thermal conductance of the coating. Thermal conductance of the coating must be known within resonable accuracy so that coating thickness can be designed to provide the correct thermal resistance when coating performance is evaluated in a rocket engine test firing.

Time and resources did not allow for a sophisticated method of measuring heat flux to be followed through a point of confidence. However, the following three different approaches for determining heat flux were taken within the scope of this program: (1) calculation using the Fourier heat conduction equation, (2) calculation using calorimetric data, and (3) measurement using a commercial heat flux gage.

To calculate heat flux using the Fourier equation, thermal conductivity of phosphate-bonded ZrO_2 had to be known. Thermal conductivity was determined directly by the flash diffusivity method (Appendix G), and indirectly by comparing calorimetric data between identical specimens from the arc-plasma jet test, one being coated with phosphate-bonded ZrO_2 and the other being coated with phosphate-free ZrO_2. The ZrO_2 coating in the latter specimen was applied by arc-plasma spraying. Purpose of the latter method was to test the original assumption in Task I that until reliable data are available, the thermal conductivity of phosphate-bonded ZrO_2 will be considered to be the same as that of phosphate-free ZrO_2 data reported in the literature. Results using the Fourier equation indicated that (1) arc-plasma jet tests in this program were actually run at 20 Btu/in.^{2}-sec, and higher in some tests, and (2) the thermal conductance of phosphate-bonded ZrO_2 was, within experimental accuracy, the same as that of melt-sprayed ZrO_2. Results using calorimetric data led to the same conclusion.

The heat flux gage indicated that tests were run at lower heat flux levels, below 7 Btu/in.^{2}-sec. Data obtained using the heat flux gage apparently in error, however, as will be discussed later in this Appendix.

An explanation of the use of the three methods, plus sample calculations using typical test data, are presented in the following sections.

CALCULATION USING THE FOURIER EQUATION

Selection of Data

Heat flux through the coated system was calculated using the one-dimensional Fourier heat conduction equation.

$$Q/A = \frac{(T_{hs} - T_{cs})}{(R_c + R_m)}$$

where

R = t/k

Q/A = heat flux, Btu/in.^{2}-sec

T_{hs} = hot-side surface temperature of the coating, F

T_{cs} = cold-side surface temperature of the metal, F

R_c = thermal resistance of the coating, in.^{2}-sec-F/Btu

R_m = thermal resistance of the metal, in.^{2}-sec-F/Btu

t = thickness, inches

k = thermal conductivity, in.-sec-F/Btu

When all parameters on the right-hand side of the equation are known, calculation of Q/A is straightforward. For the purpose of this calculation, all parameters on the right-hand side were measured during testing, estimated, or obtained from the literature. Selection of values is explained below:

T_m is 50 F above the saturation temperature of the coolant water (Ref. 1), or ca. 350 F under test conditions.

R_m was calculated using thermal conductivity data reported in the literature and the measured thickness of the Hastelloy-X substrate. The value was 60 in.^{2}-sec-F/Btu (see Appendix A).

T_c was obtained by using the optical pyrometer temperature plus a correction factor for emittance of the coated system. Emittance of ZrO_2, which vaires between 0.4 and 0.6 between 1500 and 4000 F (Ref. 2), was assumed to be 0.5. For an emittance of 0.5 and an optical pyrometer temperature of 4000 F, for example, the correction factor was 377 F (Ref. 3). But this correction factor seemed too high because the corrected melting temperature of phosphate-bonded ZrO_2 would be about the same as that for phosphate-free ZrO_2. Equivalent melting temperatures for the two materials could be the same provided that the phosphate in the outer layer of the cementitiously bonded ZrO_2 volatilized leaving a phosphate-free layer of ZrO_2. Nevertheless, a smaller correction factor was used to obtain low-side heat flux values. (All estimations and corrections were made so that a low-side heat flux would be obtained.) The correction factor that was finally used was the difference between the reported and observed melting temperatures of phosphate-free ZrO_2. Observed melting temperature was ca. 4450 F, whereas reported melting temperature was 4625 F (Ref. 4). Thus, a correction factor of 175 F, which was rounded off to 200 F, was used. Assumption was made that emittance of melt-sprayed and phosphate-bonded ZrO_2 coating was the same.

R_c was calculated by dividing coating thickness by coating thermal conductivity. Thickness was measured with a micrometer before testing and, in some cases, microscopically after testing. Thermal conductivity of melt-sprayed ZrO_2 was estimated by assuming that it was the same as ZrO_2 with a porosity of 10 percent at an average temperature of 2750 F. A value of 2.5×10^{-5} Btu/in.-sec-F (Ref. 4 and 5) was used. This value was used for the phosphate-bonded ZrO_2 coating also because, as shown later in this section and in Appendix G, thermal conductivity of both coatings is the same within experimental accuracy.

Results

Data from three typical arc-plasma jet tests were used for illustrative calculations (Table C-1). The calculated heat flux through specimen 72-6 was 15 or 16 Btu/in.^{2}-sec in each test. Heat flux did not increase through this specimen when power was increased to the arc-plasma jet because coating thickness also increased. It was coincidence that heat flux remained constant in the four different test areas. Heat flux through specimens 72-4, which had a comparable coating thickness, varied between 18 and 22 Btu/in.^{2}-sec. Calculated heat flux of a similar specimen, except that it had a coating thickness of about 2 mils, is noteworthy. The heat flux that was required to drive surface temperature to comparable levels, 3800, 3920, and 4000 F, was in the neighborhood of 45 Btu/in.^{2}-sec, or more than double the design heat flux level.

Thus, it is reasonable to conclude that heat flux was at, and well above, the design value of 20 Btu/in.^{2}-sec in the arc-plasma jet tests that were run in this program.

TABLE C-1

CALCULATED HEAT FLUX THROUGH TYPICAL SPECIMENS TESTED IN THE ARC-PLASMA JET AS MEASURED BY THREE METHODS

Specimen No.	Arc Amperage	Coating Thickness, mils	Surface Temperature (Optical Pyrometer), F	Heat Flux, Btu/in.^{2}-sec	
				Using the Heat Conduction Equation	Using Calorimetric Data*
72-6	255	4.2	3650	15	12
	280	4.2	3730	16	13
	277	4.5	3850	15	14
	305	5.0	4000	15	17
72-4	270	3.8	3500	22	11
	310	4.6	3700	20	15
	315	5.1	3725	18	14
	360	4.8	4130	21	18
	370	5.2	4040	19	17
55-2	350	2	3800	46	17
	375	2	3920	47	19
	400	2.5	4000	39	22
Copper Plate With Heat Flux Gage	200	--	--	2**	9
	250	--	--	3**	11
	300	--	--	4**	15
	350	--	--	5**	18
	400	--	--	7**	26

*An area of 0.07 in.^{2} was used to calculate flux, and values were reduced by 33 percent to compensate for spurious heat input.

**Calculated using the heat flux gage data.

CALORIMETRIC MEASUREMENT

Procedure

In theory, the procedure for measuring heat flux using the calorimetric method is simple: the increase in heat content of the cooling water per unit time is divided by the test area. Flowrate of the coolant water was measured with a standard flowmeter*, and water temperature was measured with an electrically insulated, iron-constantan thermocouple.

In practice, however, measurement was complicated by two factors. One, a realistic value for heated area was difficult to determine. Two heat-affected zones were observed in some specimens during testing, depending on the type of optical filter that was used, and in posttest examination with the unaided eye. Test area as measured by several techniques is presented below:

Description of the Area	Method of Measurement	Measured Diameter, inch	Area, in.^{2}
Outer Ring	(1) Measurement with a cathetometer during testing, and (2) measurement with a ruler of the heat-affected area after testing	7/16	0.151
Inner Circule	(1) Size of the arc-plasma gun orifice (which was also the approximate size of the arc-plasma jet), and (2) measurement of the heat-affected area after testing	5/16	0.0754
	Measurement of the brightent spot with a cathetometer and with a steel ruler during testing	5/32	0.0191

The second reason results were unreliable was that a realistic value for heat input through the test area to the cooling water was difficult to obtain. Heat input values were too high because spurious heat got to the cooling water through the copper frame of the specimen holder and through the rest of the coated specimen; i.e., through the large portion of coated area outside of the small test area.

---

*Model 8-112, Brooks Rotometer Company, Hatfield, Pennsylvania

Two studies were made to obtain approximate correction factors. In the first study, heat input from the arc-plasma jet through a copper plate, which was held in the standard test fixture, was compared to heat input through a flattened 3/8-inch-diameter, water-cooled copper tube. Reasoning was that the tube would only intercept a relatively small portion of spurious heat from the arc-plasma jet compared to the large amount of spurious heat that was picked up by the large specimen holder, 5 by 2 inches. The entire surface of the specimen holder was heated during testing by conduction through the copper frame and by convection of the arc gases that spilled around the fixture. Results are reported below as heat input to the cooling water (Btu/sec):

Arc Amperage	Copper Tube	Copper Plate
300	0.8	1.8
350	1.2	2.1
400	1.3	2.4

The data indicate that total heat input through a plate-type specimen is approximately double the heat input through the test area.

In the second study, most of the heat that would normally pass through the test area was intercepted by a flattened 3/8-inch, water-cooled copper tube before it got to the test specimen.

All of the heat input to the specimen in this test, thus, was spurious. Results are reported as heat input to cooling water (Btu/sec) on the following page.

Specimen	Arc Amperage	Heat Input to Specimen, Btu/sec	
		With Copper Tube Intercepting the Arc-Plasma Jet	Without Copper Tube
Copper Plate With Heat Flux Gage	200	43	—
	250	50	—
	300	61	103
	350	65	112
	400	75	161

These results also indicated that approximately one-half of the total heat input to the cooling water was spurious; i.e., it did not pass through the test area.

Results

Results of typical calculations using calorimetric data are given in Table C-1. An area of 0.07 $in.^2$ was used to calculate heat flux and resultant values were reduced by 33 percent to account for spurious heat input through the copper frame and through the remainder of the coated specimen. A correction of 50 percent based on the uncoated copper specimen was considered high because less spurious heat would flow through a coated Hastelloy-X specimen.

Calculated values varied between 12 and 26 $Btu/in.^2$-sec which brackets the design heat flux value of 20 $Btu/in.^2$-sec.

HEAT FLUX GAGE

Description

The heat flux gage*, which was based on the one-dimensional Fourier heat conduction equation consisted of three thin, flat, circular wafers of copper-constantan-copper that were sandwiched together and diffusion bonded. Electrically insulated thermocouple wires for measuring temperature at the two interfaces (i.e., temperature drop across the thickness of the constantan wafer) were extended out of the back of the gage. Heat flux was calculated from the measured temperature drop and the known thickness and thermal conductivity of the constantan wafer. Accuracy of constantan thickness was measured (by the gage manufacturer) to the nearest 1/10,000 inch, and thermal conductivity as a function of temperature was reported** to the third decimal point in watts/cm/C. The gage was not calibrated.

---

*Heat flux gage G-15-6, Greyrad Corporation, Princeton, New Jersey.

The gage was imbedded in the center of a 4.5-inch copper sheet having the same thickness as the gage, 1/16 inch. Gage diameter was 1/8 inch so that it fit inside the arc-plasma-jet-heated area, thereby reducing radial heat loss. A 1/32-inch gap electrically and thermally insulated the constantan wafer from the copper plate. The copper plate was mounted in a standard arc-plasma jet test fixture such that the back face was cooled the same as coated Hastolloy-X specimens.

The plan was to test the gage first without a coating and then with a 3.5-mils-thick phosphate-bonded ZrO_2 coating. Before the coating could be applied, however, the gage developed a water leak so that testing had to be stopped. Solder on the back side of the gage flowed toward the hot-side surface, creating water leaks and shorting the thermocouples. The gage was not repaired in time to continue testing.

Results

In the first series of calibration runs, the surface of the heat-flux gage was in the as-received condition, smooth and uncoated; in the second series of runs, it was roughened by grit blasting with -100 mesh garnet. Tarnish formed on the gage during the first run and remained there for all runs. Emittance, thus, may have been closer to that of ZrO_2, about 0.5, than to a polished metal surface of about 0.1.

**By the supplier, Driver-Harris Company, Harrison, New Jersey

Calibration data for power settings from 200 to 400 amperes are listed in Table C-1 and C-2. Coated specimens were typically tested at settings between 250 and 350 amperes. Calculated heat flux at a power setting of 250 was 2.6 Btu/in.^{2}-sec on the smooth surface and 3.1 Btu/in.^{2}-sec on the roughened surface. These values are considered low, however. Heat flux through the uncoated metal specimen must be at least as much as, and most likely more than, that through a coated specimen. The previously described methods demonstrated that heat flux through a specimen coated with 3.5 mils of ZrO_2 under the same test conditions is about 20 Btu/in.^{2}-sec.

Possible reasons that the measured heat flux through the gage was low included (1) solder holding the gage in place migrated during testing and changed the emf characteristics of the thermocouple junctions, (2) reported thickness of the constantan wafer was in error, (3) low emittance of the copper surface, (4) shorting due to copper or tungsten impurities deposited by the arc-plasma jet, and (5) excessive radial heat flow.

Change in heat flux as a function of distance from the center of this arc-plasma jet is shown by the data in the middle of Table C-2. Observation showed that the brightest stream of plasma gases overlapped the 1/8-inch-diameter gage an estimated 1/16 inch. This is supported by the data in Table C-2 which show that as the gage was raised and lowered 1/16 inch, the heat flux only dropped to 2.2 and 2.5 from 2.6 Btu/in.^{2}-sec. Heat flux was even proportionally high, 1.5 Btu/in.^{2}-sec, when this center stream of the jet was moved away from, but adjacent to, the gage. This datum shows that the high heat flux area is much larger than a diameter of 3/16 inch.

TABLE C-2

HEAT-FLUX GAGE DATA

Surface Condition	Arc Amperage	Temperature of Constantan Wafer, F		Thermal Conductivity of Constantan at Average Test Temperature, Btu/in.-sec-F x 10^4	Gage Heat Flux, Btu/in.^{2}-sec
		Cold Side	Hot Side		
(A)	200	172	206	2.78	1.6
	250	215	369	2.93	2.6
	250	215	270	2.93	2.6
	300	275	349	3.11	3.8
		280	356	3.14	4.0
	350	314	412	3.26	5.3
		319	417	3.28	5.4
	400	348	417	3.41	7.0
	250	192	224	2.83	1.5
(Gage was positioned adjacent to, but outside of, the arc-plasma jet)					
	250	215	261	2.91	2.2
(Gage was positioned 1/16 inch off-center toward the top)					
	250	207	258	290	2.5
(Gage was positioned 1/16 inch off-center toward the bottom)					
(B)	200	192	235	2.83	2.0
	200	199	245	2.88	2.2
	250	301	340	3.01	3.1
	300	293	374	3.19	4.3

Surface Condition A: Smooth, uncoated, and tarnished due to testing.
Surface Condition B: Uncoated, gritblasted with -100 mesh garnet, and tarnished due to testing.

Test Condition:
Argon Plasma gas
1-inch distance, arc-plasma gun to gage
24.5 lb/min coolant water flowrate
0.0060-inch constantan thickness

COMPARISON OF PHOSPHATE-BONDED AND PHOSPHATE-FREE ZrO_2 COATINGS IN ARC-PLASMA JET TESTS

Purpose and Procedure

The assumption that the thermal conductivity of phosphate-bonded ZrO_2 is similar to that of phosphate-free ZrO_2 was supported by the following experiments. Comparative merit in thermal protection between melt-sprayed ZrO_2 (Phosphate-free) and phosphate-bonded ZrO_2 was obtained by comparing coatings of the about same thickness under the same test conditions. Which ever coating system allowed the least heat to pass through to the cooling water, or had the highest surface temperature under equivalent test conditions, was the most protective; i.e., had the highest thermal resistance. Although some differences between the coatings were inherent (i.e., surface roughness, emittance, porosity, and thickness, they were minor within the scope of this type of calculation. Thickness of both types of coatings was not identical because selection of specimens with equal coating thickness was based on micrometer measurements, whereas the final thickness value was based on microscopic measurements which were usually different from the micrometer measurements.

Test procedure was to adjust the power of the arc-plasma jet to produce surface temperatures (optical pyrometer) of 3500, 3750, and 4000 F. These test temperatures were difficult to obtain, however, because accurate adjustment of the power controls during operation was not always possible and because temperature sometimes increased slightly during the test. Power is reported as arc amperage because voltage remained relatively constant between 28 and 30 volts while amperage was varied rom 255 to 390.

Results

The test data, which is shown in Table C-3 and Figures C-1 and C-2 includes that of thin (nominally 4 mils) and thick (nominally 10 mils) melt-sprayed ZrO_2 and phosphate-bonded ZrO_2 (formulation B45) coatings.

TABLE C-3

CALORIMETRIC DATA FOR PHOSPHATE-BONDED $Zr0_2$ AND ARC PLASMA-SPRAYED $Zr0_2$ COATED HASTELLOY-X SPECIMENS

Specimen No.	Coating		Arc Amperage	Surface Temperature (Optical Pyrometer), F	Increase in Coolant Water Temperature, F	Calculated Heat Flux (Using the Heat Conduction Equation) (4), Btu/in.^{2}-sec
	Composition (1)	Thickness, mils				
72.6	Phosphate-Bonded $Zr0_2$	4.2 (2)	255	3630	3.14	15
	(Formulation B45)	4.2	280	3730	3.23	16
		4.5	277	3850	3.55	15
		5.0	305	4000	4.27	15
48-2	Melt-Sprayed $Zr0_2$	--	268	3480	3.00	--
		4.0 (2)	320	3670	3.82	16
				(plus many small hot spots at 4000)		
			360	3740	--	16.3
				(plus many hot spots at 4050)		
		3.9	390	4000	4.63	19.5
				(plus hot spots at 4200; hot spots increased in temperature and the coating fused at 4550)		

(1) The $Zr0_2$ in both specimens is from the same source, Norton Company.

(2) Mounted sections of the test area were measured using a microscope with a calibrated eye piece.

(3) Based on the micrometer measurement. These specimens were not ceramographically mounted for examination.

(4) Assumptions: Coolant-side temperature was 350 F in all cases. True surface temperature was the optical pyrometer temperature +200 F. Thermal resistance of the Hastelloy-X was 60 in.^{2}-sec-F/Btu. Thermal conductivity of $Zr0_2$ was 2.5×10^{-5} Btu/in.-sec-F.

TABLE C-3

(Concluded)

Specimen No.	Coating		Arc Amperage	Surface Temperature (Optical Pyrometer), F	Increase in Coolant Water Temperature, F	Calculated Heat Flux (Using the Heat Conduction Equation)$^{(4)}$, Btu/in.^{2}-sec
	Composition$^{(1)}$	Thickness, mils				
49-4	Melt-Sprayed $Zr0_2$	$9^{(3)}$	280	3750 (a few small hot spots)	2.27	8.2
			280	3540 (many small hot spots)	2.52	8.1
			305	3800 (many small hot spots)	2.72	8.7
			330	3800 to 4100 (so many hot spots that they were almost touching each other)	3.09	9.0
			360	4300 (hot spots were touching)	3.32	9.9
			380	4450	3.55	10.0
73-3	Phosphate-Bonded $Zr0_2$ (Formulation B45)	$10.5^{(3)}$	280	3550	2.73	7.1
			283	3750 to 3950	—	7.7
			300	3950 to 4030 (incipient melting)	3.14	8.0

(1) The $Zr0_2$ in both specimens is from the same source, Norton Company.

(2) Mounted sections of the test area were measured using a microscope with a calibrated eye piece.

(3) Based on the micrometer measurement. These specimens were not ceramographically mounted for examination.

(4) Assumptions: Coolant-side temperature was 350 F in all cases. True surface temperature was the optical pyrometer temperature +200 F. Thermal resistance of the Hastelloy-X was 60 in.^{2}-sec-F/Btu. Thermal Conductivity of $Zr0_2$ was 2.5 x 10^{-5} Btu/in.-sec-F.

The thick coatings were tested so that differences in degree of thermal protection between the two types of coatings would be exaggerated.

The data for the two types of coatings are difficult to compare for several reasons. One, coating thicknesses of the two types of coating were not the same. This fact was discovered after the tests were completed. Repeating the tests with a number of specimens in hope that at least one of each would be of comparable thickness was not practical. Two, surface temperature of the melt-sprayed ZrO_2 coating was indefinite because of the formation of many small hot spots. These spots were several hundred degrees hotter than the rest of the coating in some cases and increased in population with temperature. Three, surface temperature and change in cooling water temperature data were questionable for the thick phosphate-bonded ZrO_2 coating. The coating cracked during testing and eventually spalled. Even a minute separation between the coating and Hastolloy-X substrate while calorimetric data was being collected would have caused an appreciable error due to the increase in the effective thermal resistance of the heat-barrier system.

Data in Fig. C-1 and C-2 were plotted as surface temperature versus two different parameters that are proportional to heat flux; viz., amperage input to the arc-plasma jet and rise in coolant water temperature.

Although the data must be compared and analyzed with qualifications, it shows that the two coatings are similar in degree of thermal protection within the accuracy of this test. The phosphate-bonded ZrO_2 coating was slightly more protective as shown in Fig. C-1 because for a given amperage value (amperage is assumed to be proportional to heat flux) its surface temperature is higher. But the surface temperature should be higher in this case because thickness of the coating was slightly greater.

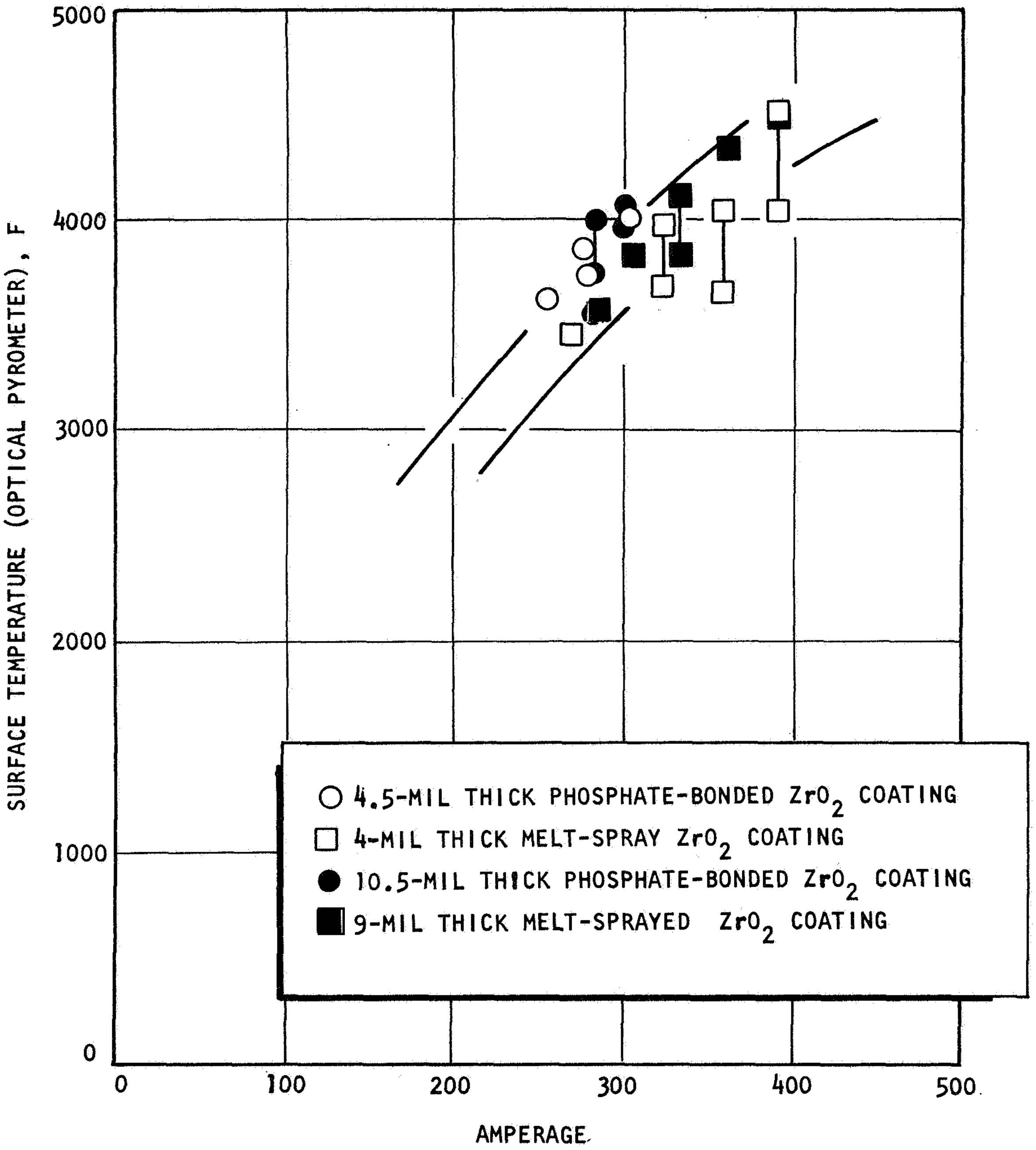

Figure C-1. Comparison of Calorimetric Data of Phosphate-Bonded and Melt-Sprayed ZrO_2 Coatings, Amperage Versus Surface Temperature

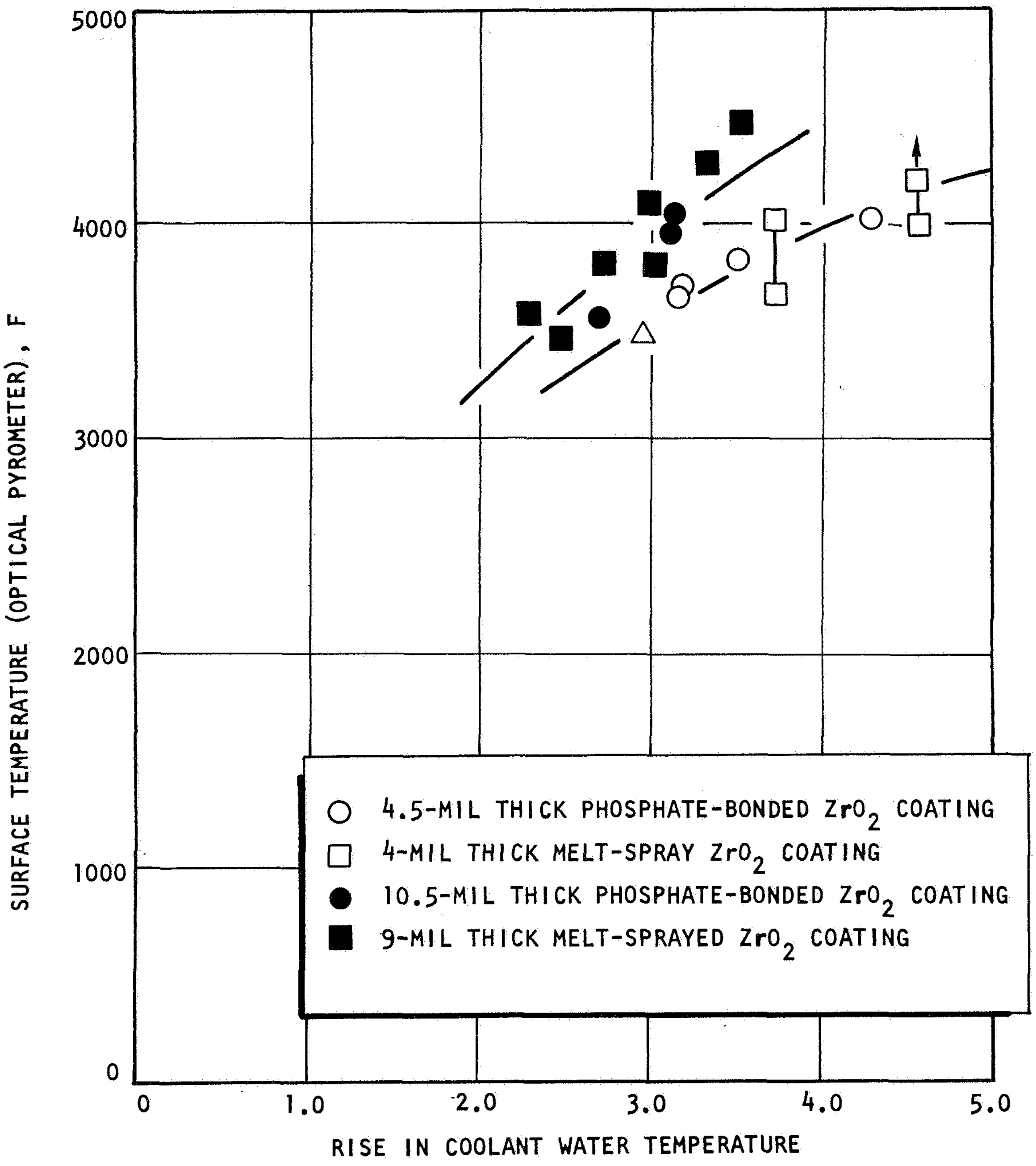

Figure C-2. Comparison of Calorimetric Data of Phosphate-Bonded and Melt-Sprayed ZrO_2 Coatings, Rise in Coolant Water Temperature Versus Surface Temperature

REFERENCES

1. Jens, W. H. and P. A. Lattes, ANL 4627, 1 May 1957.
2. Thermophysical Properties of Solid Materials, Vol. III; Ceramics, WADC TR 58-476 (AD265597), p 276, November 1960.
3. Campbell, I. E., High Temperature Technology, John Wiley & Sons Inc., New York, p 341, 1956.
4. Data Sheet, Norton Company, Refractories Division, Worchester, Massachusetts.
5. Campbell, I. E., High Temperature Technology, John Wiley & Sons Inc., New York, p 271, 1956.

APPENDIX D

PARTICLE SIZE DISTRIBUTION STUDY

The purpose of the following study was to obtain high bulk density of ZrO_2 powders by recombining selected size distributions of available raw materials. All ZrO_2 powders were -200 mesh.

Packing efficiency was conveniently characterized by the bulk density. Procedure for determining bulk density of powders was simple, expedient, yet meaningful, and the data, as shown on the following figures, was reproducible. The procedure was as follows. Twenty-gram batches of powder were first weighed to 0.01 gram and thoroughly dry blended by hand. Then, the blend was poured in a 10-cc graduated cylinder, the powder was compacted by one of three methods, and bulk density was calculated by dividing weight by volume. Methods of compaction were (1) vibration, (2) vibration with a 160-gram weight on top of the powder, and (3) manually tapping (vertically) the base of the graduated cylinder on a rigid surface until the powder no longer compacted. About 100 firm taps were usually required.

In the packing-efficiency study, blends of two size fractions were considered. These size fractions were (1) a -200 +325 mesh, coarse fraction and (2) a -325 mesh, fine fraction. Larger-size fractions were not considered because the diameter of individual powders would be larger than the thickness of the 3.5-mil coatings that were being developed for this program. Because the range of particle sizes that can be used is limited, packing studies of more than two fractions was impractical, and, consequently, only two size fractions were studied.

Two types of fine and coarse fractions were employed. The first fine fraction, denoted as "Fine A", was the -325 mesh fraction of -90 mesh Zirnorite H grog (Norton Company). The second fine fraction, denoted as "Fine B", was as-received -325 mesh Zirnoirite I powder, which reportedly contained a higher proportion of extremely fine particles than Fine A.

The first coarse fraction, denoted as "Coarse A", was the -200 +325 mesh fraction of -90 mesh Zirnorite H grog, whereas the second coarse fraction, denoted as "Coarse B", was the -200 mesh fraction of -90 mesh Zirnorite H grog.

On combining various proportions of Coarse A and Fine A, the variations found for bulk density are shown in Fig. D-1. A maximum density was found with a blend of 40 weight percent Coarse A and 60 weight percent Fine A.

However, the as-received -200 mesh fraction of grog (Coarse B) was found to have a somewhat higher bulk density than the best reconstructed blend. Screen analysis revealed that this powder was a blend of approximately 50-percent Coarse A and 50-percent Fine A. Apparently, the reconstructed blends could not be mixed efficiently.

The packing efficiency of Coarse B grog, could not be improved by adding Coarse A or Fine A. Densities of the mixtures studied are represented by the shaded circles in Fig. D-1.

Combinations of Coarse B and Fine B (instead of Fine A) were studied next (Fig. D-2). A maximum density (3.73 g/cc) was found for tamped blends with 20 weight percent Fine B. This value was higher than the value of 3.57 g/cc that was found for an equivalent mix using Fine A instead of Fine B.

If compaction by vibration was utilized, instead of compaction by tamping, much lower densities were found. Densities of the blends in which the mixture was compacted freely by vibration are shown in Fig. D-2. These are compared in Fig. D-2 to densities obtained when a 160-gram weight was placed on top of the powder in the graduated cylinder during the vibratory compaction process. In both cases, maximum packing efficiency was found when the blend contained 10 weight percent Fine B.

Regardless of the method of compaction, the best packing was found when 10 to 20 weight percent Fine B was added to Coarse B.

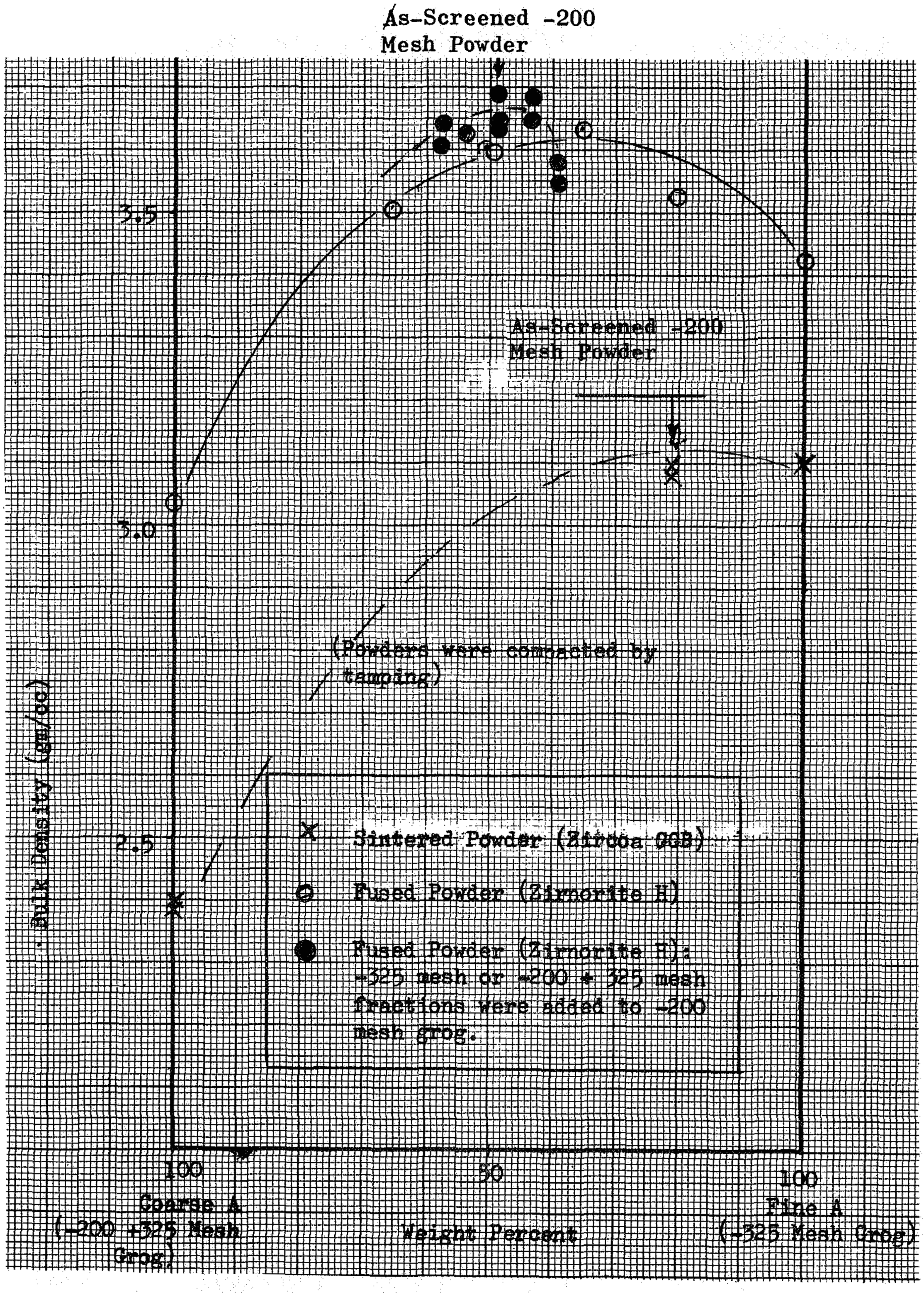

Figure D-1. Bulk Density of Blends of -200 + 325 Mesh and -325 Mesh Zirconia Grog.

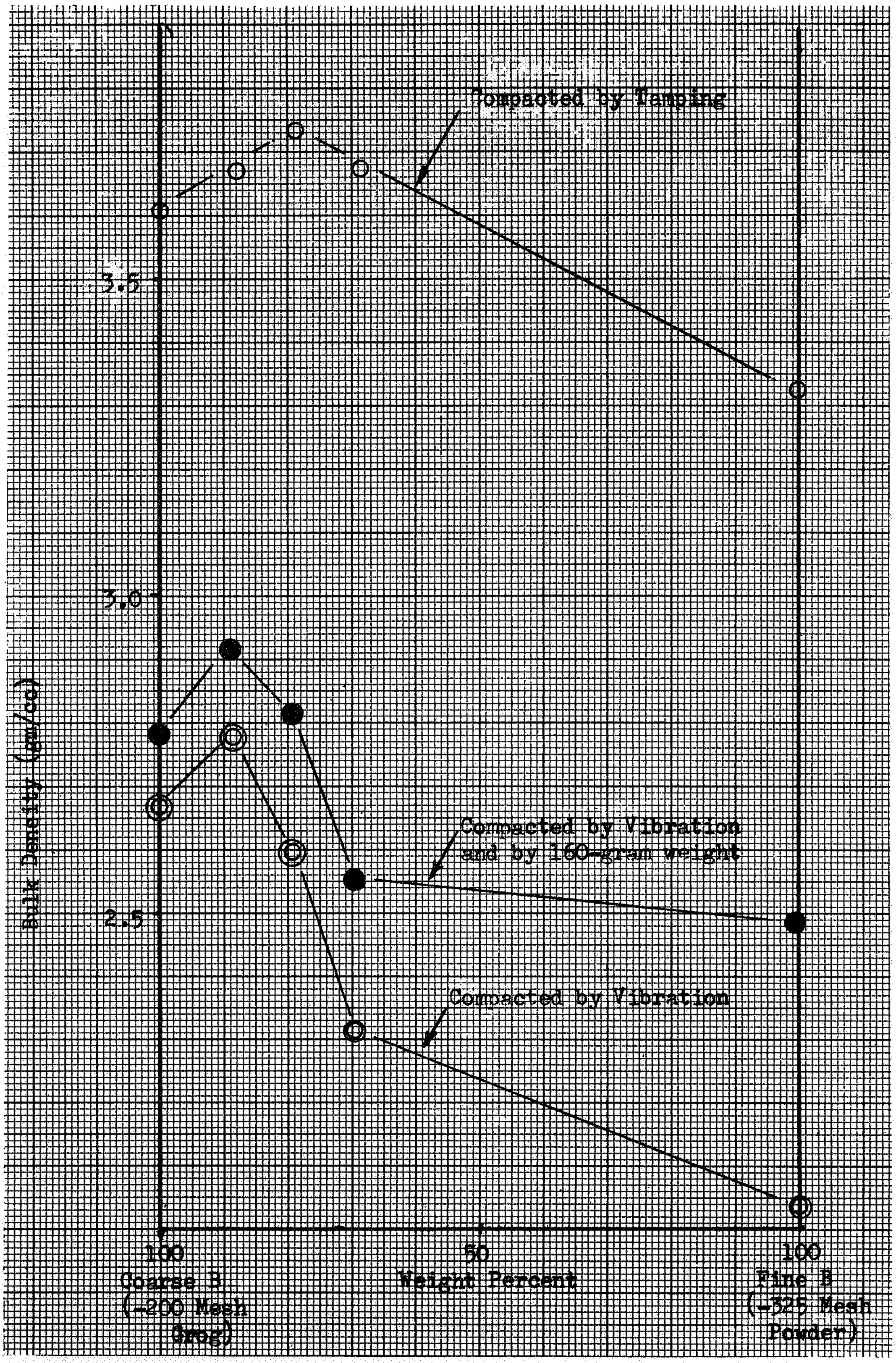

Figure D-2. Bulk Densities of Blends of -200 Mesh Grog and -325 Mesh Powder

APPENDIX E

SPECIAL SUBSTRATE PREPARATION STUDIES

GLASS BASE COATING

The purpose of the glass coating that was interposed between the Hastelloy-X substrate and the phosphate-bonded ZrO_2 (B45) coating was twofold: the glass will anneal at service temperatures (i.e., between 1200 and 1500 F), thereby relieving strains in the phosphate-bonded ZrO_2 coating, and it will attach the phosphate-bonded ZrO_2 coating to the metal substrate more strongly than it is possible without the glass coating. Adherence of the glass coating to the metal will be much stronger than that of the phosphate-bonded ZrO_2 coating to the metal. All glasses can be chemically bonded to any metal (Ref. 1, 2, and 3) and chemical bonding is at least 10-times stronger than mechanical bonding. On the other surface, the phosphate-bonded ZrO_2 coating can be bonded to the glass substrate by either of two techniques. One, development of chemical bonding between the two oxide materials should be possible and this has been indicated by the strong bonding of the B45 coating to smooth glass slides. To enhance this bonding by creating more surface area, the glass substrate can be roughened by a light grit blasting or chemical etch. Two, development of the best possible bonding can be accomplished by fusing the B45 coating to the surface of the glass coating. This was done by flash firing the coating at 1900 F for 1 minute.

The glass coating selected for this study was Ferro 5210-2C*, a commercial product that was developed at Solar Division of Internation Harvester Company and has been in use for many years. Firing temperature (application temperature) is 1800 to 1900 F depending on time at temperature, and the glass will anneal at ca. 1200 F, the service temperature for this application.

---

*Ferro Corporation, Cleveland, Ohio.

The first task of this study was to find the best firing temperature/time relationship. Coated panels of Hastelloy-X were fired at 1600, 1700, 1800, and 1900 F for 5 minutes. Coatings fired below 1900 F for 5 minutes were underfired; the surface was rippled and had a matte finish. Coatings fired at 1900 F were very good; surfaces were flat and glossy, indicating that the fine glass particles had fused into a dense, continuous coating. Firing time at lower temperatures, 1700 and 1800 F, was increased to 15 minutes but firing was still imcomplete. Thus, firing parameters were set at 1900 F for 5 minutes.

Adherence of the 5210-2C glass to the Hastelloy-X metal was tested by bending coated 1/2- by 2-inch tabs back and forth around a metal mandrel that was covered with masking tape. The number of bends required to break off the coating and the size of the mandrel are pertinent, but the most useful information from this test is the appearance of the metal substrate after the coating has been broken off. The number of flexes required to break a glass coating by bending over a given mandrel is as much a function of glass strength, surface condition, and thickness as it is of adherence. Even a strongly adherent glass coating will break off on the first bend if it is very thick, whereas a poorly adherent glass coating can withstand several bends before breaking off if it is very thin. Thus, the critical observation is the condition of the metal where the coating broke off: a clean metal substrate shows poor adherence, whereas at other extreme, a metal substrate completely covered with adherent glass fragments shows excellent adherence.

All coatings that were fired on clean but untreated Hastelloy-X surfaces showed poor bonding. Any glass can be made to chemically bond to a metal under certain controlled conditions, but finding the conditions can be difficult. Fortunately, for a silicate glass applied on Hastelloy-X, finding these conditions was relatively straightforward. One reason was the adherent, uniform oxide layer that can be formed on the Hastelloy-X surface, which was one of the reasons Hastelloy-X was selected. Chemical bonding is produced when the right amount of oxide forms on the metal surface, dissolves in the glass, and saturates it at the interface. The easiest way of producing strong chemical bonding then is to produce the needed amount of oxide on the metal before coating. So the problem, then, is to find a combination of preoxidation and coating application parameters that produce strong adherence.

To this end, Hastelloy-X substrates were oxidized at 1800 and 2000 F for 1 hour, and then the glass was applied at 1900 F for 5 minutes. Adherence of coatings applied over the substrates preoxidized at 2000 F for 1 hour was excellent. This set of application parameters, preoxidation at 2000 F for 1 hour and coating fired on at 1900 F for 5 minutes, was selected without further investigation.

MACROETCHING STUDY

Four etchants for Hastelloy-X were selected for evaluation. Compositions were:

1. Aqua Regia	HNO_3 (concentrated) HCl (concentrated) H_2O	5 milliliters 25 milliliters 30 milliliters
2. Nitric-Hydrofluoric	HNO_3 (concentrated) HF (48 percent)	20 milliliters 15 drops
3. Nitric Acid	HNO_3 (concentrated) H_2O	30 milliliters 70 milliliters
4. Ferric Chloride	$FeCl_3$ HCl (concentrated) H_2O	10 grams 2 milliliters 95 milliliters

For an initial evaluation of these etchants, Hastelloy-X tabs (1/2 by 2 inches) were put in about 50 milliliters of solution so that only half of the tab was immersed. Specimens were etched for 17 hours at ambient temperature. Results were:

Etchant	Immersed Hastelloy-X Surface
1. Aqua Regia	The metal surface was severely corroded at the etchant/air interface. Grain boundary corrosion appeared at a magnification of X50 to be as deep as the width of the grains. Roughness diminished rapidly in the emmersed part away from the air/etchant interface.
2. Nitric-Hydrofluoric	Etching was barely visible at a magnification of X50.
3. Nitric Acid 4. Ferric Chloride	No etching at a magnification of X50 was visible

Finding an ideal macroetchant and determining optimum etching parameters was beyond the scope of this program. Selectively etching grain boundaries to provide a rough surface with undercuts without, at the same time, impairing the metallurgical properties of the metal is a complex undertaking (Ref. 4). The aim of this study was, then, only to provide a satisfactory macroetch for showing that the technique was or was not better suited to this program than grit blasting or other methods of improving adherence. Thus, further studies were limited to aqua regia because it etched many times faster and deeper than the other etchants.

To speed etching, the aqua regia was heated while being stirred continuously. No visible etching was observed in a short time, less than 1 hour, until the aqua regia was heated so that it fumed and boiled at approximately 200 F. Then etching was rapid and sufficient within 1 minute. Apparently etching was by a vapor phase.

Degree of etching was difficult to control and it appeared to be uneven, particularly in several specimens which had several deep pits on the surface. Effect on the strength and ductility of the 0.015-inch-thick Hastelloy-X was not determined, but the etched surface provided an excellent substrate for applying a coating. Surface roughness varied between 150 and 280 microinches rms compared to a high of 200 microinches rms for grit blasted surfaces.

Etching surfaces that had been grit blasted was unsatisfactory. Etching attacked the peaks of the grit blasted surface faster than the other areas, thereby smoothing the grit blasted surface, at least initially, rather than roughening it. There was no advantage, therefore, in starting with a grit blasted surface.

REFERENCES

1. King, B. W., H. P. Tripp, and W. H. Duckworth: "Nature of Adherence of Porcelain Enamels to Metals," J. Amer. Ceramic Soc., 42, (11) 1959, pp. 504-525.
2. Pash, J. A., and R. M. Fulrath: "Fundamentals of Glass-to-Metal Bonding: VIII. Nature of Wetting and Adherence," J. Amer. Ceramic Soc., 45 (12), 1962, pp. 592-596.
3. Pash, J. A.: "Glass-Metal Interface and Bonding," Modern Aspects of the Vitreous State, Vol. 5, pp. 1-28, Butterworths, Washington, D. C., 1964.
4. Laszlo, T. S.: "Mechanical Adherence of Flame-Sprayed Coatings," Bull. Amer. Ceramic Soc., 40 (12), pp. 751-55, 1961.

APPENDIX F

ARC-PLASMA JET TEST DATA OF SPECIMENS COATED WITH PHOSPHATE-BONDED ZrO_2

NOTES RELATING TO DATA

1. An asterisk (*) after a coating thickness value means that the measurement was made microscopically on a mounted section using a calibrated eye piece. Otherwise all measurements were made before testing using a micrometer.

2. Test Phase Explanation:

Phase A:	Steady-state conditions while surface temperature was measured with an optical pyrometer and change in coolant water temperature was recorded; time was 3 minutes unless otherwise specified
Phase B:	Twenty-five thermal shocks
Phase C:	Steady-state conditions long enough to measure surface temperature, about 2 minutes

3. Abbreviations:

NC = no change

TS = thermal shock(s)

HS = hot spot(s)

LPSM = examination of the surface under the low-power stereomicroscope

HPLM = examination of mounted sections using the high-power, light microscope

NR = not recorded

ARC-PLASMA JET TEST SPECIMEN NO. 38-2 **DATE:** 14 June 1968

Purpose or Special Notes: Oxygen at a 1:5 ratio was mixed, within argon. The oxygen was added through the powder-feed port of the arc-plasma gun.

Slurry B29: 10 parts ZrO_2
1.05 parts BS No. 4

Water Flowrate (NR)

Test Area	Coating Thickness, mils	Amperes	ΔT_{water}, F	Test Phase	Surface Temperature, F	Comments
1	1.8	400	6.6	A	3900	NC
		(without O_2)		B	–	NC
				C	–	Temperature was 3750 with HS at 3900 F
						LPSM: NC
2	1.6 2-1/2*	450	7.3	A	3900	HS (4550 F) formed after 2 minutes
		(without O_2)		B	–	NC
				C		10 small HS (4500 F) formed in center
						LPSM: NC
3	1.8	450	6.0	A	3500	NC
		(with O_2)		B	–	NC
				C		NC
						LPSM: NC
4	1.7 1-1/2 to 2-1/4*	550	7.5	A	3700	NC
		(with O_2)		B	–	NC
				C	3700	NC except one HS (4350 F)
						LPSM: Indication that some ZrO_2 grain were dislodged from the surface
5	1.8	600	–	A	3900	Burnout occurred when the specimen was moved to center the arc-plasma jet
		(with O_2)				LPSM: NC except that molten Hastelloy-X flowed over the surface. No cracking or spalling.

ARC-PLASMA JET TEST SPECIMEN NO. 39-1 DATE: 6 June 1968

Purpose or Special Notes:

Slurry B29 : 10 parts ZrO_2
1.05 parts BS No. 4

Water Flowrate (NR)

Test Area	Coating Thickness, mils	Amperes	ΔT_{water}, F	Test Phase	Surface Temperature, F	Comments
1	3.4	400	-	A	4000	One faint HS formed
				B	-	NC
				C	4000	NC
		450	-	A	4100	1 small HS formed
2	3.9 1-3/4 to 2-3/4*					Burnout occured after 130 seconds LPSM: Coating fused around the burned through hole but it did not crack or spall
3	4.4 2-1/2*	450	-	A		Immediate burnout LPSM: Coating fused around the burnout. The coating can be lifted off.

ARC-PLASMA JET TEST SPECIMEN NO. 39-2 DATE: 6 June 1968

Purpose or Special Notes:

The specimen was tested a second time at the end of the program using an argon/5% hydrogen plasma gas.

Slurry B29 : 10 parts ZrO_2 Water Flowrate 27 lb/min
1.05 parts BS No. 4

Test Area	Coating Thickness, mils	Amperes	ΔT_{water}, F	Test Phase	Surface Temperature, F	Comments
1	~2.5	350	3.9	A	3800	NC
				B	–	NC
				C	3800	NC except small HS (4000 F)
2	~2.5	400	4.9	A	4080	Four HS (4170 F) on right side
				B	–	Three small spalled areas
				C	4080	NC
4	~2	-	4.1	A	4000	NC, 2 1/2-minute duration
		Argon/5% hydrogen arc gas was used in the following tests:				
4	~2	200*	4.8	A	3900**	NC, 1-minute duration
5	~2	180*	4.5	A	3500**	NC, 1 3/4-minute duration
6	~2	160*	3.8	A	3350**	NC, 2 1/4-minute duration LPSM: The ZrO_2 grains appeared grey in a white m matrix in areas 4, 5, and 6.

*At 49 volts compared to 29 volts when pure argon was used.

**Temperature measurement was difficult to estimate because of the formation of many hot spots on the surface of the coating.

NOTE: Distance from the specimen to the arc-plasma gun was 1.2 inches when the Ar/5% H_2 plasma gas was used; distance was 1.0 inch in all tests when pure argon was used.

ARC-PLASMA JET TEST SPECIMEN NO. 40-2 **DATE:** 27 June 1968

Purpose or Special Notes; No fluorine was used in the formulation.

Slurry : 10-g ZrO_2
1.05-g H_3PO_4

Water Flowrate (NR)

Test Area	Coating Thickness, mils	Amperes	ΔT_{water}, F	Test Phase	Surface Temperature, F	Comments
1						No data was collected
2	2.1 3-3/4*	350	5.0	A	3670	
				B	–	Spot in center apparently spalled after two TS (it did not; see LPSM)
				C	3670	NC
						LPSM: The coating did not spall but there was a dark spot on the surface
						HPLM; 1. Coating separated from substrate, but many small fragments adhered 2. Close packing of the ZrO_2 grains was noted
3	3.2 2-1/2 to 3-1/2*	400	6.2	A	4080	NC
				B	–	HS formed but no spalling
				C	4080	HS (4130 F)
						LPSM: NC
						HPLM: 1 and 2. Same comments as in area 2. 3. Outer 2/3 of the coating sintered
4	2.9	450	–	A		Started melting immediately; burnout occurred in 20 seconds

NOTE: One half of the coated specimen was soft. Tests were performed on the half of the coated specimen that was hard.

ARC-PLASMA JET TEST SPECIMEN NO. 46-2 **DATE:** 15 July 1968

Purpose or Special Notes;

Slurry B35 **:** 10 parts ZrO_2
0.50 parts BS No. 4

Water Flowrate 27-1/2 **lb/min**

Test Area	**Coating Thickness, mils**	**Amperes**	**ΔT_{water}, F**	**Test Phase**	**Surface Temperature, F**	**Comments**
1	1-3/4 to 4* at edge	350	4.3	A	3800	NC
				B	–	NC
				C	–	NC
						LPSM: NC except surface may be smoother
						HPLM: 1. Coating was adherent 2. No indication of sintering
2	1-1/4 to 2-3/4*	375	5.0	A	4400	HS in center; possibly fused
						LPSM: Center of test area was fused. The center was fused less and cracks formed in the periphery where fusion was more pronounced
						HPLM: Surface fused
3	1-1/4 to 2-1/4*	350	4.3	A	4000	NC
				B	–	NC
				C	4000	NC
						LPSM: NC; coating was hard. No fusion or change in texture was noted
						HPLM: Incipient sintering at surface. No other change

ARC-PLASMA JET TEST SPECIMEN NO. 54-2 DATE: 9 August 1968

Purpose or Special Notes; The coating was applied as two layers. The first layer was cured before the second was applied.

Slurry B44 : 10 parts ZrO_2
0.5 parts BS No. 4

~~Water~~ Flowrate 26-1/2 lb/min

Test Area	Coating Thickness, mils	Amperes	ΔT_{water}, F	Test Phase	Surface Temperature, F	Comments
1	6.3	300	4.0	A	3880	Temperature was 3760 at start
				B	–	Temperature increased after 12 TS. Spalled after 17 TS
2	7.0	325	3.2	A	4480	Melted and started to flow. Stopped after 1 minute
3	6.8	300	2.6	A	4100	Temperature increased to 4300 F after 2 minutes where incipient melting was observed HPLM: The two layers of coating separated
4	6.8	275	2.7	A	3700	NC
				B		HS formed after 15 TS. Spalled after 21 TS. (Coatings visibly separated from the substrate but did not break off.) HPLM: Boundary between the two layers of coating was visible in some areas but not in others

ARC-PLASMA JET TEST SPECIMEN NO. 55-2 **DATE:** 16 July 1968

Purpose or Special Notes: This specimen was sprayed with the same slurry immediately after the tubular NASA test specimen was prepared.

Slurry B45 : 10 parts ZrO_2
1.1 parts BS No. 4

Water Flowrate 27 lb/min

Test Area	Coating Thickness, mils	Amperes	ΔT_{water}, F	Test Phase	Surface Temperature F	Comments
1	3.4 1-3/4 to 2-1/2*	350	3.9	A	3800	Two very small HS, NC
				B	-	NC
				C	3800	NC
						LPSM: NC
						HPLM: 1. Coating was separated from substrate. This could very easily have happened during sectioning the specimen for mounting. 2. Consequently most of the coating was broken away during polishing because it was not supported by the metal substrate. 3. Sintering was observed nearer the surface.
2	2.2 1-3/4 to 2-1/2*	375	4.5	A	3920	Two very small HS (4170 F) formed after 2 minutes
				B	-	NC except HS increased to 4450 F
				C	3920	NC
					-	LPSM: Very small fused beads on the surface
					HPLM:	HPLM: 1. Coating was attached to the metal in all areas 2. Some thin areas suggested that the top layer broke off.

ARC-PLASMA JET TEST SPECIMEN NO. 55-2 (CONT.)DATE:

Purpose or Special Notes:

Slurry :

Test Area	Coating Thickness, mils	Amperes	ΔT_{water}, F	Test Phase	Surface Temperature, F	Comments
						3. Incipient sintering was observed at the surface
3	3.2 2.3*	400	5.1	A	4000	
				B		Very small HS (4530 F) in single files forming snake-like patterns
				C	4000	NC
						NOTE: It is significant that this coating did not spall and that the temperature did not increase during Phase C.
						LPSM: Very small fused beads on the surface.
						HPLM: 1. Most of the coating was detached from the substrate. 2. Consequently most of the coating broke off during polishing. 3. Sintering was observed at the surface.

ARC-PLASMA JET TEST SPECIMEN NO. 58-2 **DATE:** 1 August 1968

Purpose or Special Notes:

Slurry B44: 10 parts ZrO_2
0.5 parts BS No. 4

Water Flowrate $24\frac{1}{2}$ lb/min

Test Area	Coating Thickness, mils	Amperes	ΔT_{water}, F	Test Phase	Surface Temperature, F	Comments
1	4.5,5*	300	3.8	A	3450	Distance was 1-1/8 inch instead of 1 inch. Test was repeated at 1 inch in the same spot.
		300	–	A	3540	NC
				B	–	NC
				C	–	NC
						LPSM: NC
						HPLM: NC
2	5*	350	4.7	A	4200	Temperature increased to 4400 F in the center, then after 2 minutes to 4460 F where melting was observed.
						LPSM: Slight surface fusion and microcracks.
						HPLM: Sintering and fusion (See Fig. 12a)
3	4.8	325	4.0	A	3850	Temperature decreased to 3800 F
				B	–	HS formed after seven TS. Spalled after nine TS.
						LPSM: Large fused area; cracked and spalled
4	4.9	325	3.9	A	3815	NC
				B	–	Spalled after seven TC.
						LPSM: Fused and cracked.
						HPLM: Detached from substrate
						NOTE: Failure was caused by poor adherence.

ARC-PLASMA JET TEST SPECIMEN NO. 66-1 **DATE:** 8 August 1968

Purpose or Special Notes: The coated Hastelloy-X specimen was dried, cured, and tested without removing from the test fixture. In other words, the coated specimen was not flexed or crimped due to straightening in test fixture.

Slurry B44 : 10 parts ZrO_2
0.5 parts BS No. 4

Water Flowrate 27.5 lb/min

Test Area	Coating Thickness, mils	Amperes	ΔT_{water}, F	Test Phase	Surface Temperature F	Comments
1	6.1	300	3.1	A	3600	NC
				B	–	HS formed after four TS, spalled after 12 TS.
2	6.1	350	4.0	A	4320	Started to melt after 50 seconds
3	5.9	325	3.5	A	4065	NC
				B	–	Started spalling at the edge by the gasket. Stopped after 18 TS.
4	6.0	300	3.2	A	3650	NC
				B		Coating spalled after six TS. A HS formed during Phase A so the jet was moved to another area where no HS formed. Failure occurred at the original HS where adherence was poor.

ARC-PLASMA JET TEST SPECIMEN NO. 68-2 **DATE:** 8 August 1968

Purpose or Special Notes:

Slurry B45 : 10 parts ZrO_2
1.1 parts BS No. 4

Water Flowrate 26 lb/min

Test Area	Coating Thickness, mils	Amperes	ΔT_{water}, F	Test Phase	Surface Temperature F	Comments
1	4.6	300	3.5	A	3800	NC
				B	3800	NC
				C	3800	NC
2	4.1	350	3.7	A	4030	HS (4160 F) at 10:o'clock
				B	–	NC
				C	–	NC

ARC-PLASMA JET TEST SPECIMEN NO. 72-1 **DATE:** 21 October 1968

Purpose or Special Notes: Calibration Studies

Slurry B45 : 10 parts ZrO_2
1.1 parts BS No. 4

Water Flowrate 24.5 lb/min

Test Area	Coating Thickness, mils	Amperes	ΔT_{water}, F	Test Phase	Surface Temperature F	Comments
1	4.3	275	2.6	A+	3450	3650 F at start
2	4.3	360	3.7	A+	3820	NC
3	4.5	350	3.8	A+	3725	NC
4	5.0	398	4.5	A+	4000	BS (4100 F) in center
5	5.2	298	3.4	A+	3500	Decreased to 3450 F, Edge of coated specimen chipped; ΔT_{water} was therefore high
		359	3.7	A+	3750	

ARC-PLASMA JET TEST SPECIMEN NO. 72-2 DATE: 20 October 1968

Purpose or Special Notes: Calibration Study. Measurement of test area diameter with a cathetometer.

Slurry B45 : 10 parts ZrO_2
1.1 parts BS No. 4

Water Flowrate 24.5 lb/min

Test Area	Coating Thickness, mils	Amperes	ΔT_{water}, F	Test Phase	Surface Temperature, F	Comments
1	4.8	280	-	A+	3500	NC
2	5.3	390	-	A+	4000	HS (4500 F) in center
3	5.4	320	-	A+	3700	NC
						Measurements which varied from 0.125 to 0.188 inch diameter, were inaccurate because the size, for one thing, was dependent on the type of optical filter that was used.

ARC-PLASMA JET TEST SPECIMEN NO. 72-3 DATE: 15 October 1968

Purpose or Special Notes;

Slurry B45 : Water Flowrate 24.5 lb/min

Test Area	Coating Thickness, mils	Amperes	ΔT_{water}, F	Test Phase	Surface Temperature, F	Comments
1	4.4	300	3.5	A	3560	NC
		350		A	3680	HS ~3800 F; NC
				B	–	NC
				C	–	NC
2	4.2	300	3.8	A	3700	NC
3	4.5	370	4.7	A	4000	NC
4	3.4	288	3.1	A	3500	NC
5	4.2	370	–	A	–	Temperature increased to 4000 F, then 4200 F where HS formed, and then to 4500 F

ARC-PLASMA JET TEST SPECIMEN NO. 72-4 DATE: 22 October 1968

Purpose or Special Notes: Calibration studies and test area measurement with a steel rule that was clamped near the test area.

Slurry B45: Water Flowrate 24.5 lb/min

Test Area	Coating Thickness, mils	Amperes	ΔT_{water}, F	Test Phase	Surface Temperature, F	Comments
1	3.8	270	2.7	A	3500	NC
2	4.6	310	4.0	A+	3700	NC Measured test area with a steel ruler during testing. Hot area in center ~5/32 inch diameter. There is a ring around the most severely heated area about 3/16 wide. This ring is about 3/8 inch OD.
3	5.2	370	4.5	A+	4040	HS in center was 4200 F. Temperature increased while test area was being measured until the coating melted at 4540 F. Test area diameter was ~5/32 inch.
4	5.2	310	–	A	–	Spalled immediately
5	5.1	315	3.6	A+	3725	NC. Test area diameter was 5/32 to 3/16 inch. Temperature in outer ring was 3450 F. This area was selected for examination with the electron-beam microprobe.
6	4.8	360	4.6	A+	4130	Temperature was 4000 at start Test area diameter was 5/32 inch. Outer ring OD was 7/16 inch and temperature was 3540 F.

ARC-PLASMA JET TEST SPECIMEN NO. 72-6 **DATE:** 28 October 1968

Purpose or Special Notes; Calibration Study. Compare with specimen 48-2 (see Appendix C).

Slurry B45 : Water Flowrate 24.5 lb/min

Test Area	Coating Thickness, mils	Amperes	ΔT_{water}, F	Test Phase	Surface Temperature, F	Comments
1	4.2	255	–	A	3465	NC
		260	–	A	3560	NC
2	4.1, 4.2*	255	3.1	A	3650	Temperature was 3550 F at start. HPLM: No effects as a result of testing were observed (Fig. 11a)
3	4.0, 4.2*	280	3.2	A	3730	NC HPLM: Incipient sintering at the surface.
4	4.0	280	–	A	3730	NC
				B	–	HS formed after seven TS; 25 TS were completed.
		297	–	A	3800	NC
				B		NC
		320	–	A	3830	NC
				B		NC
5	4.2, 4.5*	277	3.6	A	3850	NC HPLM: Grains at the surface had sintered; no defects. (Fig. 11b)
6	4.6, 5.0*	305	4.3	A	4000	NC
		330	–	A	4060	HS (4300 F) formed in center; coating then fused and the temperature increased to 4430 F. HPLM: Grains at the surface to a depth of 1 mil sintered to a high density; affected area was 1/8 inch wide. (Fig. 11c).

ARC-PLASMA JET TEST SPECIMEN NO. 73-3 **DATE:** 15 November 1968

Purpose or Special Notes; Calibration Study. Compare with specimen 49-4 (see Appendix C).

Slurry B45: **Water Flowrate** 24.5 **lb/min**

Test Area	Coating Thickness, mils	Amperes	ΔT_{water}, F	Test Phase	Surface Temperature, F	Comments
1	10-1/2	280	3.0	A	3550	NC
				B	-	NC
				C	3550	NC
2	11	283	-	A	-	Spalled immediately.
3	11	283	-	A	3950	
4	10-1/2	300	3.1	A	4030	Incipient melting
				B	-	Spalled after 11 TS. It had been cracked before testing.

ARC-PLASMA JET TEST SPECIMEN NO. 73-T DATE: 14 November 1968

Purpose or Special Notes: The coating was applied on a type 347 stainless-steel tube, 0.450 inch OD, 0.012 inch wall thickness. Most of the coating spalled before testing in large axial strips.

Slurry B45 : Water Flowrate (NR)

Test Area	Coating Thickness, mils	Amperes	ΔT_{water}, F	Test Phase	Surface Temperature, F	Comments
1	5.0	280	-	A	3410	NC
2	7.7	285	2.1	A	3450	NC
3	6.3	305	2.3	A	3700	NC
				B		NC
				C		NC
4	8.0	358	2.5	A	4000	NC
				B		Started to melt after 20 TS

(a)

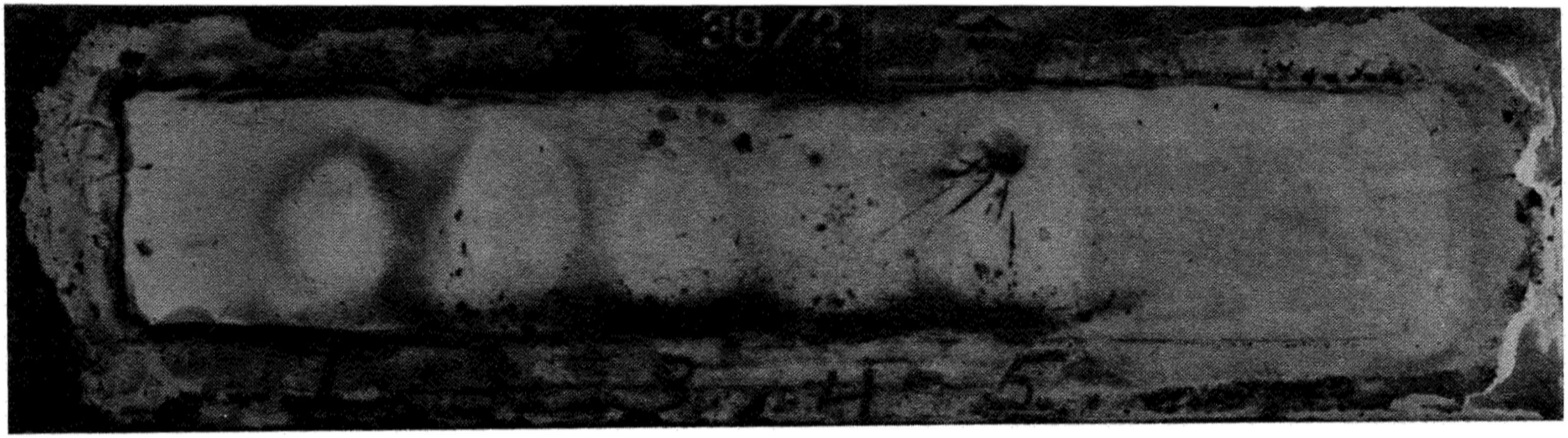

Test Area:	1	2	3	4	5
Coating Surface Temperature	3900 F	3900 F	3500 F	3700 F	3900 F
Number of Thermal Shocks:	25	25	25	25	-
Special Notes:	No Failure	No Failure	No Failure	No Failure	Burnout occured due to high power input

O_2 was added to the argon plasma gas

Figure F-1. Selected Specimens After Testing in the Arc-Plasma Jet. (Magnification ~X1-1/2: All specimens are 1-1/2 by 4-1/2 inches.)

(b)

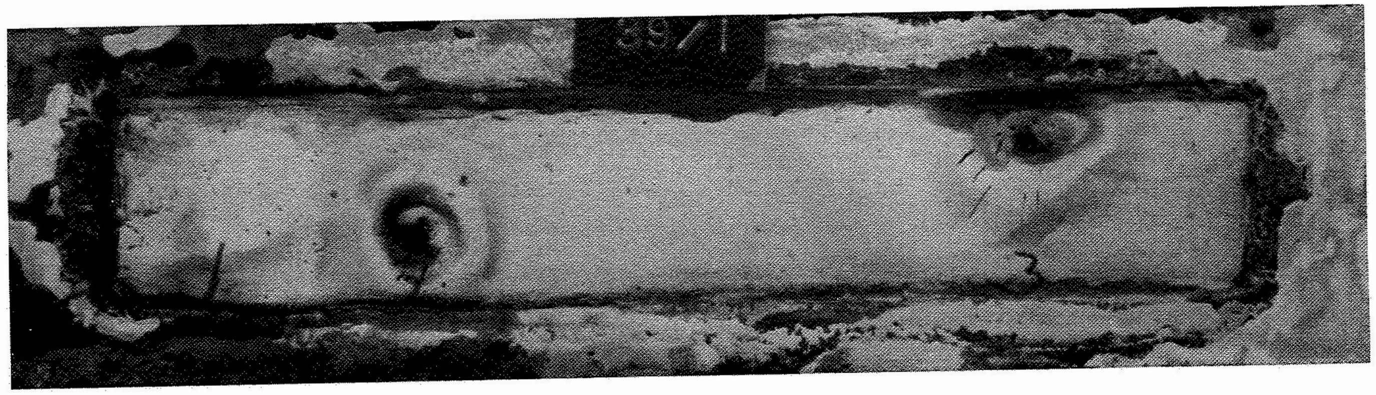

Test Area:	1	2	3
Surface Temperature:	4000 F	-	-
Number of Thermal Shocks:	25	-	-
Special Notes:	No Failure	Burnout due to insufficient cooling	Burnout due to insufficient cooling

(c)

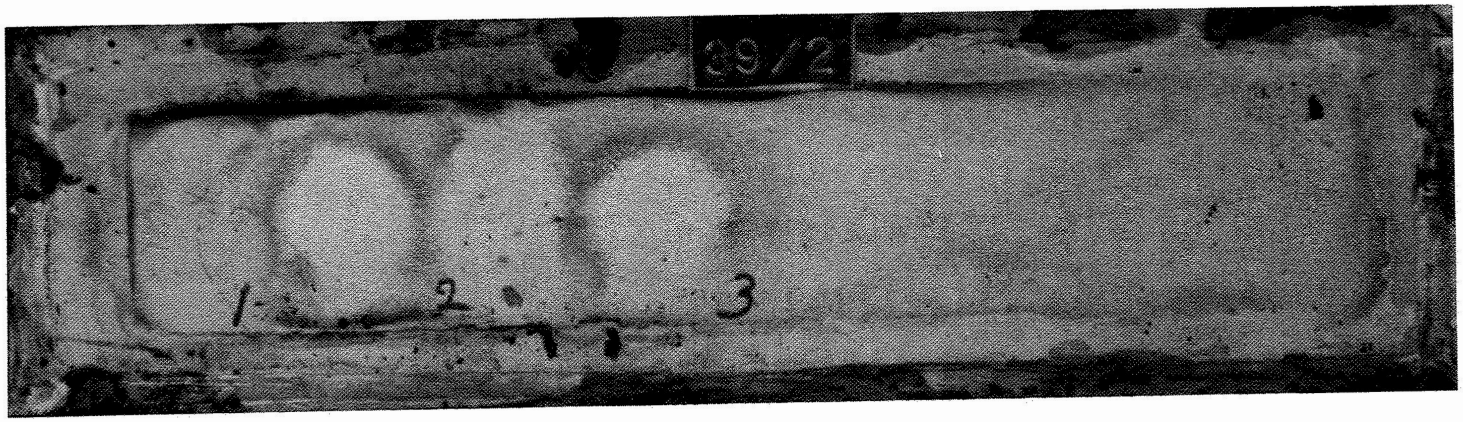

Test Area:	1	2	3
Surface Temperature:	3800 F	4080 F	-
Number of Thermal Shocks	25	25	-
Special Notes:	No Failure	No Failure	-

Figure F-1. (Continued)

(d)

Test Area:	2	3	4	1 (Mislabeled on the specimen)
Surface Temperature:	3670 F	4080 F	-	-
Number of Thermal Shocks:	25	25	-	-
Special Notes:	No Failure	No Failure	Burnout due to insuffic insufficient cooling	-

(e)

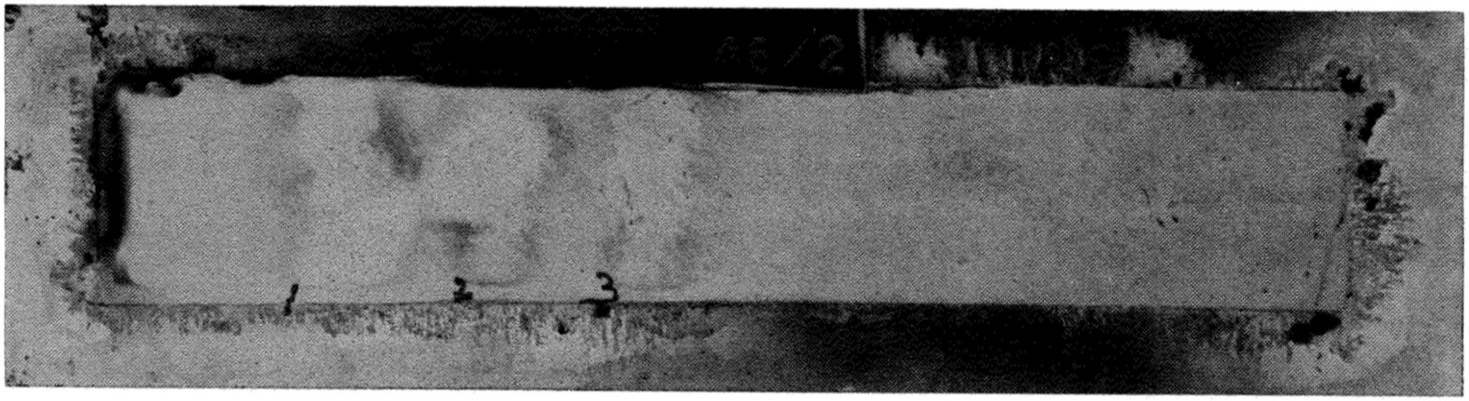

Test Area:	1	2	3
Surface Temperature:	3800 F	4400 F	4000 F
Number of Thermal Shocks:	25	-	25
Special Notes:	No Failure	Fused in Center	No Failure

Figure F-1. (Continued)

(f)

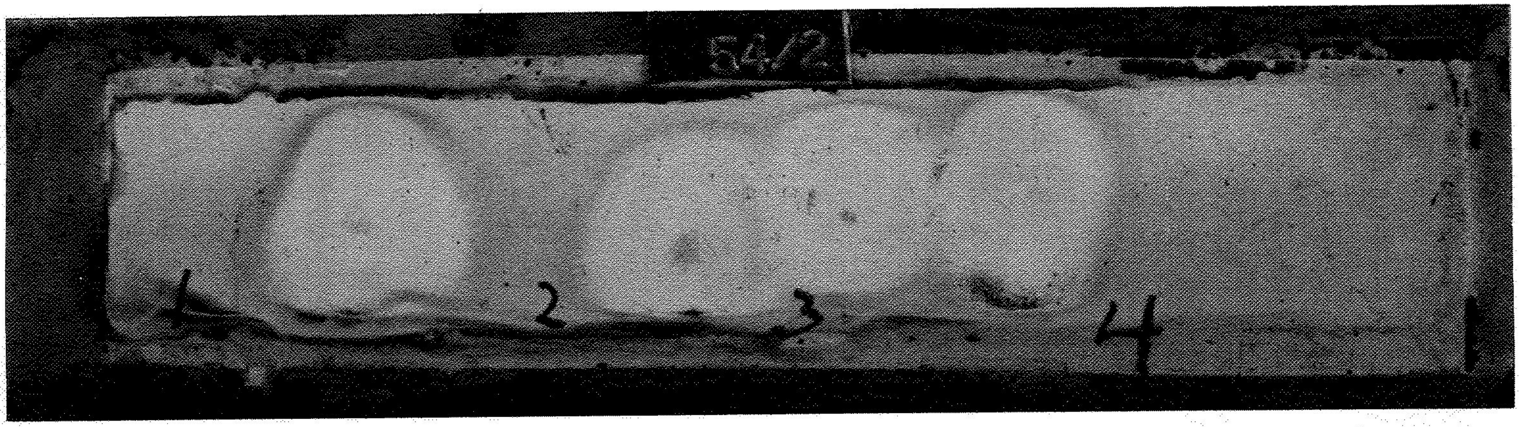

Test Area:	1	2	3	4
Surface Temperature:	3880 F	4480 F	4300 F	3700 F
Number of Thermal Shocks:	17	-	-	21
Special Notes:	This coating was excessively thick, 7 mils, and was applied to two layers			

(g)

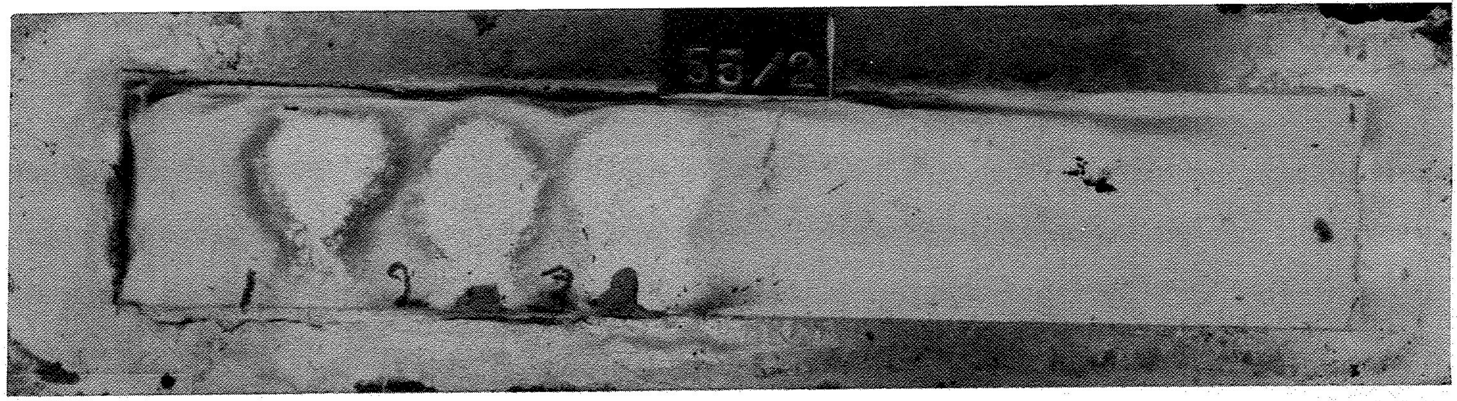

Test Area:	1	2	3	
Surface Temperature:	3800 F	3920 F	4000 F	
Number of Thermal Shocks:	25	25	25	
Special Notes:	No Failure	No Failure	No Failure	Spalling at edges was caused by hot spots as the arc-plasma jet passed by the gasket at the edge of the coated area.

Figure F-1. (Continued)

(h)

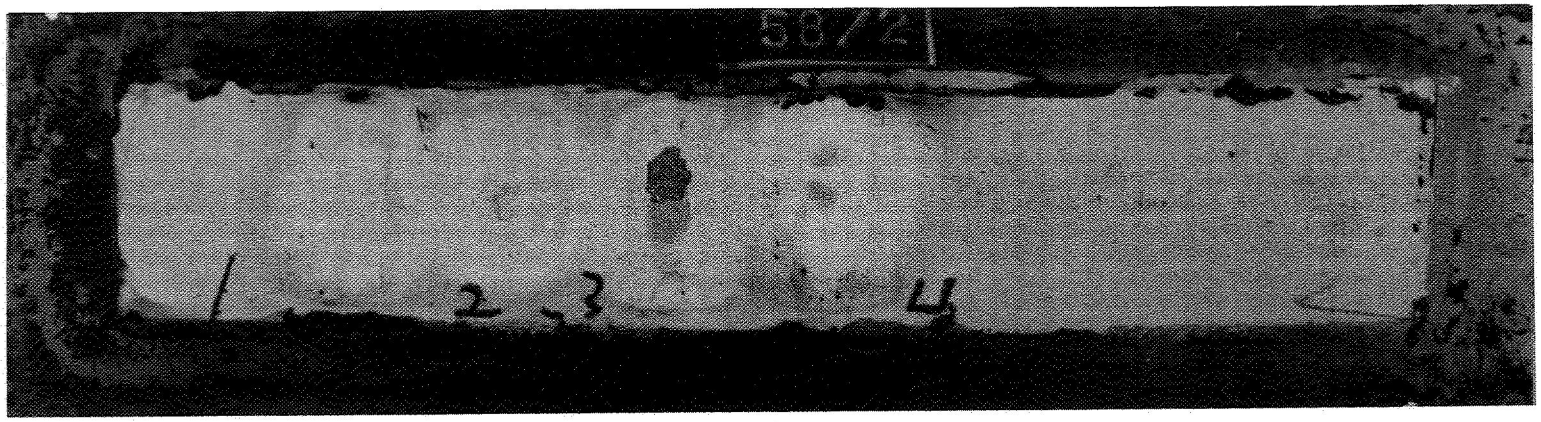

Test Area:	1	2	3	4
Surface Temperature:	3450 F	4460 F	3850 F	3815 F
Number of Thermal Shocks:	25	-	9	7
Special Notes:	No Failure	Melted	Spalled	Spalled

NOTES: Areas 3 and 4 were the only failures in this program for a coated specimen such as this.

(i)

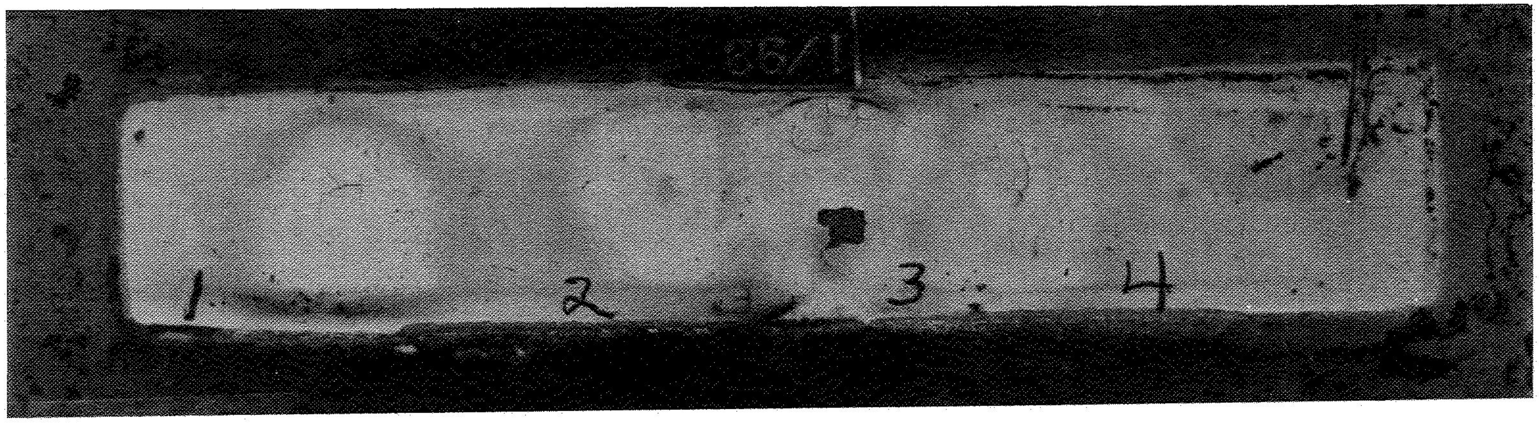

Test Area:	1	2	3	4
Surface Temperature:	3600 F	4320 F	4065 F	3650 F
Number of Thermal Shocks:	12	-	18	6
Special Notes	Spalled	Melted	Started spalling at the edge of the gasket coating	Spalled

NOTE: This coating was 6 mils thick.

Figure F-1. (Concluded)

APPENDIX G

THERMAL DIFFUSIVITY MEASUREMENT OF PHOSPHATE-BONDED ZrO_2

The flash thermal diffusivity technique described by Parker, et al. (J. Appl. Phys, 32, 1679 (1961)) was used except that the pulsed energy was supplied by a ruby laser instead of a xenon flash lamp. A 5-mil chromel-alumel thermocouple, spring-loaded to the back face of the sample, was used to measure the sample temperature. Corrections for heat losses due to radiation were applied to measurements taken above 500 C using the method of R. D. Cowan (J. Appl. Phys. 34, 926 (1963)), and measurements were made in a stainless-steel tube furnace.

The sample was supplied by Rocketdyne, in the appropriate shape (a 1/4-inch-diameter wafer) and thickness (0.0420 inch), and with the required metallized coatings. The wafer was made from an overly thick disc by polishing it to the correct thickness after the material was cured. A thick slurry (10.0 grams of ZrO_2, 1.05 grams of Binder Solution #4, and no water) was manually forced into a 1/4-inch diameter by 1/8-inch deep hole drilled in Teflon stock. The rod was removed after the initial set, and a slow drying and curing schedule was used to avoid cracking: 1 day at room temperature, 2 hours at 100 F, 2 hours at 180 F, 2 hours at 212 F, and finally 1 hour at 600 F. The specimen was then outgassed at 2500 F for 1/2 hour at about 10^{-5} torr. The front face of the sample was coated with a thin layer of platinum and the back face was coated with a thin layer of chromium. Metallic coatings were applied by vapor deposition in a vacuum. The thickness included the metallic coatings, which were <1 percent of the total thickness. The platinum effectively absorbs the laser energy at the front face, and the chromium acts as an electrical conductor between the two legs of the thermocouple. Density of the sample was 4.4 g/cm^3.

Accuracy of the measurements was checked by measuring the thermal diffusivity of an Armco iron sample at room temperature. The values obtained agreed within 1 percent of the best literature values for this material.

The accuracy of the values reported for materials less pure than Armco iron, such as the phosphate-bonded zirconia, would normally be ±5 percent. For reasons stated below, however, the uncertainty of the data, as applied to this particular phosphate-bonded zirconia sample, are believed to be ±30 percent. The main source of uncertainty in the measured values is due to inhomogeneity of the sample. Pores and cracks were readily visible on the surfaces with the unaided eye. The extent of the effects of pores and cracks within the sample is not known. Nonuniformity among samples could increase the uncertainty to ±40 to 50 percent for the material.

The data are tabulated in Table G-1 and shown in Fig. G-1. Because of the high porosity plus the very low thermal diffusivity of the material, gas entrapped within the sample contributed significantly to the total diffusivity of the sample. The gas (air) pressures are tabulated to show the extent of the effect. Data were not reproducible until the sample was outgassed thoroughly. Measurements obtained after outgassing the sample, were found to be in good agreement. Difference in the values measured on 10/23 and 10/25 may be due to nonuniform porosity and composition and errors in dimensional measurements. The best data are considered to be the average of the 10/23 and 10/25 data.

The sample dropped off the holder on two occasions, both at slightly above 500 C. This may have been due to the thermal expansion differential between the sample and the stainless-steel sample holder.

The above thermal diffusivity data are recorded in AI Laboratory Notebook B312751.

Thermal conductivity for the phosphate-bonded ZrO_2 can be calculated from the relationship

$$K = \alpha \rho C$$

where

K = thermal conductivity

α = thermal diffusivity

C = specific heat

ρ = density

TABLE G-1

THERMAL DIFFUSIVITY DATA OF PHOSPHATE-BONDED ZIRCONIA

Date, 1968	Temperature, C	Pressure ($x\ 10^6$), torr	Thermal Diffusivity, cm^2/sec
10-4	24*	(1 atm)	0.0072
	24	(1 atm)	0.0071
	28*	80	0.0056
	30	80	0.0051
	28	80	0.0053
	154	100	0.0039
	154	100	0.0035
	140	100	0.0039
10-7	26	2	0.0030
	25	2	0.0033
	24*	600	0.0069
	24	80	0.0068
	310	60	0.0044
	306	55	0.0045
	302	—	0.0043
	435	50	0.0039
	439	—	0.0041
10-23	15*	2	0.0033
	16	2	0.0032
	135	2	0.0027
	138	2.5	0.0028
	240	5.5	0.0025
	241	5	0.0022
	386	8.5	0.0020
	386	8	0.0019
10-25	14*	1.5	0.0038
	16	1.5	0.0037
	519	10	0.0024
	520	10	0.0023
	693	15	0.0022
	695	15	0.0022
	854	45	0.0018
	855	40	0.0022
	965	100	0.0024
	977	100	0.0022
	1005	200	0.0022
	1007	200	0.0017

*Location of thermocouple on sample changed.

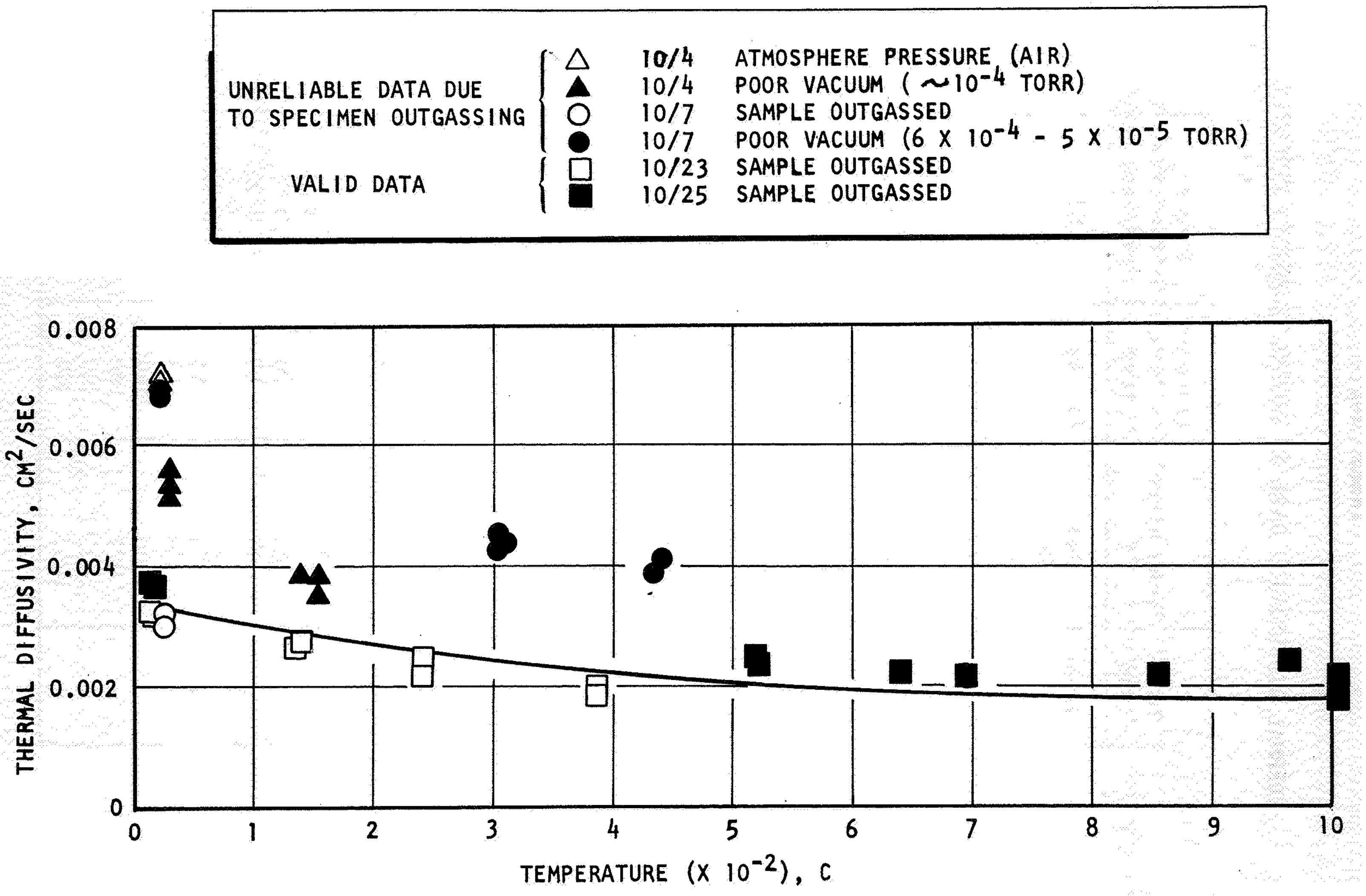

Figure G-1. Thermal Diffusivity of Phosphate-Bonded Zirconia

Thermal conductivity at 1800 F, for example, is 8.4×10^{-6} Btu/in.-sec F using the values $\alpha = 0.002$ cm^2/sec (Fig. G-1), C = 0.17 cal/g C (Ref. 1), $\rho = 4.4$ g/cm^3 and a conversion factor of 5.6×10^{-3} (Ref. 2). These data are for vacuum , but the thermal conductivity data can be modified to account for air at 1 atmosphere in the pores by adding a value of approximately 0.8 Btu/in.-sec-F (Ref. 3). This factor varies slightly depending on pore size and temperature. The 0.8 Btu/in.-sec-F value is for about a 1-mil pore size which is representative of the phosphate-bonded ZrO_2 material. The conductivity of air in a 1-mil pore increases as a function of temperature to about 1800 F and then decreases rapidly after about 2400 F. Thermal conductivity of the specimen in 1 atmosphere of air then would be $(8.4 + 0.8) \times 10^{-6}$ or 9.2×10^{-6} Btu/in.-sec-F. This compares very closely with the value reported in the literature (Ref. 4): Thermal conductivity for ZrO_2 at 1800 F with a porosity of 28 percent is 10×10^{-6} Btu/in.-sec-F. Thus, according to the results of the flash diffusivity measurements, the thermal conductivity of phosphate-bonded ZrO_2 (formulation B45) is about the same as that of pure ZrO_2.

REFERENCES

1. Shaffer, P. T. B., High-Temperature Materials, p. 387, Plenum Press, New York, 1964.
2. DeZeik, C. J., "Coversion Tables for Engineers and Scientists," SAMPE Journal, p. 46, April/May 1968.
3. Kingery, W. D., Property Measurements at High Temperature, p. 97, John Wiley & Sons, New York, 1959.
4. Goldsmith, A., et. al., Thermophysical Properties of Solid Materials: Vol. III - Ceramics, p. 271, November 1960.

DISTRIBUTION LIST

No. of Copies

National Aeronautics and Space Administration
Lewis Research Center
21000 Brookpark Road
Cleveland, Ohio 44135

Attention: Contracting Officer
Chemical Rocket Procurement Section 13
Mail Stop 500-210

National Aeronautics and Space Administration
Washington, D.C. 20546

Attention: Code RPL 2
Code RPX 1
Code RRM 1

Scientific and Technical Information Facility
NASA Representative, Code CRT
Post Office Box 33
College Park, Maryland 20740 6

National Aeronautics and Space Administration
Langley Research Center
Langley Station
Hampton, Virginia 23365

Attention: Robert R. Howell
Mail Stop 208 1
Librarian 1

National Aeronautics and Space Administration
Goddard Space Flight Center
Greenbelt, Maryland 20771

Attention: Librarian 1

National Aeronautics and Space Administration
Marshall Space Flight Center
Huntsville, Alabama 35812

Attention: K. Chandler, R-P&VE-PA 1
Librarian 1
V. F. Seitzinger, R-P&V-MNC 1

No. of Copies

National Aeronautics and Space Administration
Ames Research Center
Moffett Field, California 94035

Attention Librarian 1

National Aeronautics and Space Administration
Manned Spacecraft Center
Houston, Texas 77085

Attention: J. G. Thibodaux 1
Librarian 1

Jet Propulsion Laboratory
4800 Oak Grove Drive
Pasadena, California 91103

Attention: Librarian 1

National Bureau of Standards
U.S. Department of Commerce
Washington, D.C. 20546 1

Department of the Air Force
Air Force Materials Laboratory (AFSC)
Wright Patterson Air Force Base, Ohio 45433

Attention: MAMC (J. J. Krochmal) 1

Department of the Air Force
Air Force Rocket Propulsion Laboratory
Attention: RPM 1
Edwards Air Force Base, California 93523

Department of the Army
Picatinny Arsenal
Scientific & Technical Information Branch
Attention: SMUPA-VA6, Librarian 1
Dover, New Jersey 07801

U.S. Army Materials Research Agency
Watertown, Massachusetts 1

Department of the Navy
Naval Research Laboratory
Attention: Code 2027 1
Washington, D.C., 20390

	No. of Copies
General Motors Technical Center 12 Mile and Mound Road Warren, Michigan Attention: Dr. Richard Murie, Dept. 55	1
General Telephone & Electronics Laboratory, Inc. Bayside, New York	1
IIT Research Institute 10 West 35th Street Chicago, Illinois 60616 Attention: Document Library	1
International Harvester Company Solar Division San Diego, California 92112	1
Itek Corporation Vidya Division 1450 Page Mill Road Palo Alto, California 94304 Attention: Librarian	1
LTV Aerospace Corporation LTV Vought Aeronautics Division Attention: Librarian P.O. Box 5907 Dallas, Texas 75222	1
The Marquardt Corporation Attention: Librarian P.O. Box 2013 South Annex Van Nuys, California 91409	1
McDonnell-Douglas Corporation Douglas Missile and Space Systems Division Attention: Librarian A2-260 3000 Ocean Park Blvd. Santa Monica, California 90406	1
Monsanto Research Corporation Attention: Security Office 1515 Nicholas Road Dayton, Ohio 45407	1

No. of Copies

Norton Research Corporation
Attention: Technical Information Center
70 Memorial Drive
Cambridge, Massachusetts 02142

Philco Ford Corporation
Aeronutronic Division
Attention: Technical Information Service Acquisitions 1
Ford Road
Newport Beach, California 92663

Southern Research Institute 1
Menlo Park, California

Stanford Research Institute
Document Center for Propulsion Sciences 1
333 Ravenswood Avenue
Menlo Park, California 94025

Sylvania Electric Products, Incorporated 1
Silcor Division
Hicksville, New York

Teleflex, Incorporated
Sermetal Division 1
P.O. Box 187
125 South Main Street
North Wales, Pennsylvania 19454

TRW Systems, Incorporated
Attention: Technical Information Center 1
One Space Park
Redondo Beach, California 90278

Union Carbide Corporation
P.O. Box 324
Tuxedo, New York 10987

Attention: Technical Librarian 1

United Aircraft Corporation
Attention: Acquisitions Librarian 1
400 Main Street
East Hartford, Connecticut 06108

No. of Copies

Department of the Navy
Naval Air Systems Cmd.
Attention: AIR-330 1
Washington, D.C. 20360

DMIC
Battelle Memorial Institute
Columbus Laboratories
505 King Avenue
Columbus, Ohio 43201

Attention: Information Specialist 1

Defense Ceramic Information Center
Battelle Memorial Institute
Columbus Laboratories
505 King Avenue
Columbus, Ohio 43201

Attention: Manager of Technical Information 1

Chemical Propulsion Information Agency
Applied Physics Laboratory - JHU 2
8621 Georgia Avenue
Silver Spring, Maryland 20910

Rocketdyne, a division of 20 + Spares
North American Rockwell Corporation
6633 Canoga Avenue
Canoga Park, California 91304

Attention: S. C. Carniglia
991-374
BA40

Aerojet-General Corporation
P.O. Box 15847
Sacramento, California 95813

Attention: W. J. Lewis, Dept. 0726 1

Aerojet-General Corporation
Attention: Technical Library - 2432-2015A
P.O. Box 15847 1
Sacramento, California 95813

No. of Copies

Aerospace Corporation
Attention: Technical Information Center-Document Group 1
P.O. Box 95085
Los Angeles, California 90045

Battelle Memorial Institute
Columbus Laboratories
505 King Avenue
Columbus, Ohio 43201

Attention: D. E. Kizer 1

Bell Aerosystems Company
Attention: Technical Library 1
P. O. Box 1
Buffalo, New York 14240

Bell Telephone Laboratories 1
Mountain Avenue
Murray Hill, New Jersey 07974

Boeing Company
Attention: Aerospace Library 8k-38 1
P.O. Box 3999
Seattle, Washington 98124

Central Research Laboratory
Allied Chemical Corporation
P.O. Box 309
Morristown, New Jersey 07960

Attention: E. R. Degginger 1

DuPont Company
Eastern Division
Attention : Report Clerk. A. R. Steward
Gibbstown, New Jersey 08027 1

General Dynamics Corporation
P.O. Box 12009
San Diego, California 92112

Attention: Library & Information Services 1

General Electric Company
Attention: FPD Technical Information Center 1
Building 700, Mail Zone N-32
Cincinnati, Ohio 45215

	No. of Copies
United Technology Center Attention: Technical Library P.O. Box 358 Sunnyvale, California 94088	1
University of California Lawrence Radiation Laboratory Attention: Technical Information Division P.O. Box 808 Livermore, California 94550	1
University of Dayton Dayton, Ohio	1
University of Denver Denver Research Institute Attention: Security Officer P.O. Box 10127 Denver, Colorado 80210	1
University of Utah Attention: Dr. S. D. Brown Salt Lake City, Utah 84112	1
Vitro Laboratories West Orange, New Jersey	1

UNCLASSIFIED
Security Classification

DOCUMENT CONTROL DATA - R & D

(Security classification of title, body of abstract and indexing annotation must be entered when the overall report is classified)

1. ORIGINATING ACTIVITY *(Corporate author)*
Rocketdyne, a Division of North American Rockwell Corporation, 6633 Canoga Avenue, Canoga Park, California 91304

2a. REPORT SECURITY CLASSIFICATION
UNCLASSIFIED

2b. GROUP

3. REPORT TITLE
Protective Coating System for a Regeneratively Cooled Thrust Chamber

4. DESCRIPTIVE NOTES *(Type of report and inclusive dates)*
Final Report, 30 June 1967 Through 31 January 1969

5. AUTHOR(S) *(First name, middle initial, last name)*
H. W. Carpenter

6. REPORT DATE
29 August 1969

7a. TOTAL NO. OF PAGES

7b. NO. OF REFS
14

8a. CONTRACT OR GRANT NO.
NAS3-11187

b. PROJECT NO.

c.

d.

9a. ORIGINATOR'S REPORT NUMBER(S)
R-7775

9b. OTHER REPORT NO(S) *(Any other numbers that may be assigned this report)*
NASA CR-72569

10. DISTRIBUTION STATEMENT

11. SUPPLEMENTARY NOTES

12. SPONSORING MILITARY ACTIVITY
NASA, Cleveland, Ohio

13. ABSTRACT

A slurry-applied ceramic coating was developed for thermal protection of a Hastelloy-X thrust chamber wall in a high-performance, regeneratively cooled, hydrogen/oxygen-fueled rocket engine. Several cementitiously bonded coating systems were considered analytically and through examination of the literature. Based on screening-type arc-plasma jet tests that simulated the thermal conditions of the reference engine, one coating system appeared capable of meeting all program objectives. This coating was a phosphate-bonded zirconia system. A thickness of 3-1/2 mils of this material (1) reduced the heat flux through a water-cooled Hastelloy-X wall from 50 to 20 Btu/in.^{2}-sec, (2) survived surface temperatures to 4000 F with a 2500 F gradient, (3) survived 25 sudden thermal shocks from 70 to 4000 to 70 F, and (4) could be applied by slurry-coating techniques.

DD FORM 1 NOV 65 1473

UNCLASSIFIED
Security Classification

14. KEY WORDS	LINK A		LINK B		LINK C	
	ROLE	WT	ROLE	WT	ROLE	WT
Heat-Barrier Coating						
Phosphate-Bonded Zirconia						
Cementitiously Bonded Ceramics						
Regeneratively Cooled Rocket Engine						